THE INFLUENCE OF RAINFALL PATTERN ON THE STABILITY OF IDEALISED STEEP SLOPES IN BRUNEI

A thesis submitted to The University of Manchester for the degree of
Doctor of Philosophy
in the Faculty of Engineering and Physical Sciences

2008

ENA KARTINA HAJI ABDUL RAHMAN

SCHOOL OF MECHANICAL, AEROSPACE AND CIVIL ENGINEERING

ProQuest LLC.
789 East Eisenhower Parkway
P.O. Box 1346
Ann Arbor, MI 48106 – 1346

List of Contents

53 000 words

List of Tables

List of Figures

Abstract

The research presents a parametric study into the effects on stability of steep slopes of pore water pressure changes within the slopes due to infiltration as a consequence of different antecedent rainfall patterns and overall total rainfall intensity during a statistically significant rainfall period. The idealised slopes are typically steep and are found in Brunei Darussalam. The study has considered three generic soil types based essentially on their permeability. These are sandy, silty and clayey soil types. The rainfall patterns have been developed from studies of daily rainfall data from the period 1985 – 2004 provided by the Brunei Meteorological Section.

The pore water pressure was modelled as a 2 dimensional system by application of rainfall patterns on idealised slopes of two geometries. Steady state pore water pressure regimes were modified by the infiltration of rainfall into the slopes. This was modelled numerically using the finite element method. The program used was Hydrus2D. The stability of the slopes as a consequence of this infiltration was examined using a straightforward limit equilibrium analysis encapsulated in the program Slope12.01.

The study showed that both the patterns and intensity of rainfall influenced the infiltration potential into the slopes. Using a standard rainfall period it was found that at the end of each rainfall pattern the depth and shape of the wetting fronts were different for different cases of rainfall pattern. In addition to this, however, the behaviour of rainfall infiltration was also influenced by the soil permeability characteristic and the geometries of the slopes. The study also showed that a high daily intensity rainfall alone did not necessarily lead to incipient instability of the slope. The alteration of the pore water regime within the slope with time played a significant role in potential failure.

Based on the above observation, a method to predict the potential onset of failure has been developed by considering the degree of shear strength mobilisation required in the slope during the rainfall period. An approach is presented whereby the potential for slope failure at any time during the rainfall period may be assessed by inspection of simple graphs generated of required mobilised ϕ' against time for different rainfall patterns. Knowledge of the soil behaviour within a slope and its geometry provides an insight into when the slope is likely to fail.

Declaration

I declare that no portion of the work referred to in the thesis has been submitted in support of an application for another degree or qualification of this or any other university or other institute of learning.

Copyright Statement

In memory of my late father

Babah and Mama,

I am forever indebted to your love, support and prayers

Acknowledgement

I wish to acknowledge with deep sense of gratitude, the valuable guidance, advice and inspiration given by my supervisor, Dr. Caesar Merrifield who has been a source of steady motivation, encouragement and enlightenment, in the preparation of the thesis. He had given a fresh breath of air to my work.

I would also like to express my heartfelt thanks to Prof. Ian Smith and Dr. Mike Hicks. Without their support and invaluable advice, I would not have achieved what I was seeking. Special thanks to Prof. Frans Molenkamp for initiating me on this remarkable journey and Dr. William Craig for his advice, contribution and assistance. I also wish to thank staff members of the School of MACE, especially the school administration and IS support team.

My utmost and sincerest gratitude to the Government of Brunei Darussalam for the opportunity given to me and for the support that was provided to me throughout my studies.

A significant part of my work was based on many private communications and data from Brunei Darussalam. I therefore, would like to thank the Brunei Meteorological Service, Department of Civil Aviation; Brunei Public Work Department especially, Geotechnical and Geological section; Department of Town and Country Planning Brunei; Department of Environment, Park and Recreation Brunei; Brunei Survey Department and Brunei Shell Petroleum Company.

I wish to thank all my colleagues and friends, for all their inputs, constructive criticisms, assistance and advice. My stay in Manchester would have been very lonely and unhappy without them.

Above all, my deepest gratitude to my family to whom I will always be thankful for their love, understanding, continuous support, encouragement and prayers.

Notation List

A cross sectional area (m^2)

a inverse of air entry value (m^{-1})

$a(h)$ water stress response function (day^{-1})

AEV air entry value (m)

b width of the slice in the circular slip surface (m)

c' effective cohesion (kN/m^2)

E_n total normal force per unit length on one side of the slice of the circular slip surface (kN/m)

E_{n+1} total normal force per unit length on the other side of the slice of the circular slip surface (kN/m)

E_{tm} total energy per unit mass (m^2/s^2)

E_{tv} sum of the total energy of the unit volume [($kg.m/s^2$)/m^3]

FoS factor of safety of the slope (-)

g acceleration of gravity (m/s^2)

h hydraulic head (m)

h (in Richard's equation and water retention cuve) - pressure head (m)

h (in limit equilibrium analysis) - mean height of the slice of the circular slip surface (m)

h_p pressure head (m)

K permeability or the hydraulic conductivity of the soil (m/s)

K (in Richard's equation) - unsaturated coordinates of conductivity function (m/s)

K^A dimensionless anisotropy tensor for the unsaturated hydraulic conductivity (-)

K_r relative hydraulic conductivity (m/s)

K_s saturated hydraulic conductivity (m/s)

K_{ij}^A components of dimensionless anistropy tensor K^A (-)

K_{iz}^A components of dimensionless anistropy tensor K^A (-)

L length (m) used in Darcy's law

l pore connectivity parameter established to be 0.5 (-)

m parameter in the soil water retention curve (-)

N total normal force per unit length on the base of the slice of the circular slip surface (kN/m)

N' total effective normal force per unit length on the base of the slice of the circular slip surface (kN/m)

n pore size distribution index in water retention curve (-)

P0 pressure head value below which roots start to extract water (m)

POpt pressure head value below which roots extract water at maximum rate (m)

P2H pressure head value (m) below which roots no longer extract water at a maximum rate of higher potential transpiration rate (m/s)

P2L pressure head value (m) below which roots no longer extract water at a maximum rate of lower potential transpiration rate (m/s)

P3 pressure head value below which root water uptake stops (m)

Q (in Darcy's law) - discharge of water (m^3/s)

Q (in Spencer's Method) - the resultant from the interslice forces Z_n and Z_{n+1}

q specific discharge or the Darcian velocity (m/s)

r radius of the circular arc for circular slip surface (m)

S sink term (day^{-1})

S_e effective water content (-)

S_p potential water uptake (day^{-1})

T shear force on the base of the slice of a circular slip surface (kN/m)

t time (day)

t_i initial time (day)

u pore pressure water of the soil (kN/m^2)

u_a pore air pressure of the soil (kN/m^2)

u_w pore water pressure of the soil (kN/m^2)

v velocity of ground water (m/s)

W total weight per unit length of the slice of the circular slip surface (kN/m)

X_n total shear force per unit length on one side of the slice of the circular slip surface (kN/m)

X_{n+1} total shear force per unit length on the other side of the slice of the circular slip surface (kN/m)

x_i spatial coordinates ($i = 1, 2$) (m)

x_j spatial coordinates ($j = 1, 2$) (m)

Z_n parallel interslice force on one side of the slice of the circular slip surface (kN/m)

Z_{n+1} parallel interslice force on the other side of the slice of the circular slip surface (kN/m)

z elevation of the centre of gravity of the unit volume above datum (m)

α angle of inclination of the base to the horizontal of the slice in a circular slip surface (^{o})

ϕ' effective angle of shear resistance (^{o})

ϕ^b angle of shear resistance related to $(u_a - u_w)$ (^{o})

ϕ_m required mobilised angle of shear resistance to be in limiting equilibrium (^{o})

γ unit weight of the soil (kN/m^3)

θ volumetric water content (-)

θ (in Spencer's Method) - angle of inclination of the parallel interslice forces Z_n and Z_{n+1} (^{o})

θ_r residual volumetric water content (-)

θ_s saturated volumetric water content (-)

ρ density which is defined by mass over volume (kg/m^3)

σ_f total stress of the soil at failure (kN/m^2)

σ_f' effective stress of the soil at failure (kN/m^2)

τ_f shear strength of the soil (kN/m^2)

τ_m shear strength required to maintain equilibrium (kN/m^2)

1 Introduction

The problem of slope instability in Brunei Darussalam is considered to be a minor problem but it frequently occurs; this is based upon observations from the reported cases of slope failure to the public works department in Brunei Darussalam. As much as it does not create major catastrophes as in many parts of other far eastern countries, the incidence of slope instability has become one of the main concerns in engineering practice, as slope remediation after failures that have occurred are generally very costly (Quazi, 1999).

In general, slopes may deform and eventually fail as a consequence of a number of factors. These, for instance, are the changes in the steepness of slope due to weathering and erosion; changes in overburden pressure on the slope by the placement of additional load on the crest; variation in ground water table; human activities which may give rise to local toe excavation; seismic disturbance, etc. A major concern in the Far East, in particular in Brunei Darussalam, is the effect on stability as the pore water pressure within the slopes varies due to the infiltration of rainfall into the soil slopes. An increase in pore water pressure in the soil with no increase in total stress reduces the mean effective stress and hence the frictional strength of the soil. This can induce large pre-failure deformations and eventual slope instability leading to failure. In addition to this, many slopes have been over-steepened by natural erosion (Dykes, 1994) to the extent that their stability is under threat especially in some developed areas.

The interaction between the groundwater in the soil and the hydrological cycle is of particular interest to society, for instance in hydrological engineering it is required for the management of the water resources, e.g. for the determination of drainage and irrigation. It is necessary to estimate the seepage through dams, the seepage losses from channels and the groundwater recharge rates, while for the quality control of water the prediction of pollutant attenuation may be needed. In geotechnical engineering, the relationship between the hydrological cycle, the soil and the groundwater is used in the study of the stability of soil structures; e.g. in the case of foundations and stability analyses of retaining walls, embankments and slopes.

The interaction between the atmosphere and the soil, i.e. the transfer of moisture and energy through the soil surface, greatly influences the nature of the upper portion of the soil profile (Blight, 1997). This upper layer is known as the unsaturated zone, and is located between the ground surface and the groundwater table (Lu and Likos, 2004). In order to understand the behaviour of these slopes, it is essential to study the soil properties and the groundwater infiltration behaviour in the unsaturated zone separately from the formulation of the relative stability or instability of a slope and the climate pattern before these can be combined to achieve the aim of the overall research. This study is, therefore, concerned with the stability of slopes under a range of rainfall conditions occurring in Brunei Darussalam.

1.1 Aims and objectives

The overall aim of the research is to improve the understanding of the behaviour of water infiltration into slopes with the commensurate generation of transient pore water pressure regimes due to different rainfall patterns and the consequential effect this has on the overall stability of steep slopes in different types of soil in Brunei in order to develop a method to predict when a failure might occur in these slopes.

The objectives of the research are to;-

- Examine the transient distribution of pore water pressure in typical slopes of different soil and conductivity characteristics when subjected to idealised rainfall regimes.
- Examine the effect of the changes in pore water pressure on the stability of slopes when rainfall intensity and total amount of rainfall are varied.
- Investigate the position of critical slip surfaces generated within slopes during a rainfall period.
- Determine the degree of shear strength mobilisation i.e. characterised by the mobilised internal angle of shear (ϕ' value) of the soil within the slope at which failure occurs in each case. This is the overall angle of internal resistance for the soil required to be mobilised in order for the slope to be in limiting equilibrium

- Develop a method to predict when a failure could be induced based upon the slope geometry, soil properties and the characteristics of the rainfall on the slope.

1.2 Methodology

A parametric study was designed in order to achieve the objectives of the research. Firstly, it involved the study of the soil conditions, slope geometries and the climate conditions - especially the daily rainfall pattern that is associated with Brunei Darussalam. The parametric study later involved the numerical modelling of rainfall infiltration into slopes of idealised geometry by finite elements and the slope stability analysis by the method of limit equilibrium.

1.2.1 Studying the soil data and slope geometries

In order to understand the soil types in Brunei Darussalam, a total of 47 soil investigation reports were gathered from the Public Works Department, Brunei Darussalam. Other literature e.g. (Carsel and Parrish, 1988; Griffiths and Lu, 2005; van Genuchten 1980) were also used to understand the behaviour and parameters of the unsaturated soil near the surface. These parameters were required for the numerical analysis. In addition to this, the general nature of the slopes such as slope angle and the topography of Brunei Darussalam were examined using previous literature and reports, e.g. (Dykes 1994; Negara Brunei Darussalam Master Plan, 1986; Sandal 1996)

1.2.2 Understanding rainfall patterns in Brunei

The Meteorological Section, Brunei Darussalam, maintains most of the historical rainfall records for the country. A comprehensive database of daily rainfall figures was obtained through this office for the 20 years period from 1st January, 1985 to 31st December, 2004. The data were mainly derived from the Brunei International Airport. The data were evaluated so that rainfall behaviour could be identified and

formatted for inclusion in the numerical model. The senior officer of the Meteorological Section in Brunei Darussalam provided further explanation and details associated with the data in order to understand further the climatic conditions in the area of Brunei (Haji Sirabaha, 2004).

1.2.3 Numerical and limit equilibrium analyses

The numerical modelling to study the pore water pressure changes due to rainfall was carried out using a finite element program, Hydrus2D. It is a commercially available software package distributed by the International Groundwater Modelling Centre, Colorado. Hydrus2D is capable of modelling both the saturated and unsaturated water flow by using Richards' equation in two dimensions. The software adopts a Galerkin linear finite element solution technique to solve the governing equations on triangular elements.

The second part of the parametric study was to determine the degree of stability of the standard slopes under different pore water pressure conditions using a limit equilibrium analytical technique. The software used was Slope12.01, which is commercially available. The Slope12.01 package is distributed by Geosolve Ltd. The software allows the user to prescribe different methods of slope stability analysis within limits which are applicable to both circular and non circular slip surfaces, e.g. Swedish circle (Fellenius) method, Bishop's simplified method, Spencer's method and Janbu's method.

1.3 Structure of the thesis

Chapter 1 introduces the basis of the research. It explains the general background, the aim and objectives of the work. It also describes the methodology of the research, as well as the structure of the thesis.

Chapter 2 presents the background to the research question in Brunei Darussalam in general and a review of previous studies on the effect of rainfall on slope. In

addition to this, the theoretical basis of groundwater flow and slope stability analysis is also presented.

Chapter 3 and Chapter 4 define the problem and the research methodology in more detail. Chapter 3 mainly describes the soil hydraulic properties, slope geometries and rainfall behaviour that are related to the parametric study. The development of a rainfall pattern model is included at the end of Chapter 3. This rainfall model is one of the essential input parameters for the water infiltration numerical analysis.

In Chapter 4 the basis of the parametric study is presented. It explains the preparation of the numerical analysis in Hydrus2D and the development of the limit equilibrium model based on Slope12.01. The limitations and the difficulties of numerical and equilibrium modelling are also explained in this chapter.

Chapter 5 presents the results and discussion associated with the numerical modelling of pore water pressure changes due to the application of rainfall on slopes.

Chapter 6 presents the results and discussion associated with the limit equilibrium analysis of rainfall influenced slopes.

Chapter 7 presents the argument and the basis of the development of the general method to predict the onset of failure in slopes in Brunei based on knowledge of the slope geometry, soil characteristics, rainfall characteristics and subsequent pore water pressure changes in the slopes.

Chapter 8 presents a summary of and overall conclusions for the research and recommendations for future work.

2 Literature Review

2.1 Brunei Darussalam – An overview

Brunei Darussalam is located along the northern coastline of Borneo, a large island situated in the southern region of the South China Sea (Figure 2.1). Brunei Darussalam is often referred to as Brunei – a term which will be used extensively in this text. Brunei has an area of 5 770 km^2 and can be classified into four main districts; Brunei and Muara district, Tutong district, Belait district and Temburong district. The capital of Brunei Darussalam is Bandar Seri Begawan, which is located in Brunei and Muara district. Most construction is currently taking place in this capital or close to Bandar Seri Begawan.

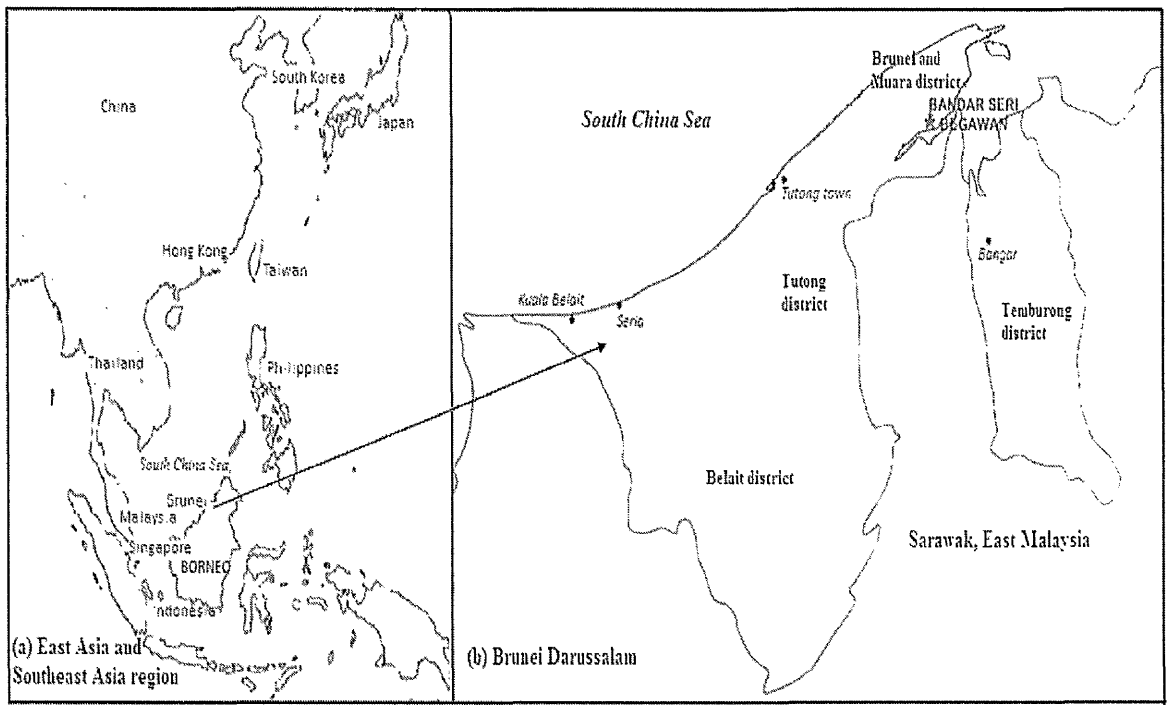

Figure 2.1 (a) Location of Borneo island in the region of East Asia and Southeast Asia Region (b) Four districts of Brunei Darussalam – Brunei and Muara, Belait, Tutong and Temburong district

In geological terms Brunei experiences rapid lateral and vertical changes. The country lies at the centre of large northwest Borneo geosynclines where 33 km of tertiary sediments have been deposited (Abdul Halim, 1992). Most of the land surface of Brunei Darussalam is developed on bedrock of tertiary age (Abdul Halim,

1992; Jali and Choudhury, 1992). These tertiary formations have been affected by folding, faulting, uplift and subsequent tropical erosion. The quaternary geological formations are considered to be a recent development and the uplifting and tilting process helps to protect a youthful landscape that is vigorously being weathered and eroded.

The Negara Brunei Darussalam Master Plan (1986), stated that slopes in Brunei are always greater than 12°, most of these slopes are steeper than 20° and many in excess than 30°. This occupies about 64% of the total land area of Brunei Darussalam. The hillsides generally comprise residual soils typically 2-3 m deep overlying weathered bedrock and are highly sensitive to erosion. 5% of the total land area consists of gentle slopes of less than 12° and 31% of the total land area is lowlands with very soft alluvium deposits and peat. In addition to this, it should also be noted that 70% of the total area of the country is still covered with forest.

Brunei Darussalam has an equatorial climate. It is characterised by plenty of sunshine, highly variable rainfall and little temperature variation throughout the year (Sandal, 1996). It has a daytime temperature as high as 37°C and annual rainfall as high as 3359 mm. Whilst low precipitation is considered unusual in equatorial regions, low monthly rainfall occasionally does occur at various times in each year. There is evidence that the variation of the monthly precipitation can vary widely, from time to time, even though the variation in total annual rainfall varies slightly. Inspection of data over the last twenty years shows that the highest monthly rainfall was recorded in August, 1998 and it was 711.9 mm. This high monthly rainfall was associated with La-Nina season in 1998-1999 (Haji Sirabaha, 2005). La-Nina is the one of the modes of the ocean atmospheric cycle called El-Nino Southern Oscillation (ENSO) which occurs in the tropical Pacific Ocean (Henson, 2008). ENSO is the change in the atmospheric pattern due to fluctuations in the surface temperature and difference in pressure in the tropical pacific ocean (Burroughs, 2007). The study of rainfall patterns in Brunei Darussalam for the 20 year period from 1985-2004 is analysed and presented in more detail in Chapter 3.

2.2 Tropical residual soils

Jali and Choudhury (1992) divide the soils in Brunei into four groups. These are;- peat or organic soils, alluvial deposits and cohesive soils, alluvial deposits and non cohesive soils, and residual soils. Alternatively, as suggested by Singh and Huat (2004), soils may generally be categorised into two, i.e. transported and residual soils. Transported soils are soils that are formed elsewhere and transported to a different location, whereas residual soils are soils that are formed from insitu weathering which accumulate and remain at the same position.

In this research the main concern will be on tropical residual soils like those found in Brunei Darussalam. Residual soils that are found in Brunei are derived from tertiary sedimentary rock by the process of chemical and mechanical weathering (Jali and Choudhury, 1992). Chemical weathering is the breaking down of rock minerals into secondary soils, typically by chemical reaction, for instance oxidation, reduction and hydration whereas mechanical weathering is the breaking down of rocks into smaller particles by physical force, for example by the action of temperature, rain and wind. These form clastic soils (Blyth and De Freitas, 1984; Singh and Huat, 2004; Wicander and Monroe, 1995). It should be noted, however, that the rate of chemical weathering in humid and tropical regions is higher than the rate of mechanical weathering (Summerfield, 1991).

The development of residual soils from parent rocks by the weathering process solely depends on the nature of the rock, the environmental circumstance, e.g. the climatic and topographic conditions and time (Singh and Huat, 2004). For these reasons, the characteristics of residual soils vary from one region to another (Rahardjo et al., 2004). Jali and Choudhury (1992) suggested most shale in Brunei contains organic substances, the consequence of which is to make the shale softer than would be expected in an organic poor environment. When this shale is exposed to sunshine and rainfall, the cyclic drying and wetting process will tend to disintegrate the shale easily.

Residual soil is considered to be heterogeneous, existing largely in an unsaturated environment and has high permeability of the order of 10^{-4} m/s to 10^{-6} m/s (Brand,

1992; Lumb, 1965). Due to their unsaturated characteristics, residual soils are considered to have high shear strengths (Fredlund and Rahardjo, 1993). However due to its high porosity and permeable nature associated with relic fabric amongst other factors, water can easily infiltrate into the residual soil during a period of rainfall and when the rainfall results in full saturation of the soil, the shear strength will reduce considerably.

2.3 Slope instability and its relationship to rainfall

Due to the behaviour and characteristics of residual soil described in the previous section, there are a number of problems associated with the stability of residual soil slopes in the tropical regions which received high rainfall throughout the year (Alonso et al., 1995; Au, 1993; Brand et al., 1984; Dykes, 1994; Gasmo et al., 2000; Lumb, 1975; Rahardjo et al., 2001; Tsaparas, 2002; Tsaparas and Toll, 2002).

Lumb (1975) correlated statistically the relationship between rainfall and landslides from 1950 to 1973 in Hong Kong. The study was based on daily rainfall events and, importantly, the 15 days antecedent rainfall prior to failure occurring. It was found that slope failures usually occurred when daily (24 hours) rainfall exceeded 100 mm and the 15 days cumulative antecedent rainfall exceeded 350 mm. However, Lumb (1975) explained that heavy rainfall did not necessarily produce slope failure. In some cases, after the occurrence of a serious slope failure due to rainfall, no further slope failure occurred or it was found that the risk of slope failure was considered minor near the neighbouring area even though the rainfall intensity was higher.

Dykes (1994) studied the temporal variations in slope stability with respect to the seasonality of rainfall and moisture conditions of the soil of the undisturbed National Park rainforest area in southern part of Brunei. The area is expected to experience 24 shallow landslides every year with recurrence intervals of up to 10 000 years on the same slope (Dykes, 1994). It was noted that the shallow slope failures were the result of saturation of the upper soil layers by perched groundwater above the impermeable bedrock.

Vargas et al. (1990) studied numerically the pattern of water flow in slopes in Brazil using a finite element method. They assumed that the slope surfaces became saturated immediately once there was rainfall, thus maintaining a zero pore water pressure at the surface. The analysis did not allow any evaporation, influence of vegetation, runoff or hysteresis. Vargas et al. (1990) described the behaviour of a wetting front as it developed in a semi-infinite homogenous slope, keeping the pore water pressure either negative or as null. The slip surface was shallow, due to the decrease in the near surface shear strength affected by the decrease in the negative pore water pressure close to the slope surface. They also showed that the position of the bedrock under the homogenous layer affected the pore water pressure distribution within the slope. When the impermeable bedrock was closer to the surface, positive pore water pressure developed in the upper part of the slope. However, when the bedrock was more permeable, a positive pore water pressure was obtained at the toe of the slope. They concluded that the pattern of the pore water pressure distribution due to rainfall was similar for both fine and coarser soil material. However, the time interval to reach certain position of saturation was different. They confirmed that the same seepage pattern was produced when the ratio of rainfall to the coefficient of permeability at saturation of the soil was similar. Nevertheless, there would also be time phase differences depending on the value of coefficient permeability at saturation.

By using a numerical model, Alonso et al. (1995) showed that both the soil permeability and soil retention curve influenced the infiltration of water in an unsaturated slope. These properties would therefore control the stability of slope during rainfall. It should therefore take longer for a less permeable soil to effect a reduction in the factor of safety against failure of a slope compared to a more permeable soil. In some cases, especially for high rainfall intensity on low permeable soil, the factor of safety continues to decrease even after termination of the rainfall. Alonso et al. (1995) proposed that this behaviour was probably responsible for the time delay in some slope failures.

By using a numerical model (Ng and Shi, 1998a; Ng and Shi 1998b) suggested that the dominant influences on the stability of steep unsaturated slopes in colluvium in Hong Kong were initial ground water level, rainfall intensity and antecedent rainfall

influence. The development of perched in water table was observed above the main water level. The negative pore water pressure decreased in this zone as the rainfall intensity increased. However it was found that high rainfall intensity did not necessarily create a larger rise in the shallow main ground water level. High rainfall intensity itself reduced the factor of safety, but this factor of safety would have been affected further by the presence of the antecedent rainfall. Ng and Shi (1998a) and Ng and Shi (1998b) also developed a critical time of 7 days for an antecedent rainfall when the factor of safety representing the stability of the slope reached its minimum value.

Gasmo et al. (2000) studied further numerically the effect of infiltration on the stability of an unsaturated soil slope due to rainfall in Singapore. They found that large amounts of infiltration were obtained at the crest of the slope and for a high intensity rainfall, a rate of infiltration (m/s) larger than the value of permeability of the soils within the slope at saturation could also be achieved. They also described the condition when the soil permeability increased as the soil moisture content, hence degree of saturation, increased, thus increasing the infiltration rate until a steady state condition was obtained. Besides infiltration, Gasmo et al. (2000) also studied the effect of evaporation on pore water pressure distribution in slopes. The negative pore water pressure increased due to the applied evaporation and decreased due to applied rainfall. However, in comparison to field data, the application of evaporation in numerical models appears to show an excessive increase in the negative pore water pressure prevailing within the vadose zone.

Rahardjo et al. (2001) studied further the affect of antecedent rainfall on slopes in Singapore. An antecedent rainfall of 5 days duration was assumed prior to the application of a major rainfall event. They showed clearly that the antecedent rainfall played a major role in the changes of pore water pressure and slope instability in Singapore which agrees with Ng and Shi (1998a) and Ng and Shi (1998b). However, unlike Ng and Shi (1998a) and Ng and Shi (1998b), Rahardjo et al. (2001) found that the main ground water level rose before the major rainfall started.

Tsaparas (2002) and Tsaparas et al. (2002) investigated the influence of initial conditions and the coefficient of permeability due to the application of antecedent and major rainfall on slope stability in Singapore. They showed that changes in pore water pressure and the location of the wetting front were more significant in highly permeable soil than less permeable soil during a major rainfall event. They identified that the initial conditions e.g. ground water level was not important when antecedent rainfall was involved. In addition to this, for soil with high permeability, the introduction of antecedent rainfall has little influence on the changes in the slope stability.

Based on previous studies, they showed that antecedent rainfall was one of the factors that contributed to the instability of unsaturated residual slopes. However, other studies such as Brand et al. (1984) identified that antecedent rainfall was not particularly important for slope instability in Hong Kong and slope instability was mostly affected by short duration high intensity rainfall. Rahardjo et al. (2001) suggested that the role of antecedent rainfall varied depending on the soil properties at the location, the surface condition of the slopes, and the variability of tropical rainfall and microclimate conditions. Different studies have quantified different periods of antecedent rainfall. Lumb (1975) used a 15-day period of antecedent rainfall in Hong Kong in his studies, Ng and Shi (1998a) suggested a 7-day period of antecedent rainfall during which time the factor safety became critical. Other recent studies by Rahardjo H. et al. (2008) used a 5-day period of antecedent rainfall for soil conditions in Singapore. Further field studies by Rahardjo H. et al.(2008) suggested that the amount of antecedent rainfall to generate the highest possible pore water pressure profile is different depending on the texture and permeability of the soil. From their findings, it was found that the worse case of pore water pressure changes due to the application of rainfall on low permeability soil only produced little changes in the factor of safety in comparison with higher soil permeability.

As described above, the use of numerical modelling in predicting the onset of slope instability is very common. However, the complexity of how rainfall infiltrates into the slope should be addressed. Discrepancies have been found between the field data and the computed results (Gasmo et al., 2000; Tsaparas and Toll, 2002). Introduction of evo-transpiration effects in numerical models results in a higher value

of negative pore water in comparison with the field data (Gasmo et al., 2000). Tsaparas and Toll (2002) introduced a thin layer of permeable membrane in their numerical model which represented the pathway of roots from vegetation in order to create a more appropriate pore water pressure distribution comparable to the field observations.

Despite the complexity and discrepancies of using numerical modelling, it still provides a better and more economical understanding of pore water pressure distribution during rainfall than that which may be measured and is a valuable tool for parametric studies.

2.4 Theory

As implemented in the Hydrus2D numerical model, the study of the pore water pressure changes in the slopes due to rainfall infiltration requires the study of groundwater flow through porous media and an understanding of the hydraulic properties of the soil. Therefore this section presents the derivation of the governing flow equations and the model of the hydraulic properties incorporating unsaturated soil. In addition to this, the formulation of a limit equilibrium analysis as applied in Slope12.01 is included.

2.4.1 Groundwater flow

The ground water flow is controlled by laws of physics and thermodynamics such that the difference in energy from one point to another moves the water from one region to another (Fetter, 2001). The sum of total energy of the unit volume of fluids, E_{tv} at any point comprises kinetic energy, gravitational potential energy and energy of fluid pressure as described in Equation 2.1,

$$E_{tv} = \frac{1}{2}\rho v^2 + \rho g z + u \qquad (2.1)$$

where, E_{tv} is the sum of the total energy of the unit volume (M/LT^2), ρ is the density which is defined by mass over volume (M/L^3), v is the velocity (L/T), g is the acceleration of gravity (L/T^2), z is the elevation of the centre of gravity of the unit volume above a datum (L) and u is the pressure of the fluid (M/LT^2).

By dividing the equation above by ρ, the total energy per unit mass, E_{tm} (L^2/T^2) is produced as shown in Equation 2.2,

$$E_{tm} = \frac{v^2}{2} + gz + \frac{u}{\rho} \tag{2.2}$$

The sum of the three components above is constant when the fluids are considered ideal, i.e. the condition when the flow is in steady state and the fluid is both incompressible and frictionless. Under these conditions the density does not change with change in pressure and no energy is required to overcome the frictionless fluid, thus the condition remains constant. By dividing Equation 2.2 by g, Equation 2.3 is produced,

$$\frac{v^2}{2g} + z + \frac{u}{\rho g} = \text{constant} \tag{2.3}$$

From Equation 2.3, the sum of the components may be expressed as the total energy per unit weight, which is called a potential or hydraulic head, h (L), thus,

$$h = \frac{v^2}{2g} + z + \frac{u}{\rho g} \tag{2.4}$$

In general, the groundwater flow has a very small velocity, thus $\frac{v^2}{2g}$ in the above equation may be ignored, and by substituting the pressure of the fluid, $u = \rho g h_p$ in Equation 2.4, where h_p is the height of a column that gives the pressure head (L), Equation 2.4 becomes,

$$h = z + h_p \tag{2.5}$$

2.4.2 Darcy's law and Richard's equation

In the mid 1800's, Henry Darcy found out that for a given sand material, the discharge of water, Q , is proportional to the difference in hydraulic head, h , between two points and to the cross sectional area, A , and inversely proportional to the difference in length, L , between these two points (Fetter, 2001), i.e.

$$Q = -KA\left(\frac{h_1 - h_2}{L_1 - L_2}\right) \tag{2.6}$$

where Q is the discharge of water, i.e. volume of the rate of flow (L^3/T), K is the permeability or the hydraulic conductivity of soil with respect to water (L/T), $h_1 - h_2$ is the difference in hydraulic head (L) between point 1 and point 2 and $L_1 - L_2$ is the difference in length (L) between point 1 and point 2. This has become known generally as Darcy's Law. In general, the Darcy's law, expressed above by Equation 2.6, can be expressed by Equation 2.7 below,

$$Q = -KA\left(\frac{dh}{dl}\right) \tag{2.7}$$

The negative sign in Equation 2.6 and Equation 2.7 shows that the ground water flow moves from a zone of high hydraulic head to that of a low hydraulic head. The value of $\frac{dh}{dl}$ is known as hydraulic gradient. By dividing Equation 2.7 above by A on both sides, it thus becomes the well-known equation,

$$q = -K\frac{dh}{dl} \tag{2.8}$$

where $q = Q/A$ with dimensions of L/T, q is known as the specific discharge or the Darcian velocity.

Consider a two dimensional transient Darcian flow of water in a variably saturated porous media the air phase playing an insignificant role, a governing equation which is known as Richard's equation is produced as shown in Equation 2.9. This equation

is formed by combining Darcy's equation and the two dimensional continuity equation of unsaturated flow, $\frac{\partial\theta}{\partial t}=\frac{\partial q}{\partial x_i}-S$ (Charbeneau, 2000; Fredlund and Rahardjo, 1993; Simunek et al., 1999; Verruijt, 1970).

$$\frac{\partial\theta}{\partial t}=\frac{\partial}{\partial x_i}\left[K(K_{ij}^{A}\frac{\partial h}{\partial x_j}+K_{iz}^{A})\right]-S \tag{2.9}$$

where θ is the volumetric water content (L^3L^{-3}), h = the pressure head (L), S is a sink term (T^{-1}), t is time (T), x_i and x_j are the spatial coordinates over indices i and j (i,j=1,2), K is defined as the unsaturated coordinates of conductivity function (LT^{-1}) given by $K(h,x,z)=K_s(x,z)K_r(h,x,z)$ where K_s is the saturated hydraulic conductivity (LT^{-1}) and K_r is the relative hydraulic conductivity (LT^{-1}) and K_{ij}^{A} and K_{iz}^{A} are components of a dimensionless anisotropy tensor $\mathbf{K}^{A}$.

The sink term, S, in Equation 2.9 is the root water uptake and defined by $S(h)=\mathrm{a(h)}S_p$ (Feddes et al., 1978), where a(h) is the water stress response function $(0\le \mathrm{a(h)}\le 1)$ which is dimensionless as described in Figure 2.2 and S_p is the potential water uptake (T^{-1}). In order to satisfy the Feddes model, it requires five parameters as shown in Figure 2.2, these are the P0 and POpt values which are the pressure head values below which roots start to extract moisture from the soil, and at which the maximum possible rate is achieved respectively. The P2H and P2L values are the limiting pressure heads below which roots are no longer able to extract water at a maximum rate for higher and lower potential transpiration rates (L/T) respectively and P3 is the pressure head value below which root water uptake stops.

It should be noted that the water uptake, S, is assumed to be zero when the pressure head is close to that at saturation, i.e. when the pressure head is greater than P0, and also when the pressure head is lower than the pressure head at the wilting point, P3. The wilting point is the condition at which the soil becomes completely dry and when root water uptake fully stops. The value of water uptake, S, increases from P0 to POpt, and decreases from P2H (or P2L) to P3. Between POpt and P2H (or P2L), water uptake is considered maximal.

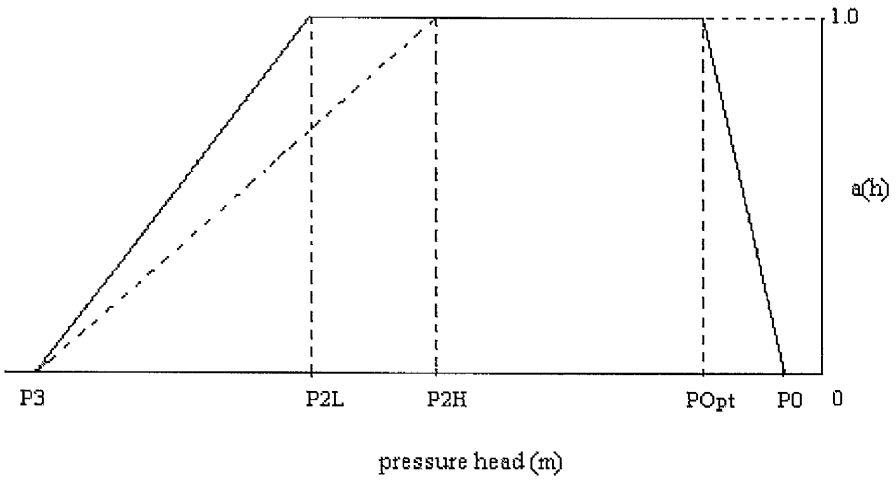

Figure 2.2 The Feddes root water uptake reduction model (from Rassam et al., 2004)

2.4.3 Unsaturated soil hydraulic properties

The relationship between $\theta(h)$ and $K(h)$ in Richard's equation is considered to be non linear. The two well known models to describe the unsaturated soil hydraulic properties are those developed by Brooks and Corey (1964) and van Genuchten (1980).

The relationship between the water content and the negative pressure head or matric suction is described by the soil water retention curve (SWRC). Figure 2.3 shows a typical soil water retention curve for both the drying and wetting phases, illustrating the potential for hysteresis. This graph shows the parameters such as the saturated volumetric water content, θ_s, the residual volumetric water content, θ_r, and the air entry value, AEV (L). The air-entry value is the pressure head at which the pores start to lose water.

Brooks and Corey (1964) described the soil water retention curve as follows,

$$S_e = \left(\frac{\text{AEV}}{h}\right)^n \tag{2.10}$$

S_e is the effective water content, i.e.

$$S_e = \frac{\theta - \theta_r}{\theta_s - \theta_r} \tag{2.11}$$

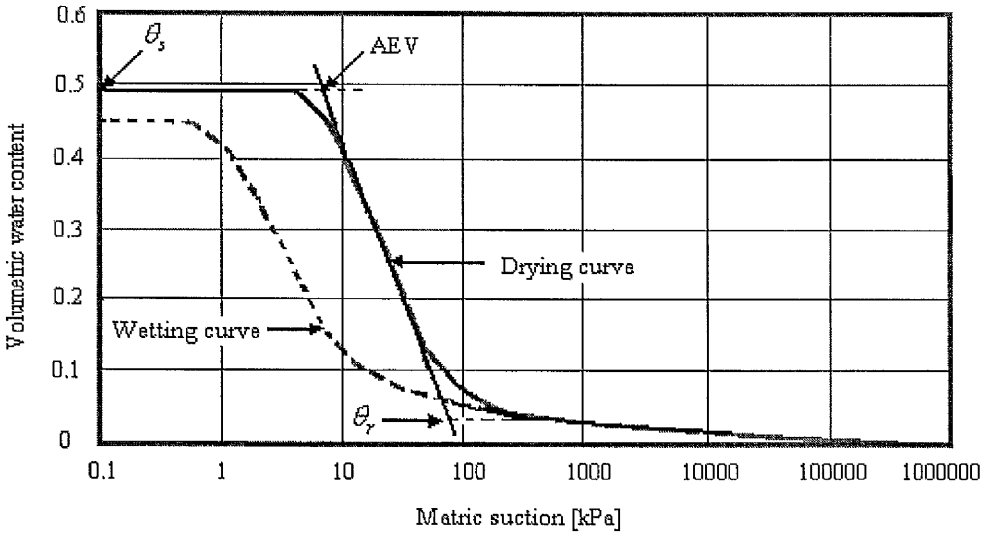

Figure 2.3 Typical soil water retention curve (from Fredlund and Xing, 1994)

By plotting $\log|h|$ versus $\log\theta$ by referring to Equation 2.10 and Equation 2.11, a linear relationship can be obtained - thus the intercept of the best fit curve gives the AEV and the inverse of the gradient of the curve gives the value of n. This value of n is known as the pore-size distribution index.

In this research, however, a van Genuchten model is used. This has been done since the van Genuchten model accommodates the air-entry values for finer soil material and gives a better S-shaped curve when plotted on semi-log scale in comparison with Brooks and Corey model (van Genuchten, 1980). The van Genuchten equation to describe the effective water content is given by,

$$S_e = \left(1 + |ah|^n\right)^{-m} \tag{2.12}$$

where a, n and m are fitting parameters of the SWRC curve, a is the reciprocal of the air entry value, AEV, and m is usually taken as 1-1/n. By substituting Equation 2.11 into Equation 2.12, θ may be found, i.e.

$$\theta = \theta_r + \frac{\theta_s - \theta_r}{\left[1 + |ah|^n\right]^m} \tag{2.13}$$

A further hydraulic parameter utilised in Richard's equation is the hydraulic conductivity function, $K(h)$. Generally, the hydraulic conductivity is defined as the soil's ability to move water within the soil pores (Delleur, 1999). For the fully saturated condition, the flow of water is considered to be continuous; however, in the partially saturated condition, due to the presence of air in the pores, the flow of water in the soil is not continuous. In the partially saturated condition, the value of *K(h)* is related to the changes in pressure head or the volumetric water content. At this stage, the value of *K(h)* is considered to be lower than the value of the hydraulic conductivity function at saturation, K_s. The K_s value is only achieved and remains constant when the soil becomes saturated.

According to Brooks and Corey (1964), the hydraulic conductivity is defined by,

$$K(h) = K_s \left(\frac{\text{AEV}}{h}\right)^{2+3n} \tag{2.14}$$

and by using the statistical pore-size distribution model from Mualem (1976), van Genuchten (1980) gives the expression;

$$K(h) = K_s S_e^{\,l} \left[1 - (1 - S_e^{\,1/m})^m\right]^2 \tag{2.15}$$

where l is the pore connectivity parameter established to be 0.5 (Mualem, 1976). Therefore, by adopting the van Genuchten model described by Equation 2.13 and Equation 2.15, the numerical analysis used in this research requires knowledge of five independent parameters, i.e. θ_r, θ_s, a, n and K_s.

2.4.4 Shear strength and limit equilibrium analysis

The shear strength of the soil is simply the ability of the soil material to resist shear (Powrie, 1997). This is therefore a primary parameter required to study the stability

of any soil mass (Craig, 1997). According to the principle of effective stress (Terzaghi, 1943), where the soil may generate soil resistance to shear only through interparticle contact, the shear strength, τ_f as defined in the Mohr-Coulomb criterion for failure or soil rupture, in terms of effective stress, σ_f' is described by,

$$\tau_f = c' + \sigma_f' \tan\phi' \tag{2.16}$$

where, c' and ϕ' are the effective cohesion and the effective angle of shear resistance respectively, mobilised by the effective stress in the soil. The values of c' and ϕ' are considered to be fundamental shear strength parameters of the soil. The shear strength parameters can be obtained in a number of ways, in both laboratory and field tests, yielding a range of values depending on the failure mode applied to the test. In a simple form they may be expressed graphically from a series of Mohr circles of stress by introducing a straight line that is tangential to these circles. An example of the typical series of Mohr circles with a failure envelope is shown in Figure 2.4.

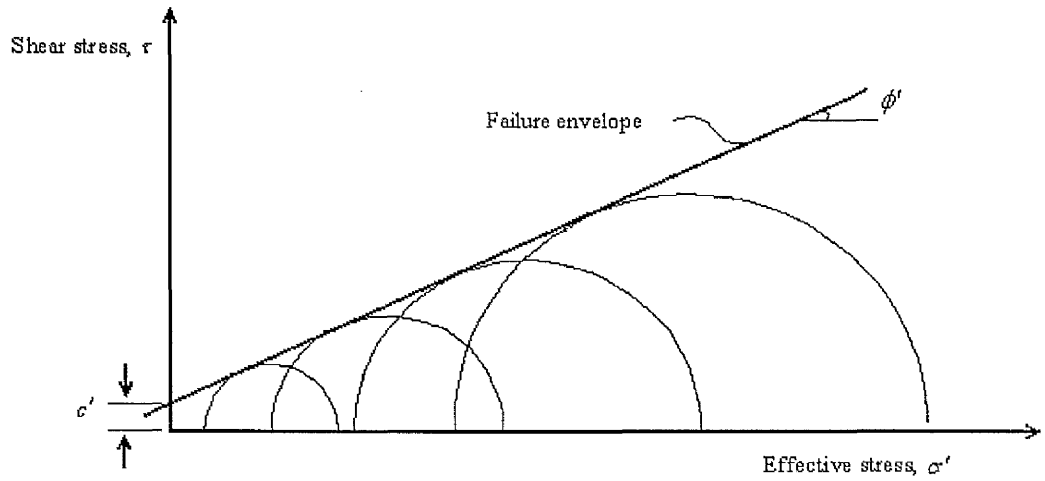

Figure 2.4 Series of Mohr circles with failure envelope (from Craig, 1997)

However, the shear strength Equation 2.16 above is mostly applicable for saturated soil, and the Mohr-Coulomb failure envelope as shown in Figure 2.4, can be extended to partially saturated soil as described by Fredlund and Rahardjo (1993). One of the shear strength equations for unsaturated soil in terms of stress state variables, $(\sigma_f - u_a)$ and $(u_a - u_w)$ can be written as follows,

$$\tau_f = c' + (\sigma_f - u_a)\tan\phi' + (u_a - u_w)\tan\phi^b \qquad (2.17)$$

where τ_f is the shear strength, c' is the effective cohesion of the soil, σ_f is the total stress of the soil, u_a is the pore air pressure, u_w is the pore water pressure, ϕ' is the angle of shear resistance related to $(\sigma_f - u_a)$ and ϕ^b is the angle of shear resistance related to $(u_a - u_w)$. In this case the shear strength parameters will be c', ϕ' and ϕ^b. These three parameters can be obtained by plotting the shear strength, τ_f against stress state variables, $(\sigma_f - u_a)$ and stress state variables, $(u_a - u_w)$ against $(\sigma_f - u_a)$ on the same graph in three dimensions, i.e. $(\sigma_f - u_a)$ in the x-direction, τ_f in the y-direction and $(u_a - u_w)$ in the z-direction.

For residual soil types in Brunei, it is probably more appropriate to consider the shear strength equation as shown in Equation 2.17 above, because the residual soil is known to be partially saturated. However, due to the limitations of the slope stability software, Slope12.01, that is used for this research, the earlier expression of shear strength as shown in Equation 2.16 has been used to represent the shear strength parameters in the slope stability analysis.

The factor of safety of a slope in this research is calculated by using limit equilibrium analysis. The factor of safety, FoS is defined as the ratio of the shear strength available, τ_f, to the shear strength, τ_m that is required to maintain equilibrium (Bishop, 1955), i.e.

$$\text{FoS} = \frac{\tau_f}{\tau_m} \qquad (2.18)$$

A circular surface of rupture, or slip plane, is assumed in the limit equilibrium analysis to obtain the magnitude of the factor of safety of the slope against failure. Figure 2.5 shows an example of a slope with a circular slip surface and typical slices with mean height, *h* and width, *b*. The circular arc has a centre of rotation, O and radius, *r*. The enlargement of the sketch of the slice, with the forces assumed to be acting on it is also shown in Figure 2.5.

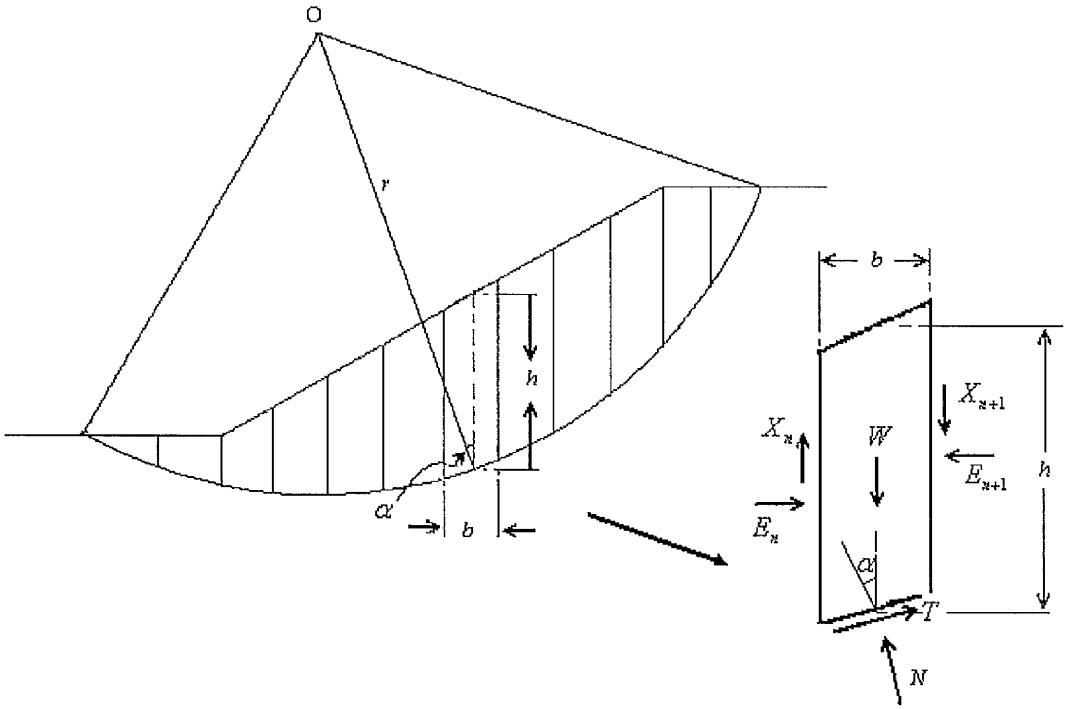

Figure 2.5 Circular slip surface with forces acting on the slice

The descriptions of the forces acting on the slice are as follows (Bishop, 1955; Craig, 1997; Duncan and Wright, 2005; Smith and Smith, 1998; Spencer ,1967).

- The total weight of the, $W = \gamma bh$ where γ is the unit weight of the soil (kN/m^3), b is the width of the slice, and h is the average height of the slice.
- The total normal force on the base of the slice, N which has two components of the effective normal force, N' and the force of water due to pore pressure, $ub \sec\alpha$, where u is the pore water pressure at the base, and α is the inclination of the base to the horizontal, thus

$$N = N' + ub \sec\alpha \tag{2.19}$$

- The shear force on the base, $T = \tau_m b \sec\alpha$, thus

$$T = \frac{\tau_f}{\text{FoS}} b \sec\alpha \quad \text{where} \quad \tau_f = c' + \sigma' \tan\phi'$$

$$\therefore \quad T = \frac{1}{\text{FoS}}(c'b \sec\alpha + N' \tan\phi') \tag{2.20}$$

- At the sides of the slice, there are two interslice forces involved, i.e. the total normal forces on the sides, E_n and E_{n+1} , and the total shear forces on the sides, X_n and X_{n+1}

By neglecting the interslice forces at the sides of the slice, i.e. by assuming $X_n - X_{n+1} = 0$ and $E_n - E_{n+1} = 0$, the condition satisfies the Fellenius (or Swedish) solution. The method only satisfies the overall moment equilibrium but does not satisfy the horizontal and vertical equilibrium. Bishop's Simplified Method assumes that $X_n - X_{n+1} = 0$; this condition satisfies vertical equilibrium and overall moment equilibrium but not horizontal equilibrium.

In this research, the refinement of Bishop's Simplified Method which is also known as Spencer's Method is used. This is because firstly, the Spencer's Method satisfies the condition of horizontal, vertical and moment equilibrium for the slip as a whole, and secondly, since the research is associated with the stability of steep slopes, it is appropriate to use this method as recommended by Borin (2003).

Spencer's Method is carried out by assuming that the interslice forces are inclined and parallel (Spencer, 1967). Thus, by removing the forces of E_n, E_{n+1}, X_n and X_{n+1} in Figure 2.5, the parallel interslice forces of Z_n and Z_{n+1} as shown in Figure 2.6 are considered to satisfy the complete equilibrium procedure of Spencer's method. The value of θ is the angle of inclination of the parallel interslice forces, Z_n and Z_{n+1}, to the horizontal axis. For the equilibrium condition, the resultant, Q, from the interslice forces, Z_n and Z_{n+1}, is produced. The resultant, Q, must meet three other forces i.e. the total weight of the slice, W, the total normal force at the base, N, and the shear force at the base, T, through the point of intersection.

By determining the forces normal and parallel to the base of the slice, the following expression as described by Spencer (1967) is produced,

$$Q = \frac{\frac{c'b}{\text{FoS}}\sec\alpha + \frac{\tan\phi'}{\text{FoS}}\left(W\cos\alpha - ub\sec\alpha\right) - W\sin\alpha}{\cos(\alpha-\theta)\left[1+\frac{\tan\phi'}{\text{FoS}}\tan(\alpha-\theta)\right]} \qquad (2.21)$$

By assuming the interslice forces are parallel, the equation for force equilibrium can be expressed as,

$$\sum Q = 0 \tag{2.22}$$

And for moment equilibrium by taking the sum of moments about the centre of the rotation, O, where the radius, r, is constant, the equation can be illustrated as,

$$\sum [Q\cos(\alpha - \theta)] = 0 \tag{2.23}$$

For complete limit equilibrium analysis, Equation 2.22 and Equation 2.23 must satisfy one another. From these two equilibrium expressions, different values of FoS can be obtained by selecting different values of θ. As a result, two relationships of resultant FoS against assumed θ, due to force equilibrium and moment equilibrium equations can be plotted. The interception of these two curves gives the real value of the factor of safety, FoS, and the corresponding angle of inclination, θ, which satisfy the equilibrium Equation 2.22 and Equation 2.23 above.

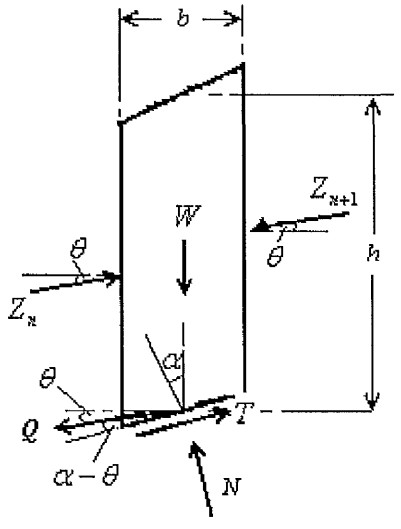

Figure 2.6 The forces acting on the slice for Spencer's Method (from Spencer, 1967)

3 Definition of the Problem and Research Methodology

3.1 Introduction

In general, the formation of steep slopes in Brunei is largely due to the processes of tropical weathering and erosion. However, the weathering process sometimes produces a layer of weathered material on the slope surface that is able to support vegetation (Quazi, 1999). This vegetation is instrumental in the reduction of the process of erosion and surface run off. Roots from this vegetation help to lower the water table in the soil, reducing the pore water pressure below the water table and increasing the soil suction in the unsaturated zone (Blight, 1997). Nevertheless, removal of natural vegetation can cause a serious hazard on any sloping land during rainfall. This is because the bare soil lost its mechanical reinforcement from the roots of vegetation to hold the soil together, thus it becomes more prone to severe erosion and direct water infiltration during rainfall.

The geological formations in Brunei also influence slope deformation and stability. Based on Quazi (1999), some landslides occurring in some developed areas like Bandar Seri Begawan and Jerudong are believed to be due to the breakdown or dissolution of poorly cemented sandstone and mudstone. Thus, seepage of ground water can loosen the soil.

Another factor that has been noted concerning the stability of slopes in sandstone and mudstone is the angle of inclination of these strata within the slope. It is possible that slope failures that have occurred in Bandar Seri Begawan are not just due to poorly cemented sandstones but also due to the angle of inclination of the potentially weak interfaces affected by excavation and how they are related to the slope angle. It can be shown that landslides are more likely to occur when the angle of inclination of a weaker layer within the sequence is parallel to slope (Blyth and De Freitas, 1984).

In many third world countries, human interference through excavation of slopes for rapid urbanisation very often creates unstable slopes that have the potential to fail resulting in disastrous consequences for both property and people resident at the base of the slopes. In Brunei, slope failures may occur even after several years of

construction and this is normally triggered during or immediately after heavy rainfall (Quazi, 1999). There is sufficient evidence in Bandar Seri Begawan that there is a serious lack of understanding of slope characteristics and environmental conditions which are a consequence of, and affected by, the rapid development of urban expansion. Slope stability problems are usually only recognised after failures, or gross deformation of slopes has occurred. The remediation and rehabilitation of slopes after failure are often very difficult and are generally very costly.

An investigation has shown that during the period 1999-2001, a total of 139 cases of slope failure were reported to the Public Work Department of Brunei Darussalam. Data for the periods before and after this period are not available but it is not unreasonable to assume that similar numbers of failures have been reported annually.

Approximately 70 cases of slope failure were reported in 1999, 32 cases in 2000 and 37 cases in 2001. In 1999, the reported cases were double compared to the years 2000 and 2001. This is probably the consequence of the El-Nina phenomenon in 1998-1999.

There are a number of factors that should be considered in this research, these include the geometry of the slope, properties of the soil and the manner of infiltration of rainfall into the soil. This research reports the findings of a parametric study carried out to investigate the combined effects of these parameters on essentially steep slopes in Brunei. This chapter discusses further the validity of the variables that were used in the parametric studies.

3.2 The effect of slope geometry in the study

In a climate where there is high rainfall such as in Brunei Darussalam, the weathering conditions on the relatively weak sedimentary rock produce steep slopes in upland areas (Jali and Choudhury, 1992). Inspection of the Negara Brunei Darussalam Master Plan (1986) shows that more than half of the total land area consists of steep slopes greater than 12^{o}, most of which are steeper than 20^{o} and some exceed 35^{o}. Very steep slopes, having slope angles as high as 50^{o} are commonly found in undisturbed mountainous areas of Temburong. Slope angles, however, have

been found to seldom be controlled by the dip angle of the underlying bedrock (Quazi, 1999).

Dykes (1994) recorded the slope surface angles of about 67 slopes in the Temburong area. These data are shown in Figure 3.1. Even though most of the very steep slopes are found in the undisturbed area of the Temburong district, in rapid urbanisation areas of Brunei, steep slopes are sometimes produced due to inappropriate practices of excavation (Quazi, 1999). Based on the findings of Dykes (1994) and Quazi (1999), it was decided to investigate the effects on two slope angles of 1V:0.5H and 1V:1H in this research. In Brunei, these slope angles are effectively recognised as steep slopes.

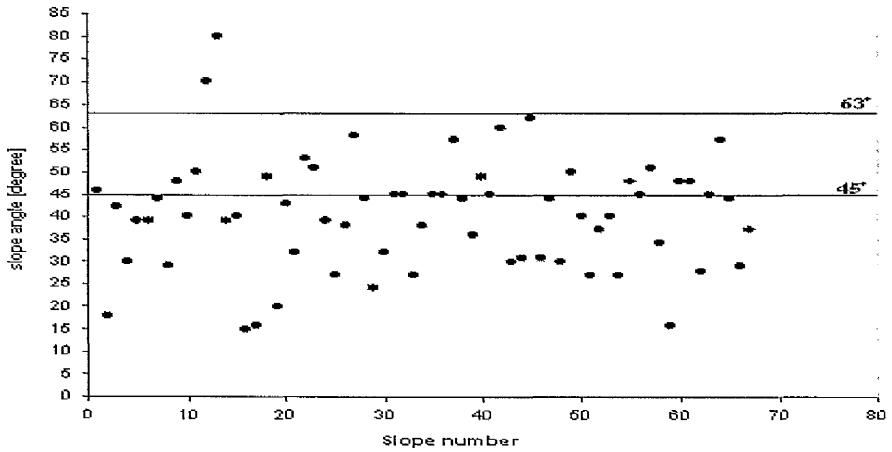

Figure 3.1 Slopes angles recorded by Dykes (1994) for Temburong district in Brunei Darussalam

3.1 Range of soil properties of slopes investigated in this study

In order to understand the soil properties of Brunei Darussalam, data from 47 soil investigations from the public works department, Brunei, were analysed. The data were gathered from 4 districts; 26 investigations from the Brunei and Muara districts, 6 sets of data from the Tutong district, 6 data sets from the Belait district and 9 from the Temburong district. The location of these 4 districts was shown earlier in Figure 2.1.

The soil investigation data were collected from developed areas in Brunei Darussalam. According to BS5930 (1999), most of the soil was described as sandy SILT or CLAY, silty SAND or clayey SAND. It was noted that GRAVEL and

PEAT were also present in some areas. From the 47 soil investigations, it was concluded from the borehole logs and associated SPT values, that in some areas of Brunei the soil tends to be soft or loose near the surface, getting stiffer and denser with depth. In some areas, decayed vegetation and wood pieces were found close to the surface. Weathered sandstone fragments were also recorded in some zones as deep as 18m. Different colours of weathered sandstone were also noted with depth, suggesting a high rate of weathering of the sandstone. The bulk density varied from 1.07 Mg/m^3 for peaty clay to 2.52 Mg/m^3 for mudstone, siltstone and silty clay.

It should be noted that there are limitations to these data sets. The soil investigation data only helps to understand the soil types in Brunei Darussalam in general engineering strength terms. However, soil hydraulic parameters for the unsaturated conditions that are required for the numerical analysis as described in Chapter 2 were not available. Therefore, these data were obtained from other literature, for instance from Carsel and Parrish (1988), Lu and Likos (2004), Schaap and Leij (2000) and Schaap et al. (2001). In addition, it should also be noted that there was, and still is, no coherent data available from ground water monitoring in Brunei. This is based on personal communication with personnel from the Public works department of Brunei Darussalam.

Initially, three saturated hydraulic conductivities, K_s of 1 x 10^{-4} m/s, 1 x 10^{-5} m/s and 1 x 10^{-6} m/s were chosen for the parametric study. These permeability values were based on recommended permeability values suggested by Lumb (1965) and Brand (1992) for residual tropical soils. From these saturated hydraulic conductivities values, other soil hydraulic input parameters as described in Chapter 2 were derived for the numerical analysis. These included;-

- the residual volumetric water content, θ_r
- the saturated volumetric water content, θ_s
- the inverse of air entry values, a (m^{-1})
- and the pore size distribution index, n

These were derived from the collected data of Lu and Likos (2004), Schaap and Leij (2000) and Schaap et al. (2001).

Schaap et al. (2001) developed a neural network computer programme, Rosetta, which employs five hierarchical pedotransfer functions (PTFs) for the prediction of van Genuchten (1980) water retention parameters and saturated hydraulic conductivity, K_s. Most of the hydraulic data that were used in Rosetta were obtained from soils in temperate and subtropical climates of North America and Europe. By using the United States Department of Agriculture (USDA) textural classes (Schaap et al., 2001), Rosetta produced six parameters, θ_r, θ_s, a, n, K_s and l as shown in Table 3.1 below. Lu and Likos (2004) also illustrated the typical ranges of hydraulic soil parameters for various soils as shown in Table 3.2.

Table 3.1 Water retention parameters and saturated hydraulic conductivity derived from Rosetta (Schaap et al, 2001) with respect to USDA textural classes

	Texture classes	θ_r	θ_s	a (m^{-1})	n	K_s (m/s)	l
1	Sand	0.053	0.3747	3.53	3.1798	7.44E-05	0.5
2	Loamy sand	0.0485	0.3904	3.47	1.7466	1.22E-05	0.5
3	Sandy loam	0.0387	0.387	2.67	1.4484	4.43E-06	0.5
4	Sandy clay loam	0.0633	0.3837	2.11	1.3298	1.53E-06	0.5
5	Loam	0.0609	0.3991	1.11	1.4737	1.39E-06	0.5
6	Silt loam	0.0645	0.4387	0.51	1.6626	2.11E-06	0.5
7	Clay loam	0.0792	0.4418	1.58	1.4145	9.47E-07	0.5
8	Silt	0.0501	0.4887	0.66	1.6769	5.06E-06	0.5
9	Clay	0.0982	0.4588	1.5	1.2529	1.71E-06	0.5
10	Sandy clay	0.1169	0.3854	3.34	1.2067	1.31E-06	0.5
11	Silty clay loam	0.0901	0.482	0.84	1.5202	1.29E-06	0.5
12	Silty clay	0.1108	0.4808	1.62	1.3207	1.11E-06	0.5

Table 3.2 Water retention parameters and saturated hydraulic conductivity from Lu and Likos (2004)

Soil types	θ_r	a (m^{-1})	n	K_s (m/s)
Sand	0.05 - 0.1	1 – 5	4 - 8.5	10^{-2} - 10^{-5}
Silt	0.08 - 0.15	0.1 – 1	2 - 4	10^{-5} - 10^{-9}
Clay	0.1 - 0.2	0.01 - 0.1	1.1 - 2.5	10^{-9} - 10^{-13}

Inspection of Table 3.1 and Table 3.2 above, shows that a range of water retention parameters can be obtained for a parametric study. Values of θ_r, θ_s, a, n, and l can be obtained based on the chosen saturated hydraulic conductivity, K_s , as mentioned above. It is assumed that in this study, the sandy soil has a K_s value of 1 x 10^{-4} m/s,

whilst silty and clayey soils have K_s values of 1 x 10^{-5} m/s and of 1 x 10^{-6} m/s respectively. The final water retention parameters and saturated hydraulic conductivity values adopted for this research are illustrated in Table 3.3 below. It should be emphasised that the water retention parameters that were obtained in Table 3.3 were related to the K_s values adopted rather than the soil types that were observed in Table 3.1 and Table 3.2. However, throughout the presentation in this thesis, the soil is differentiated by the name of the soil type rather than the K_s value of the soil.

It should be noted that the water retention parameters should be compatible with the numerical software, Hydrus2D which tentatively noted in previous literature. A few analyses need to be executed in order to find the best fit soil hydraulic parameters for the parametric studies, to eliminate problems and inconsistencies in the numerical simulation; for instance increasing the pore size distribution index, n by 0.1 from 1.5 to 1.6 results in a reduced runtime, acceptable mass balance results and consistent number of iterations per realisation. It should be noted, however, that a smooth numerical simulation not only depends on the soil hydraulic parameters but also on the mesh design within the slope geometry, the applied amount of rainfall to the surface of the slope geometry and the boundary conditions associated with the geometry of the model. This is explained further in Chapter 4.

Table 3.3 Water retention parameters and saturated hydraulic conductivity for parametric studies

Soil types	θ_r	θ_s	a (m^{-1})	n	K_s (m/s)
Sandy soil	0.05	0.35	5.00	3.00	1 x 10^{-4}
Silty soil	0.07	0.42	1.50	2.00	1 x 10^{-5}
Clayey soil	0.10	0.50	1.00	1.60	1 x 10^{-6}

3.4 Climate and the understanding of the rainfall pattern in Brunei

The study of the soil water balance requires all the factors involved in the circulation of the water near the surface of the earth to be considered. The sun's radiation can be considered as the beginning of the hydrological process. As the sun heats the earth surface, water is lost as gaseous water vapour to the atmosphere by the

processes of evaporation and transpiration. Thereafter through the process of condensation, the water vapour reverts to the liquid state in the form of clouds and, at a particular atmospheric condition, precipitation is produced. The precipitation in the form of rainfall or snow returns to the earth's surface; directly to the sea, rivers or lakes, ground surface and it may also be intercepted by vegetation. It should be noted that the precipitation in the equatorial region is mainly in the form of rainfall and it varies from showers to thunder storms. When rainfall reaches the ground, pools of water form at the ground surface, which may infiltrate into the soil or be dispersed on the ground as runoff over a sloping ground surface.

In Brunei, generally, there is only a relatively small variation in the temperature throughout the year. This can be seen in Table 3.4 and Figure 3.2 showing the maximum and minimum temperatures recorded by the Meteorological Section throughout the year of 2000. Figure 3.2 also shows the relative humidity over the same period. It should be noted that in the equatorial region, the variations in temperature are diurnal, and mainly between day and night rather than between seasons (Lockwood, 1974).

Table 3.4 Mean maximum and minimum temperature for Brunei during 12-months period in year 2000

Months	Max. mean temperature (°C)	Min. mean temperature (°C)
January	32.8	22.3
February	32.0	22.1
March	33.0	22.7
April	33.6	22.6
May	35.0	22.8
June	33.4	22
July	34.6	23
August	34.4	22.3
September	34.1	22
October	34.8	22.2
November	32.8	21.7
December	33.0	22.6

Changes in temperature also reflect the variation in the relative humidity; the relative humidity also varies by a small degree throughout the year (Figure 3.2). As with the temperature in the equatorial region, the variation in relative humidity also occurs on a diurnal basis. Throughout the day, the maximum relative humidity can be found

between late afternoon and early morning when the temperature is considered to be low and at a minimum. The minimum relative humidity can be reached around mid-afternoon when the temperature reaches its maximum value (Dale, 1963).

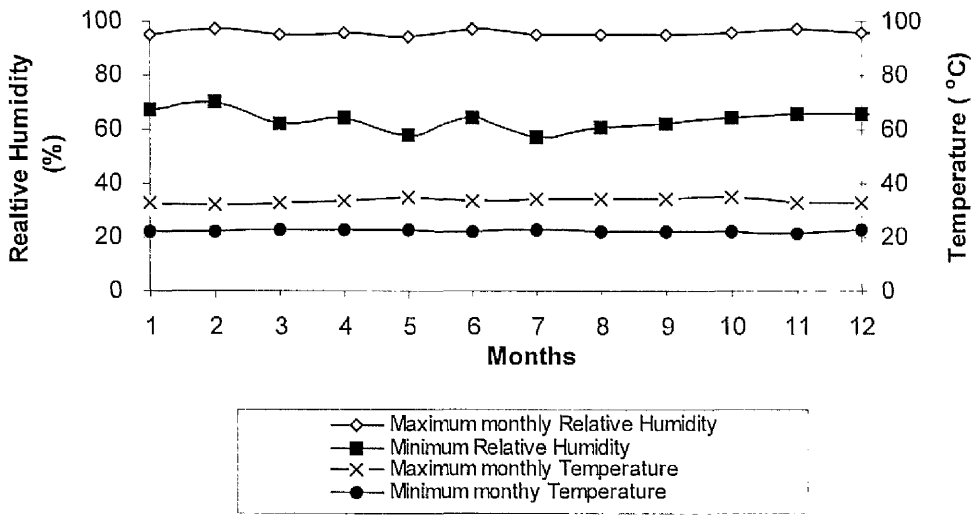

Figure 3.2 The maximum and minimum monthly relative humidity (%) and the maximum and minimum monthly temperature (^{o}C) for 2000

The equatorial regions are known to have a large amount of water surplus throughout the year and no water deficit (Blight, 1997; Brunig, 1970; Lockwood, 1974). Based on A-pan Evaporation data from the Meteorological section in Brunei, the maximum daily evaporation for the 20 year period from 1985 - 2004 was recorded in August, 2004 and it was 11.9 mm. The daily mean evaporation for the same 20 year period was 5.2 mm. Higher evaporation was coinciding with low cloudiness and rainfall (Sandal, 1996). Using Thornthwaite's empirical equation, Brunig (1970) recorded that the actual and potential annual evapotranspiration values at Kuching, Sarawak in Borneo Island are both equal to 1728 mm with monthly amounts between 118 mm and 165 mm and no soil water deficit.

In this research however, the main focus for data is the rainfall pattern in Brunei Darussalam. Rainfall is one of the most important variables in our parametric studies. Thus, a better understanding of rainfall behaviour is required in order to develop a suitable rainfall pattern for the investigation of rainwater seepage into the soil. This is illustrated in more details in the following subsections.

3.4.1 Overview of annual and monthly rainfall in Brunei

Rainfall in the equatorial region is abundant. Brunei receives more than 2000 mm rainfall every year with a mean annual rainfall of 2759 mm, which was taken over a period from 1985 to 2004. Based on data for the 20 year period from 1985-2004, the lowest recorded rainfall was 2153 mm which occurred in 1990 and the highest rainfall was 3399 mm falling in 1988.

The region of South East Asia experienced El-Nino seasons during 1986-1987, 1991-1992 and 1997-1998 and La-Nina seasons during 1988-1989 and 1998-1999. In South East Asia region, El-Nino period is the time when rainfall is below average leading to drought whereas La-Nina is when the rainfall is above average. However, the severity of these two modes of El Nino Southern Oscillation (ENSO) is different from one country to another and it should also be noted that El-Nino is usually followed by La-Nina (Burroughs, 2007). Table 3.5 shows that the highest monthly rainfall was recorded in August of 1998 during a La-Nina period, where the monthly average rainfall was 711.9 mm. However, at the beginning of the year when Brunei experienced El-Nino season, the recorded rainfall was only at trace level, thus the combination of La-Nina and El-Nino period in 1998 still produced an annual rainfall that was close to the average annual value calculated from 1985 to 2004. This was probably the reason why it was difficult to observe whether the country experienced any ENSO phenomenon by just observing the total annual rainfall as shown in Figure 3.3.

The mean monthly rainfall for the period 1985-2004 for Brunei is shown in Figure 3.4. Rainfall in Brunei occurs throughout the year and the heaviest rainfall occurs between October and January. Brunei rainfall is influenced by the North East Monsoon between November and March, and the South West Monsoon between May and September. The months of April and October are known as the transition periods between these two monsoons.

Table 3.5 The monthly rainfall recorded at Brunei International Airport for the 20 year periods from 1985 – 2004

STN. No. 96315 BRUNEI AIRPORT
UNIT: millimetre (mm) PERIOD : 1985-2004

YEAR	JAN	FEB	MAR	APR	MAY	JUN	JUL	AUG	SEP	OCT	NOV	DEC	ANN
1985	305.5	137.8	72.7	263.5	285.8	87.6	172.3	18.0	244.1	381.4	284.0	521.2	2773.9
1986	305.2	113.3	120.6	180.1	68.3	279.0	72.6	265.2	172.3	372.1	398.8	174.4	2521.9
1987	24.8	131.3	33.5	59.8	273.4	288.2	199.1	360.9	142.0	250.7	388.2	249.3	2401.2
1988	277.1	220.1	220.0	203.5	219.6	165.5	301.1	468.0	356.4	201.3	486.2	280.5	**3399.3**
1989	151.4	300.9	186.4	193.9	201.6	168.7	78.8	80.2	344.4	272.1	462.7	245.1	2686.2
1990	387.8	0.6	112.1	293.9	197.8	183.8	161.0	46.3	186.8	185.8	276.3	120.8	**2153.0**
1991	71.7	53.2	46.1	302.5	287.4	215.9	69.2	110.3	233.3	391.7	177.1	279.0	2237.4
1992	201.8	20.6	3.1	119.8	387.8	269.9	247.3	85.4	116.3	311.5	305.6	250.9	2320.0
1993	28.8	52.0	20.3	191.8	329.7	190.4	472.0	71.2	177.8	287.5	410.0	320.6	2552.1
1994	358.2	67.3	121.5	257.4	158.9	178.5	94.8	397.3	136.0	279.0	288.5	316.1	2653.5
1995	179.1	90.0	184.6	83.5	209.6	204.6	364.7	451.0	212.1	257.2	313.5	513.0	3062.9
1996	503.5	200.6	112.8	288.2	274.4	170.4	252.9	295.0	168.1	396.0	317.5	315.5	3294.9
1997	241.2	248.0	7.0	141.7	523.6	189.6	294.7	63.5	273.9	351.3	488.1	94.5	2917.1
1998	**8.0**	**21.0**	**Trace**	**114.8**	**59.0**	**235.2**	**373.2**	**711.9**	**307.7**	**252.1**	**230.7**	**531.4**	**2845.0**
1999	469.8	348.3	169.2	191.8	323.1	68.7	126.3	196.3	307.7	580.7	197.3	380.3	3359.5
2000	209.8	303.8	149.6	316.0	132.6	461.5	21.3	339.1	348.3	309.9	252.8	273.6	3118.3
2001	621.0	192.6	207.7	268.5	164.9	386.5	64.5	129.8	208.1	482.7	308.0	173.7	3208.0
2002	145.4	34.7	113.9	337.1	317.8	133.4	164.3	317.1	164.2	218.0	410.5	233.7	2590.1
2003	60.0	29.5	132.8	302.2	169.1	183.8	303.8	286.6	63.5	467.1	152.1	661.6	2812.1
2004	157.9	44.8	154.6	214.0	237.3	56.1	212	138.3	445.5	202.6	212	210.1	2285.2
Months	20	20	20	20	20	20	20	20	20	20	20	20	20
Mean	235.4	130.5	114.1	216.2	241.1	205.9	202.3	241.6	230.4	322.5	318.0	307.3	2759.6
Max	621.0	348.3	220.0	337.1	523.6	461.5	472.0	711.9	445.5	580.7	488.1	661.6	3399.3
Min	8.0	0.6	Trace	59.8	59.0	56.1	21.3	18.0	63.5	185.8	152.1	94.5	2153.0

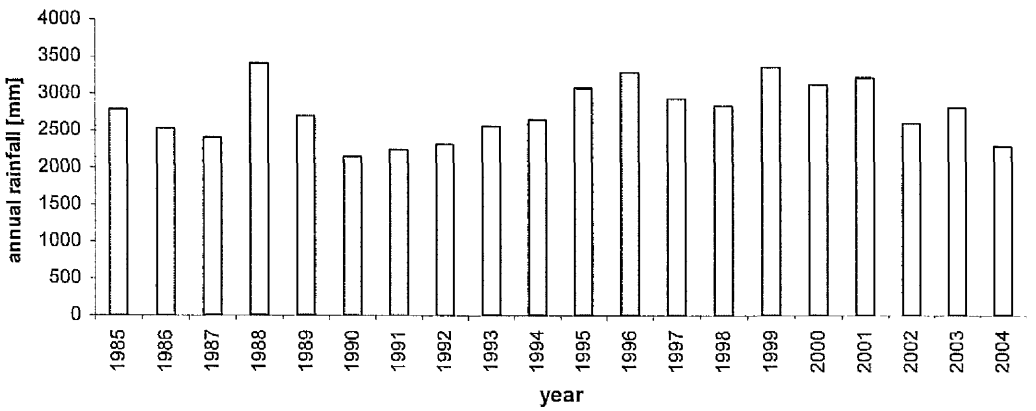

Figure 3.3 Annual rainfall recorded in Brunei International Airport from 1985-2004

In general, the North East Monsoon brings heavy rainfall and the South West Monsoon signifies drier weather. It should be noted, however, that in February and March the north easterly monsoon brings a dry wind from the Pacific Ocean thus also creating relatively dry weather in Brunei. The months of February and March are in fact the two driest months of the year.

Figure 3.5 illustrates further the variation of the monthly rainfall in Brunei from January 1985 to December 2004. Even though the mean monthly rainfall shows considerable monsoon seasons in Brunei, Figure 3.5 shows that differences of rainfall pattern can be significant from time to time.

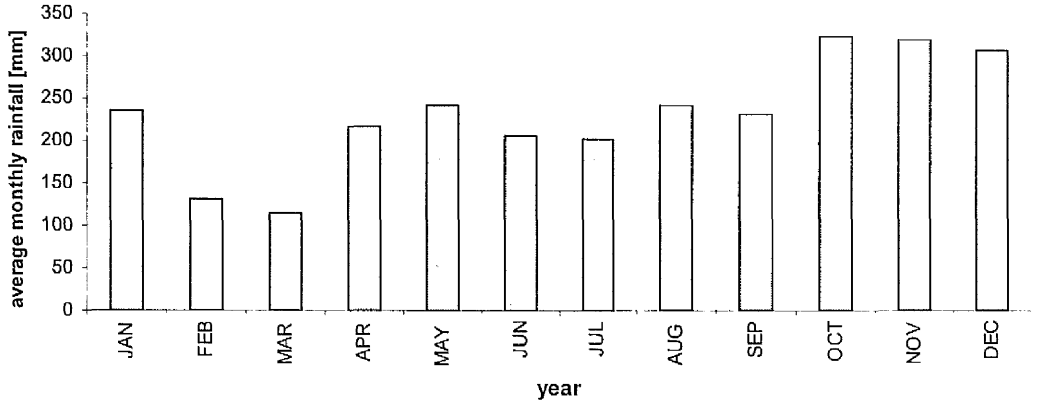

Figure 3.4 Average monthly rainfall for 20 years period from 1985-2004

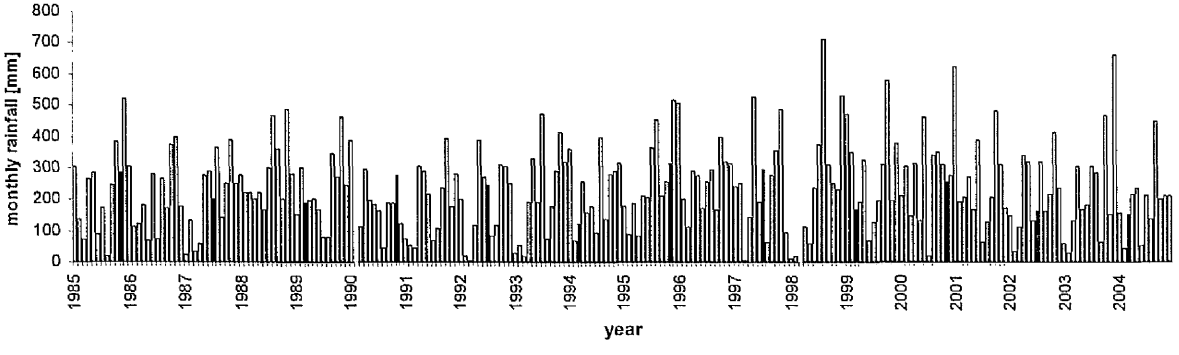

Figure 3.5 Amount of monthly rainfall recorded in Brunei International Airport from 1985-2004

3.4.2 Daily cumulative rainfall

Another method of understanding the pattern of rainfall is by analysing the accumulation of 30 days rainfall at every 10 days interval. This procedure was prepared for each year from 1985 - 2004. The initial time, $t_i = 0$ was taken as the 1st of January in each year, and with 10 day intervals the end value, $t_i = 330$ days was on the 26th of November in the same year or on the 27th of November during leap years. Figure 3.6 shows an example of a 30 days cumulative rainfall graph with 10 days intervals for 1985. For the rest of the years, the plotted graphs of the 30-days cumulative rainfall pattern for each year are illustrated in Appendix A.

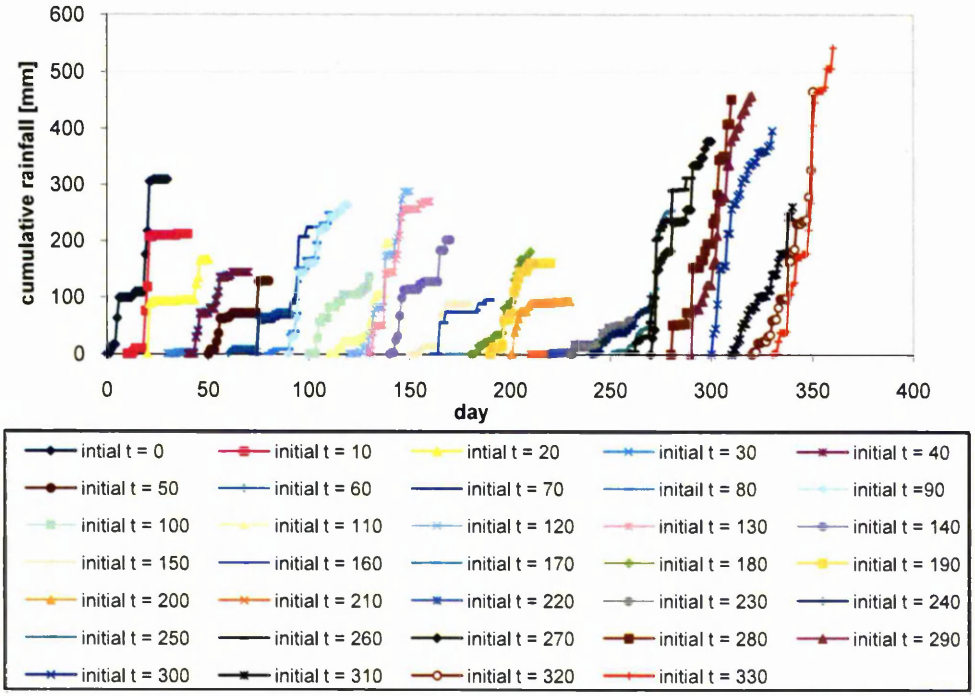

Figure 3.6 The 30-days cumulative rainfall with 10 days intervals from the initial time, $t_i = 0$ to $t_i = 330$ for the year 1985

From these 30-days cumulative graphs, the maximum value of a total 30-days cumulative rainfall for each year from 1985 to 2004 is tabulated in Table 3.6. The maximum 30-days cumulative rainfall was calculated to be in 1998 with total rainfall recorded of 695.21 mm. This value was achieved after a 30 day period of rainfall from an initial time, $t_i = 200$ days, which was on 19 July, 1998. The calculated value was lower than the recorded value of 711.9 mm that was noted in August, 1998 from monthly rainfall data at Brunei International Airport. Calculating the total cumulative rainfall by this method probably underestimated the highest possible 30-

day cumulative rainfall throughout the year as it depends on the initial time at which the rainfall was measured. However, by inspection of the 30-day cumulative rainfall pattern for a 20 year period, it shows that daily rainfall varied considerably from time to time, and the maximum amount of 30-day cumulative rainfall could be obtained at any time of the year.

Table 3.6 The maximum amount of 30-days cumulative rainfall calculated during each year between 1985 and 2004.

Year	Initial time, t_i (day)	Date of t_i	Maximum cumulative rainfall for 30 days (mm)
1985	330	26 Nov	541.50
1986	280	7 Oct	397.10
1987	290	17 Oct	525.50
1988	220	7 Aug	502.11
1989	300	27 Oct	550.20
1990	0	1 Jan	329.00
1991	130	10 May	391.70
1992	120	29 Apr	451.01
1993	170	19 Jun	483.30
1994	310	6 Nov	389.00
1995	200	19 Jul	478.70
1996	0	1 Jan	503.42
1997	110	20 Apr	568.03
1998	200	19 Jul	695.21
1999	270	27 Sep	608.92
2000	250	6 Sep	488.63
2001	0	1 Jan	617.62
2002	100	10 Apr	416.52
2003	320	16 Nov	580.12
2004	250	6 Sep	411.30

From Figure 3.6, a further plot of cumulative rainfall against time was obtained by plotting a number of cumulative rainfall distributions normalised as shown in Figure 3.7. This was done by selecting six of the 30-day cumulative rainfall graphs at the end of 1985. The selected graphs from Figure 3.6 were chosen for the initial times, t_i = 280 days, 290 days, 300 days, 310 days, 320 days and 330 days and normalised so that there all have the same total 30-days rainfall of 505.8 mm. The value of 505.8 mm was chosen mainly because it was the highest of the 30-days cumulative rainfall amount that was recorded in 1985. However, it should be noted that any 30-days cumulative rainfall amount can be used to normalise the whole graphs. Figure 3.7

shows a clear variation in rainfall pattern over the different periods and suggests an alternative and perhaps a better approach in the development of rainfall patterns that may be appropriate to use in a parametric study. Such an approach provides rainfall distributions with time which are characteristically different and which may provide an environment of precipitation and subsequent infiltration which would result in very different transient pore water pressure regimes within a slope with time hence an indication as when a slope failure may occur due to these pore water pressure changes during rainfall.

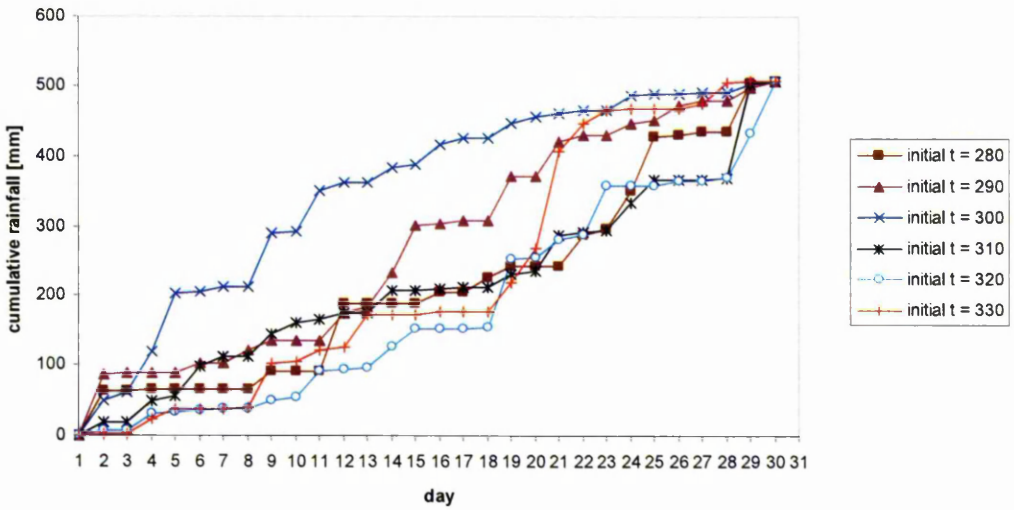

Figure 3.7 Normalised 30-days cumulative rainfall obtained in 1985 from initial time, t_i = 280 days to t_i = 330 days

3.4.3 Development of rainfall pattern for parametric studies

By using the same concept of normalisation described in the previous section, a simpler method was created by looking at the frequency distribution. The frequency distribution was set up to study the identical occurrence of the daily rainfall amount for 20 years period. The frequency table is shown in Table 3.7. There were 7305 daily rainfall data available for the 20 years period from 1985-2004. The frequency table was constructed by dividing the amount of daily rainfall into 5 mm intervals. The first column in Table 3.7 shows the number of intervals involved, the second column is the bin centre, i.e. the middle value of every 5 mm daily rainfall intervals and the third column is the number of occurrences of identical daily rainfall for 20 years period.

Table 3.7 Calculation of frequency of rainfall data

No.	Bin centre (daily rainfall) [mm]	No. of occurrences [days]	No. of days (based on total 35 day occurrences)
1	0	2885	**13.82272**
2	2.5	1739	8.331964
3	7.5	899	4.307324
4	12.5	467	2.237509
5	17.5	295	1.413415
6	22.5	229	1.097194
7	27.5	149	0.713895
8	32.5	163	0.780972
9	37.5	88	0.421629
10	42.5	81	0.388090
11	47.5	53	0.253936
12	52.5	42	0.201232
13	57.5	34	0.162902
14	62.5	38	0.182067
15	67.5	23	0.110198
16	72.5	19	0.091034
17	77.5	18	0.086242
18	82.5	14	0.067077
19	87.5	9	0.043121
20	92.5	13	0.062286
21	97.5	6	0.028747
22	102.5	8	0.038330
23	107.5	5	0.023956
24	112.5	2	0.009582
25	117.5	7	0.033539
26	122.5	4	0.019165
27	127.5	2	0.009582
28	132.5	3	0.014374
29	137.5	4	0.019165
30	142.5	2	0.009582
31	147.5	1	0.004791
32	152.5	1	0.004791
33	157.5	0	0
34	162.5	1	0.004791
35	167.5	1	0.004791
Total no. of days in 20 years =		7305	
Total no. of days for parametric study =			35

By assuming the 35 intervals in column 1 were equal to 35 days of rainfall occurrences these were used in the parametric study. The fourth column was set up to recalculate the number of days of rainfall that occurred within the 35 day period. Thus, the calculation in the fourth column i.e. No. of days = (No. of occurrences/total no. of days in 20 years x 35), e.g. the highlighted bold number in the second row in Table 3.7 was calculated as 2885/7305 x 35 = 13.82272 days, which means that there

were approximately 14 days of no rainfall in 35 day period. This calculation was repeated for each interval in Table 3.7.

For the numerical analysis, column 4 and column 2 in Table 3.7 were recomputed, so that the number of days of rainfall in column 4 was stated in terms of whole numbers. The new calculated data are shown in Table 3.8. It should be noted that the first seven intervals in Table 3.7 were each converted directly as whole numbers. However, there were three parts, i.e. from intervals 8 to 9, intervals 10 to 13 and intervals 14 to 35 (as shown in Table 3.7), where the values were summed together to give a total whole of one day period and a daily rainfall intensity. By converting the original number of days in Table 3.7 into whole numbers as shown in Table 3.8, it reduced the total number of days from 35 to 34. The total amount of rainfall for 34 days period is 310.26 mm, and a cumulative rainfall pattern was plotted based on the tabulated frequency data as shown in Figure 3.8. Such rainfall pattern and the total rainfall amount were achieved based on 20 years daily rainfall data, and has been adopted as the basic rainfall pattern for the parametric study. However, based on Table 3.6, it was found that the total amount of cumulative rainfall can be higher than 310.26 mm. Thus, it was felt appropriate to also consider a higher amount of rainfall within the domain for the parametric study in order to observe how much variation in rainfall actually affected the pore water pressure changes and hence influenced the stability of the slope. An example of the increase in 34-days rainfall amount by 30% and 60% is also shown in Figure 3.8.

Table 3.8 Recomputed data from frequency calculation for parametric study

no. of days	days in a whole number	rainfall [mm]
0.87	1	85.32
1.01	1	48.19
1.20	1	34.25
0.71	1	27.50
1.10	1	22.50
1.41	1	17.50
2.24	2	12.50
4.31	4	7.50
8.33	8	2.50
13.82	14	0.00
Total rainfall for 34 days =		310.26

From the basic rainfall pattern with a total cumulative rainfall for the 34 day period of 310.26 mm (Figure 3.8), two other rainfall patterns were developed to illustrate periodic variations within the domain but having the same maximum cumulative rainfall. All three distributions are shown in Figure 3.9. In the case of pattern 1, the distribution of rainfall was set so that the maximum rainfall intensity was experienced on the first day of the 34 day period for the number of days for which it was computed. In this case it was 85.32 mm for a period of one day (see Table 3.8).

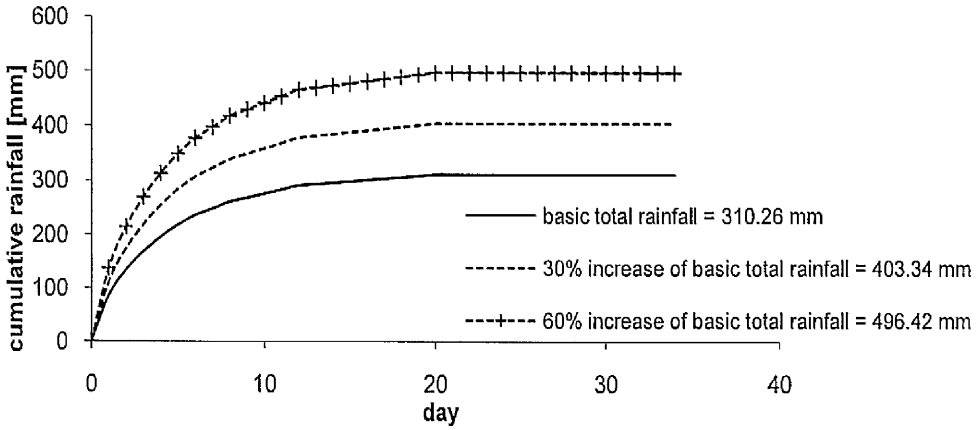

Figure 3.8 Cumulative rainfall pattern for total 34-days rainfall of 310.26 mm, 403.34 mm with 30% increase and 496.42 mm with 60% increase

The daily rainfall for the subsequent days was then determined by setting a decreasing magnitude for the number of days computed in turn. The second distribution was the inverse of the first i.e. the rainfall intensity per day increased from zero on day one to 88.35 mm on the last day. The third pattern assumed that the rainfall was distributed evenly throughout the month. These three rainfall patterns were used in the parametric study. In addition to this, three further rainfall patterns increased by 60% above the basic rainfall patterns were included in this study. The use of the input rainfall data for numerical analysis is described further in Chapter 4.

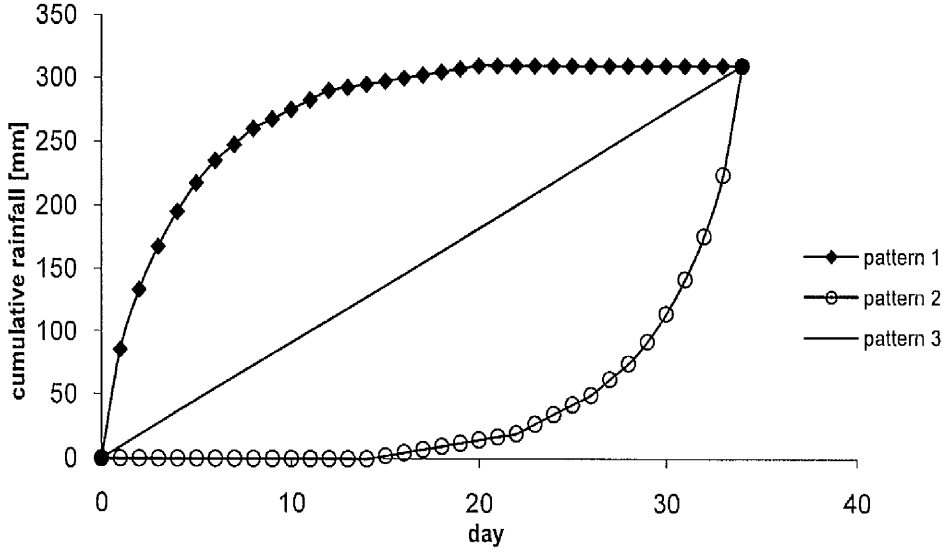

Figure 3.9 Three rainfall pattern for the parametric study with the same total amount of rainfall of 310.26 mm

4 Description of Parametric Study

4.1 Introduction

The parametric study was designed to model the effects of different intensities of antecedent rainfall on the stability of steep slopes of different slope angle and material properties. This required the model to be subjected sequentially to;

- An intensity of antecedent rainfall for a specific duration
- Monitoring of the development of the infiltration front within the slope
- A determination of the stability of the slope at times subsequent to the period of rainfall.

This chapter describes how the process was developed and how the sequence was used to provide the input data to determine the state of the slope at critical times after a period of rainfall.

The first part of the parametric study required the observation of pore water pressure changes in the slopes subjected to specific precipitation regimes which included variation of rainfall patterns. As mentioned in Chapter 1, the finite element program Hydrus2D was used to analyse the effect of rainfall infiltration into the slopes. This chapter describes the development of the numerical model. This includes;

- the design of the slope geometry
- the design of the finite element mesh
- Derivation of material and hydrogeological input data; for example saturated hydraulic conductivities, bulk densities, porosities, vadose zone partially saturated flow parameters including matric suction indices
- Derivation of appropriate rainfall intensities.

The intended output from this section of the analysis was the values of pressure head at selected locations within the slope domain.

The second part of the parametric study, to determine the effect of these transient changes of pore water pressure in the slope on its intrinsic stability, was to express the stability of the slope in terms of either a factor of safety or the required mobilisation of an angle of internal friction. This was achieved by the use of a standard limit equilibrium analysis using the software, Slope12.01. The development of the limit equilibrium model in Slope12.01 is also included in this chapter.

A preliminary analysis was first carried out before the final model was set up. The purpose of doing a preliminary analysis was initially to get some familiarisation of Hydrus2D and Slope12.01 software, and later a more detail study needed to be carried out for the overall parametric study. In the case of the validation of Hydrus2D, the geometry of the slope domain, the mesh design, the initial condition of ground water level and pressure heads distribution, the boundary condition, the input hydraulic parameters, the time steps and iterations criteria were all considered in the preliminary study in order to ensure that these factors were compatible with one another and numerically acceptable for the parametric study. In order to make sure that the results of different types of soil could be compared to each other, all the factors mentioned above needed to be similar for all soil cases that were considered in this research. This helped to minimise any possible inconsistency in the output from the parametric study. During the preliminary study, and as confirmed by Rassam et al. (2004), it was found that there were certain aspects that needed to be considered for the design of the parametric study. For instance, avoiding placing the initial ground water level at soil surface prevented the condition of a diverging numerical solution. Introducing a finer mesh for high permeable soil proved to be very important when high rainfall intensity was applied onto the slope in order to prevent any numerical inconsistency. Allowing small time steps and creating a stable hydrostatic initial condition helped to simulate the numerical solution smoothly.

Similarly, in the case of using the Slope12.01 software, a preliminary study was also carried out in terms of designing the piezometric grids within the slope domain and deciding the type of slip surface that would be considered reasonable for the parametric study. During the preliminary study considering the piezometric grids, for instance, it was found that the potential slip surface due to rainfall was mainly

formed at a shallow position beneath the slope, thus the design placed the grids more appropriately around the slope area.

4.2 Geometry of slopes

The geometries of the slopes chosen for analysis are presented in Figure 4.1 Two typical slope geometries have been chosen. Both are 20 m high, having slope angles of 1V:0.5H and 1V:1H respectively. The models consist essentially of homogenous soils overlying an impermeable hard rock at depth.

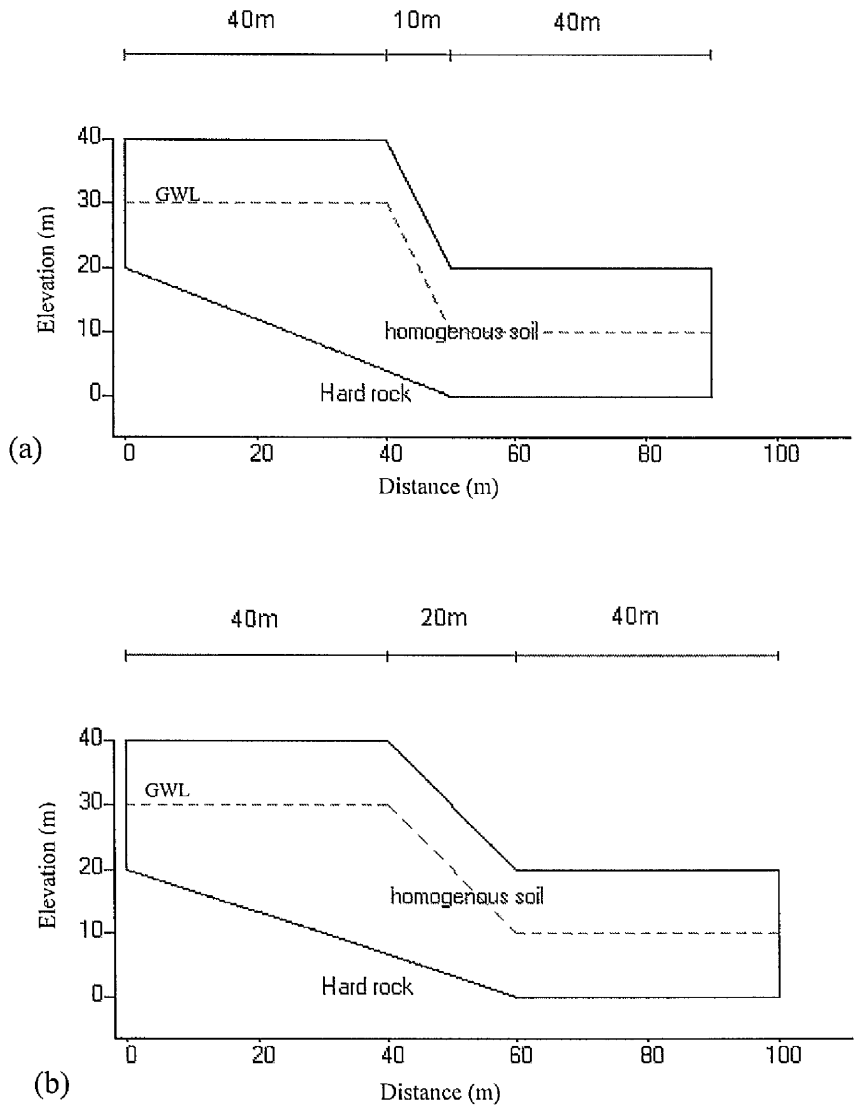

Figure 4.1 Geometry of (a) 1V:0.5H slope and (b) 1V:1H slope for infiltration and slope stability analysis

Based on soils typically found in Brunei three types were selected representing the typical range of permeabilities which have been derived from the literature. These are;-

- a sandy soil with $K_s = 1 \times 10^{-4}$ m/s,
- a silty soil with $K_s = 1 \times 10^{-5}$ m/s and
- a clayey soil with $K_s = 1 \times 10^{-6}$ m/s.

The left and right hand boundaries of the soil model were set to be 40 m away respectively from the crest and the toe of slope. This was required to avoid any influence of the flow boundaries at the sides of the model on pore water pressure changes within the slope area. A soil/rock interface was inferred from experience of relict soils. An inclined soil/rock boundary which did not influence either the pore water flow or the stability of the slope was assumed to reduce the number of elements required for the numerical analysis. The water table was initially set level at a depth of 10 m below the ground surface. This, however, was not the steady state ground water condition. This was found numerically prior to the application of the first rainfall to the slope. This is illustrated later in this chapter.

4.3 Preparation of the numerical model for analysis using Hydrus2D

The preparation of the numerical model for the parametric study involved a number of stages. One of the initial stages of preparing the numerical model was to input the time information which was associated with the numerical solution in Hyrdus2D. For all the analyses, the initial time step was 1e-005 day and the minimum and maximum time permitted value of the time step was 1e-008 day and 5 days respectively. The initial time step was the starting time of the calculation and the step throughout the numerical solution lay between or was equal to the minimum and maximum allowed time value. The time step was automatically adjusted at each time level according to the iteration range that was necessary to reach convergence (Simunek et al., 1999).

Other stages which were associated with the preparation of the numerical model are described in the subsections below. This includes the design of the mesh and the

establishment of the boundary conditions for the applied geometry, the creation of the steady state flow of ground water in the slope domain for the initial condition at t = 0, and the summary of other variables used for the numerical analysis.

4.3.1 Mesh design and applied boundary conditions

The geometry and the mesh design for the models having slopes of 1V:0.5H and 1V:1H used in the numerical analysis are shown in Figure 4.2. The generation of the mesh was achieved as follows (Simunek et al., 1999);-

- The total number of nodes was first applied at seven sides of the domain i.e. at the boundaries of the geometry.
- A nodal density of 0.1 was applied at the upper part of the boundary in order to achieve a finer mesh distribution near the ground surface. Nodal density is a real number between 0.01 and 100 that characterises the local density of boundary points. The program differentiates nodal left density and right density.
- When the values of both densities are equal, then nodal density will be continued, i.e. the distance between one node to another node on all sides of the boundaries will be equal. However, when the values of these two densities are different, then the distance between nodes will also be different.
- Nodal density controls the number and size of elements within the slope domain. However, it should be noted that it does not affect the total number of nodes that was first applied on the boundaries of the geometry.
- Once the number of nodes and density have been applied at the boundaries, Hydrus2D generates the mesh automatically.

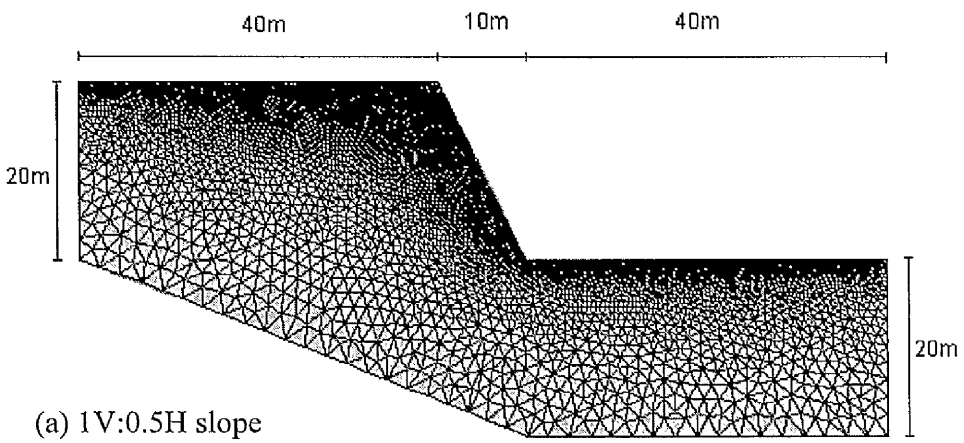

(a) 1V:0.5H slope

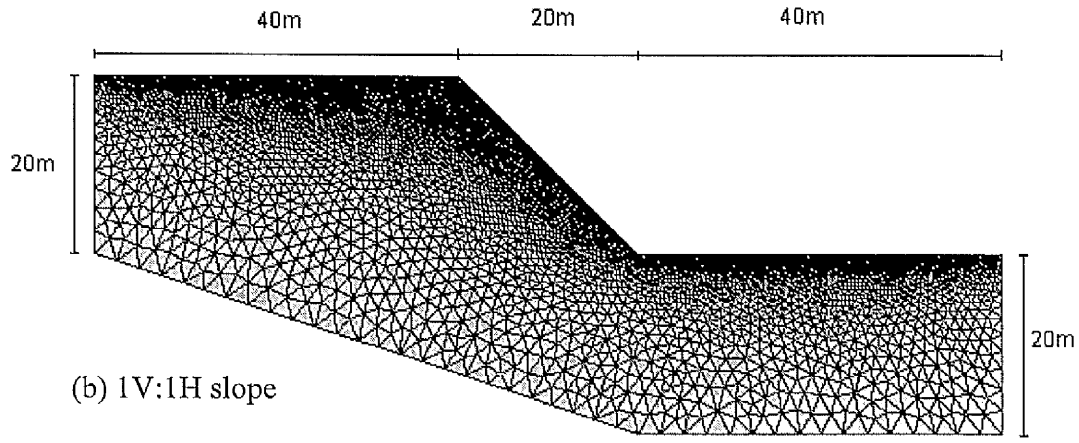

Figure 4.2 Mesh design of (a) 1V:0.5H slope and (b) 1V:1H slope for numerical analysis in HYDRUS2D

The designed slope has four boundary conditions, i.e. an atmospheric boundary condition, two constant head boundary conditions and a no flow boundary condition. The atmospheric boundary condition was applied at the surface of the geometry which allowed rainfall to infiltrate into the ground. At the left hand side and the right hand side of the geometry, a constant head boundary was set up in order to identify the position of the groundwater table which allowed a lateral regional flow in the domain. It should be noted, however, that the pressure head on the constant head boundaries remained constant throughout the analysis. This is a restriction of the program. The no flow boundary was applied at the bottom part of the geometry which prevented water from coming in and out through the lower boundary. This boundary condition represented a separation line between the homogenous soil and impermeable bedrock below. It should also be recognised that the existence of boundaries at the lower part and both sides of the geometry must have no influence on the pore water changes in the slope area.

4.3.1.1 Sensitivity of mesh density

The number of nodes, elements and density of the mesh influence the performance and the result of the numerical analysis. A finer mesh produced a more accurate numerical result; however an increase in node number increased the running time of

the analysis. Thus, in order to produce an acceptable performance as well as reasonable results, a finer mesh was only introduced at the upper part of the domain given that the research enquiry was concentrated on the behaviour of the upper part of the domain in order to observe the effect of rainfall on the stability of slopes. In addition, the introduction of an inclined boundary at the lower part of the domain also served to reduce the number of elements, thus the running time for the numerical analysis.

The 1V:0.5H slope had 7605 nodes and 14 713 elements. However, in the case of the model comprising clayey soil with a saturated hydraulic conductivity of K_s = 1 x 10^{-6} m/s, the number of nodes and elements were reduced to 5226 and 10 021 respectively. During this study, however, it was found that the running time for less permeable soil was longer than the running time for more permeable soil and it was worst for the slope comprising clayey soil. Thus, reducing the number of nodes and elements in clayey soil essentially reduced the runtime by as much as 60% i.e. from 20 hours to 7.9 hours. The reduction in node number did not affect the result of the pore water pressure changes near the surface. This is because the mesh density near the surface remained as fine as the original mesh so that the upper surface would not be affected due to these changes. For all slopes with a ratio 1V:1H, the number of nodes and elements were 7159 and 18 817 respectively.

4.3.2 Creating an initial steady a state water flow condition

For all cases, the water table was initially at 10 m below the ground surface. This is shown in Figure 4.1. The initial pore water pressure was hydrostatic, thus the initial minimum pressure head at the ground surface was -10 m. However, before rainfall was applied to the surface of the geometry, the steady state condition of pore water pressure within the slope domain, both above and below the ground water level was determined. This was done directly by using Hydrus2D as it has the ability to run until it reaches a steady state flow condition. The new position of the ground water table when the steady state condition was achieved is shown in Figure 4.3 for both 1V:0.5H and 1V:1H slopes. This new condition of pore water pressure distribution was used as the initial condition for the parametric study.

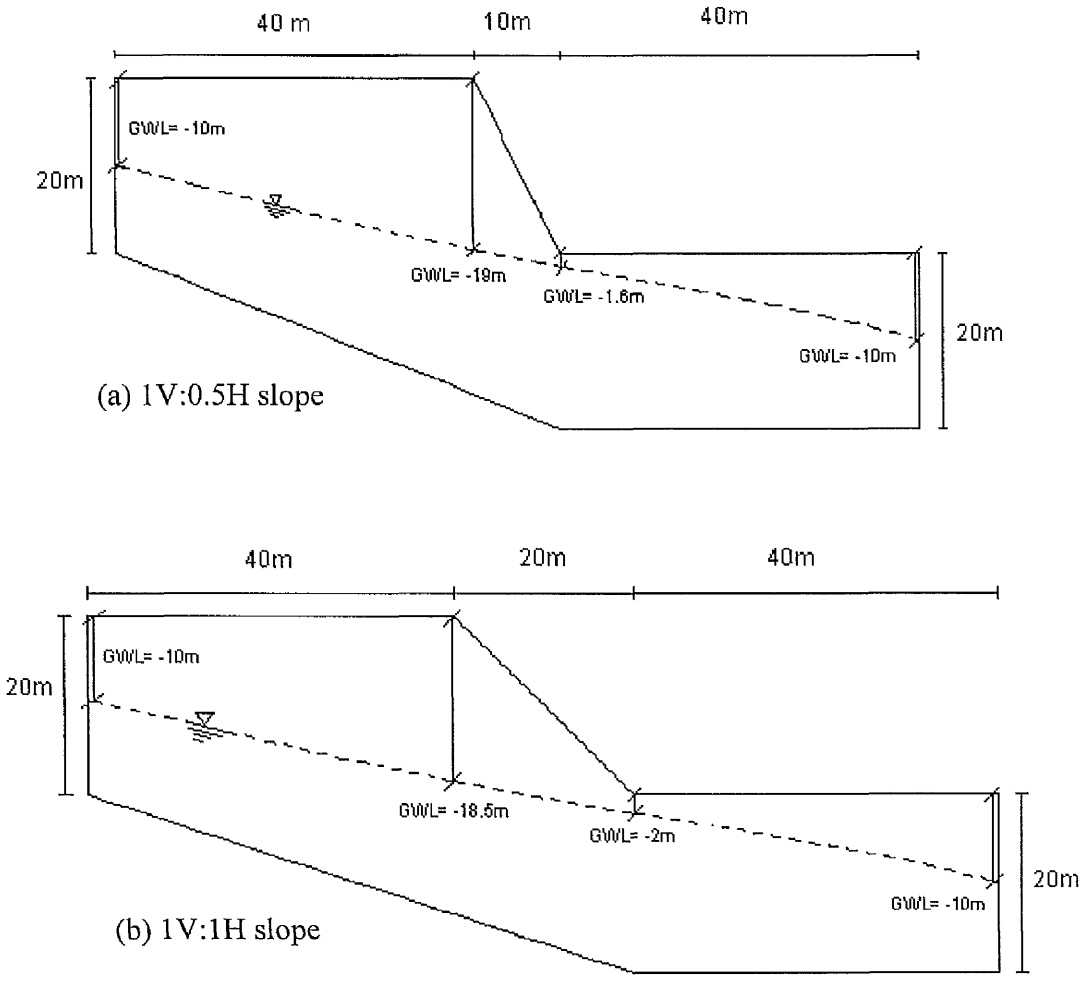

Figure 4.3 Location of ground water level (GWL) at steady state condition for (a) 1V:0.5H slope and (b) 1V:1H slope

4.3.3 Variable parameters in the analysis

The variable parameters for the parametric study included the soil types upon which depended on the saturated hydraulic conductivity of the soil, the rainfall intensities and total cumulative rainfall during the 34 days period, and the variation of rainfall patterns. The development of these parameters was discussed in Chapter 3.

36 numerical analyses were carried out in order to achieve the objectives of the parametric study and these are summarised in Table 4.1 below. The second column in Table 4.1 represents the name of the project slopes that were used in the numerical analysis and throughout this thesis. The third column shows the geometry of each

project as the ratio of vertical to horizontal, (V: H). The fourth column is the saturated hydraulic conductivity, K_s, adopted for the homogeneous soil for each project slope. The fifth and the sixth columns in Table 4.1 respectively illustrate the total cumulative 34-days rainfall and the type of rainfall pattern for each project slope. The summary of each rainfall pattern is shown in Table 4.2.

Table 4.1 Summary of the numerical analyses for the parametric study

No.	Project	Geometry (V:H)	*Ks* [m/s]	total rainfall [mm]	Rainfall pattern (see Figure 3.9)
1	S31-a1	1:0.5	1×10^{-4}	310	1
2	S31-a2	1:0.5		310	2
3	S31-a3	1:0.5		310	3
4	S31-b1	1:0.5	1×10^{-5}	310	1
5	S31-b2	1:0.5		310	2
6	S31-b3	1:0.5		310	3
7	S31-c1	1:0.5	1×10^{-6}	310	1
8	S31-c2	1:0.5		310	2
9	S31-c3	1:0.5		310	3
10	S33-a1	1:0.5	1×10^{-4}	496	1
11	S33-a2	1:0.5		496	2
12	S33-a3	1:0.5		496	3
13	S33-b1	1:0.5	1×10^{-5}	496	1
14	S33-b2	1:0.5		496	2
15	S33-b3	1:0.5		496	3
16	S33-c1	1:0.5	1×10^{-6}	496	1
17	S33-c2	1:0.5		496	2
18	S33-c3	1:0.5		496	3
19	S41-a1	1:1	1×10^{-4}	310	1
20	S41-a2	1:1		310	2
21	S41-a3	1:1		310	3
22	S41-b1	1:1	1×10^{-5}	310	1
23	S41-b2	1:1		310	2
24	S41-b3	1:1		310	3
25	S41-c1	1:1	1×10^{-6}	310	1
26	S41-c2	1:1		310	2
27	S41-c3	1:1		310	3
28	S43-a1	1:1	1×10^{-4}	496	1
29	S43-a2	1:1		496	2
30	S43-a3	1:1		496	3
31	S43-b1	1:1	1×10^{-5}	496	1
32	S43-b2	1:1		496	2
33	S43-b3	1:1		496	3
34	S43-c1	1:1	1×10^{-6}	496	1
35	S43-c2	1:1		496	2
36	S43-c3	1:1		496	3

Table 4.2 consists of four main columns, the first column identifies the day within the 34 days rainfall period. The second column shows the daily rainfall intensity for Pattern 1 rainfall, similarly, the third and the fourth column shows the daily rainfall intensity for Pattern 2 and Pattern 3 for that particular day respectively. Each column of rainfall pattern has been divided into two sub columns, the first sub column is the original daily rainfall intensity which was calculated from the frequency distribution table as described in Chapter 3 and the second sub column is the daily rainfall intensity when rainfall was increased by 60%. The last row in Table 4.2 is the amount of cumulative rainfall after 34 days period.

Table 4.2 Rainfall pattern and daily intensities for parametric study.

TIME	**PATTERN 1** rainfall [mm/day]		**PATTERN 2** rainfall [mm/day]		**PATTERN 3** rainfall [mm/day]	
Day	Original pattern	60% increase	Original pattern	60% increase	Original pattern	60% increase
0	0	0	0	0	0	0
1	85.32	136.51	0	0	9.13	14.60
2	48.19	77.10	0	0	9.13	14.60
3	34.25	54.80	0	0	9.13	14.60
4	27.50	44.00	0	0	9.13	14.60
5	22.50	36.00	0	0	9.13	14.60
6	17.50	28.00	0	0	9.13	14.60
7	12.50	20.00	0	0	9.13	14.60
8	12.50	20.00	0	0	9.13	14.60
9	7.50	12.00	0	0	9.13	14.60
10	7.50	12.00	0	0	9.13	14.60
11	7.50	12.00	0	0	9.13	14.60
12	7.50	12.00	0	0	9.13	14.60
13	2.50	4.00	0	0	9.13	14.60
14	2.50	4.00	0	0	9.13	14.60
15	2.50	4.00	2.50	4.00	9.13	14.60
16	2.50	4.00	2.50	4.00	9.13	14.60
17	2.50	4.00	2.50	4.00	9.13	14.60
18	2.50	4.00	2.50	4.00	9.13	14.60
19	2.50	4.00	2.50	4.00	9.13	14.60
20	2.50	4.00	2.50	4.00	9.13	14.60
21	0	0	2.50	4.00	9.13	14.60
22	0	0	2.50	4.00	9.13	14.60
23	0	0	7.50	12.00	9.13	14.60
24	0	0	7.50	12.00	9.13	14.60
25	0	0	7.50	12.00	9.13	14.60
26	0	0	7.50	12.00	9.13	14.60
27	0	0	12.50	20.00	9.13	14.60
28	0	0	12.50	20.00	9.13	14.60
29	0	0	17.50	28.00	9.13	14.60
30	0	0	22.50	36.00	9.13	14.60
31	0	0	27.50	44.00	9.13	14.60
32	0	0	34.25	54.80	9.13	14.60
33	0	0	48.19	77.10	9.13	14.60
34	0	0	85.32	136.51	9.13	14.60
SUM [mm]	310.26	496.42	310.26	496.42	310.26	496.42

4.4 Obtaining pressure head values from output results

At the end of each numerical simulation, the output was verified to ensure that the results were numerically acceptable. The mass balance was inspected and the maximum allowable error was < 2%. The mass balance is the calculation of the numerical error in the water balance computation within the domain. Hydrus2D introduces two values or quantities, the first quantity is the change in the absolute water storage for all elements and the second quantity is the sum of absolute fluxes that come in and out of the domain (Simunek et al., 1999). The difference between these two quantities is called the mass balance error. It should be noted that when rainfall exceeds the infiltration capacity of the soil, any excess water on the surface of the domain is removed instantaneously by Hydrus2D. The iteration time information was also examined and was not permitted to be higher than the applied maximum number of iterations. The reported flux should also be realistic. These verifications were obtained from the post-processing in Hydrus2D. The running time for each simulation varied depending upon the type of soils in the slopes, rainfall patterns and rainfall intensity.

The pore water pressure distribution before and after the simulation was also obtained through post-processing within Hydrus2D. These included the contours of pressure head, volumetric water content and the velocity vector of pore water pressure changes. The profile for pore water pressure distribution with depth is also illustrated by examination of the cross section between two coordinates within the domain. The results from post-processing in Hydrus2D gave a better understanding of the effect of the rainfall infiltration on the behaviour of the pore water pressure changes in the slopes examined.

The cross sectional values of pressure head with depth around the slope area were required for the slope stability analysis. For this purpose, a grid was designed around the slope area in Hydrus2D which was similar to the grid that was used later to define the geometrical parameters for the failure surfaces in Slope12.01. As Slope12.01 only allows 20 by 20 piezometric grids, the values of pressure head with depth were also collected manually at 20 cross sectional points in Hydrus2D. As

shown in Figure 4.4, for 1V:0.5H slopes, 20 cross sectional pressure head values were taken from x = 38.97 m to x = 51.03 m, and the interval between the first two columns was 1.0 m, then the interval changed by approximately 0.6 m for the next 17 columns and the interval between the last two columns was also 1.0 m ; whilst for 1V:1H slopes, these values were taken from x = 39.10 m to x = 60.05 m at approximately 1.1 m interval, this process was repeated at each required time. When all 20 sets of cross sectional pressure head data were recorded, these data were converted to piezometric head values as acceptable input to Slope12.01.

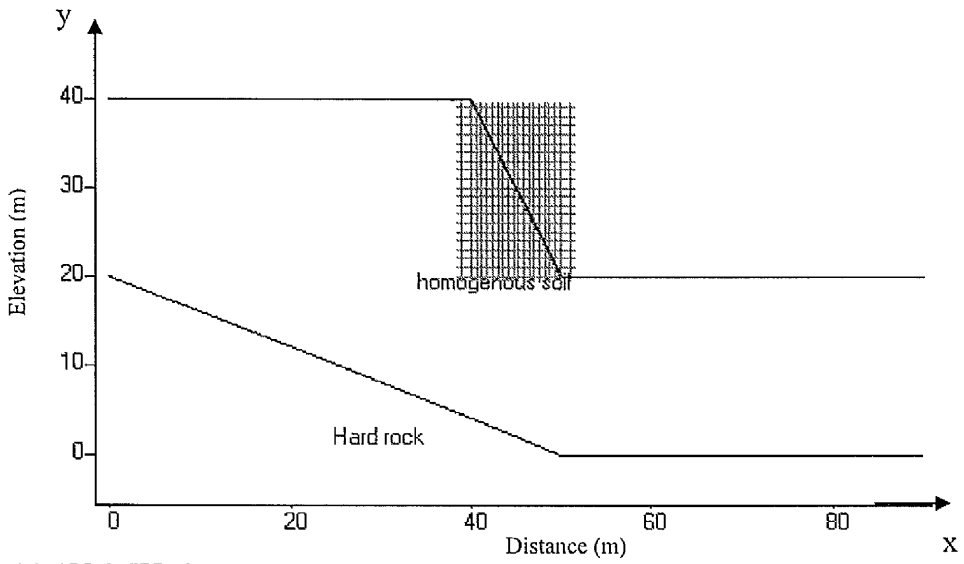

(a) 1V:0.5H slope

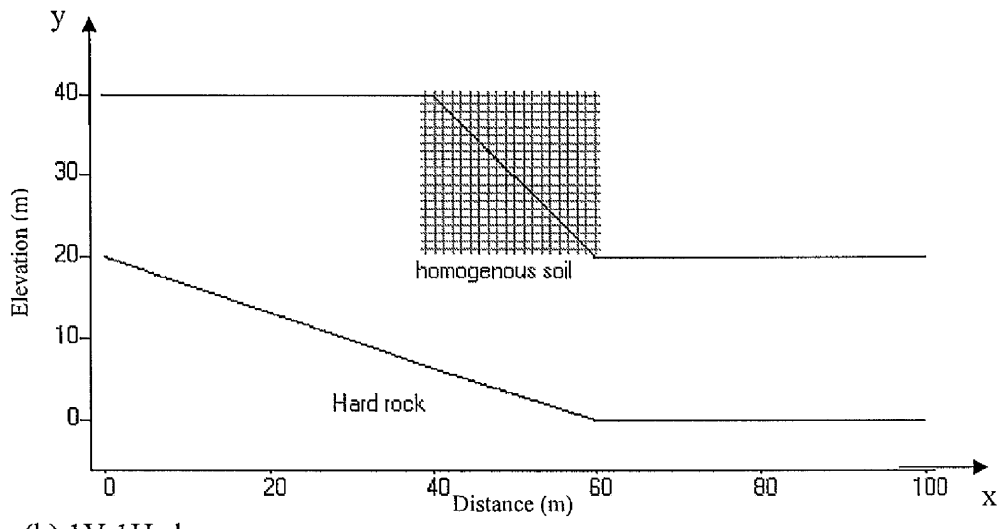

(b) 1V:1H slope

Figure 4.4 The area of the piezometric grids for (a) 1V:0.5H slope and (b) 1V:1H slope

4.5 Limitations of the numerical analysis

As mentioned in Chapter 2, it is essential to consider all the hydraulic properties above and below the soil surface in the numerical analysis in order to create a condition similar to a realistic field situation. However, introducing evaporation and transpiration in a numerical study is a complex matter. In Hydrus2D itself, introducing evaporation during a period of no rainfall produced a very high negative pore water pressure near the surface, and a sudden application of rainfall on the negative pore water pressure created instability in the numerical performance. This problem has been confirmed by Rassam et al. (2004). Due to this instability, the program usually terminated before it was completed. In order to avoid this problem, evaporation on the soil was not included in the parametric study. The consequence of avoiding the inclusion of evaporation probably overestimated the safety factor of the slope and probably the position of critical slip surface.

Another hydraulic property that has not been considered in this study is transpiration. Hydrus2D allows transpiration by introducing a model of root water uptake in the numerical analysis. This parameter is described in Chapter 2 as the sink term, S as shown Equation (2.9). However, there is a lack of field data available from Brunei for this model. Nevertheless, a few analyses were carried out by using some default parameters that were suggested in the Hydrus2D manual for root water uptake models. It was found, quite understandably, that the depth of the wetting front due to rainfall was shallower in soils with root water uptake than on soil without it. On the other hand, for the limit equilibrium analysis, the position of slip surface and the factor of safety were similar for both cases, i.e. the presence of root water uptake model did not affect the location of the slip surface or the derived factor of safety against failure for the slope. Thus, it was considered acceptable to exclude transpiration and root water uptake model for the parametric study in this case.

4.6 Development of the limit equilibrium model in Slope12.01

The limit equilibrium analysis in Slope12.01 was set up following the development of the numerical model in Hydrus2D. Unlike the slope geometry in Hydrus2D, both

upper homogenous soil and lower impermeable hard rock layers were considered in Slope12.01. This geometry is shown in Figure 4.1.

Setting up the model in slopes12.01 included identifying the soil properties in both layers for stability analyses. The required parameters are bulk densities of the soil below and above ground water level, and effective stress parameters to describe the shear strength of the soil. The position of the ground water level, values of piezometric grids and the definition of slip surface were also set up for the analyses. This is explained in the next sub sections in more detail.

4.6.1 Setting up piezometric grids in slopes

In Slope12.01, piezometric grids are used to identify the value of piezometric heads where the porewater distribution is not hydrostatic in slopes. Before the values of piezometric grids in the slope geometry were set up, the locations of the ground water levels were positioned at the ground surface. This is necessary since one of the limitations of the Slope12.01 program is that it can only identify the values of piezometric grids below the position of ground water level, whereas any values above the ground water level are ignored. Therefore, in order for Slope12.01 to recognise values over the entire piezometric grid, both the negative pressure head values and the positive pressure head values that are located in the model, a notional ground water level needs to be positioned on the ground surface.

Slope 12.01 only allows 20 by 20 piezometric grids in the x and y directions. For all slope models in the parametric study, all 400 piezometric heads grid nodes were used and positioned strategically around the slope area. A few assessments were initially carried out to find the best 20 by 20 piezometric grid areas that would be used for all limit equilibrium analyses. The chosen grids were designed to give the lowest factor of safety which probably could be considered as the most critical locations for the critical failure surfaces for the analysis.

The area occupied by the 20 by 20 piezometric head grid nodes for the 1V:0.5H and 1V:1V slopes were illustrated earlier in Figure 4.4. It should be noted that the grid was so designed that the coordinates for the piezometric grids in Slope12.01 were

similar to the coordinates of the pressure heads derived from Hydrus2D. The output results of the pressure heads with depth from Hydrus2D were converted into piezometric head values and inputted into the piezometric grids in Slope12.01. For 1V:0.5H slopes, the first coordinate for the piezometric grid was at x = 38.97 m and y = 39 m, and the increments were at 1.0 m and -1.0 m in x and y direction respectively to the second column; then the increments changed by approximately 0.6 m and -1.0 m in x and y direction respectively for the next 17 columns; and the increment between the last two columns were 1.0 m and -1.0 m in the x and y directions respectively. For 1V:1H slopes, the first coordinates for the piezometric grid were at x = 39.10 m and y = 40 m, and the increments were at 1.1 m and -1.0 m in the x and y directions respectively.

However, as shown in Figure 4.4, approximately half of the piezometric grids were outside the slope domain. It should be noted that Slope12.01 determines the value of the porewater pressures along the potential slip surfaces by interpolation between the closest piezometric head values. Thus, almost half of the grids which were far outside the slope domain and out of the range during the calculation of pore water pressure in the slip surface were ignored.

4.6.2 Setting up common points and centres of circles

Slope12.01 allows circular and non-circular slip surfaces to be generated for the stability analysis. Before finalising the type of slip surface that was going to be used throughout the analysis, a few analyses were first carried out to find the appropriate slip surface for slope problem. From the preliminary study it was decided to use a circular slip surface as it gave the lowest factors of safety relative other types of slip surfaces.

To compute the factor of safety for a circular slip surface, the centre and the radius of the circle need to be determined. Slope12.01 allows the user to build in a grid of potential centres for the centres of the potential slip surfaces and a set of common points in the slope area. The common point is the point through which the circle passes in order to define the potential slip surface within the slope itself and it is required to specify the radius of the circle (Borin, 2003). A set of common points is

defined by the x-y coordinates of the first point, their spacing in the x and y directions and the total number of points. By establishing the grid centres of a circle and a set of common points, Slope12.01 automatically generates the ideal centre of the circle with a circle's circumstance which passes through any set of common points, hence forming a circular slip surface of the slope which gives the lowest factor of safety.

It should be noted that Slope12.01 has the ability to extend the grids of the centre of the circle automatically in the event the lowest factor of safety is not found within it. However, for the case of common points, this is not the case so a few sets needed to be tested in order to find the most sensitive points through which the slip surface might pass that gave the lowest value for the safety factor. For both the 1V:0.5H and the 1V:1H slopes, common points were positioned very close to the ground surface. This was done to avoid any miscalculation on a very shallow slip surface that might possibly exist near the slope surface. These slips would have been generated due to the program allowing the very low effective stresses close to the surface dominating the magnitude of the shear resistance. The program did not allow for any non-linearity in the low effective stress region in the constitutive equation for shear resistance. Shallow common points also allowed Slope12.01 to calculate the factor of safety for both shallow and deep slip surfaces until it found the magnitude of the lowest factor of safety. It should also be highlighted that, for each common point, Slope12.01 only shows the lowest factor of safety for the most critical slip surface, the position of this circular slip surface and the coordinate of the centre of the circle. The grids for the centre of the circle and the set of common points for 1V:0.5 and 1V:1H slopes are shown in Figure 4.5.

For the 1V:0.5H slopes, the coordinate for the first corner of the centre of the circle was x = 35.0 m and y = 30.0 m and the grid increments were 2.0 m for both x and y directions. There were 25 by 25 node grids in the x and y directions to describe the centres of the potential failure circles. Slope12.01 does extend these grids whenever it is required. The coordinate for the first common point was x = 40.0 m and x = 39.0 m and located just below the crest. There were 20 common points all together and the increments between each common point were 0.5 m and -1.0 m in x and y directions respectively.

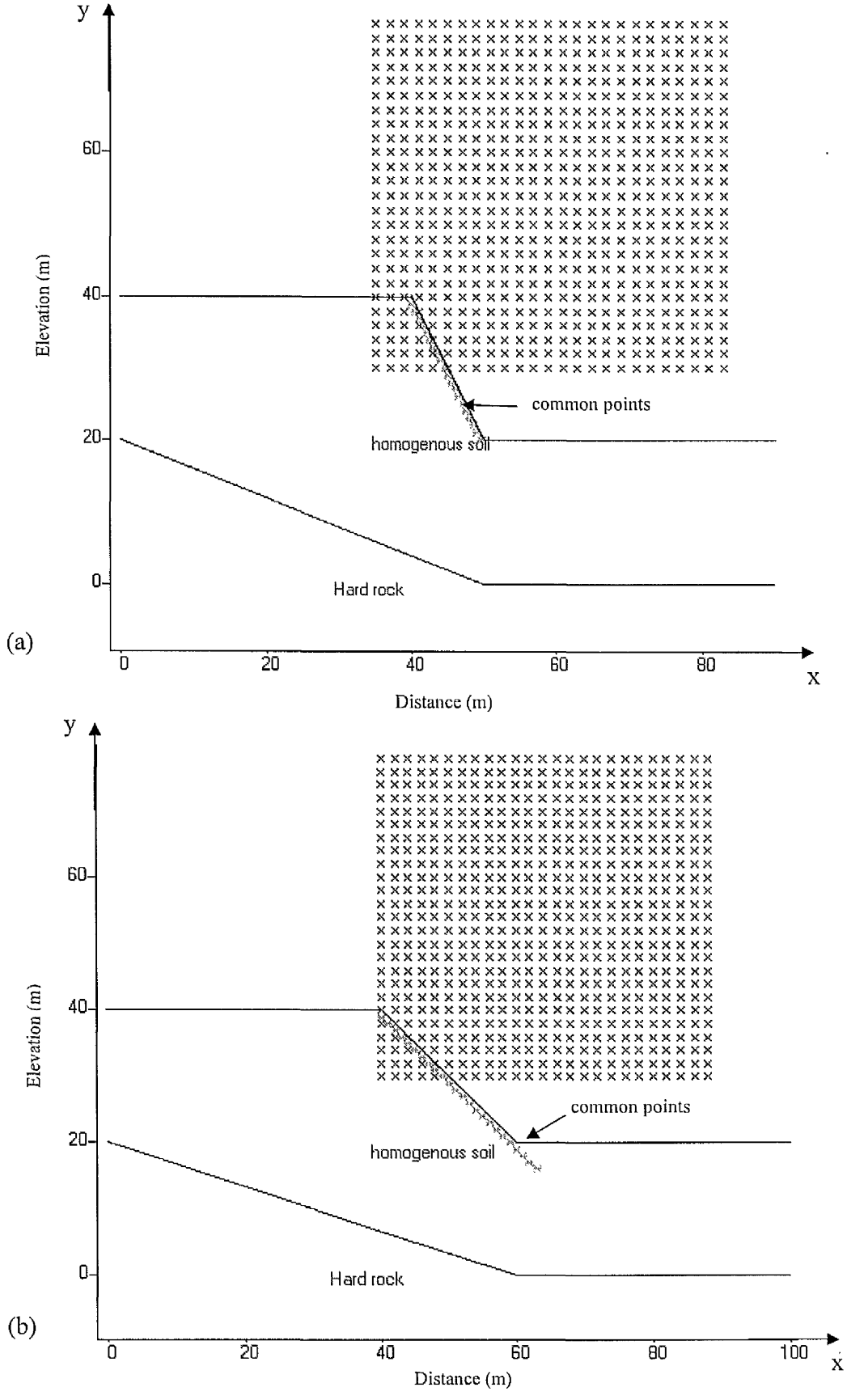

Figure 4.5 The grids of the centre of the circle and common points for (a) 1V:0.5H slope and (b) 1V:1H slope

For the 1V:1H slopes, the coordinate for the first corner of the centre of the circle was x = 40.0m and y = 30.0m and the grid increments were also 2.0 m for both x and y directions. There were also 25 by 25 node grids in the x and y directions for the centres of the circles. The coordinate for the first common point was x = 40.0 m and x = 39.0 m and located just below the crest. There were 24 common points all together and the increments between each common point was 1.0 m and -1.0 m in the x and y directions respectively.

4.6.3 Input parameters for the analysis

Other input parameters that were required for the limit equilibrium analysis were the parameters to describe the shear strength of the soil. All the soil parameters were held constant so that the factor of safety of the slope was only influenced by the porewater pressure changes in the slope due to the rainfall.

For the upper layer of the soil, i.e. for all three types of soil, the bulk unit weight above and below ground water level was taken as 20 kN/m^3. The drained cohesion, c', and the angle of shear resistance, ϕ', of the soil were adopted as 5.0 kN/m^2 and 38^o respectively. The drained cohesion, c', was implemented from Dykes (1994) for soil that was found in Temburong district. It is understood that the ϕ' value is considered to be unrealistic for clayey soil, however it should be noted that the first stage of the study involved the change in factor of safety of the slope which influenced by the changes of pore water pressure due to rainfall whilst all other shear strength soil parameters were kept constant. In the later stage of the study however, the ϕ' value was converted to a mobilised shear angle, ϕ_m, that which is required to be mobilised to keep the slope in limiting equilibrium as described later in Chapter 7. For the lower impermeable layer where it was assumed that the hard rock remained stable throughout the analysis, the bulk unit weight adopted for the hard rock was 25 kN/m^3, the cohesion value, c' and the angle of shear resistance, ϕ', were 500.0 kN/m^2 and 50^o respectively.

4.7 Obtaining factors of safety (FoS) from the output

The output results of the pressure head values from Hydrus2D were first converted to piezometric head values before they were inputted in Slope12.01. Slope12.01 analysed these data, and the lowest value of the factor of safety for each common point was generated. From these generated values, only the lowest value of the factor of safety from all common points was recorded. This process was repeated for many time steps. The time steps were different depending on the applied rainfall pattern.

At the early stage of the analysis, Slope12.01 only calculated the factor of safety of the slope due the changes in piezometric grids whilst the rest of the parameters remained constant. However, in subsequent analysis, for each piezometric grid data point, the angle of shear resistance, ϕ', was modified until a mobilised phi, ϕ_m, was found. The mobilised phi value, ϕ_m, is defined as the phi value of the soil when the slope is in limiting equilibrium, i.e. the factor of safety, FoS = 1. This procedure was repeated for all time steps during the 34-days rainfall period.

In summary, there are two factors that were obtained from Slope12.01, i.e.

- The changes in the factor of safety (FoS) with time for each rainfall pattern.
- The mobilised phi, ϕ_m for each time during a particular rainfall pattern.

4.8 Limitations of the limit equilibrium analysis

The limit equilibrium analysis requires an advance assumption regarding the shape and location of the slip failure surface. There is a probability, however slight, that the most critical slip surface was not detected. However by keeping the coordinates of the common points very close to the soil surface this probably reduced the degree of risk. The other downside of the limit equilibrium analysis is that the deformation of the slope and its progression to failure due to rainfall cannot be modelled, and the

factor of safety against failure of the slope needs to be calculated manually at each required time.

Slope12.01 only allows 20 by 20 node piezometric head grids in both the x and y directions, thus an optimised size of piezometric grids were required to be found. Slope12.01 calculates the value of pore water pressure in a slip surface by using interpolation between four nearest piezometric head values. If any point on the slip surface is outside the grid, the piezometric value is obtained between two closest grids. The more evenly distributed piezometric grids around the domain probably gave more accurate calculations of the pore water pressure in the slip surface, hence the factor of safety. On the other hand, locating the allowable 20 by 20 node piezometric grids close to the slope area should have been acceptable, given that the main focus of the study was to observe the effect of rainfall on the pore water pressure changes near the surface of the slope.

A further disadvantage or limitation of the Slope12.01 software rather than the limit equilibrium analysis itself is that the 400 piezometric head values need to be input in the piezometric table individually, i.e. the values could not be imported directly from the EXCEL spread sheet after converting the pressure head values to the piezometric head values. Thus, this proved to be a rather time consuming exercise as different piezometric head values were required for each different time step for one particular rainfall pattern.

There was one parameter of shear strength that is considered for unsaturated soil as suggested by Fredlund and Rahardjo (1993) which is not included in Slope12.01. This parameter is based upon the extended Mohr-Coulomb failure criterion for unsaturated soil, ϕ^b. As a result, there is a probability that the calculation of the factor of safety of the slope is underestimated during the condition of unsaturated flow.

Despite the limitation of the limit equilibrium analysis, Slope12.01 is still able to give an idea of the sensitivity of the effect of different rainfall patterns on slopes for the parametric study.

5 Effect of rainfall on groundwater behaviour

5.1 Introduction

This chapter discusses the changes in pore water pressure distribution within the slope when different rainfall patterns and total amounts of rainfall were applied. Rainfall was applied to a slope of standard height (H=20 metres) for a constant 34 days in each case (See Chapter 4). The cases considered are summarised in the table below.

Table 5.1 The summary of the cases considered in this research study

Characteristic	Cases		
Slope Angle	1V:1H	1V:0.5H	
Slope Material	Sandy soil	Silty soil	Clayey soil
Total cumulative rainfall	310mm	496mm	
Rainfall Pattern	1	2	3

Thirty six separate cases were considered. The cases are grouped in terms of the generic slope soil type and geometry in the first instance and then within these sub-divisions the discussion considers the effects of the total cumulative rainfall and the manner in which it is distributed in time.

Each sub section discusses the effects of the changes in pore water pressure at different time depending on the applied rainfall pattern. Given the difference in characteristics of the rainfall intensities at various times during the 34 day rainfall period for rainfall patterns 1, 2 and 3, the pore water pressure distribution was observed as follows;-

Rainfall Pattern 1

Observed at the end of days;- 1, 3, 6, 20, 34.

Rainfall Pattern 2

Observed at the end of days;- 22, 26, 31 and 34.

Rainfall Pattern 3

Observed at the end of days;- 8, 17, 26 and 34.

The chosen observation time points were based upon the inspection of rainfall intensity applied. By looking at Table 4.2, the daily rainfall intensity was changing for the first six day period of Pattern 1 rainfall. It is probably important to observe the daily changes in pore water pressure due to the changes in daily rainfall intensity. However, taking daily pore water pressure data from Hydrus2D would be time consuming, thus for the first six days of Pattern 1 rainfall, the pore water pressure was only observed at the end of t = 1 day, t = 3 days and t = 6 days. The pore water pressure was also examined after a period of low intensity rainfall at the end of t = 20 days. It should be noted that, this was also the time when the rain ended. Finally, the pore water pressure at the end of t = 34 days, i.e. the last day of Pattern 1 rainfall was also noted after a period of 14 days of no rainfall.

In order to observe the effect of the lower daily rainfall intensity on slopes, two observation time points were taken at the end of t = 22 days and t = 26 days of Pattern 2 rainfall. It should be noted that, there was no rainfall for the first 14 days period of Pattern 2 rainfall. The third observation time point was taken at the end of t = 31 days, simply because it was the time before the higher daily rainfall intensity was applied, and finally at the end of t = 34 days when Pattern 2 rainfall ended after receiving the highest daily rainfall intensity during the 34 days duration.

For Pattern 3 rainfall, the observation time points were taken at the end of t = 8 days, 17 days, 26 days and 34 days. This is because the daily rainfall intensity was constant throughout the 34 days duration of Pattern 3 rainfall, thus it is appropriate to consider these four observation time points at approximately equal time intervals.

It should be noted that Hydrus2D software presents the distribution of pore water pressure in the slope geometry in terms of pressure head values. In this chapter, therefore, the illustrations of the changes of pore water pressure with depth due to rainfall are shown in terms of pressure head values, in metres, with depth.

The initial distribution of pore water pressure in the slope domain, in terms of pressure head values at t = 0 is illustrated in Figure 5.1 for both 1V:0.5H and 1V:1H slopes. It should be noted that Figure 5.1 was the steady state condition of ground water flow that was illustrated earlier in Chapter 4.

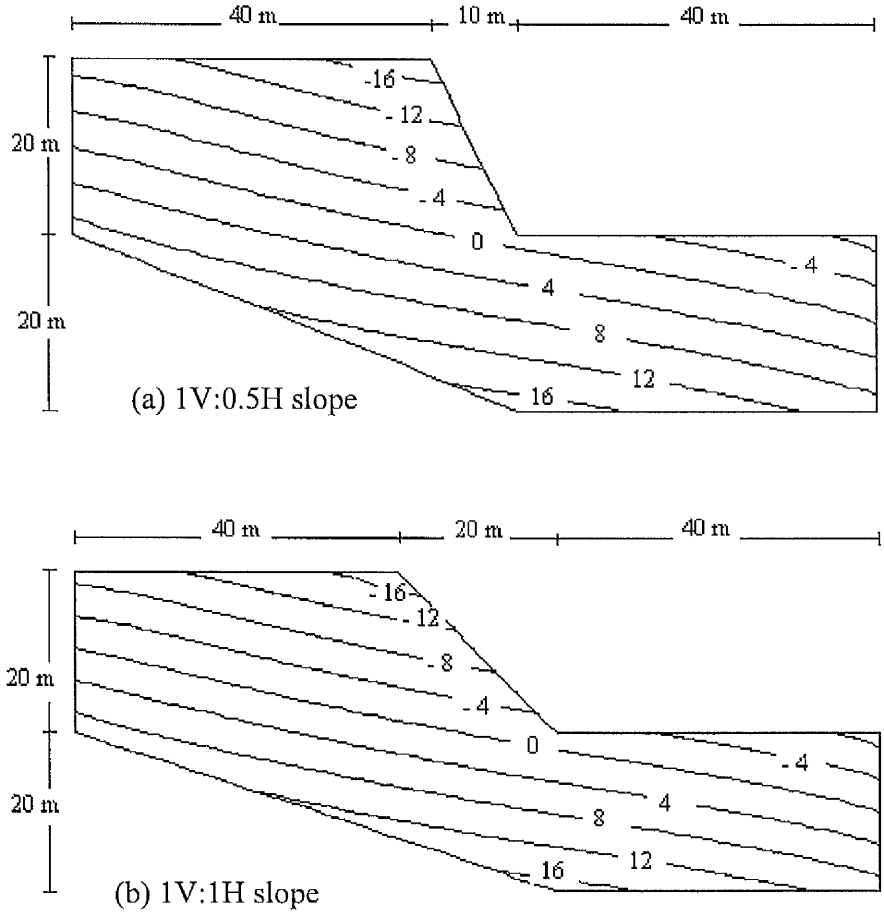

Figure 5.1 The initial distribution of pressure head values at t = 0 for (a) 1V:0.5H slopes and (b) 1V:1H slopes

5.2 The influence of the infiltration of rainfall into a sandy soil slope with time

This section discusses the changes in pore water pressure in the sandy type soil for both 1V:0.5H and 1V:1H slopes, having a height of 20 metres. The effect of the three different rainfall patterns with the same cumulative rainfall of 310 mm on a 1V:0.5H slope is examined; subsequently the pore water pressure changes are considered when the cumulative rainfall amount increased to 496 mm. The variation

of the pore water pressures in the 1V:1H slope under the same conditions is subsequently examined in the same way.

5.2.1 The effect on pore water pressure distribution in a 1V:0.5H sandy type soil slope subjected to different rainfall patterns of duration 34 days with a total rainfall of 310 mm

The distribution of pore water pressure on a section below the crest of the slope in terms of pressure head values with time for different rainfall pattern with the same total rainfall amount of 310 mm is shown in Figure 5.2. The high magnitude negative pore water pressure immediately below the ground surface increased to approximately zero as water started infiltrating into the ground. The wetting front moved downwards as more rainfall infiltrated into the ground. In the case of Pattern 1 rainfall, the rain stopped at the end of t = 20 days, however the location of the wetting front continued to progress downwards even after a period of fourteen days of no rainfall.

In the case of Pattern 2 rainfall, no rain fell for the first 14 days of the rainfall standard period. The rainfall only started on Day 15 and increased slowly until it reached its highest intensity of 85.32 mm/day on Day 34. After a 34 day period and a total of 310 mm cumulative rainfall, the depth of the wetting front did not progress further than 4.5 m into the slope.

In the case of Pattern 3 rainfall which was a constant rate of rainfall intensity of 9.13 mm/day, the depth of the wetting front increased with the total cumulative amount of rain which fell. However, at the end of 34 days rainfall, the depth of the wetting front was no deeper than 8.5 m deep.

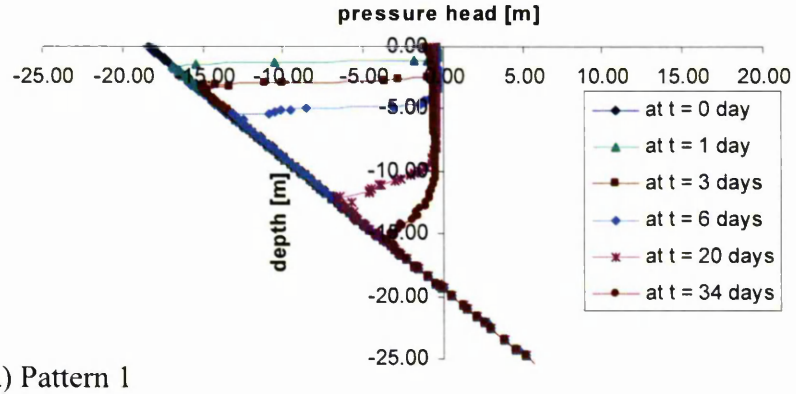

(a) Pattern 1

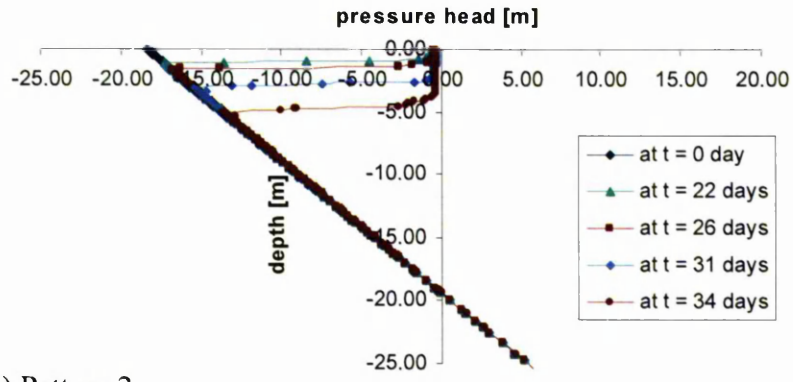

(b) Pattern 2

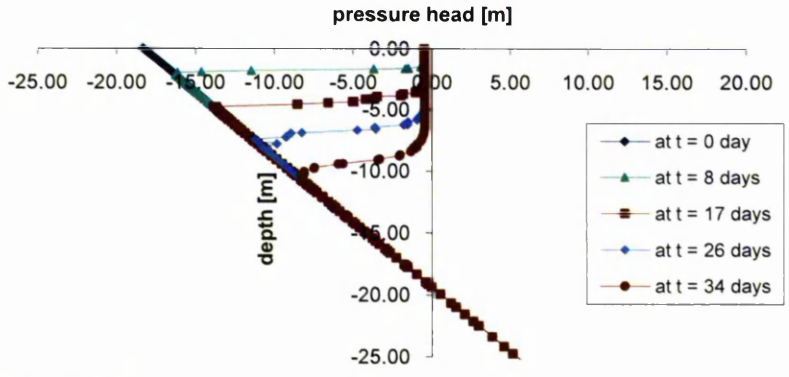

(c) Pattern 3

Figure 5.2 Distribution of pressure head on a section below the CREST of the 1V:0.5H SANDY soil slope at different times for (a) Pattern 1 (b) Pattern 2 and (c) Pattern 3 rainfall for a cumulative total of 310 mm in the 34 day period.

For the same total amount of rainfall, Figure 5.2 shows that the rainfall pattern plays an important role in the development of pore water pressure changes and the depth to which the wetting front will penetrate in a sandy type soil slope. After 34 days of rainfall, the depth of the wetting front was the deepest for Pattern 1 rainfall and the shallowest for Pattern 2 rainfall. It can be seen that for Pattern 1 rainfall the water continued to infiltrate into the ground even after rainfall stopped, thus suggesting that for Pattern 2 and Pattern 3 rainfall, the wetting front would probably continue to penetrate after the 34 days of rainfall.

Figure 5.3 illustrates the changes in pore water pressure at the toe of the slope during the period of rainfall. It shows that for Pattern 1 rainfall, infiltration due to the high intensity rainfall at the start of the rainfall period again increased the pore water pressure immediately below the ground surface with immediate effect to close to 0 kN/m^2. However, as the intensity of the rainfall reduced slowly to zero with time, the pore water pressure slowly became more negative and by the end of t = 34 days, the pore water pressure was approximately -10kN/m^2 just beneath the toe of the slope. The ground water level increased slightly and reached its maximum position at the end of t = 6 days from the initial position of 1.73 m to 1.63 m below ground level.

In the case of Pattern 2 rainfall, as the rainfall intensity increased gradually, the pore water pressure also increased slowly at the toe of the slope and at the end of t = 34 days, the elevation of the ground water level increased slightly to 1.55 m. The constant rate of Pattern 3 rainfall also resulted in the increase in pore water pressure at the toe of the slope, however as shown in Figure 5.3(c), this value of pore water pressure remained equal from the end of t = 8 days until the end of t = 34 days. Again there is clear evidence that the degree of rainfall intensity affects the behaviour of pore water pressure changes in sandy type soil slopes. At the end of t = 34 days, the ground water level increased to 1.65 m from its initial position of 1.73 m below ground level.

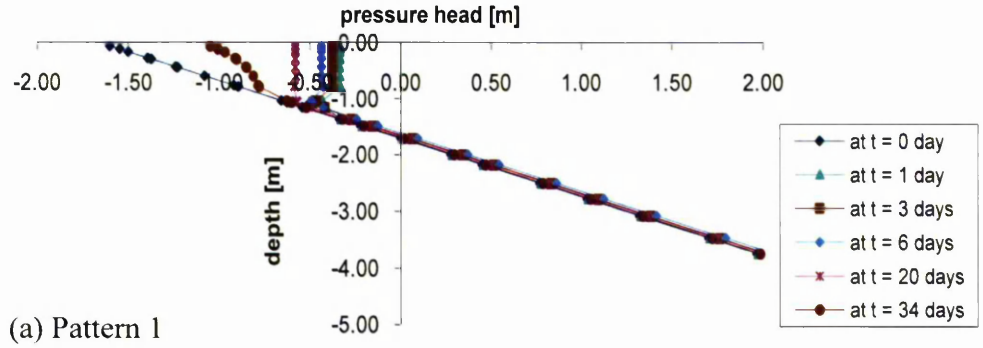

(a) Pattern 1

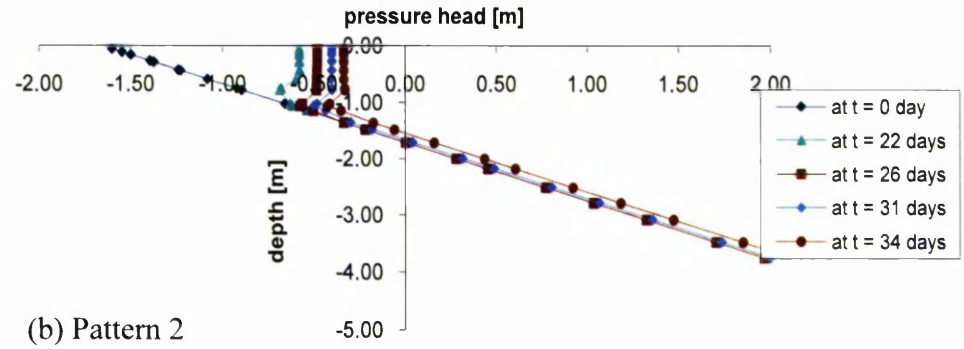

(b) Pattern 2

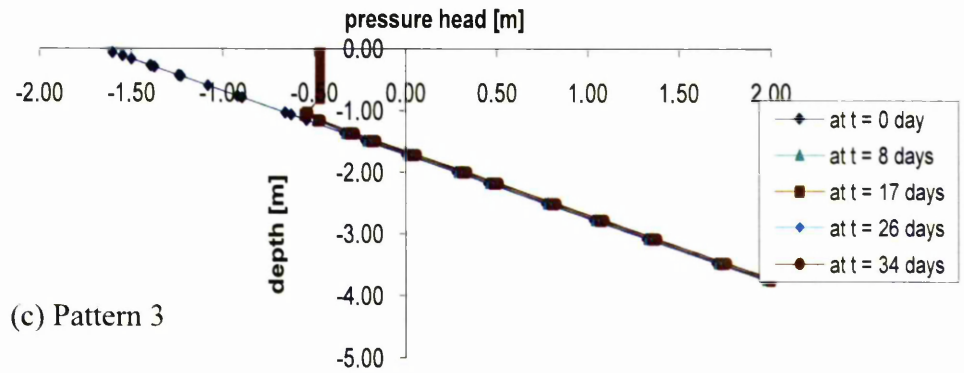

(c) Pattern 3

Figure 5.3 Distribution of pressure head on a section below the TOE of the 1V:0.5H SANDY soil slope at different times for (a) Pattern 1 (b) Pattern 2 and (c) Pattern 3 rainfall of a cumulative total of 310 mm in the 34 day period.

5.2.2 The effect of an increase of 60% in the base case cumulative rainfall during a 34 days period on the pore water pressure behaviour in a 1V:0.5H sandy type soil slope

When the rainfall intensity and the total rainfall amount was increased by 60%, the analysis showed that the depth of the wetting front at the same time after the start of the rainfall was also increased, however the pattern of the pore water pressure changes was similar with that of the lower intensity rainfall. For Pattern 1, Pattern 2 and Pattern 3 rainfalls, at the end of t = 34 days, the wetting front was deeper by a further 3.0 m (20%), 2.0 m (44%) and 5.5 m (65%) respectively. The magnitude of pore water pressure behind the wetting front, however, remained at approximately zero kN/m^2. The changes of the pore water pressure at the crest of the 1V:0.5H sandy slope, for different rainfall patterns at higher intensity rainfall is shown in Figure 5.4.

On the section below the toe of the slope, even though the pattern of the pore water pressure distribution was similar to that generated by the lower (base case) intensity rainfall, there was a slight increase in the ground water level (i.e. perceived level of atmospheric pressure) for all rainfall patterns as shown in Figure 5.5. In the case of infiltration into the slope of sandy soil, the high intensity rainfall tended to cause an immediate increase in the negative pore water pressure in the vadose zone and an increase in the ground water level at the toe of the slope. When the rainfall terminated the ground water level moved back towards its initial position and the pore water pressure above the ground water level became more negative. In comparison with behaviour during the lower (base case) rainfall, the ground water level after rainfall periods of Pattern 1, Pattern 2 and Pattern 3 moved further upwards to 1.52 m, 1.35 m and 1.60 m respectively from the initial position of 1.73 below ground level .

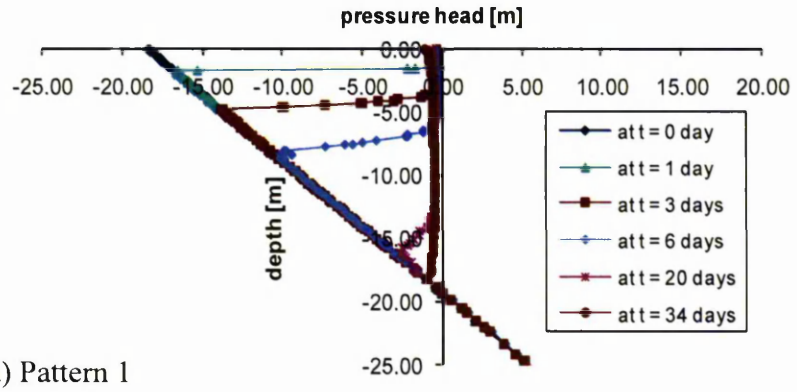

(a) Pattern 1

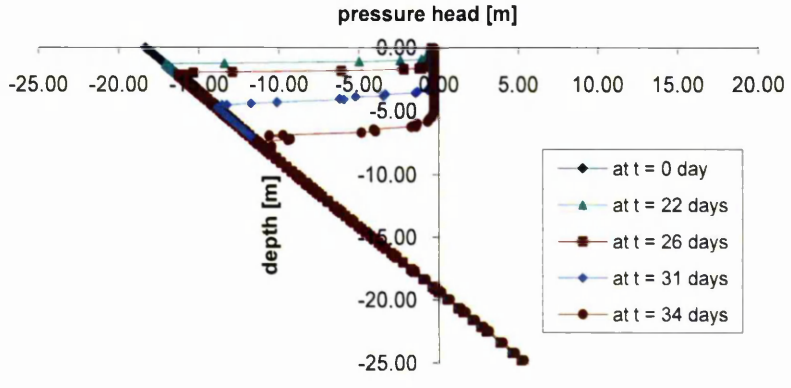

(b) Pattern 2

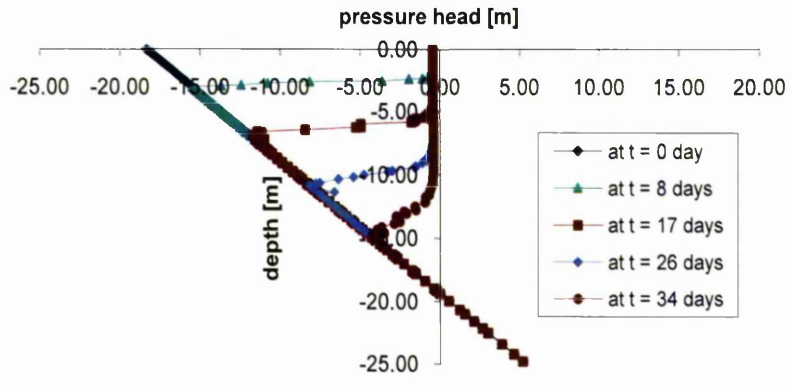

(c) Pattern 3

Figure 5.4 Distribution of pressure head on a section below the CREST of the 1V:0.5H SANDY soil slope at different times for (a) Pattern 1 (b) Pattern 2 and (c) Pattern 3 rainfall for a cumulative total of 496 mm in the 34 day period.

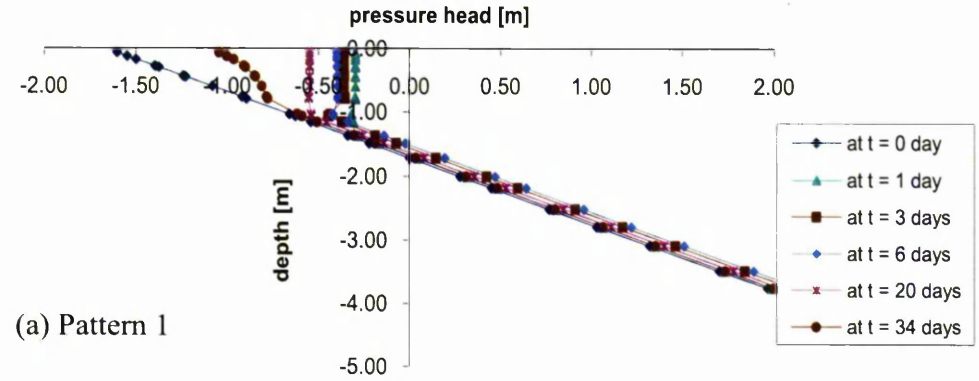

(a) Pattern 1

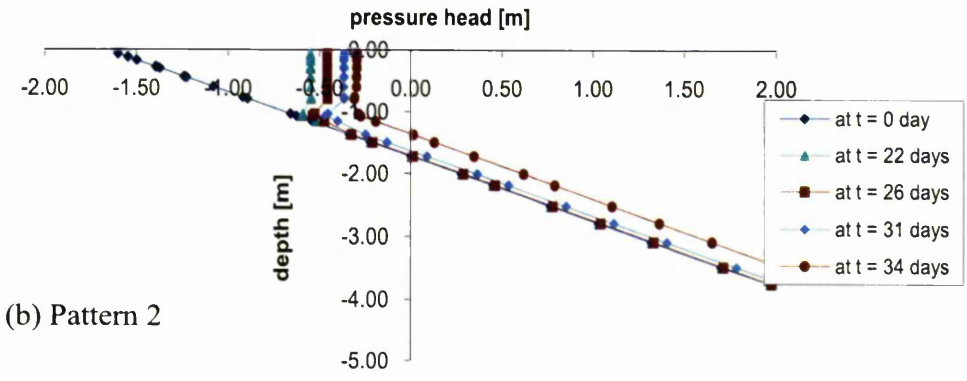

(b) Pattern 2

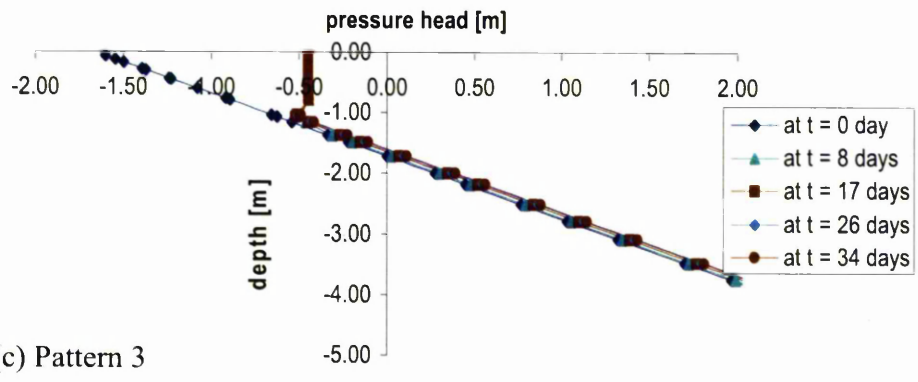

(c) Pattern 3

Figure 5.5 Distribution of pressure head on a section below the TOE of the 1V:0.5H SANDY soil slope at different times for (a) Pattern 1 (b) Pattern 2 and (c) Pattern 3 rainfall for a cumulative total of 496 mm in the 34 days period.

5.2.3 The effect on pore water pressure distribution in a 1V:1H sandy type soil slope subjected to different rainfall patterns of duration 34 days with a total rainfall of 310 mm

The changes in pore water pressure on the section below the crest of 1V:1H sandy slope for different rainfall patterns shows the same behaviour as that for the 1V:0.5H sandy slope. This is shown in Figure 5.6 for the base case rainfall intensity with total 34 day rainfall amount of 310 mm. The depths of the wetting front at the end of 34 days for all rainfall patterns were shallower for 1V:1H slopes than for 1V:0.5H slopes. The difference in depth of the wetting front on the section below the crest of both slopes (1V:1H and 1V:0.5H) for Pattern 1, Pattern 2 and Pattern 3 rainfalls were 4.0 m, 0.5 m and 1.5 m respectively. What is clear is that the difference in the wetting fronts was the least for Pattern 2 rainfall.

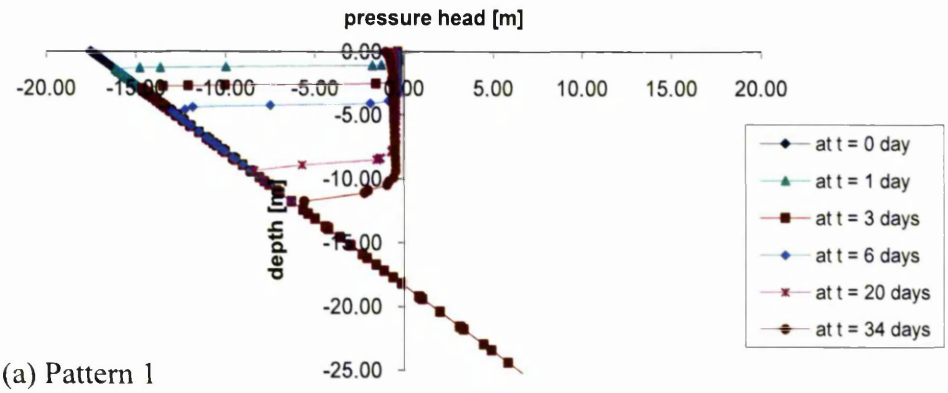

(a) Pattern 1

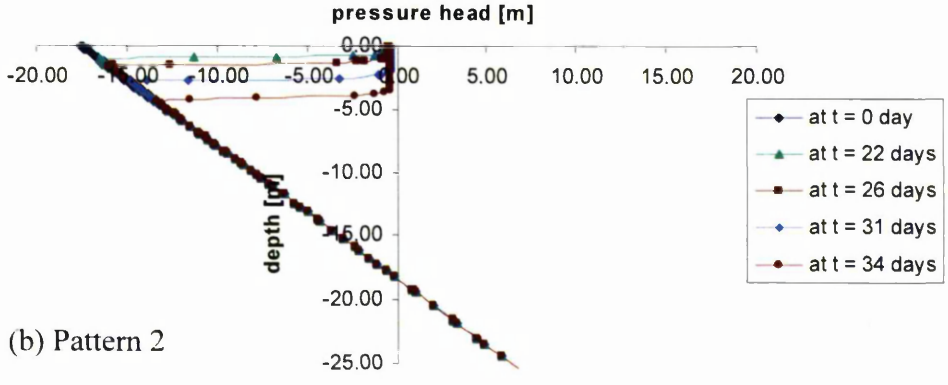

(b) Pattern 2

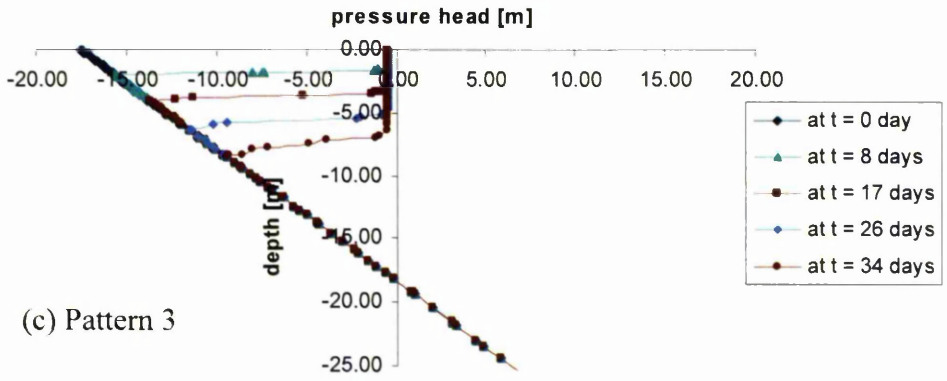

Figure 5.6 Distribution of pressure head on a section below the CREST of the 1H:1V SANDY soil slope at different times for (a) Pattern 1 (b) Pattern 2 and (c) Pattern 3 rainfall for a cumulative total of 310 mm in the 34 day period.

On the section below the toe of the slopes, however, it can be seen from Figure 5.7 that the wetting fronts due to different rainfall patterns were deeper for 1V:1H slopes than for 1V:0.5H slopes. Clear changes of pore water pressure near the surface of the ground may be seen beneath the toe of the slopes. Similar to 1V:0.5H slopes, the effect of the initial high intensity of Pattern 1 rainfall reduced the negative pore water pressure instantly below the toe of the slopes. As the rainfall intensity reduced to zero, the pore water pressure became more negative. When Pattern 2 rainfall was applied with increasing rainfall intensity with time, the negative pore water pressure reduced and the wetting front increased with time. As for the application of Pattern 3 rainfall, it appears that the rate of water infiltration remained constant as a consequence of the constant rainfall intensity. The depth of the ground water was initially at 2.15 m deep and only decreased in depth to 2.05 m, 2.01 m and 2.08 m respectively at the end of t = 6 days for Pattern 1 rainfall, and at the end of t = 34 days for both Pattern 2 and Pattern 3 rainfalls.

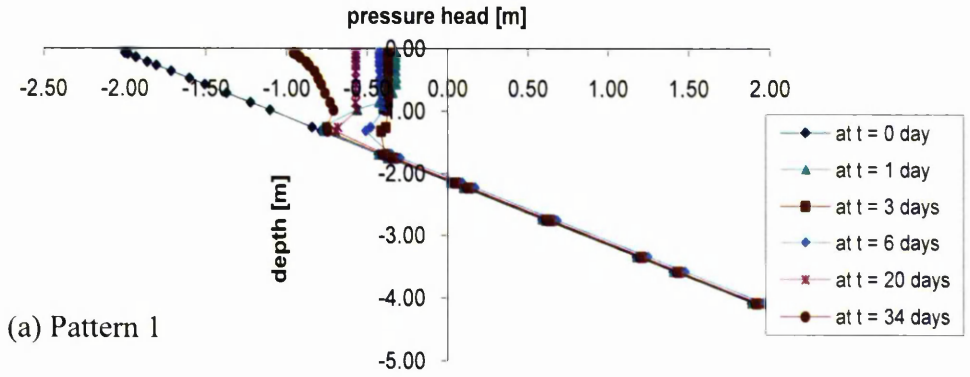

(a) Pattern 1

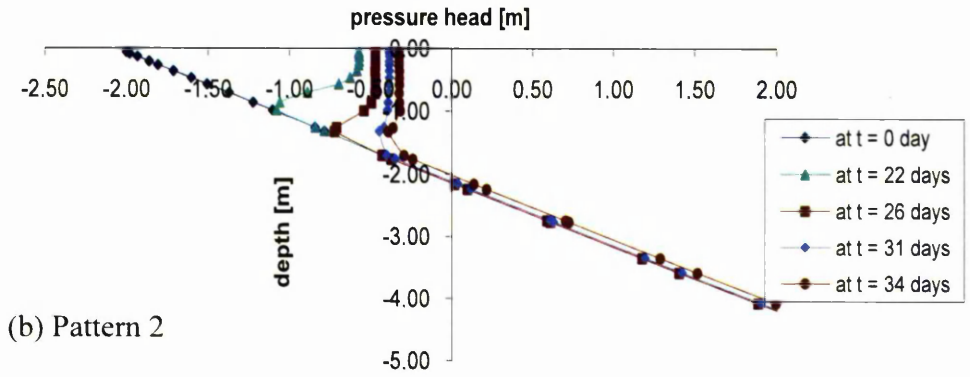

(b) Pattern 2

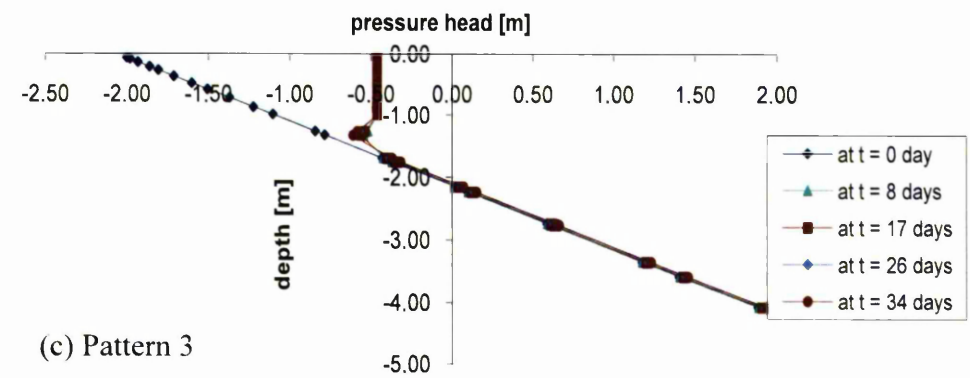

(c) Pattern 3

Figure 5.7 Distribution of pressure head on a section below the TOE of the 1H:1V SANDY soil slope at different times for (a) Pattern 1 (b) Pattern 2 and (c) Pattern 3 rainfall for a cumulative total of 310 mm in the 34 day period.

5.2.4 The effect of an increase of 60% in the base case cumulative rainfall during a 34 days period on the pore water pressure behaviour in a 1V:1H sandy type soil slope

The distribution of pore water pressure on a section below the crest of the slope due to a 60% increase in the base case rainfall intensity over the 34 day period is shown in Figure 5.8. As in the case of the application of the higher rainfall intensity to the 1V:0.5H sandy slopes, the application here of higher intensity rainfall increased the advancement of the wetting front in 1V:1H sand slopes relative to that in the base case rainfall condition. For Pattern 1, Pattern 2 and Pattern 3 rainfall, the wetting front location moved downwards by 4.0 m (36% increase), 1.0 m (25% increase) and 3.5 m (50% increase) respectively relative to the base case. It should be noted however, for all rainfall patterns, the wetting fronts at the end of t = 34 days beneath the crests in 1V:1H slopes were still shallower than the wetting fronts in 1V:0.5H slopes.

As shown in Figure 5.9, the behaviour of pore water pressure on a section below the toe of the slopes shows a similar pattern to the behaviour of pore water pressure for base case rainfall as shown in Figure 5.7. For all three of the rainfall patterns, as higher rainfall continued to infiltrate into the toe of the slopes, the depth of the ground water decreased from the initial position of 2.15 m to the maximum position of approximately 1.95 m depth at the end of t = 6 days of Pattern 1 rainfall, and to approximately 1.83 m and 2.03 m depth respectively at the end of t = 34 days for Pattern 2 and Pattern 3 rainfall. The position of ground water level achieved its maximum position at the earlier time for Pattern 1 rainfall probably because the slope received most of the high intensity rainfall at the earlier time, whereas for Pattern 2 rainfall the ground water level was mostly effected at the end of t = 34 days due to the high daily rainfall intensity towards the end of the rainfall duration. The ground water level was the least effected during the 34 days period of the constant daily rainfall intensity of Pattern 3.

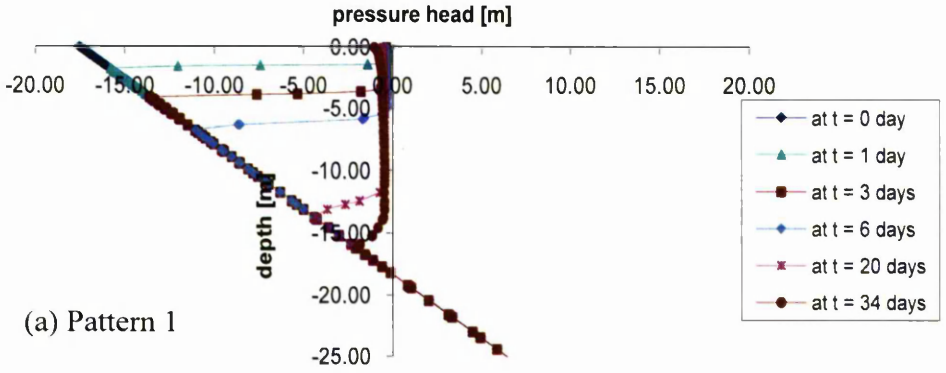

(a) Pattern 1

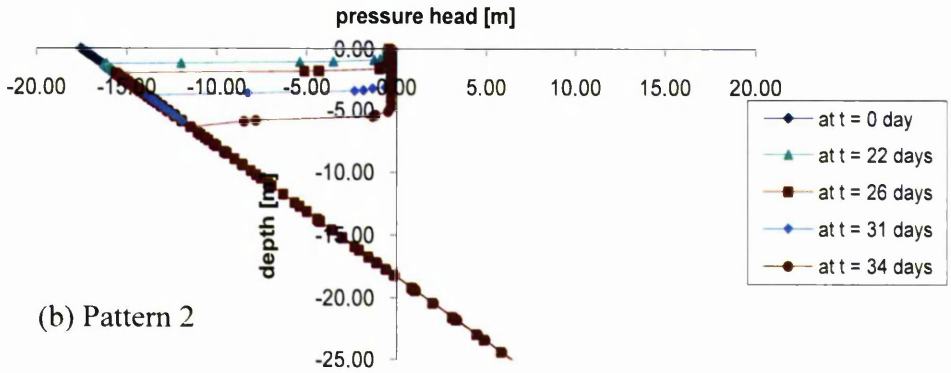

(b) Pattern 2

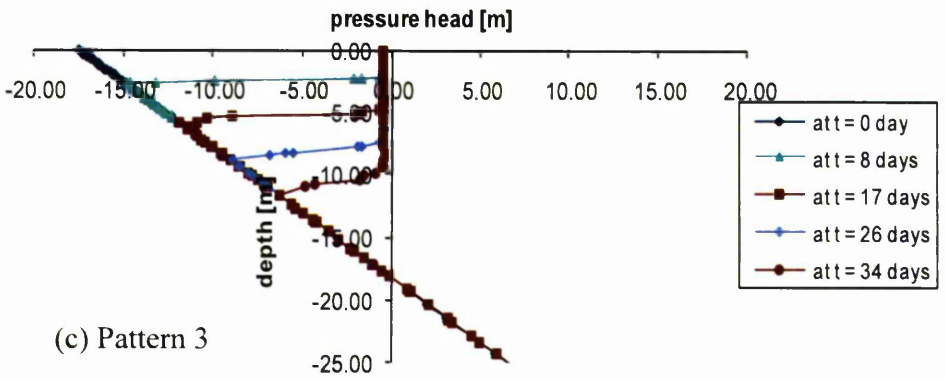

(c) Pattern 3

Figure 5.8 Distribution of pressure head on a section below the CREST of the 1H:1V SANDY soil slope at different times for (a) Pattern 1 (b) Pattern 2 and (c) Pattern 3 rainfall for a cumulative total of 496 mm in the 34 day period.

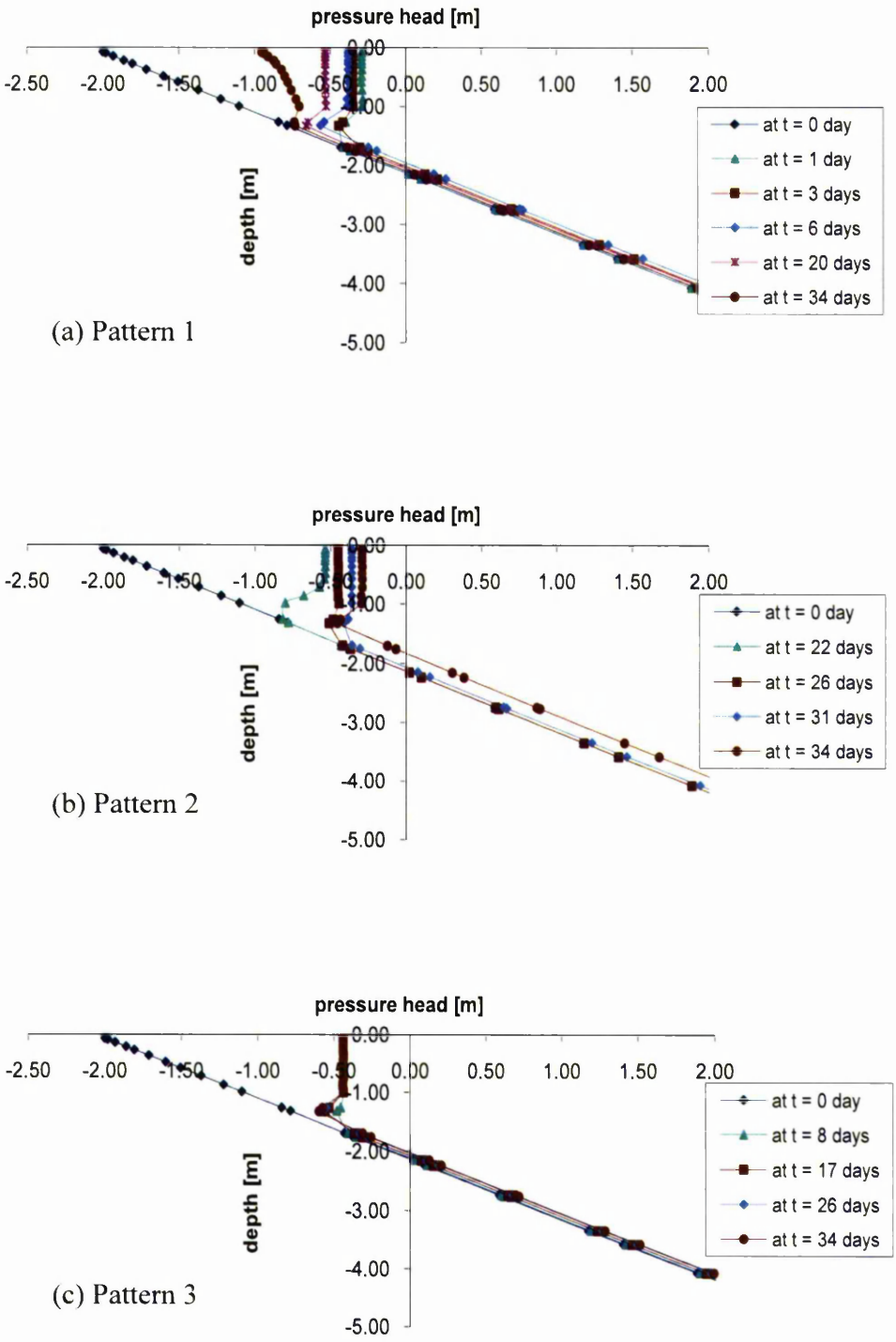

Figure 5.9 Distribution of pressure head on a section below the TOE of the 1H:1V SANDY soil slope at different times for (a) Pattern 1 (b) Pattern 2 and (c) Pattern 3 rainfall for a cumulative total of 496 mm in the 34 day period.

5.3 The influence of the infiltration of rainfall into a silty soil slope with time

A discussion of the changes in pore water pressure generated in a slope comprising a generic silty soil for both 1V:0.5H and 1V:1H slope angles is presented in this section. This section discusses the effect of different rainfall patterns developing the same total amount of rainfall of 310 mm in a 34 day period on pore water pressure changes in a 1V:0.5H slope, and the behaviour of pore water pressures due to an increase in the total amount of rainfall in 34 days from 310mm to 496 mm. The effect of different rainfall patterns and the total rainfall amount on 1V:1H silt slopes are also discussed.

5.3.1 The effect on pore water pressure distribution in a 1V:0.5H silty type soil slope subjected to different rainfall patterns of duration 34 days with a total rainfall of 310 mm

The distribution of pore water pressure due to the application of different rainfall patterns with the same cumulative total rainfall over the standard 34 days of 310 mm is shown in Figure 5.10. For the Pattern 1 rainfall (total cumulative rainfall of 310 mm) the distribution of pore water pressure on a section below the crest of the silty slope suggests that the negative pore water pressure near the surface reduced rapidly (i.e. became less negative) as high intensity rainfall infiltrated the ground. However, as the rainfall intensity reduced, the pore water pressure then became more negative. Notwithstanding this, the depth of the wetting front continued downwards even after the rain stopped. The depth of the wetting front at t = 34 days (i.e. the end of the rainfall period) was 4.5 m.

With the application of Pattern 2 rainfall, however, the negative pore water pressure reduced (became less negative) slowly even as the rainfall intensity increased. It shows that at the end of the 34 days rainfall, the wetting front on the section below the crest of slope was 1.5 m deep. As shown in Figure 5.10(c), application of Pattern 3 rainfall (constant rate of rainfall intensity) seems to give a constant depth of wetting fronts with time , and at the end of t = 34 days the wetting front was 3.0 m deep.

By comparing Figure 5.2 for a slope comprising sandy soil and Figure 5.10 for a slope comprising silty soil, it can be seen that, beneath the crest of the slope, water infiltrated more rapidly through the sandy soil slope than through the silty soil slope (this is to be expected) and the wetting front was also deeper in the case of the sandy soil than in the case of silty soil. Likewise, notwithstanding the pattern of rainfall applied to both slopes, the reduction in negativity in pore water pressure below the crest of the slope due to the application of rainfall was larger in all cases in the sandy soil than in the silty soil.

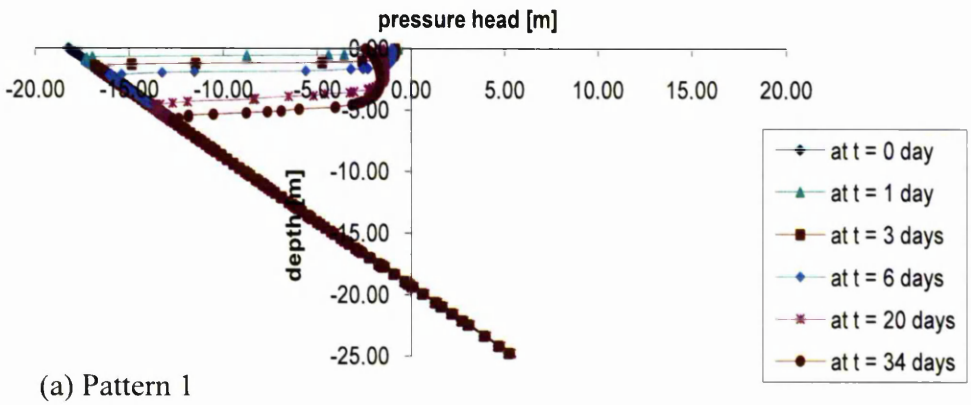

(a) Pattern 1

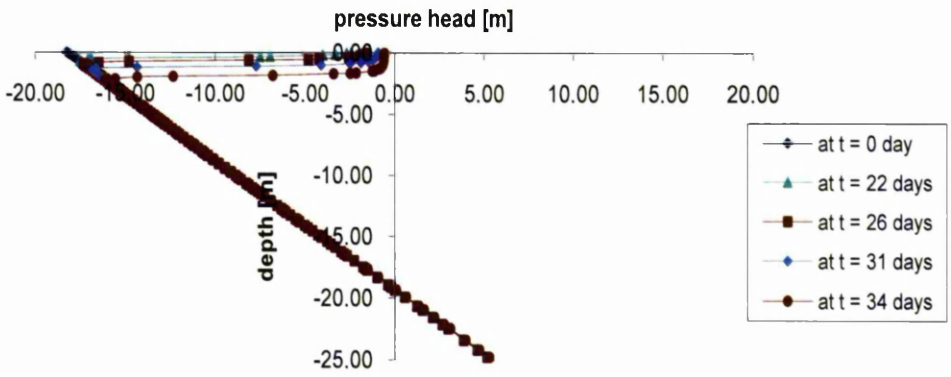

(b) Pattern 2

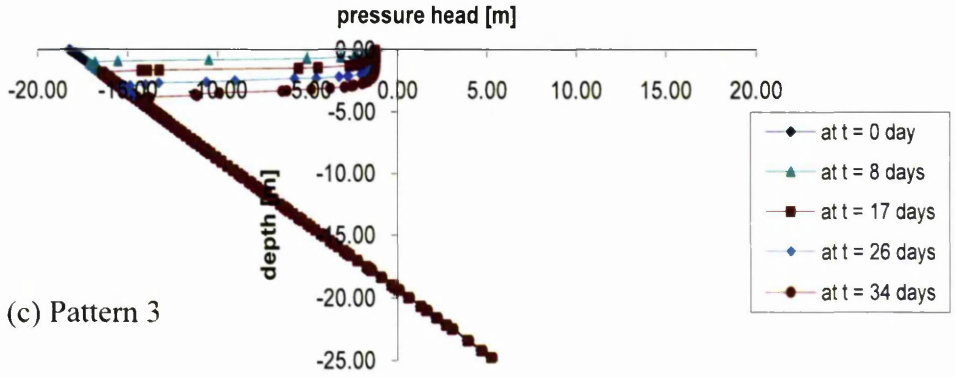

(c) Pattern 3

Figure 5.10 Distribution of pressure head on a section below the CREST of the 1V:0.5H SILTY soil slope at different times for (a) Pattern 1 (b) Pattern 2 and (c) Pattern 3 rainfall for a cumulative total of 310 mm in the 34 day period.

Figure 5.11 shows the distribution of pore water pressure due to different rainfall patterns on a section below the toe of a 1V:0.5H silt slope. Again, the changes in pore water pressure are shown clearly beneath the toe of the slope. Furthermore the rainfall intensity influenced the magnitude of increase and decrease in negative pore water pressure changes above the ground water level. In the case of Pattern 1 rainfall, the ground water level reached its highest position at the end of t = 6 days rising from the initial position of 1.73 m to 1.4 m below the ground level. In the case of Pattern 2 and Pattern 3 rainfall, it shows that the ground water level reached its highest position to 1.15 m and 1.42 m respectively at the end of 34 days of Pattern 2 and Pattern 3 rainfall

Comparison of Figure 5.3 for a slope in sandy soil and Figure 5.11 for a slope in silty soil both of equal geometry and subjected to the same total rainfall of 310 mm in 34 days, shows that the increase in ground water level on the section below the toe of the slope was greater in slopes of silty soil than in slope of sandy soil.

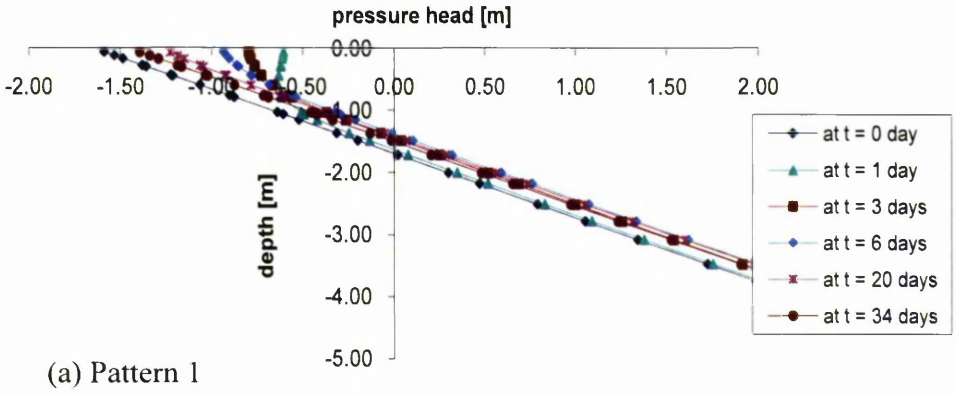

(a) Pattern 1

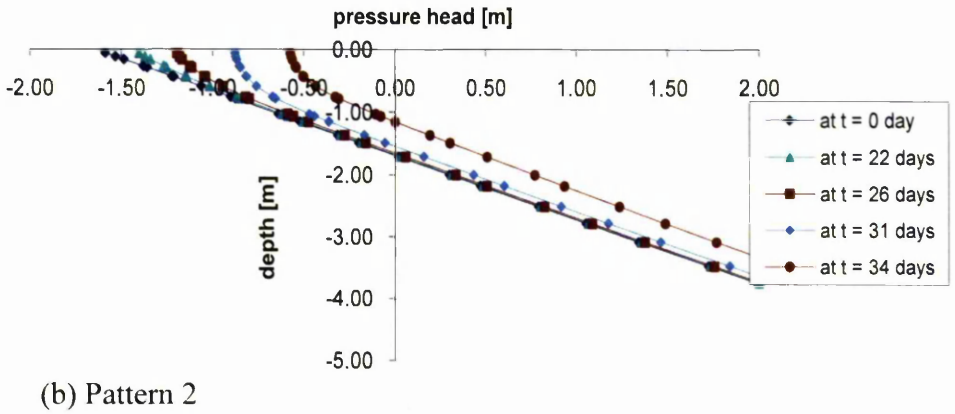

(b) Pattern 2

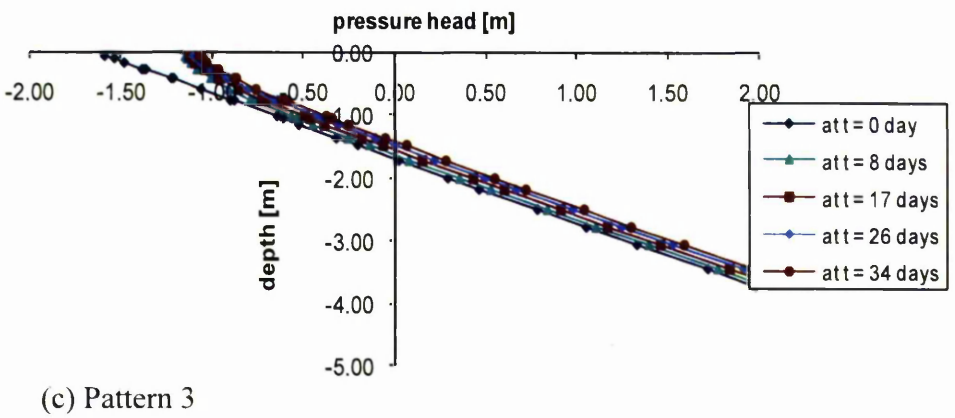

(c) Pattern 3

Figure 5.11 Distribution of pressure head on a section below the TOE of the 1V:0.5H SILTY soil slope at different times for (a) Pattern 1 (b) Pattern 2 and (c) Pattern 3 rainfall for a cumulative total of 310 mm in the 34 day period.

5.3.2 The effect of an increase of 60% in the base case cumulative rainfall during a 34 days period on the pore water pressure behaviour in a 1V:0.5H silty type soil slope

As shown in Figure 5.12, the increase of the daily, and hence the total, amount of rainfall by 60% over the same rainfall period demonstrates the same behaviour of pore water pressure variation at the crest of 1V:0.5H silty soil slope as in a slope which has been subjected to the lower rainfall intensity and total amount of 310mm in 34 days. As can be expected, however, the wetting fronts were deeper for higher rainfall amount than for lower rainfall amount for the same time periods. For Pattern 1, Pattern 2 and Pattern 3 rainfall, at the end of t = 34 days, the difference in the depth of the wetting front for the lower and higher rainfall intensities was 2.5 m (56%), 1.0 m (67%) and 1.8 m (60%) respectively. This should be noted against an increase of cumulative rainfall of 60% in each case.

Similarly, on a section below the toe of the slope, as shown in Figure 5.13, the pore water pressure changes were the same for both lower and higher levels of rainfall. However, the ground water level rise on the section below the toe of the slope was greater for the higher cumulative rainfall than for lower (base case) cumulative rainfall. For Pattern 1, Pattern 2 and Pattern 3 rainfall, the ground water level was decrease in depth further from 1.73 m to 1.09 m, 0.3 m and 1.18 m respectively. The ground water level rose the most by the end of the period of Pattern 2 type rainfall relative to the rise due to the other two rainfall patterns. In addition, this shows that the effect of the increase in the amount of rainfall by 60% also reduces the negative pore water pressure above the ground water level to a greater extent than during a rainfall period of base case rainfall intensities. This behaviour was not observed in the slopes comprising sandy soil.

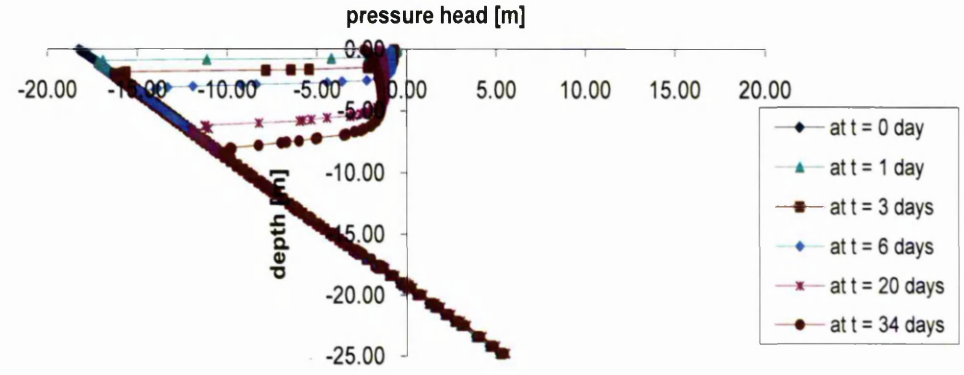

(a) Pattern 1

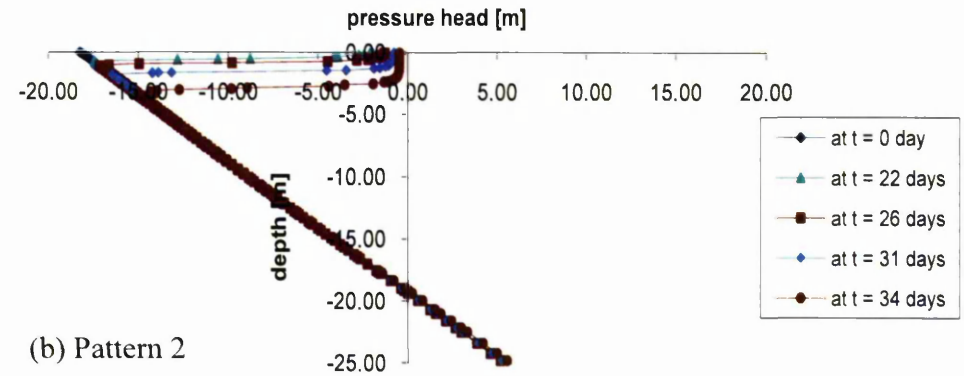

(b) Pattern 2

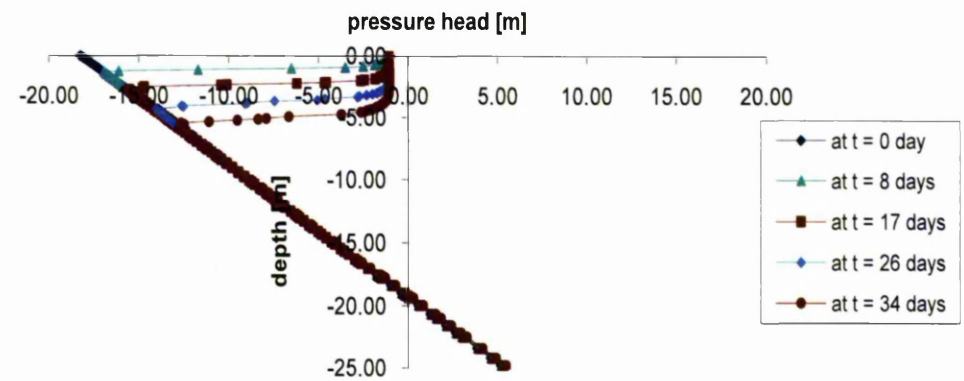

(c) Pattern 3

Figure 5.12 Distribution of pressure head on a section below the CREST of the 1V:0.5H SILTY soil slope at different times for (a) Pattern 1 (b) Pattern 2 and (c) Pattern 3 rainfall for a cumulative total of 496 mm in the 34 day period.

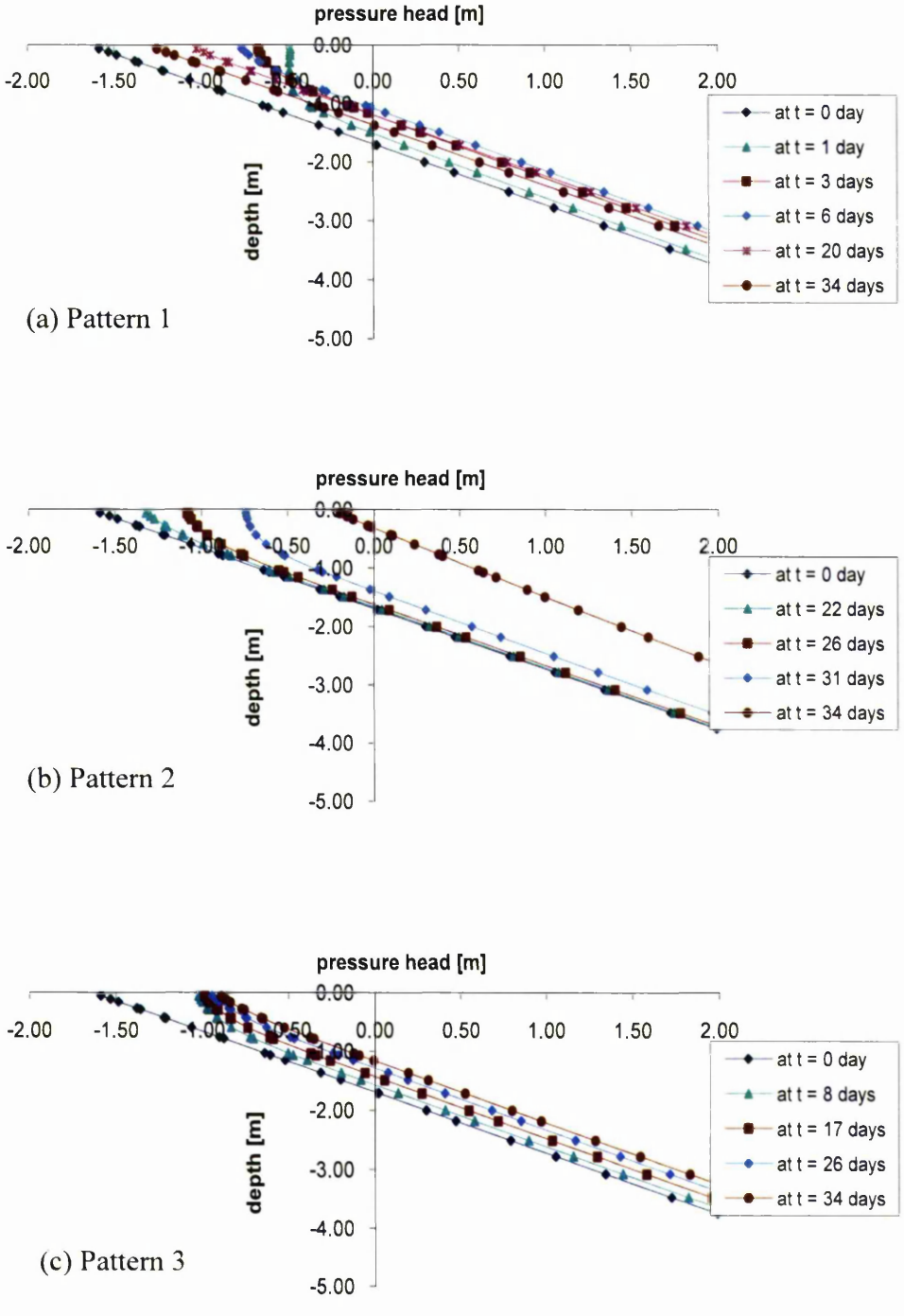

Figure 5.13 Distribution of pressure head on a section below the TOE of the 1V:0.5H SILTY soil slope at different times for (a) Pattern 1 (b) Pattern 2 and (c) Pattern 3 rainfall for a cumulative total of 496 mm in the 34 day period.

5.3.3 The effect on pore water pressure distribution in a 1V:1H silty type soil slope subjected to different rainfall patterns of duration 34 days with a total rainfall of 310 mm

Figure 5.14 shows the variation in pore water pressure due to the application of different rainfall patterns in 1V:1H silt slopes. The pore water pressure changes at the crest of the 1V:1H silt slopes were similar to those in the 1V:0.5H silt slopes. However, the depths of the wetting front on a section below the crest of the slope due to Pattern 1 and Pattern 3 rainfall into 1V:1H slopes were shallower than those due to equivalent rainfall onto 1V:0.5H slopes. The differences in the depths of these wetting fronts were 1.0 m and 0.5 m respectively for Pattern 1 and Pattern 3 rainfall. In the case of Pattern 2 rainfall, the wetting fronts on the same section below the crest of 1V:1H and 1V:0.5H slopes were similar.

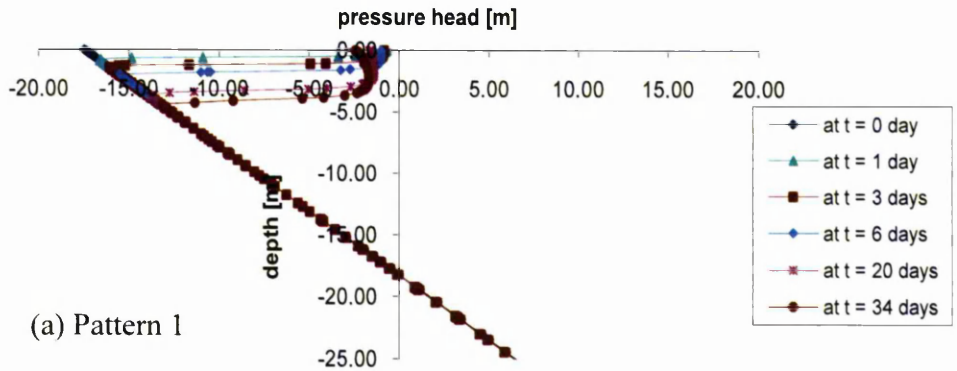

(a) Pattern 1

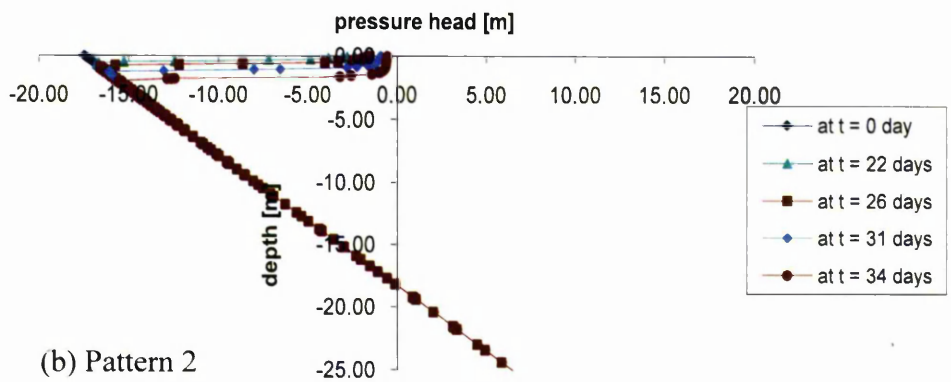

(b) Pattern 2

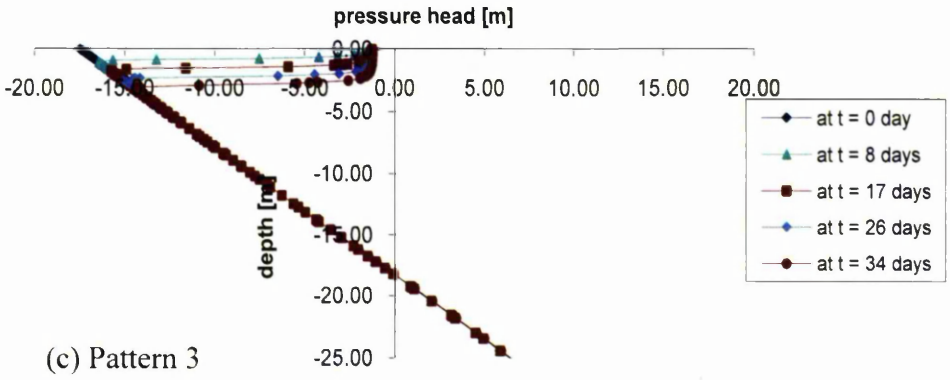

(c) Pattern 3

Figure 5.14 Distribution of pressure head on a section below the CREST of the 1H:1V SILTY soil slope at different times for (a) Pattern 1 (b) Pattern 2 and (c) Pattern 3 rainfall for a cumulative total of 310 mm in the 34 day period.

Comparison of Figure 5.11 (for 1V:0.5H silt slopes) and Figure 5.15 (for 1V:1H silt slopes) seems to show that the depth of the wetting fronts were deeper on the same section below the toe of 1V:1H silt slopes than for 1V:0.5H silt slopes, especially as observed in the case of Pattern 2 rainfall, however it was noted that for all rainfall patterns, the increased in ground water level beneath the toe of the slope was smaller in the case of 1V:1H silt slopes than in 1V:0.5H silt slopes. This was probably due to the fact that the initial ground water level on the section below the toe of the 1V:1H slopes was computed to be deeper below ground level than in the case of the 1V:0.5H slopes. For 1V:1H silty soil slope, the highest ground water level on the section below the toe of the slope was achieved at the end of t = 20 days for Pattern 1 rainfall and the increased level was only 0.28 m, moving upwards from its initial position of 2.15 m below ground level. For Pattern 2 and Pattern 3 rainfall, the ground water level increased to 1.80 m and 1.88 m respectively.

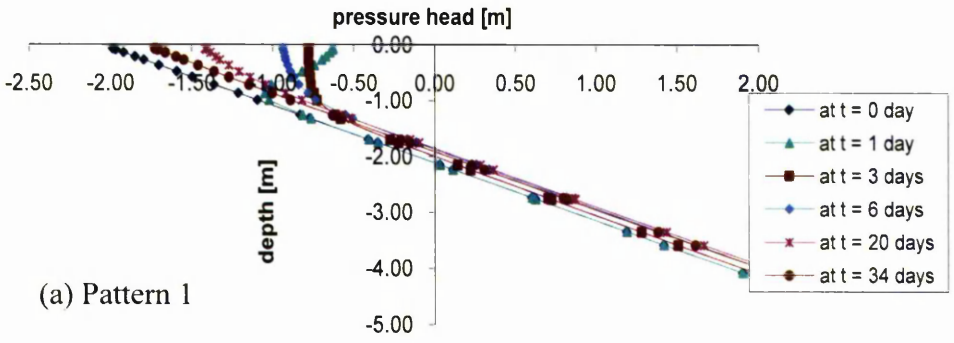

(a) Pattern 1

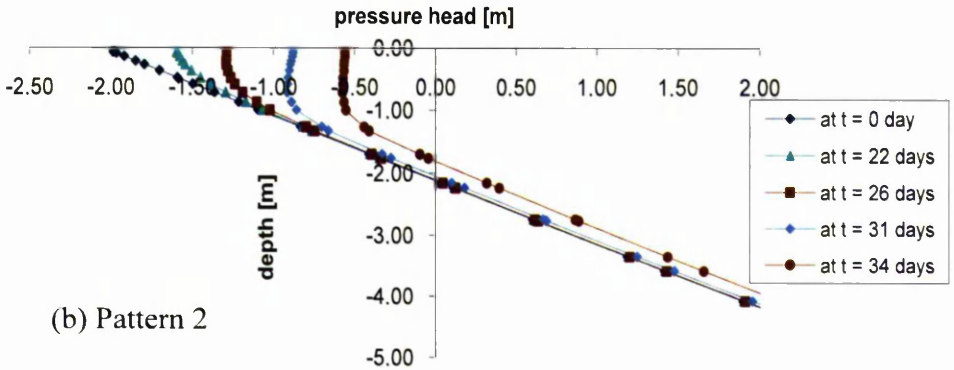

(b) Pattern 2

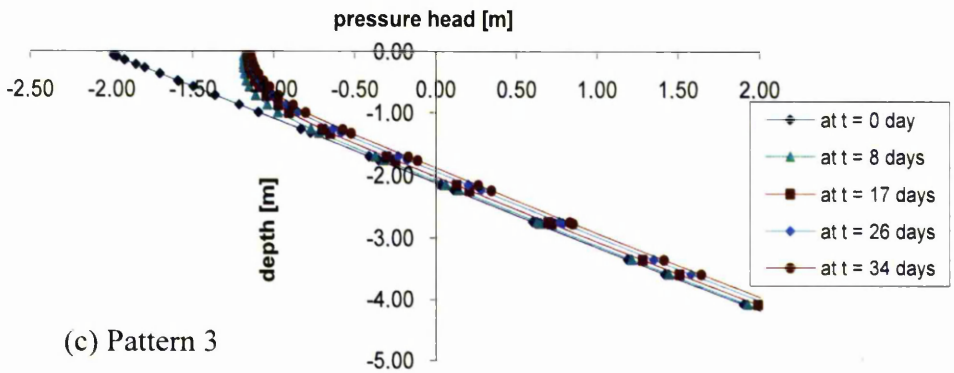

(c) Pattern 3

Figure 5.15 Distribution of pressure head on a section below the TOE of the 1H:1V SILTY soil slope at different times for (a) Pattern 1 (b) Pattern 2 and (c) Pattern 3 rainfall for a cumulative total of 310 mm in the 34 day period.

5.3.4 The effect of an increase of 60% in the base case cumulative rainfall during a 34 days period on the pore water pressure behaviour in a 1V:1H silty type soil slope

As shown in Figure 5.16, as in the case of the 1V:0.5H slopes, increasing the daily rainfall amount by 60% also had the effect of increasing the depth of the wetting front on the section below the crest of the 1V:1H slopes over equivalent time intervals. The wetting front was increased by 1.5 m (43%), 0.8 m (53%) and 1.0 m (40%) at the end of t = 34 days for Pattern 1, Pattern 2 and Pattern 3 rainfall respectively.

By comparing Figure 5.15 and Figure 5.17, the pattern of the distribution of pore water pressure on the same section below the toe of the slope remained essentially the same in the case of the higher rainfall as it was due to the lower rainfall. However, the ground water level increase was greater due to the increase in the daily rainfall by 60%. The ground water level decreased in depth further from 2.15 m to 1.63 m, 1.2 m and 1.65 m respectively for Pattern 1, Pattern 2 and Pattern 3 rainfall. The decrease of the negative pore water pressure above the ground water level (in the vadose zone) was magnified due to this increase in rainfall amount. It should also be noted that for Pattern 2 rainfall, the highest position of the ground water level was achieved at the end of t = 20 days.

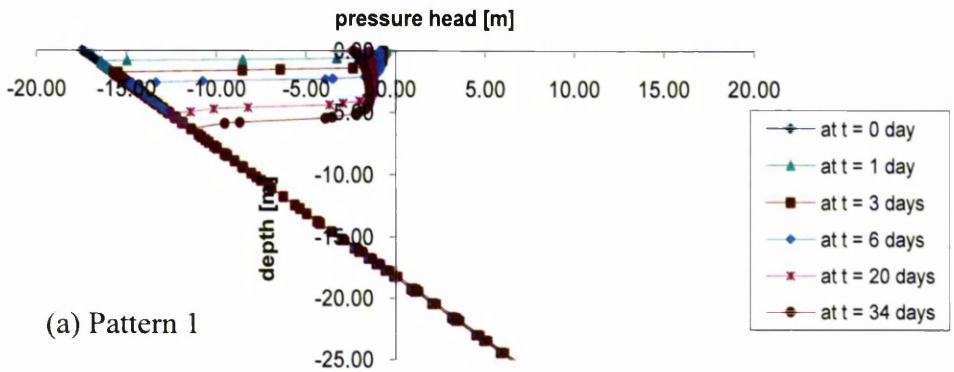

(a) Pattern 1

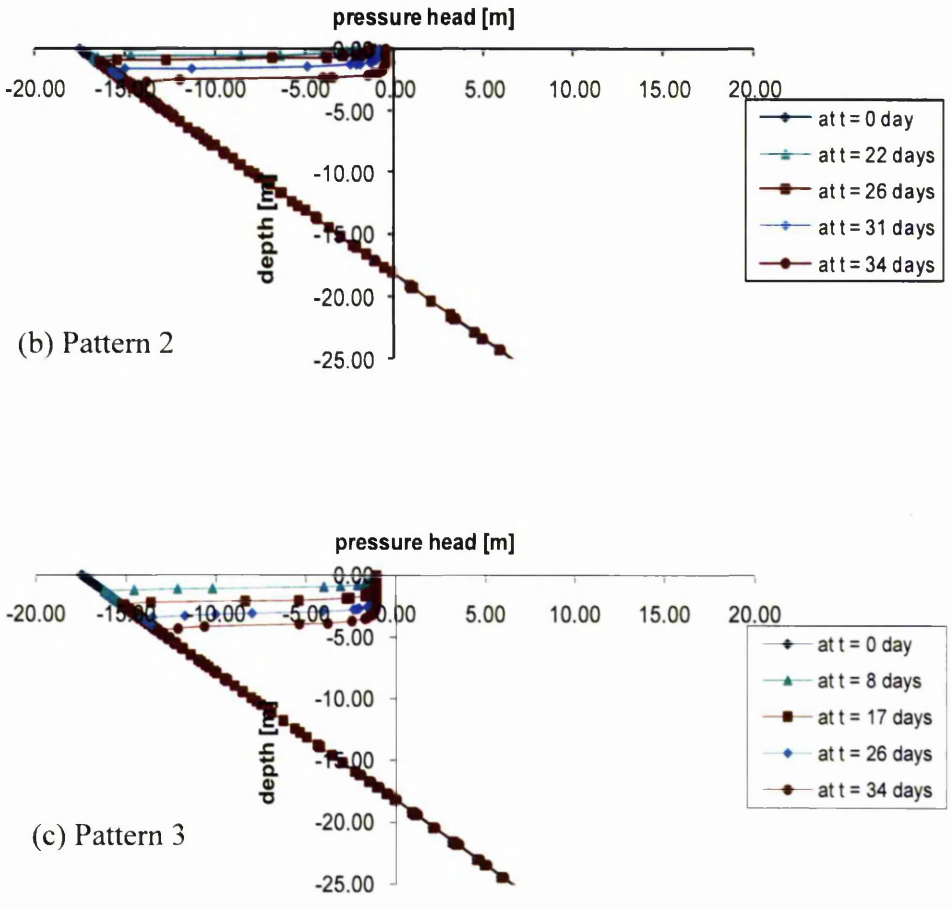

Figure 5.16 Distribution of pressure head on a section below the CREST of the 1H:1V SILTY soil slope at different times for (a) Pattern 1 (b) Pattern 2 and (c) Pattern 3 rainfall for a cumulative total of 496 mm in the 34 day period.

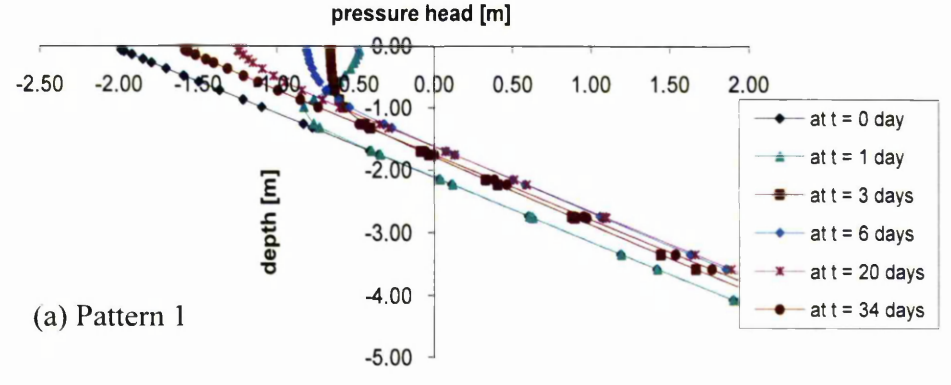

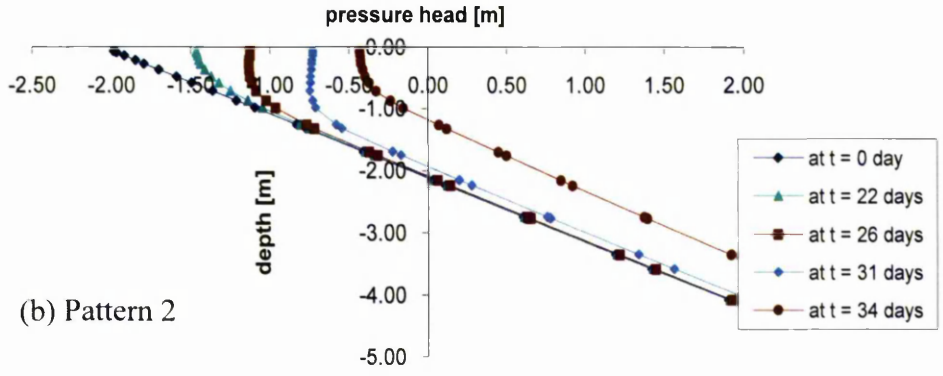

(b) Pattern 2

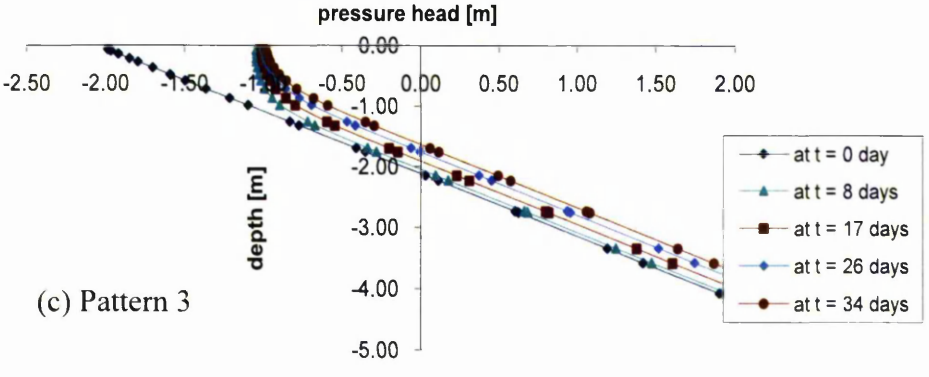

(c) Pattern 3

Figure 5.17 Distribution of pressure head on a section below the TOE of the 1H:1V SILTY soil slope at different times for (a) Pattern 1 (b) Pattern 2 and (c) Pattern 3 rainfall for a cumulative total of 496 mm in the 34 day period.

5.4 The influence of the infiltration of rainfall into a clayey soil slope with time

This section discusses the effect of different rainfall patterns resulting in the same total cumulative rainfall (310 mm) over a period of 34 days, on pore water pressure changes in a 1V:0.5H clay slope. The influence on the pore water pressure changes where the total rainfall is increased to 496 mm over the same period is then considered. Finally, the effect of lower and higher rainfall amounts with different rainfall patterns on 1V:1H clay slopes are also presented in this section.

5.4.1 The effect on pore water pressure distribution in a 1V:0.5H clayey type soil slope subjected to different rainfall patterns of duration 34 days with a total rainfall of 310 mm

The variation in pore water pressure with time on a section below the crest of a 1V:0.5H clay slope resulting from the infiltration by different rainfall patterns with the same total rainfall of 310 mm in 34 days is shown in Figure 5.18. It shows that the depths to which the wetting front moved under the influence of all three rainfall patterns in the clay soil slope were relatively shallow compared with the depths it moved in the sand and silt soil slopes. However, the pattern of pore water pressure movement in the clay soil slope is still similar to that in sand and silty soil slopes. After 34 days of rainfall in the case of Pattern 1 rainfall, the depth of the wetting front was no deeper than 2 m, likewise in the case of Patterns 2 and 3 rainfall, the depth of the wetting front at the end of the 34 day period was approximately 1 m and 1.5 m deep respectively.

Due to the high rainfall intensity at the beginning of the Pattern 1 rainfall period, the pore water pressure near the surface of the crest was found to be very close to zero in comparison with two other soil types. In fact for Pattern 2 rainfall, at the end of the high intensity period of 85.32 mm/day on Day 34, the pore water pressure near the surface of the crest reached a value of zero. Pattern 3 rainfall resulted in less reduction in the negative pore water pressure near the surface of the crest in comparison with Pattern 1 and Pattern 2 rainfall.

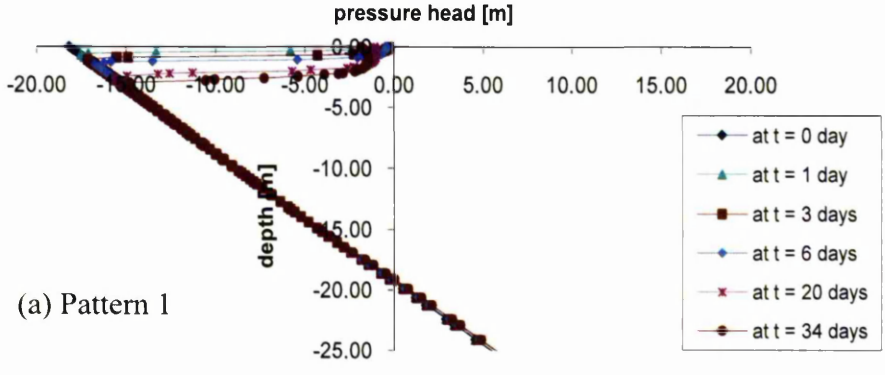

(a) Pattern 1

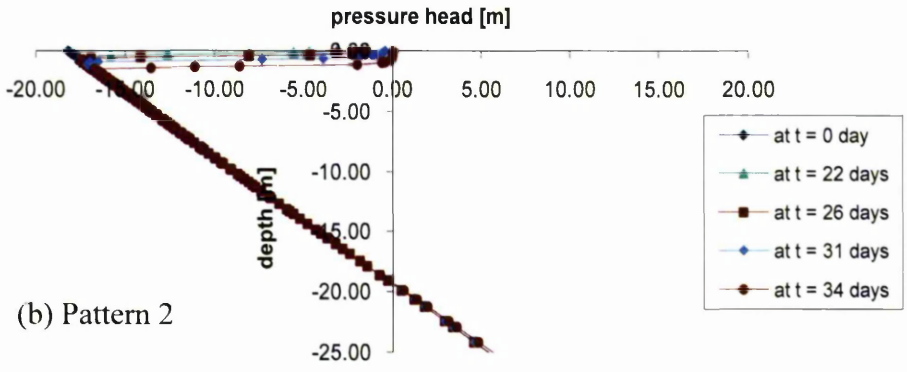

(b) Pattern 2

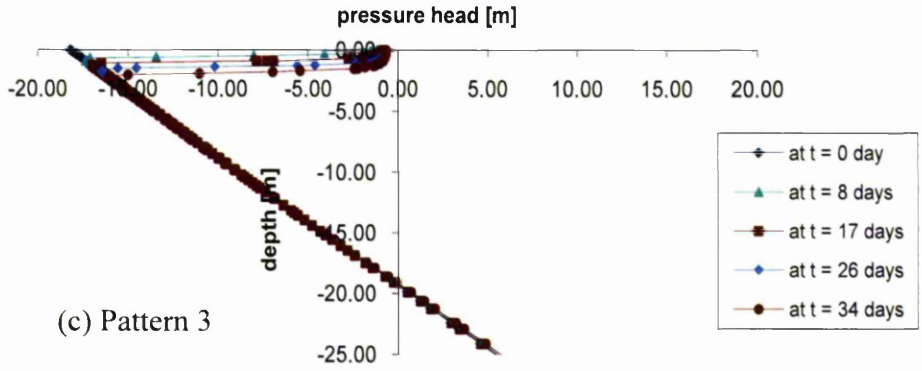

(c) Pattern 3

Figure 5.18 Distribution of pressure head on a section below the CREST of the 1V:0.5H CLAYEY soil slope at different times for (a) Pattern 1 (b) Pattern 2 and (c) Pattern 3 rainfall for a cumulative total of 310 mm in the 34 day period.

Figure 5.19 illustrates how the pore water pressure on a section below the toe of the 1V:0.5H clay slopes changed due to the application of different rainfall patterns. During the high rainfall intensity on the first day of Pattern 1 rainfall, the pore water pressure tended to zero very rapidly just below the surface of the ground. As water continued to infiltrate into the ground, it shows that at the end of t = 3 days the ground water level (or level at which the pore water was at atmospheric pressure) decreased in depth from approximately 1.73 m deep to 0.5 m deep. This ground water level continued to decrease in depth slightly until at the end of t = 6 days, and it was 0.35 m deep. However at the end of t = 20 days, the depth to the ground water

started to increase in depth to 0.8 m and the pore water pressure above the ground water level became more negative. This was probably due to the slow reduction in rainfall intensity in the Pattern 1 rainfall. After 14 days of no rainfall, it shows that at t = 34 days the depth of the ground water continued to increase in depth and the negative pore water pressure above the ground water level continued to increase.

In the case of the Pattern 2 rainfall, as the cumulative total of daily rainfall continued to increase, the negative pore water pressure near the surface continued to decrease, the ground water level increased slowly until the toe of the slope became saturated at the end of t = 33 days and the ground water level stayed at this position until the end of t = 34 days. In the case of the constant rainfall intensity i.e. Pattern 3 rainfall, the interval of the ground water level increment on the section below the toe of the slope from one observation time point to another seems to be approximately equal during the 34 days duration. This was probably due the approximate equal amount of rainfall that was received from one observation time point to another. At the end of t = 34 days, the depth to the ground water table was 0.65 m.

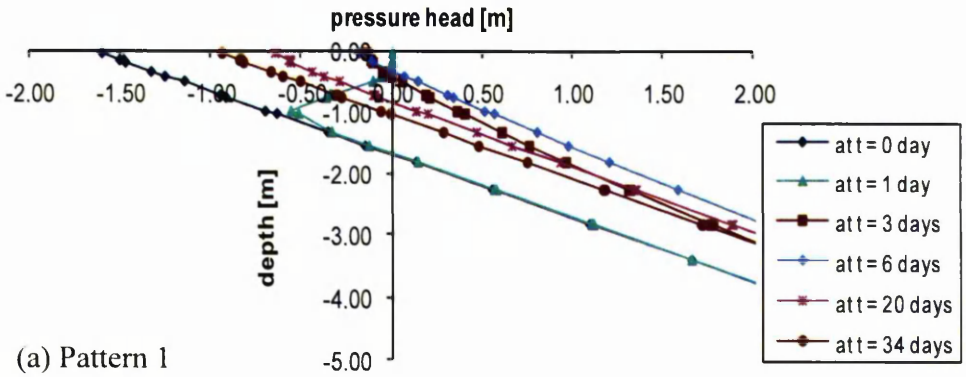

(a) Pattern 1

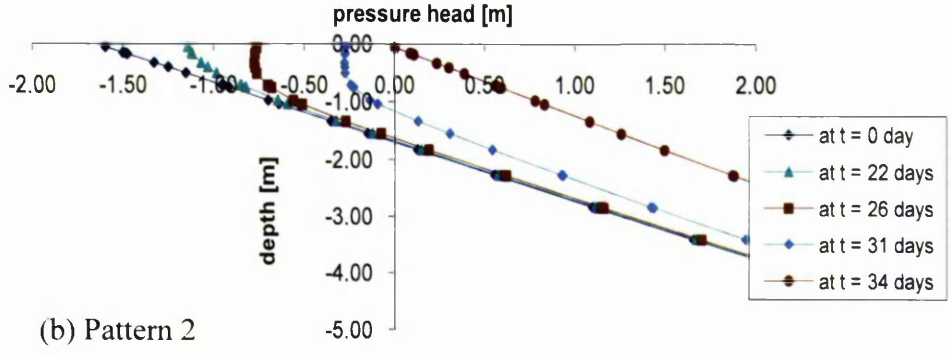

(b) Pattern 2

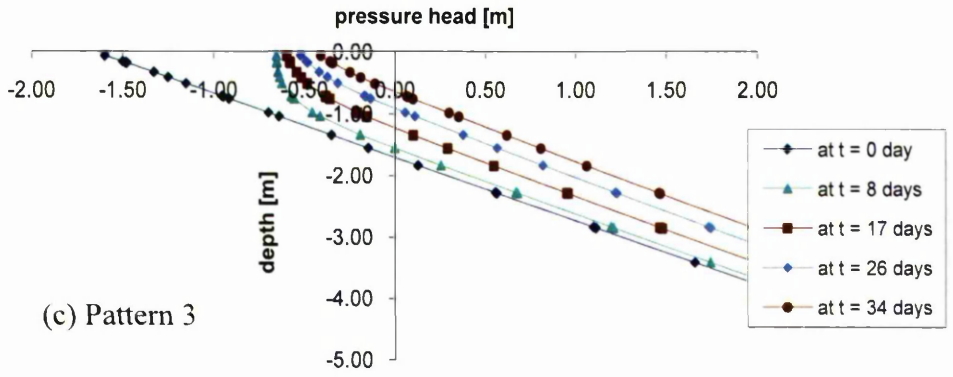

Figure 5.19 Distribution of pressure head on a section below the TOE of the 1V:0.5H CLAYEY soil slope at different times for (a) Pattern 1 (b) Pattern 2 and (c) Pattern 3 rainfall for a cumulative total of 310 mm in the 34 day period.

5.4.2 The effect of an increase of 60% in the base case cumulative rainfall during a 34 days period on the pore water pressure behaviour in a 1V:0.5H clayey type soil slope

From Figure 5.20, it can be seen that the increase in rainfall intensity by 60% for all three rainfall patterns resulted in an increase in the depth of the wetting front on a section below the crest of the slopes relative to the base case rainfall intensities as shown earlier in Figure 5.18. At the end of t = 34 days of Pattern 1, Pattern2 and Pattern 3 rainfall, the increase in the depth of the wetting front was found to be approximately 3.5 m deep (75% increase), 1.5 m deep (50% increase) and 2.5 m deep (67% increase) respectively. However, the variation of the pore water pressure distributions was similar to the variation of pore water pressure distributions observed in the case of the base case rainfall (see Figure 5.18).

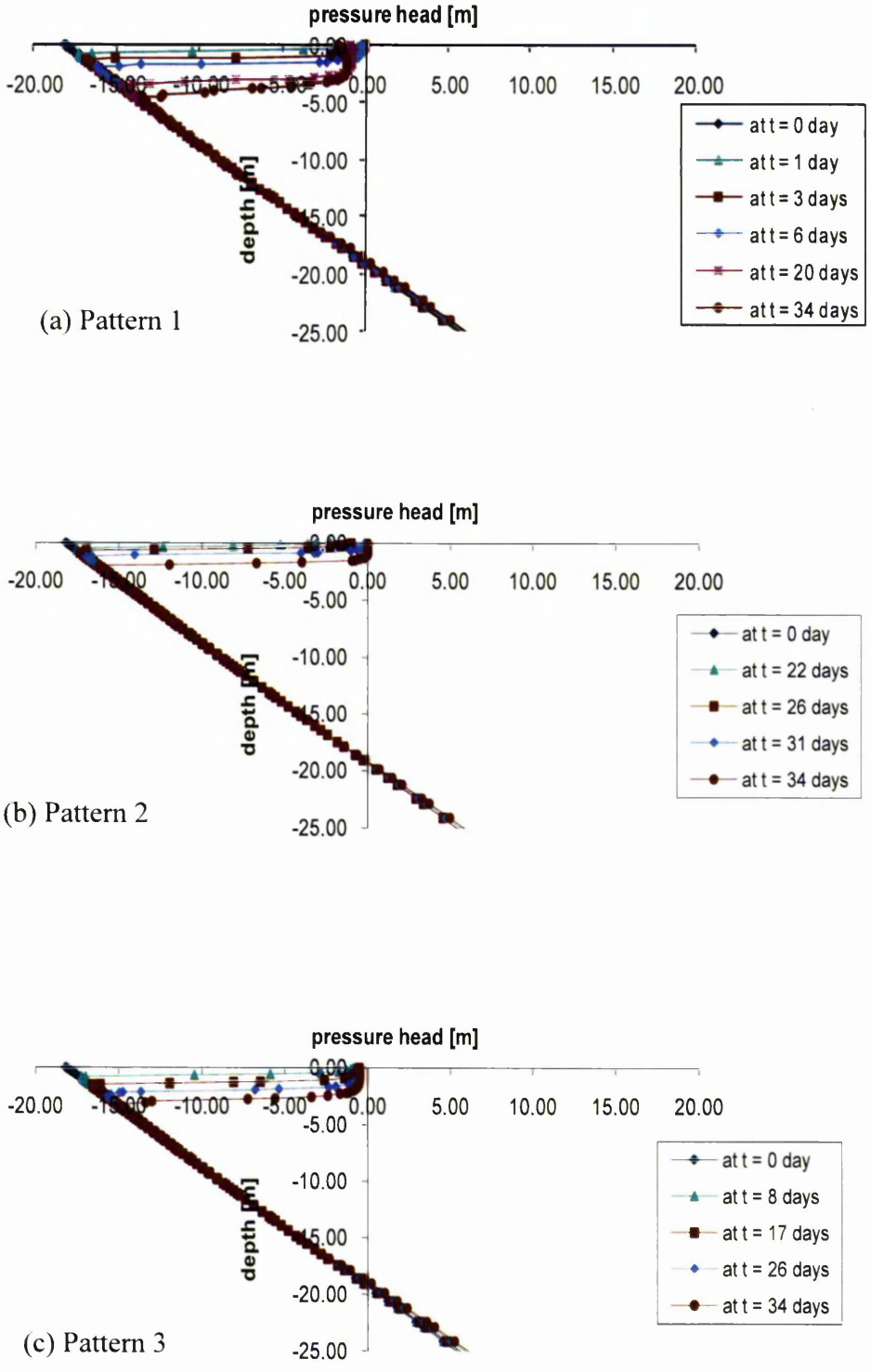

Figure 5.20 Distribution of pressure head on a section below the CREST of the 1V:0.5H CLAYEY soil slope at different times for (a) Pattern 1 (b) Pattern 2 and (c) Pattern 3 rainfall for a cumulative total of 496 mm in the 34 day period.

The changes in pore water pressure on a section below the toe of the 1V:0.5H clayey soil slope for different rainfall patterns with a 60% increase in rainfall intensity are shown in Figure 5.21. Similar to that seen in Figure 5.19 for Pattern 1 rainfall, the high intensity rainfall by t = 1 day reduced the negative pore water pressure near the ground surface effectively to zero. After t = 2 days, the ground water level on the section below the toe of the slope migrated to the ground surface effectively remaining in this position until about the end of t = 12 days. However, as the rainfall daily intensity continued to decrease, the level of ground water started to decrease with the pore water pressure above the phreatic surface became more negative.

In the case of Pattern 2 rainfall, the ground water level on the same section below the toe of the slope continued to increase as the rainfall increased. It shows that at the end of t = 31 days, the toe of the slope was already fully saturated whilst in the case of Pattern 3 rainfall, the toe was already fully saturated by the end of t = 22 days staying in this condition until the end of t = 34 days.

It should be noted that in the case of all rainfall patterns, as shown in Figure 5.21, the ground water level below the toe of the slope reached the ground surface at some time during the 34-day rainfall period. In addition to this, it also shows that in slopes comprising clayey soils there was a greater tendency for the ground water level beneath the toe of the slope to reach the ground surface during application of all three rainfall patterns compared to slopes in sandy and silty type soils.

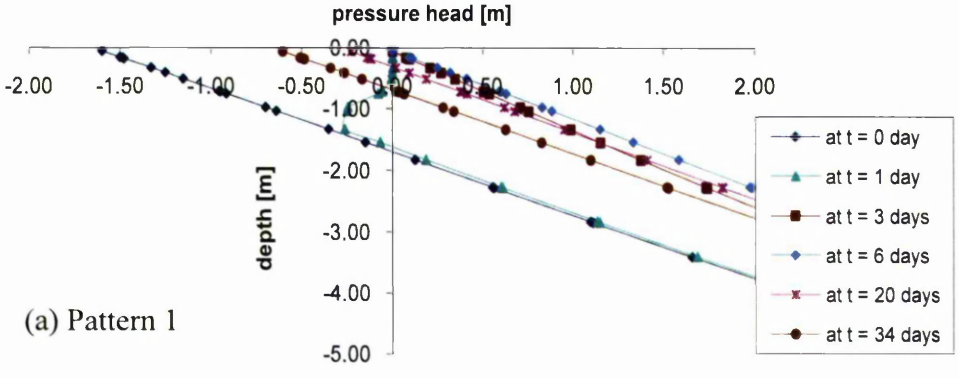

(a) Pattern 1

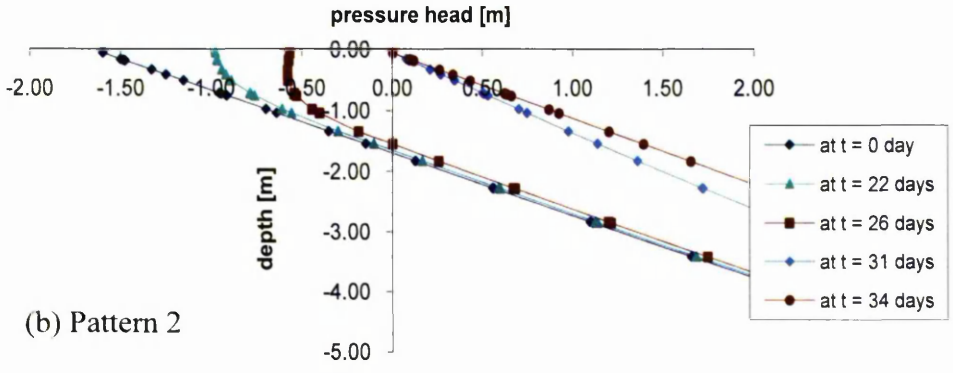

(b) Pattern 2

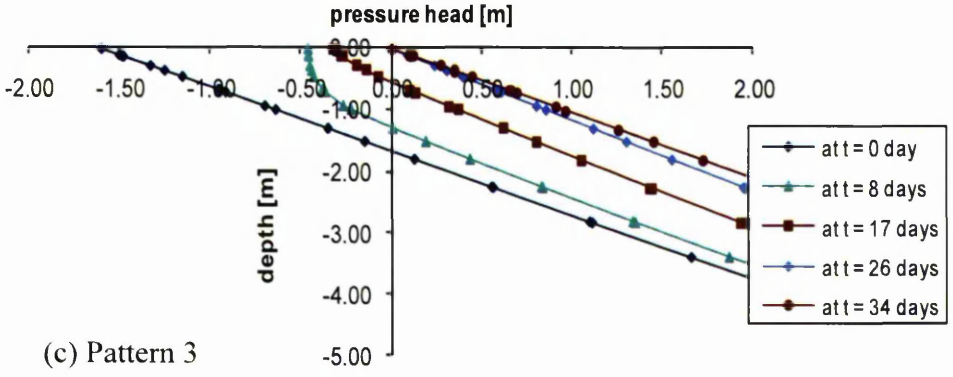

(c) Pattern 3

Figure 5.21 Distribution of pressure head on a section below the TOE of the 1V:0.5H CLAYEY soil slope at different times for (a) Pattern 1 (b) Pattern 2 and (c) Pattern 3 rainfall for a cumulative total of 496 mm the 34 day period.

5.4.3 The effect on pore water pressure distribution in a 1V:1H clayey type soil slope subjected to different rainfall patterns of duration 34 days with a total rainfall of 310 mm

As shown in Figure 5.22, the behaviour of the pore water pressure on a section below the crest of a 1V:1H clayey soil type slope due to the three different rainfall patterns shows no difference compared with that of the pore water pressure below the crest of a 1V:0.5H clay soil slope as shown earlier in Figure 5.18. It can be seen that by the end of t = 34 days, the depths of the wetting front below the crest were similar for both 1V:1H and 1V:0.5H clay slopes, i.e. for Pattern 1 rainfall, Pattern 2 rainfall and

Pattern 3 rainfall the depths of the wetting front were 2 m, 1 m and 1.5 m respectively.

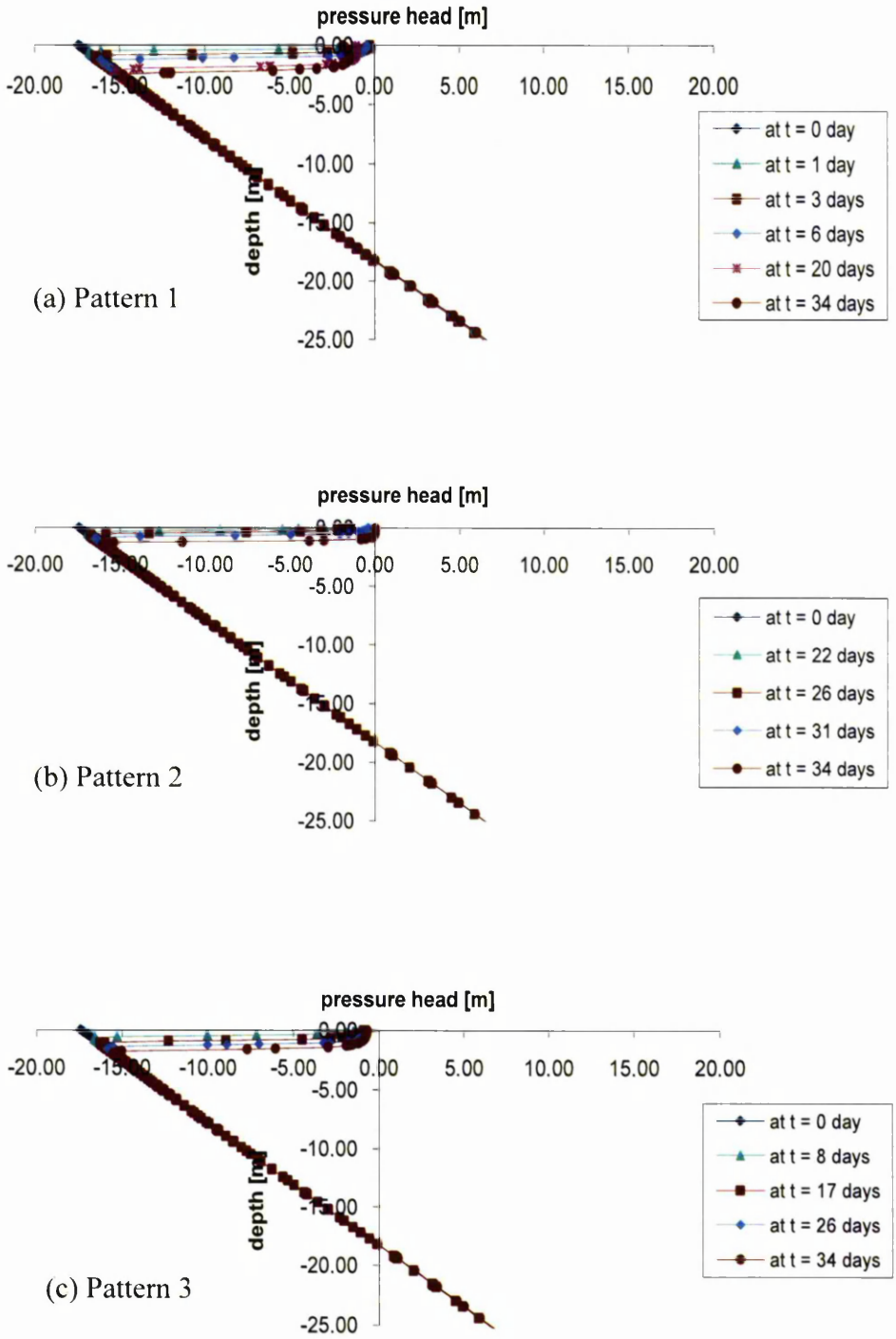

Figure 5.22 Distribution of pressure head on a section below the CREST of the 1V:1H CLAYEY soil slope at different times for (a) Pattern 1 (b) Pattern 2 and (c) Pattern 3 rainfall for a cumulative total of 310 mm in the 34 day period.

However, on a section below the toe of the slope, the increase in ground water level was relatively low compared with that seen in 1V:0.5H slopes at equivalent times in the rainfall period. In the case of Pattern 1 rainfall (Figure 5.23), the ground water level was elevated and reached its maximum position at t = 6 days, increasing from 2.15 m to 1.35 m deep. In the case of Pattern 2 rainfall, it can be seen that there was only a slight change in the ground water level at the end of t = 31 days probably due to the lower rainfall intensities at the early stages of the Pattern 2 rainfall period. However, at the end of t = 34 days, the toe of the slope became saturated instantly. At the end of t = 34 days of the Pattern 3 rainfall, the ground water level rose to a maximum at 1.33 m deep. Comparing Pattern 1 and Pattern 3 rainfall, it can be seen that the maximum depth of ground water level between these two patterns differed by only 0.02 m.

Furthermore, by comparing Figure 5.19, showing the distribution of the pressure head beneath the toe of a 1V:0.5H clayey soil slope and Figure 5.23, showing the same beneath the toe of 1V:1H clay slope, it seems that a reduction of the negative pore water pressure beneath the toe of the slope was greater in the 1V:0.5H clay slope than in the 1V:1H clay slope.

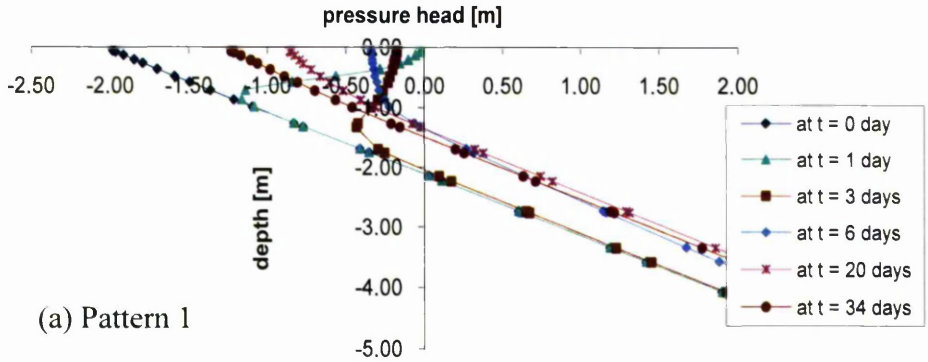

(a) Pattern 1

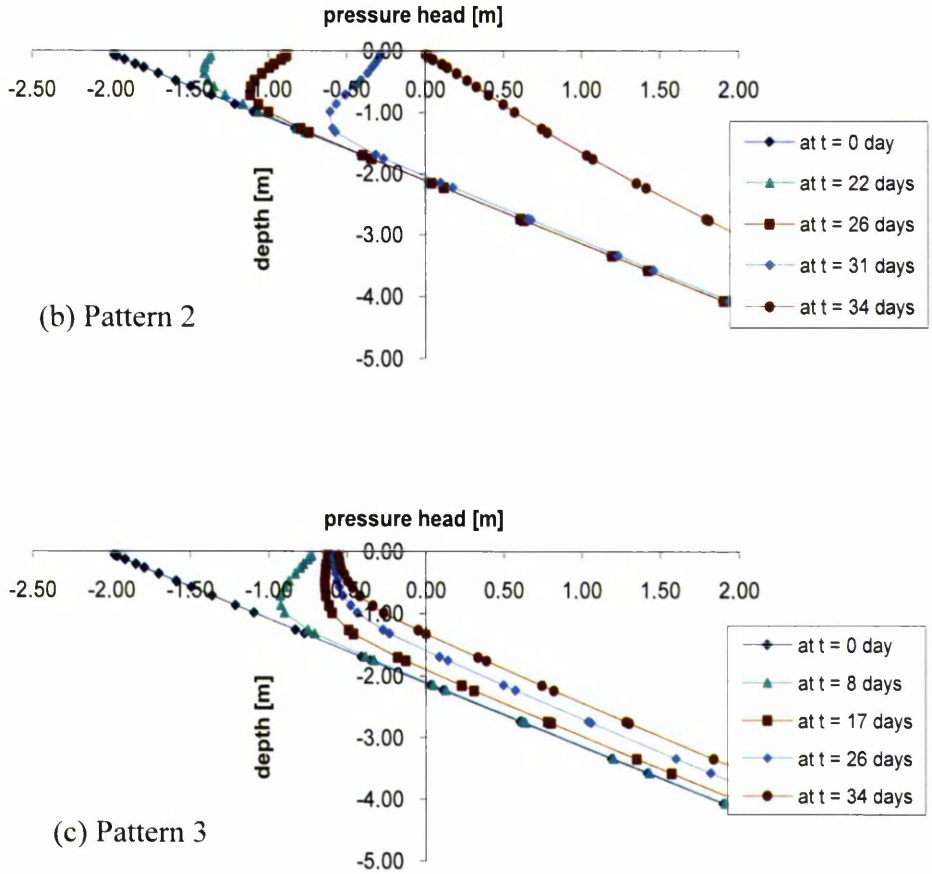

Figure 5.23 Distribution of pressure head on a section below the TOE of the 1V:1H CLAYEY soil slope at different times for (a) Pattern 1 (b) Pattern 2 and (c) Pattern 3 rainfall for a cumulative total of 310 mm in 34 day period.

5.4.4 The effect of an increase of 60% in the base case cumulative rainfall during a 34 days period on the pore water pressure behaviour in a 1V:1H clayey type soil slope

The distribution of pore water pressure changes on a section below the crest of a 1V:1H clayey soil slope due to the application of an overall rainfall intensity which is 60% greater than the base case is illustrated in Figure 5.24. The patterns of pore water pressure changes were similar for both lower and higher rainfall intensities to those in the cases of slopes in sandy and silty soils, and the depths of the wetting fronts were also deeper as a result of the higher rainfall intensity. At the end of t =

34 days, the depth of the wetting fronts were increased by 1.0 m (50%), 0.5 m (50%) and 0.5 m (33%) for Pattern 1, Pattern 2 and Pattern 3 rainfall respectively.

By comparing Pattern 1 and Pattern 3 rainfall only on 1V:1H clay slopes in Figure 5.24 and the 1V:0.5H clayey soil slopes in Figure 5.20 subjected the higher rainfall intensity of 496 mm/34 days, it shows that even though the 1V:1H slopes produced a shallower depth of the wetting front at the end of t = 34 days, these differences were small. The difference in the depths of the wetting fronts were not more than 0.5m for both rainfall patterns, whilst for Pattern 2 rainfall, the depths of the wetting fronts were equal.

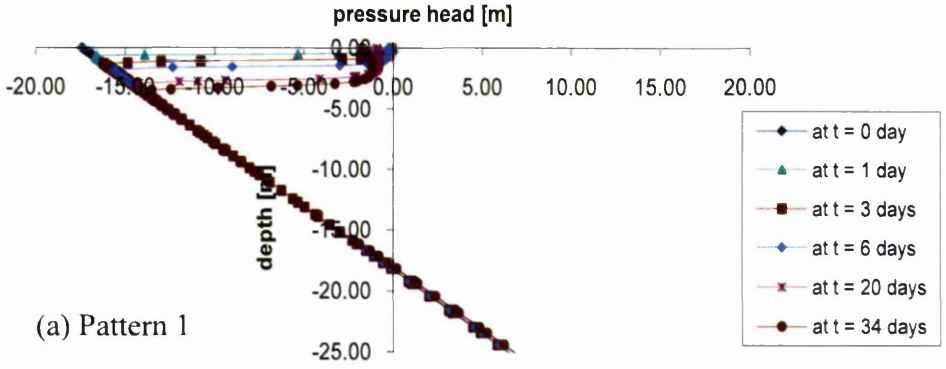

(a) Pattern 1

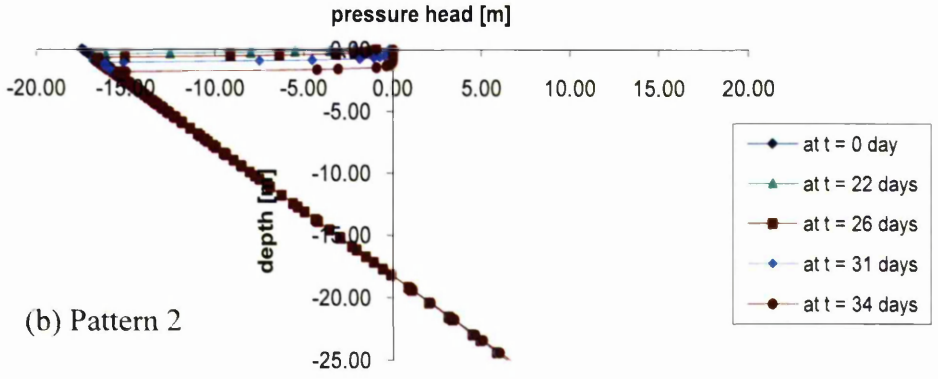

(b) Pattern 2

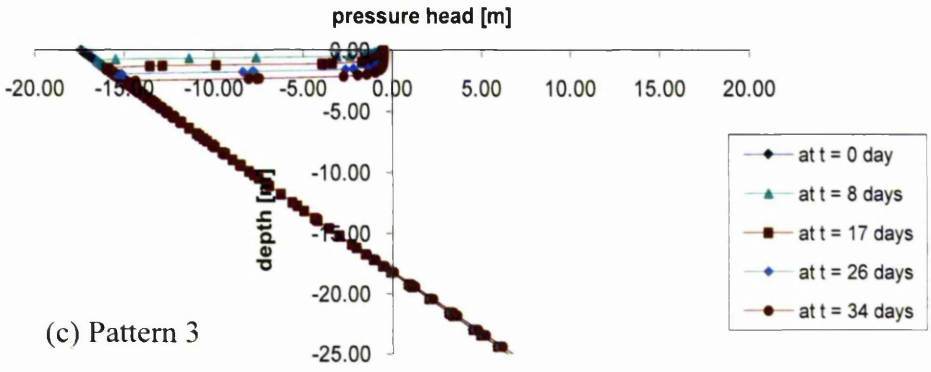

(c) Pattern 3

Figure 5.24 Distribution of pressure head on a section below the CREST of the 1V:1H CLAYEY soil slope at different times for (a) Pattern 1 (b) Pattern 2 and (c) Pattern 3 rainfall for a cumulative total of 496 mm in the 34 day period.

As shown in Figure 5.25, the increase of the daily rainfall intensity by 60% also increased the position of the ground water level on a section below the toe of the slope. It shows that for Pattern 1 rainfall, the toe of the slope became fully saturated by the end of t = 6 days. It should be noted, however, that the toe of the slope started to become saturated by the end of t = 4 days, and remained in this condition until the end of t = 9 days before the ground water level started to reduce.

In the case of Pattern 2 and Pattern 3 rainfall, the increase in the rainfall intensity had a very different influence on the pore water pressure and the ground water level. For Pattern 2 rainfall, the toe of the slopes only started to become saturated at the end of t = 32 days, and stayed at this position until the end of t = 34 days. In the case of Pattern 3 rainfall, the toe of the slope became fully saturated at the end of t = 33 days and stayed in this condition until the end of t = 34 days. These two observations were based upon the graphical display result of two-dimensional pressure head values that can be obtained in Hydrus2D.

The behaviour of pore water pressure in the 1V:1H clay slopes was in many ways similar to the behaviour of pore water pressure in 1V:0.5H clay slopes when subjected to the increased rainfall intensities.

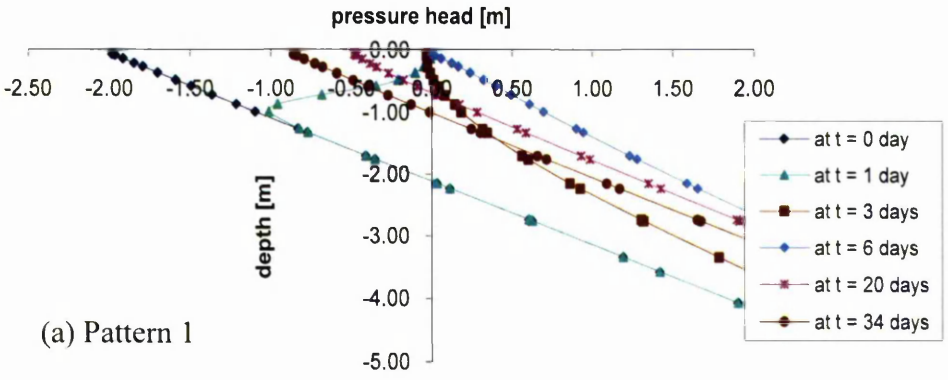

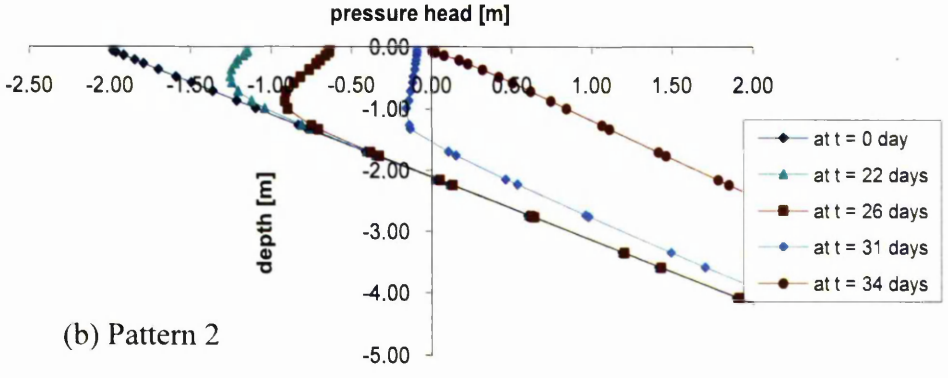

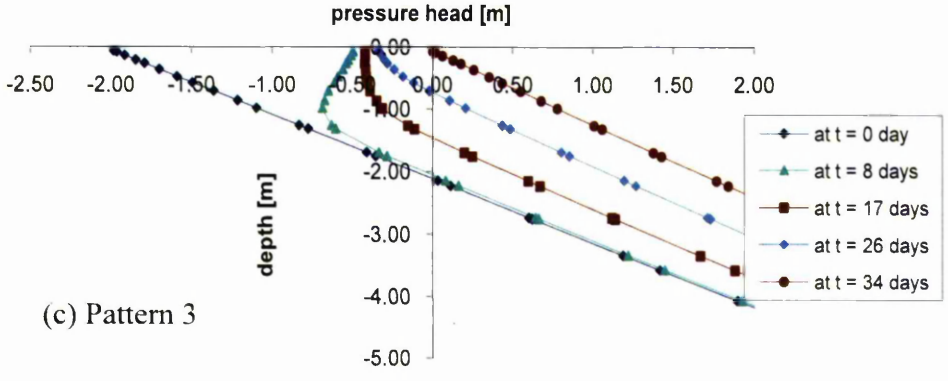

Figure 5.25 Distribution of pressure head on a section below the TOE of the 1V:1H CLAYEY soil slope at different times for (a) Pattern 1 (b) Pattern 2 and (c) Pattern 3 rainfall for a cumulative total of 496 mm in the 34 day period.

5.5 Summary of the effects of rainfall intensity and pattern on the pore water pressures within slopes of two different geometries and three soil types

A number of observations are significant in the context of predicting the stability of the slopes as the rainfall period progresses. These observations relate to the distribution of the pore water pressure within the body of the slopes with time given the soil composition of the slopes and the characteristics of the rainfall.

In general the discussion in this section is confined to the changes observed in the pore water pressures beneath the crest and the toe of the slopes respectively. Obviously the distribution elsewhere within the slope also plays a significant role in the mobilisation of resistance to failure but the characteristic behaviour at these locations are an indication of the overall behaviour of the slopes.

The observations are summarised as follows:-

1. The depth of the wetting fronts at the crest of the slopes, the time and the depth at which the ground water level reached its maximum on a section below the toe of the slopes are summarised and tabulated in Table 5.2 for slopes in sandy soil, Table 5.3 for slopes in silty soil and Table 5.4 for slopes in clayey soil.

2. For all the slopes considered in all soils, the depth of the wetting front on a section below the crest of the slopes increased when the overall rainfall intensity was increased by 60% from the base case. The effect of the increase in rainfall intensity by 60% is the most prominent at the end of Pattern 3 rainfall in the case of slopes in sandy soil, at the end of Pattern 2 rainfall in the case of slopes in silty soil and at the end of Pattern 1 rainfall in the case of slopes in clayey soil. However, the depth of the wetting front below the crest of the slope was the deepest in the case of slopes in sandy soil and the shallowest in slopes in clayey soil. This can be seen clearly at the end of t = 34 days of all three rainfall patterns.

Table 5.2 The depth of the wetting fronts on a section below the crest and the position of the ground water level (GWL) beneath the toe of sandy soil slopes

Soil and rainfall pattern	Crest	Toe		
SAND (1V:0.5H)	Depth of the wetting front at the end of t = 34 days [m]	Time at which the GWL reached its maximum position [day]	Minimum depth of rising GWL [m]	Difference in the increase in GWL from its initial position [m]
Pattern 1 (310 mm)	15	6	1.63	0.1
Pattern 2 (310 mm)	4.5	34	1.55	0.18
Pattern 3 (310 mm)	8.5	34	1.65	0.08
Pattern 1 (496 mm)	18	6	1.52	0.21
Pattern 2 (496 mm)	6.5	34	1.35	0.38
Pattern 3 (496 mm)	14	34	1.60	0.13
SAND (1V:1H)				
Pattern 1 (310 mm)	11	6	2.05	0.1
Pattern 2 (310 mm)	4	34	2.01	0.14
Pattern 3 (310 mm)	7	34	2.08	0.07
Pattern 1 (496 mm)	15	6	1.95	0.2
Pattern 2 (496 mm)	5	34	1.83	0.32
Pattern 3 (496 mm)	10.5	34	2.03	0.12

3. In each case at some stage during the rainfall period, the ground water level beneath the toe of the slopes increased to a certain level during the 34-days rainfall period. However, the magnitude of increase in the ground water level depended on the type of soil in the slope. The ground water level was least affected in slopes of sandy soil, whilst, on the other hand, for slopes in clayey soil, a saturation point was reached at the toe of the slope towards the end of Pattern 2 rainfall. When the overall rainfall intensity was increased by 60%, the toe became saturated at one time or another for all three rainfall patterns.

4. Generally, the ground water level reached its maximum level towards the end of t = 34 days for Pattern 2 and Pattern 3 rainfall. However, for Pattern 1 rainfall, the maximum ground water level was found to occur at an early stage during the 34-day period. This shows that the high intensity rainfall affected the changes in ground water level to a greater extent despite the type of rainfall pattern involved.

Table 5.3 The depth of the wetting fronts on a section below the crest and the position of the ground water level (GWL) beneath the toe of silty soil slopes

Soil and rainfall pattern	Crest	Toe		
SILT (1V:0.5H)	Depth of the wetting front at the end of t = 34 days [m]	Time at which the GWL reached its maximum position [day]	Minimum depth of rising GWL [m]]	Difference in the increase in GWL from its initial position [m]
Pattern 1 (310 mm)	4.5	6	1.4	0.33
Pattern 2 (310 mm)	1.5	34	1.15	0.58
Pattern 3 (310 mm)	3	34	1.42	0.31
Pattern 1 (496 mm)	7	6	1.09	0.64
Pattern 2 (496 mm)	2.5	34	0.3	1.43
Pattern 3 (496 mm)	4.8	34	1.18	0.55
SILT (1V:1H)				
Pattern 1 (310 mm)	3.5	20	1.87	0.28
Pattern 2 (310 mm)	1.5	34	1.80	0.35
Pattern 3 (310 mm)	2.5	34	1.88	0.27
Pattern 1 (496 mm)	5	20	1.63	0.52
Pattern 2 (496 mm)	2.3	34	1.20	0.95
Pattern 3 (496 mm)	3.5	34	1.65	0.5

5. By comparing different rainfall patterns for slopes of all soils, by the end of t = 34 days, the depth of the wetting front was the deepest in the case of Pattern 1 rainfall and the shallowest in the case of Pattern 2 rainfall. This is because for Pattern 1 rainfall, slopes received most of the rainfall during the first 20 days of the 34-days period, and during the last 14 days whilst there was effectively no further rainfall, water still continued to infiltrate into the ground. However, for Pattern 2 rainfall, the 14 days period of no rainfall was at the beginning of the rainfall period. The highest daily rainfall only occurred on Day 34, thus the time was not sufficient for the wetting front to reach the same depth as Pattern 1 rainfall by the end of t = 34 days. It is expected that the depth of the wetting front at the end of t =34 days for Pattern 3 rainfall was between the depth of the wetting fronts for Pattern 1 and Pattern 2 rainfalls. This was probably because of the nature of constant continuous rainfall for Pattern 3 for the 34 days period.

Table 5.4 The depth of the wetting fronts on a section below the crest and the position of the ground water level (GWL) beneath the toe of clayey soil slopes

Soil and rainfall pattern	Crest	Toe		
CLAY (1V:0.5H)	Depth of the wetting front at the end of t = 34 days [m]	Time at which the GWL reached its maximum position [day]	Minimum depth of rising GWL [m]	Difference in the increase in GWL from its initial position [m]
Pattern 1 (310 mm)	2	6	0.35	1.38
Pattern 2 (310 mm)	1	33 – 34	0.05	1.68
Pattern 3 (310 mm)	1.5	34	0.65	1.08
Pattern 1 (496 mm)	3.5	2 – 12	0.05	1.68
Pattern 2 (496 mm)	1.5	31 – 34	0.05	1.68
Pattern 3 (496 mm)	2.5	22 – 34	0.05	1.68
CLAY (1V:1H)				
Pattern 1 (310 mm)	2	6	1.35	0.8
Pattern 2 (310 mm)	1	34	0.08	2.07
Pattern 3 (310 mm)	1.5	34	1.33	0.82
Pattern 1 (496 mm)	3	4 – 9	0.08	2.07
Pattern 2 (496 mm)	1.5	31 – 34	0.08	2.07
Pattern 3 (496 mm)	2	33 – 34	0.08	2.07

6. Even though Pattern 2 rainfall produced the shallowest wetting fronts for all three rainfall patterns beneath the crest of the slopes, it gave the highest increase in the ground water level below the toe of the slopes in comparison with other rainfall patterns, whilst Pattern 3 rainfall affected the ground water level the least. This is probably due to the effect of high intensity rainfall at the end of Pattern 2, after a long period of antecedent rainfall.

7. By evaluating the difference between two different geometries, it can be seen that the depth of the wetting front on the section below the crest of sandy and silty slopes was deeper for the 1V:0.5H slopes than the 1V:1H slopes. However, for slopes in clayey soil, the changes of the depth of the wetting fronts were almost the same for both geometries.

8. Initially, the ground water depths beneath the toe of the slopes were located at 1.73 m deep for the 1V:0.5H slopes and 2.15 m deep for the 1V:1H slopes. Due to the high permeability in the slopes of sandy soil, water easily

infiltrated into the slope, thus making the changes in ground water depths below the toe of the sandy slopes approximately similar for both slope geometries. In slopes of silty and clayey soils, however, due to their relatively low permeability the changes in ground water depth beneath the toe were smaller in the 1V:1H slopes than in the 1V:0.5H slopes. This is probably because it took a longer time for the water to reach the ground water level located at a larger depth.

A further illustration of the distribution of pore water pressure within the slopes at the end of t = 34 days in two dimensions are illustrated in Appendix B. Instead of showing the whole domain as described in Chapter 4, the figures in Appendix B are only illustrating the enlargement around the slope area at the end of t = 34 days. This will give a clearer picture of the contours of the pore water pressure distribution around the slope area. It should also be noted that the contours of pore water pressure distribution was presented in terms of pressure head values (unit: metre, m).

6 Effect of Rainfall on Slope Stability

6.1 Introduction

This chapter discusses the effect of rainfall pattern on slope stability. The slope stability analyses in this chapter are based on effective stress principles using the pore water pressure distributions discussed in Chapter 5. A factor of safety (FoS) has been found at different times during the 34 days rainfall period depending on the rainfall pattern applied. As with the pressure head distributions developed in Chapter 5, the factor of safety was calculated at the end of t = 1 day, 3 days, 6 days, 20 days and 34 days for Pattern 1 rainfall, at the end of t = 22 days, 26 days, 31 days and 34 days for Pattern 2 rainfall, and at the end of t = 8 days, 17 days, 26 days and 34 days for Pattern 3 rainfall.

As highlighted in Chapter 4, Slope12.01 only provides the lowest value of factor of safety for each slip surface obtained from each common point and centre of circle. Thus, at the end of each run time, there are 20 circular slip surfaces for 1V:0.5H slopes and 24 circular slip surfaces for 1V:1H slopes. In this chapter however, only the lowest value of the factor of safety (FoS) for all potential circular slip surfaces at any chosen time as described above is presented.

It should be noted that the change in factor of safety of the slope with time was only influenced by the changes of pore water pressure due to rainfall whilst other shear strength soil parameters were kept constant. The shear strength parameters adopted for the slope stability analyses are given in Chapter 4.

The chapter is divided into three main sections, i.e. the presentation of the changes in the factor of safety for sand slopes, for silt slopes and for clay slopes which each experienced three different types of rainfall patterns with two different amount of total rainfall.

6.2 Presentation of the stability of the slopes in sandy type soil

At t = 0 (i.e. day zero) the FoS against failure for a 1V:0.5H slope was found to be 1.79 and the FoS for the flatter slope (1V:1H) was found to be 2.01. In Chapter 5 it is shown that water infiltrated easily into the sandy soil and the depth of wetting fronts were also greater in comparison with other two soil materials considered. This section illustrates further how these changes in pore water pressure due to different rainfall patterns affect the factor of safety of the slope against failure for both geometries, the steeper 1V:0.5H slope and the relatively flatter 1V:1H slope.

6.2.1 1V:0.5H sandy soil type slope

The application of Pattern 1 rainfall on a 1V:0.5H slope caused an almost immediate reduction in the magnitude of FoS. Table 6.1 shows how the coordinates of the common point, the centre of rotation of the critical slip surface, and the value of the factor of safety of this slip surface change with time when Pattern 1 rainfall with total amounts of 310 mm and also 496 mm was applied onto 1V:0.5H slope. The locations of critical slip surfaces at various times are clearly seen in Figure 6.1. From Table 6.1 and Figure 6.1, it can be seen that when rainfall was first applied at t = 1 day, the critical slip surface migrated to a location close to the slope, moving deeper into the slope with time. Furthermore, the magnitude of the FoS reduced slowly with time. However, by the end of t = 20 days and until t = 34 days, even though the critical slip surface was generated at deeper locations, the factor of safety tended to increase. This was probably due to the reduction in rainfall to zero towards the end of the 34-days period.

The introduction of a higher total rainfall amount of 496 mm reduced the magnitude of FoS by a greater extent at the end of t = 1 day, 3 days and 6 days in comparison with that caused by the lower total rainfall of 310 mm in 34 days. The location of the critical slip surface for the higher rainfall intensity was deeper than the slip surface generated during the lower rainfall intensity. However, at t = 20 days and t = 34 days, the magnitude of the FoS and location of the critical slip surface were similar for both lower and higher total rainfall over the 34 day period.

It should be noted, however, that the difference in magnitude of FoS as a result of Pattern 1 rainfall for the two total rainfall amounts of 310 mm and 496 mm decreased reaching zero towards the end of the rainfall period (i.e. t = 34 days). This behaviour shows that even though, as illustrated previously in Chapter 5, the wetting fronts in 1V:0.5H sandy soil slopes generated during Pattern 1 rainfall due to higher rainfall amount were deeper in comparison with the wetting fronts due to the lower rainfall intensity, the location of the critical slip surfaces and magnitudes of the factor of safety remained the same after equivalent periods of time. In both cases of Pattern 1 type total rainfall on 1V:0.5H sand slopes, it shows that the slope was in a state of failure at the end of t = 3days. Based on the lower total rainfall for 34 days period of 310 mm, it shows that 1V:0.5H sand slope potentially received 167.8 mm of rainfall by the end of period up to t = 3 days.

Table 6.1 The position of circular slip surface and the factor of safety due to the application of Pattern 1 rainfall on 1V:0.5H sand slope

Total rainfall (mm)	Time, t (day)	Cumulative rainfall (mm) at different 't'	Coordinates of the common point (m)			Critical circle				
						Centre			Radius (m)	FoS
			No	x	y	location	x	y		
	0	0	20	49.5	20	t0	53	40	20.30	1.79
310	1	85	5	42	35	t1	77	60	43.01	1.57
	3	168	1	40	39	t3	83	50	44.38	0.91
	6	235	19	49	21	t6	79	50	41.73	0.77
	20	310	19	49	21	t20	81	54	45.97	0.78
	34	310	19	49	21	t34	81	54	45.97	0.80
496	1	137	10	44.5	30	t1	73	50	34.82	1.31
	3	268	19	49	21	t3	77	48	38.90	0.78
	6	376	19	49	21	t6	83	54	47.38	0.73
	20	496	19	49	21	t20	81	54	45.97	0.78
	34	496	19	49	21	t34	81	54	45.97	0.80

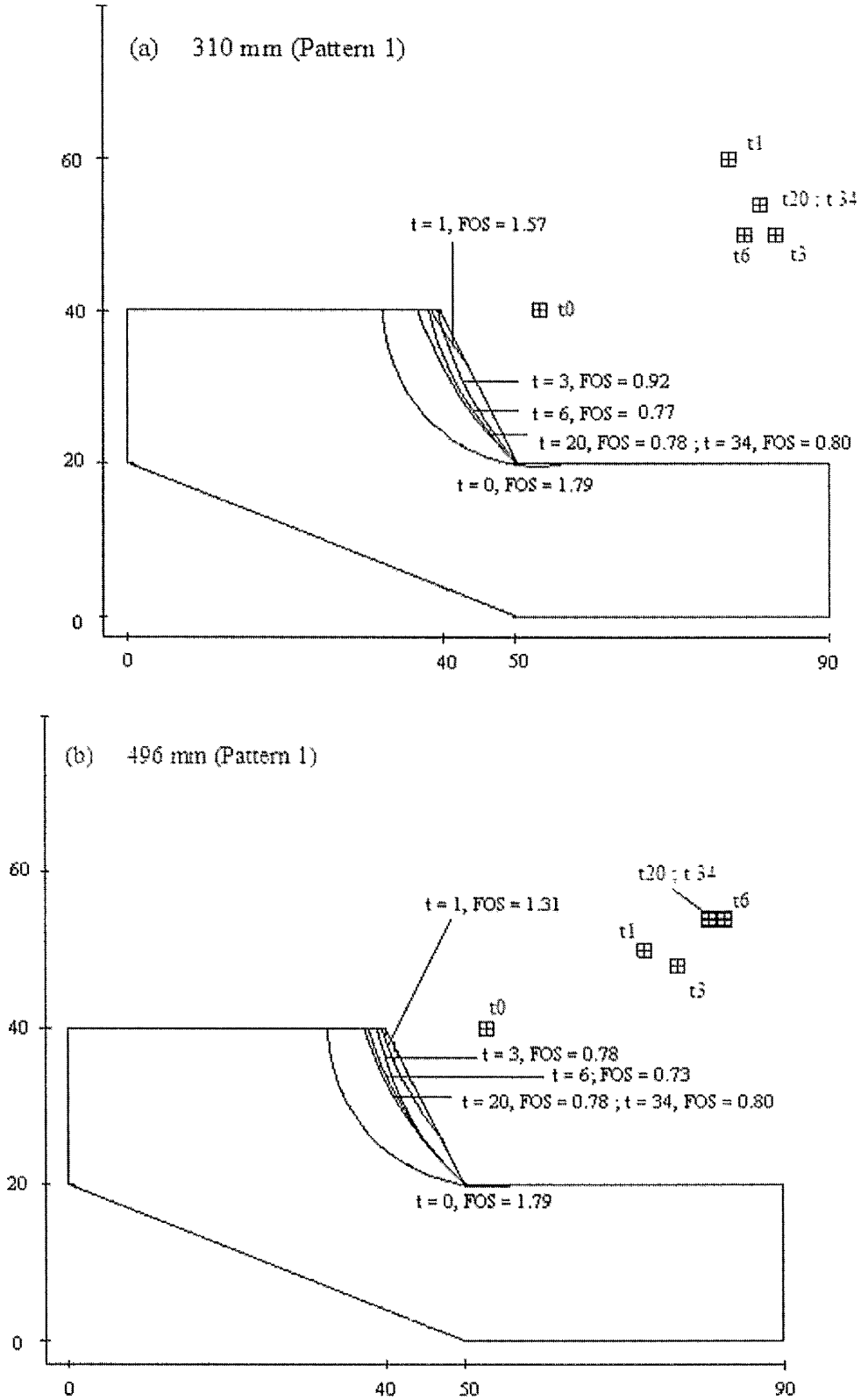

Figure 6.1 The location of the critical circular slip surface with time on a 1V:0.5H sandy soil type slope subjected to Pattern 1 rainfall with total cumulative rainfall of (a) 310 mm and (b) 496 mm

As in the case of Pattern 1 rainfall, the application of Pattern 2 rainfall on 1V:0.5H sand slope caused the critical slip surface to appear rapidly near the surface. However due to the low rainfall intensity at the beginning of Pattern 2 rainfall, the reduction of the factor of safety was smaller during the earlier stages but continued to reduce further until the end of the rainfall period.

Introduction of the higher rainfall intensity on the slope had the result of deepening the location of the critical slip surface and reducing the magnitude of the FoS further. The coordinates of the common points and the centre of the circle for the critical slip surface due to the application of Pattern 2 rainfall is tabulated in Table 6.2, and a clearer illustration of the locations of these slip surfaces with time is shown in Figure 6.2. In the case of Pattern 2 rainfall, it can be seen that the 1V:0.5H sand slope appeared to fail at the end of the period of rain (t = 31 days).

At the end of the rainfall period, i.e. at t = 20 days for Pattern 1 rainfall and at t = 34 days for Pattern 2 rainfall, it can be seen that the magnitudes of the factor of safety against failure differed by 0.02 – 0.04. Pattern 2 rainfall generated a shallower slip surface in comparison with that generated by the Pattern 1 rainfall, However, these differences are considered to be small.

Table 6.2 The position of circular slip surface and the factor of safety due to the application of Pattern 2 rainfall on 1V:0.5H sand slope

Total rainfall (mm)	Time, t (day)	Cumulative rainfall (mm) at different 't'	Coordinates of the common point (m)			Critical circle				
						Centre			Radius (m)	FoS
			No.	x	y	location	x	y		
	0	0	20	49.5	20	t0	53	40	20.30	1.79
310	22	20	20	49.5	20	t22	53	40	20.06	1.71
	26	50	5	42	35	t26	77	60	43.01	1.53
	31	143	1	40	39	t31	83	50	44.38	0.96
	34	310	19	49	21	t34	77	48	38.90	0.76
496	22	32	20	49.5	20	t22	53	40	20.30	1.62
	26	80	12	45.5	28	t26	83	54	45.63	1.26
	31	228	18	48.5	22	t31	79	50	41.40	0.81
	34	496	19	49	21	t34	83	54	47.38	0.74

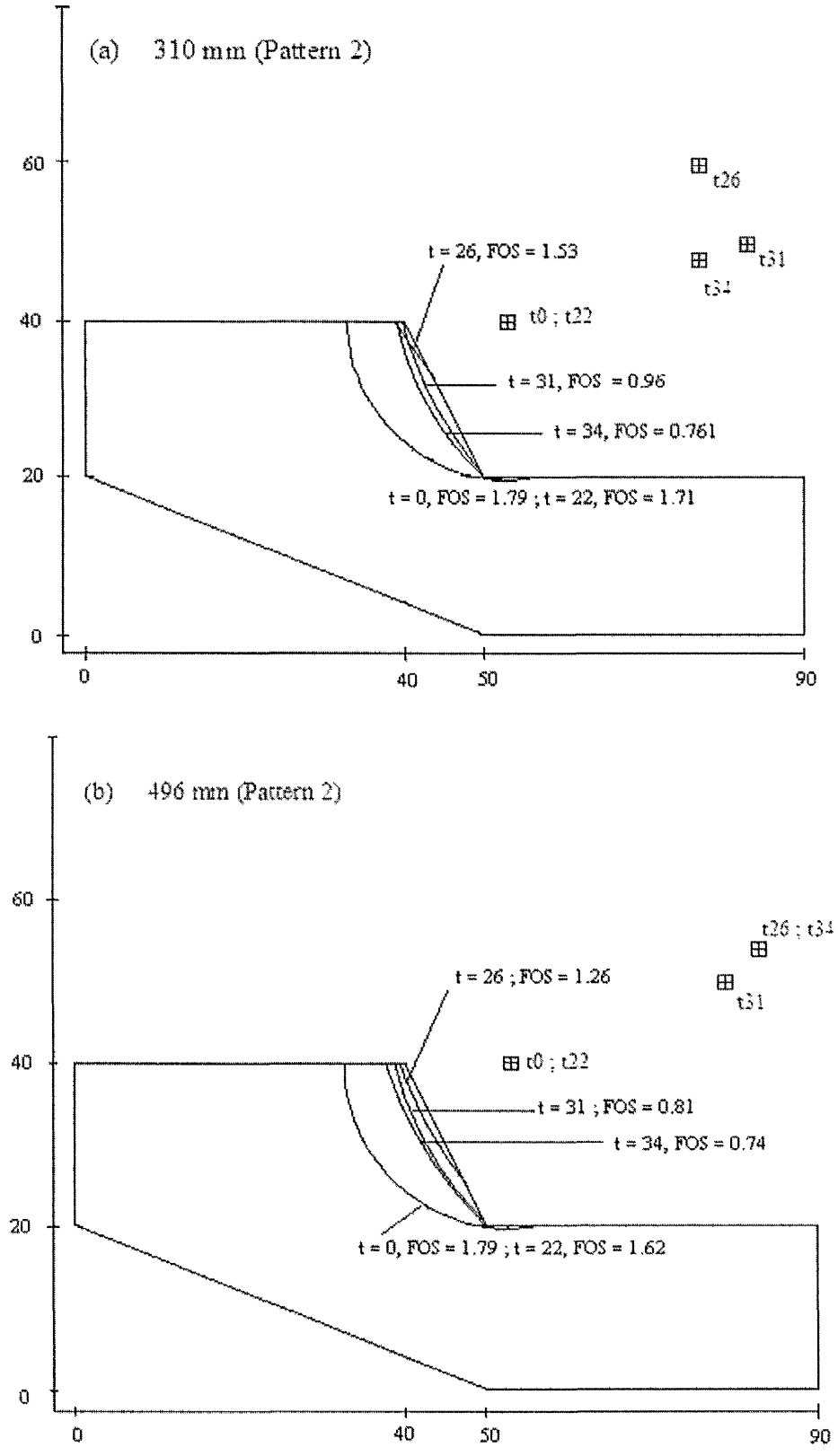

Figure 6.2 The location of the critical circular slip surface with time on a 1V:0.5H sandy soil type slope subjected to Pattern 2 rainfall with total cumulative rainfall of (a) 310 mm and (b) 496 mm

Table 6.3 shows the coordinates of the common points and the centres of the critical circular slip surfaces generated by the application of Pattern 3 rainfall on a 1V:0.5H sandy soil slope at selected times. For the lower total cumulative rainfall of 310 mm, it can be seen that the slope had already failed at the end of t = 17 days with a FoS = 0.82. The amount of rainfall received during this time was 155.2 mm. However, for the higher rate of rainfall, it shows that at t = 8 days, the FoS = 0.99. During this period the amount of rainfall applied to the slope was 116. 8 mm.

The position of these circular slip surfaces is shown in Figure 6.3(a) for total cumulative rainfall of 310 mm, and Figure 6.3(b) for total cumulative rainfall of 496 mm. Similar to previous rainfall patterns, it can be seen that the higher rainfall caused a deeper location of the critical slip surface and lowered the magnitude of the FoS further for the equivalent time within the rainfall period. However, like Pattern 1 rainfall, it shows that the location of the slip surface remained the same at t = 26 days and t = 34 days. In addition to this, unlike Pattern 1 rainfall, the FoS against failure during these two periods remained equal.

Table 6.3 The position of circular slip surface and the factor of safety due to the application of Pattern 3 rainfall on 1V:0.5H sand slope

Total rainfall (mm)	Time, t (day)	Cumulative rainfall (mm) at different 't')	Coordinates of the common point (m)			Critical circle				
						Centre			Radius (m)	FoS
			No.	x	y	location	x	y		
	0	0	20	49.5	20	t0	53	40	20.30	1.79
310	8	73	12	45.5	28	t8	83	54	45.63	1.25
	17	155	19	49	21	t17	77	48	38.90	0.82
	26	237	19	49	21	t26	81	54	45.97	0.77
	34	310	19	49	21	t34	81	54	45.97	0.77
496	8	117	13	46	27	t8	77	52	39.82	0.99
	17	248	19	49	21	t17	83	54	47.38	0.77
	26	380	19	49	21	t26	81	54	45.97	0.76
	34	496	19	49	21	t34	81	54	45.97	0.76

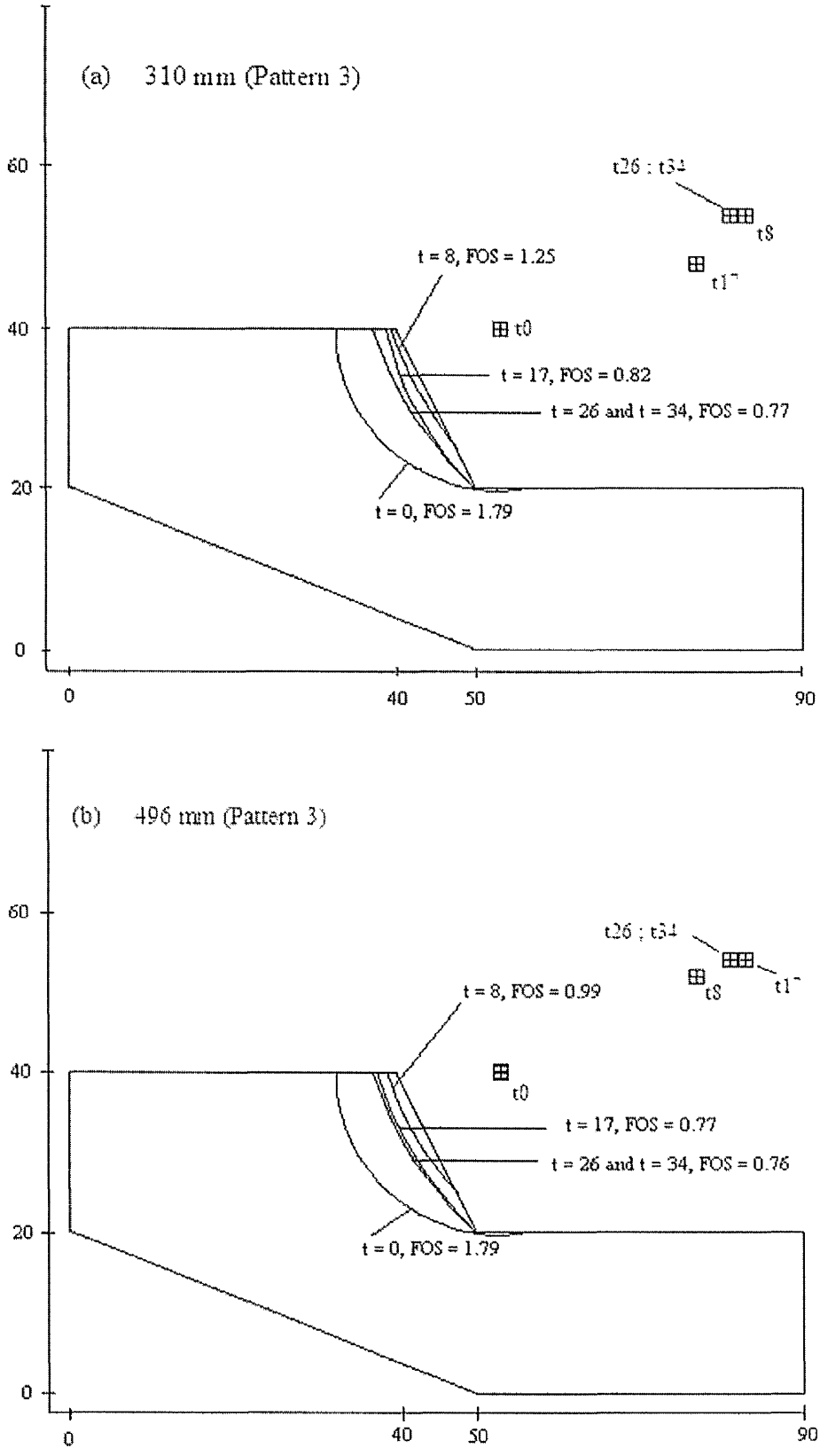

Figure 6.3 The location of the critical circular slip surface with time on a 1V:0.5H sandy soil type slope subjected to Pattern 3 rainfall with total cumulative rainfall of (a) 310 mm and (b) 496 mm

6.2.2 1V:1H sandy soil type slope

Initially at t = 0, i.e. prior to the start of the rainfall with the phreatic surface in equilibrium, the factor of safety of the 1V:1H sandy soil type slope against failure was equal to 2.01. The soil strength parameters for the 1V:1H sandy soil slope were identical to those adopted for the 1V:0.5H sandy soil slope. The changes in FoS and the coordinates of the common points and the centre of the circle with time due to the application of Pattern 1 rainfall are shown in Table 6.4 and illustrated further in Figure 6.4. The application of Pattern 1 rainfall instantly caused a reduction in the FoS against failure of the 1V:1H sand slope, however for the lower total rainfall of 310 mm, it shows that at t = 1 day, the location of the critical slip surface only migrated upwards a small distance from its initial position. A shallow circular slip surface was formed at t = 3 days, and thereafter to deepen with time.

Unlike the case of the lower rainfall amount, application of the higher rainfall intensity with total amount of 496 mm in 34 days shifted the initial circular slip surface almost instantly to close to the surface, whereupon it slowly deepened with time. By comparing the lower and the higher rainfall amount, it also shows that the higher intensity rainfall reduced the value of FoS further than the lower rainfall intensity. It was also observed that, as rainfall stopped at the end of t = 20 days, because of the distribution of rainfall within the trial period, the FoS magnitude started to increase. This behaviour was similar to that in the case of the 1V:0.5H slope. In addition to this, despite the small differences in FoS values at the end of t = 34 days, both lower and higher cumulative rainfall caused a similar positioning of the circular slip surface at the end of this period.

It should be noted that, even though there was a reduction in factor of safety due to the application of Pattern 1 rainfall, it shows that for both lower and higher rainfall intensity with total cumulative rainfall of 310 mm and 496 mm respectively, the 1V:1H sand slope remained stable (i.e. FoS >1.0) throughout the 34-day rainfall period.

Table 6.4 The position of circular slip surface and the factor of safety due to the application of Pattern 1 rainfall on 1V:1H sand slope

Total rainfall (mm)	Time, t (day)	Cumulative rainfall (mm) at different 't'	Coordinates of the common point (m)			Critical circle				
						Centre			Radius (m)	FoS
			No.	x	y	location	x	y		
	0	0	23	62	17	t0	58	40	23.35	2.01
310	1	85	22	61	18	t1	58	40	22.20	1.85
	3	168	14	53	26	t3	86	74	58.25	1.37
	6	235	19	58	21	t6	78	60	43.83	1.20
	20	310	19	58	21	t20	72	54	35.85	1.20
	34	310	19	58	21	t34	76	62	44.78	1.23
496	1	137	16	55	24	t1	74	50	32.20	1.83
	3	268	18	57	22	t3	88	72	58.83	1.22
	6	376	19	58	21	t6	76	60	42.95	1.16
	20	496	19	58	21	t20	78	66	49.24	1.21
	34	496	19	58	21	t34	76	62	44.78	1.22

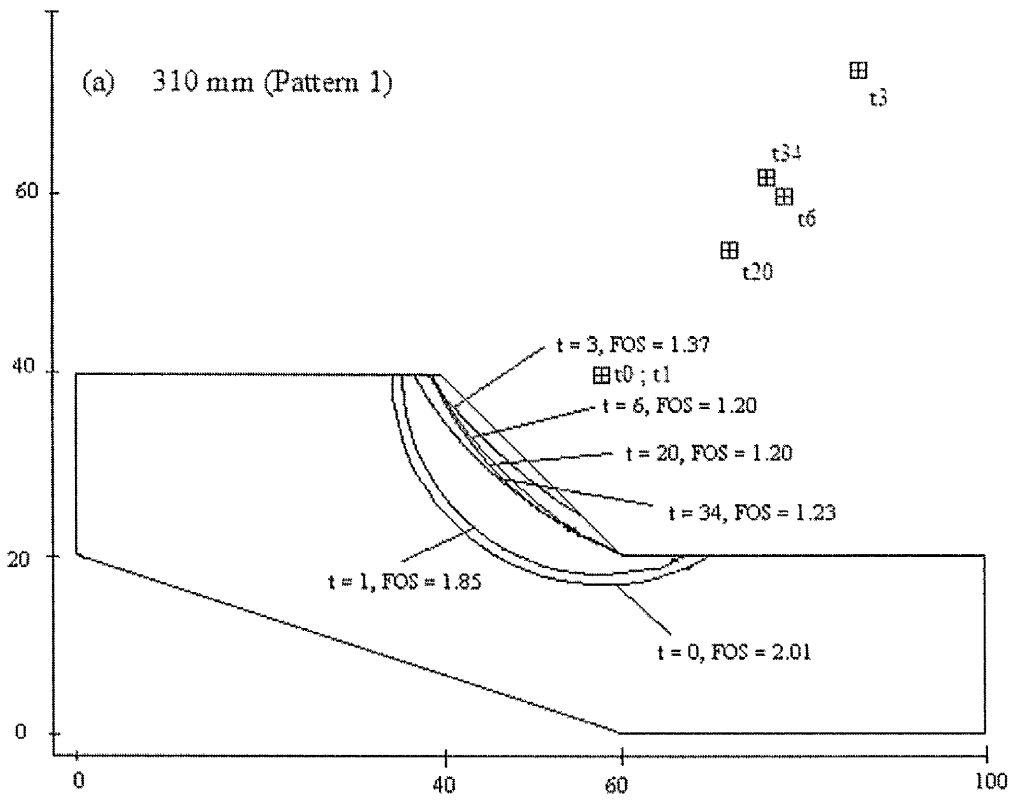

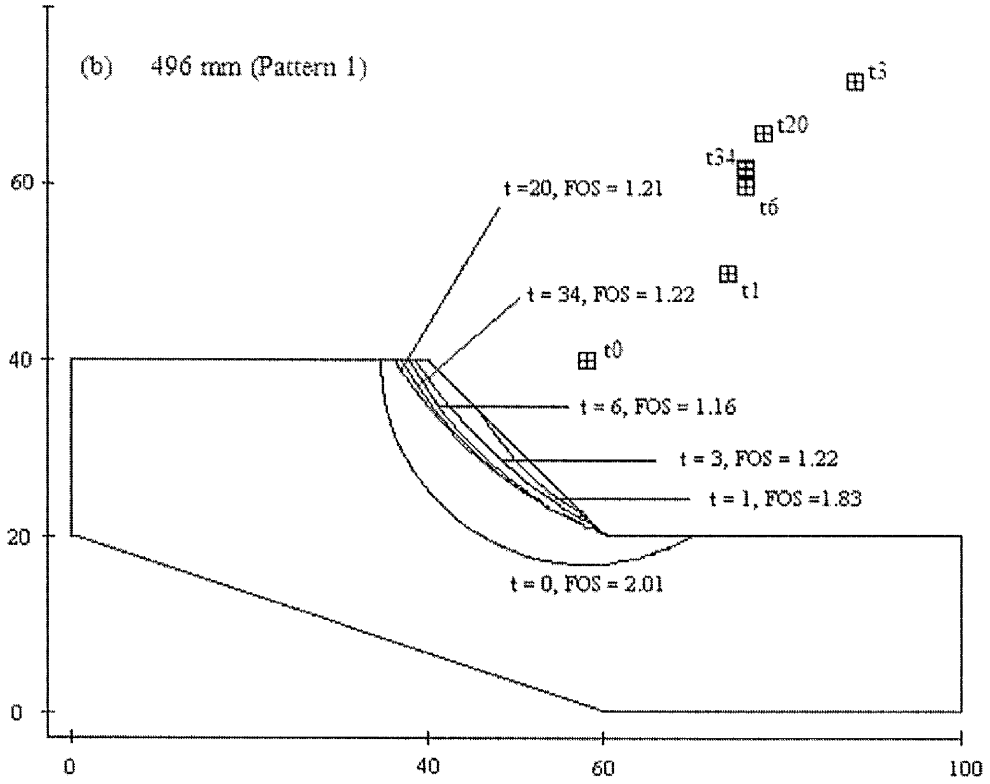

Figure 6.4 The location of the critical circular slip surface with time on a 1V:1H sandy soil type slope subjected to Pattern 1 rainfall with total cumulative rainfall of (a) 310 mm and (b) 496 mm

Similar to Pattern 1 rainfall, the factor of safety during the 34-day period of Pattern 2 rainfall remained above unity. The magnitude of the factor of safety with time and the coordinates of the common points and the centre of circle for the slip surface due to the application of Pattern 2 rainfall are shown in Table 6.5 and are illustrated diagrammatically in Figure 6.5.

At the end of t = 22 days of the lower rainfall intensity, it can be seen that the potential slip surface only migrated at a small distance away from the location of the slip surface generate initially staying at this position until the end of t = 26 days. The difference between the FoS values during this time was only 0.01. As rainfall continued, the slip surface moved closer to the surface and the FoS reduced further to 1.41, and at t = 34 days, as the FoS continued to decrease the slip surface moved deeper within the slope.

It was also observed that the location of the circular slip surface and the value of FoS at the end of t = 22 days due to the application of the higher intensity rainfall of Pattern 2 was similar to those values resulting from the lower intensity rainfall.

However, at t = 26 days, it was observed that the position of the slip surface moved closer to the surface and later slowly deepened with time. By comparing the higher and the lower rainfall amount, it can be seen that the introduction of a higher rainfall intensity caused a further reduction of the value of the factor of safety until the end of t = 34 days.

Table 6.5 The position of circular slip surface and the factor of safety due to the application of Pattern 2 rainfall on 1V:1H sand slope

Total rainfall (mm)	Time, t (day)	Cumulative rainfall (mm) at different 't'	Coordinates of the common point (m)			Critical circle				
						Centre			Radius (m)	FoS
			No.	x	y	location	x	y		
	0	0	23	62	17	t0	58	40	23.35	2.01
310	22	20	22	61	18	t22	58	40	22.20	1.87
	26	50	22	61	18	t26	58	40	22.20	1.86
	31	143	14	53	26	t31	88	76	61.03	1.41
	34	310	18	57	22	t34	86	72	57.80	1.20
496	22	32	22	61	18	t22	58	40	22.20	1.87
	26	80	15	54	25	t26	66	44	22.47	1.77
	31	228	18	57	22	t31	92	76	64.35	1.24
	34	496	19	58	21	t34	78	62	45.62	1.14

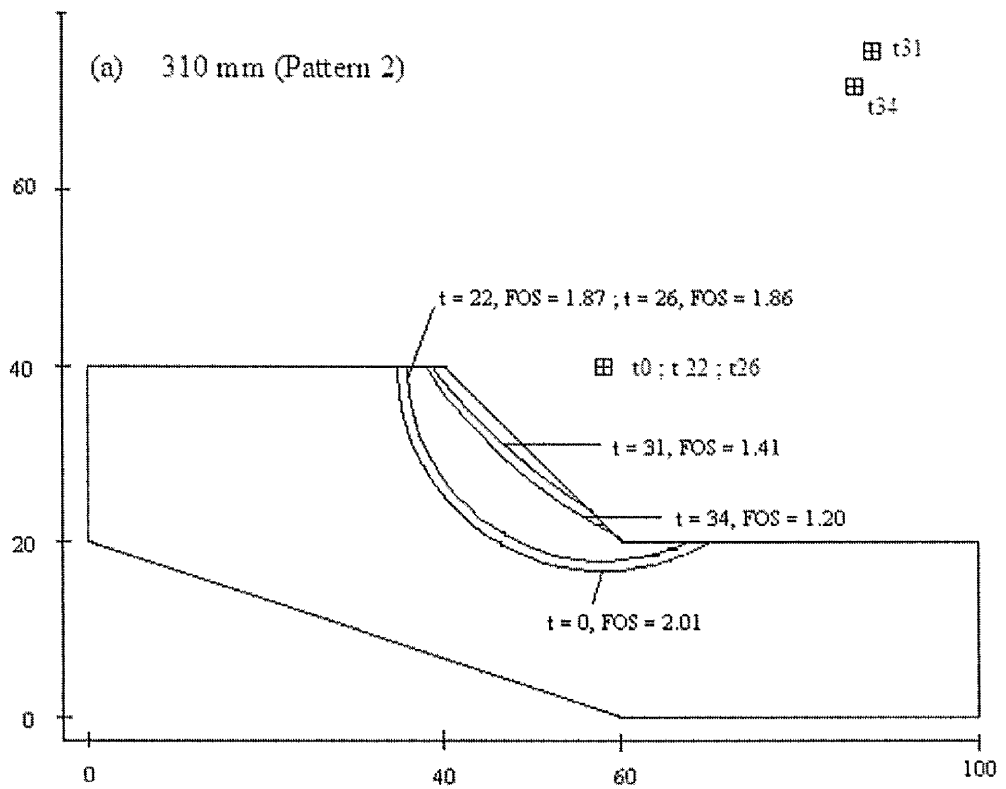

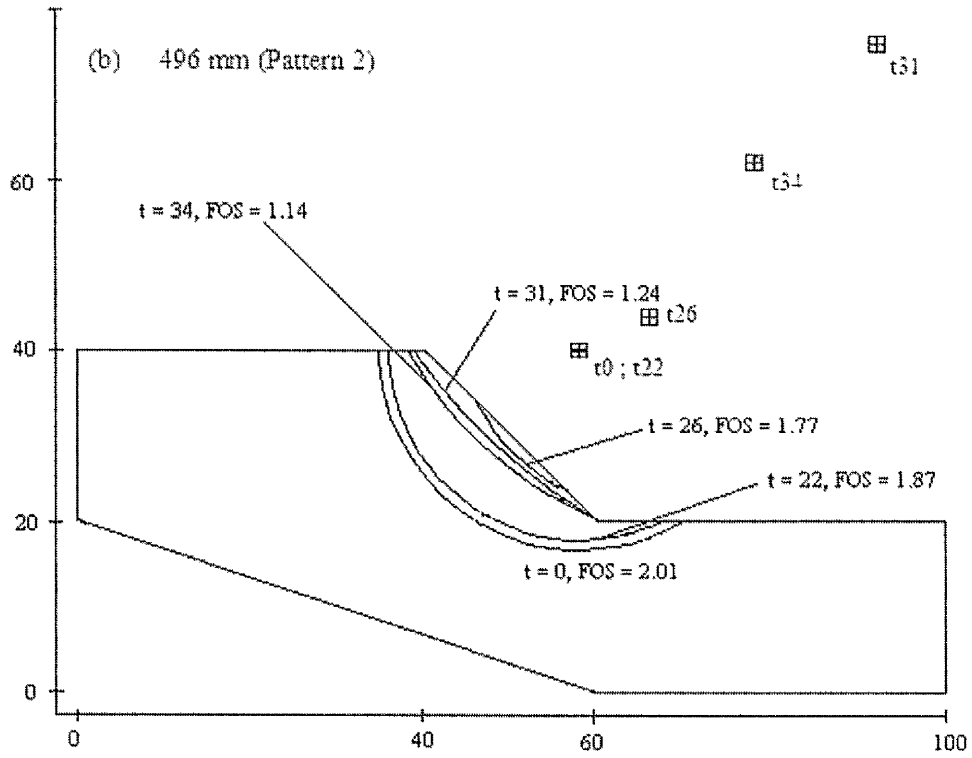

Figure 6.5 The location of the critical circular slip surface with time on a 1V:1H sandy soil type slope subjected to Pattern 2 rainfall with total cumulative rainfall of (a) 310 mm and (b) 496 mm

Table 6.6 shows the coordinates of the common points and the centres of the circles for the critical slip surfaces at different times generated by the application of Pattern 3 rainfall having a total 34-day cumulative rainfall of both 310 mm and 496 mm. A reduction of factor of safety was observed as the rainfall was applied to the surface of the 1V:1H sandy soil slope becoming constant from t = 26 days to the end of the period of rainfall. The introduction of the higher rainfall intensity caused a further reduction in the FoS. However from the end of t = 26 days onwards, the difference of the FoS magnitudes between the lower and higher rainfall intensities was only 0.01.

A better illustration of these slip surfaces can be seen in Figure 6.6. For the lower rainfall intensity, it shows that at t = 8 days, a small circular slip surface was forming at the bottom of the slopes continuing to deepen and widen with time. However, the positions of the slip surfaces at the end of t = 26 days and t = 34 days were considered to be very close to one another. Similar to previous observations during higher rainfall intensities, Figure 6.6 shows that the application of a higher overall

rainfall intensity caused the slip surface to deepen further and a constant location of the slip surface was reached at an earlier time in comparison with the lower rainfall amount.

Table 6.6 The position of circular slip surface and the factor of safety due to the application of Pattern 3 rainfall on 1V:1H sand slope

Total rainfall (mm)	Time, t (day)	Cumulative rainfall (mm) at different 't'	Coordinates of the common point (m)			Critical circle				
						Centre			Radius (m)	FoS
			No.	x	y	location	x	y		
	0	0	23	62	17	t0	58	40	23.35	2.01
310	8	73	16	55	24	t8	70	46	26.63	1.80
	17	155	18	57	22	t17	88	72	58.83	1.27
	26	237	19	58	21	t26	78	62	45.62	1.19
	34	310	19	58	21	t34	74	58	40.31	1.19
496	8	117	14	53	26	t8	88	76	61.03	1.44
	17	248	19	58	21	t17	82	68	52.77	1.19
	26	380	19	58	21	t26	76	60	42.95	1.18
	34	496	19	58	21	t34	76	60	42.95	1.18

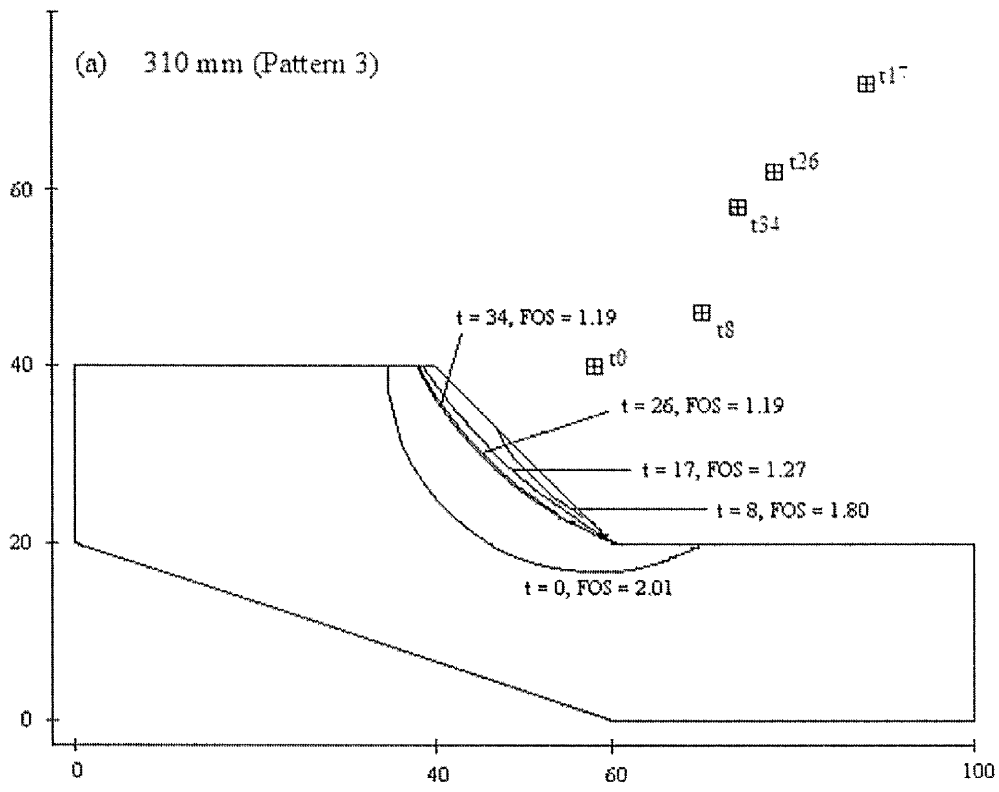

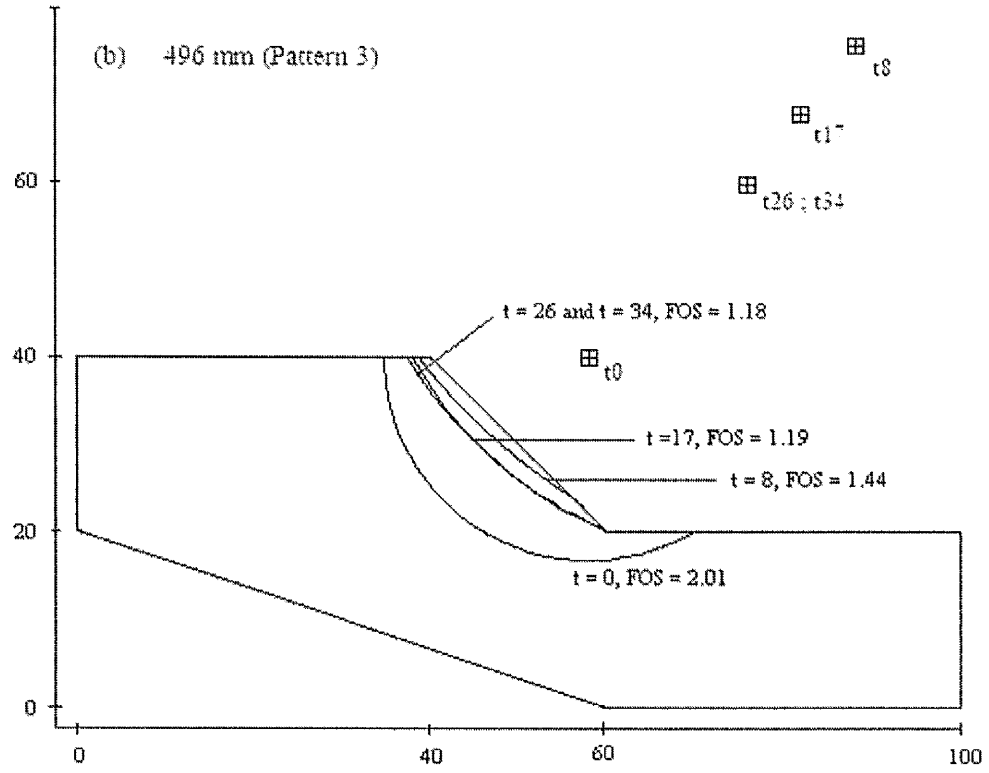

Figure 6.6 The location of the critical circular slip surface with time on a 1V:1H sandy soil type slope subjected to Pattern 3 rainfall with total cumulative rainfall of (a) 310 mm and (b) 496 mm

6.2.3 Comparison of the effects on the 1V:0.5H and 1V:1H sandy soil slopes

The changes in FoS with time as tabulated from Tables 6.1 to 6.6, for both 1V:0.5H and 1V:1H sand slopes is also illustrated in Figure 6.7.

By assuming that all rainfall infiltrated into the 1V:0.5H sandy soil slopes and by looking at Table 6.1, Table 6.2 and Table 6.3, it may be concluded that the magnitude of the FoS was less than unity when the slope had received a total amount of rainfall greater than 117 mm. However, for 1V:1H sandy soil slopes, it shows that for all rainfall patterns the slope remained stable throughout the 34 days of rainfall duration. It can also be noted that for both geometries, it shows that the introduction of a higher rainfall intensity caused a further deepening of the location of the slip surface.

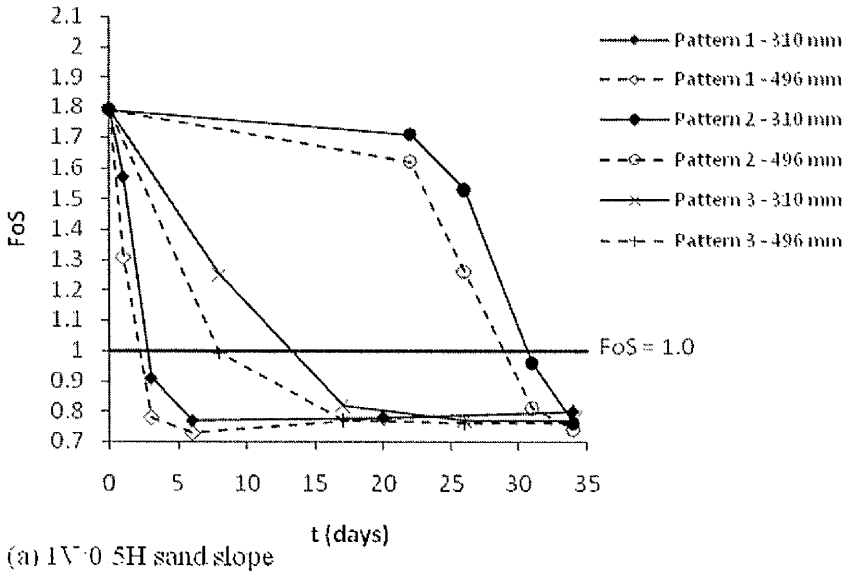

(a) 1V:0.5H sand slope

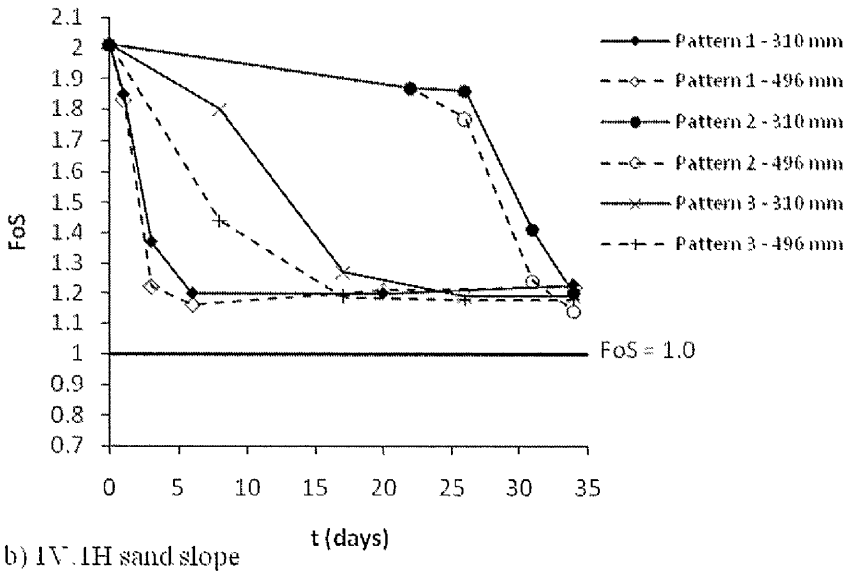

(b) 1V:1H sand slope

Figure 6.7 The changes in FoS with time for (a) 1V:0.5H sand slope and (b) 1V:1H sand slope for different rainfall patterns and total amount

From the above discussion, it can be inferred that the higher intensity of rainfall does not necessarily reduce the factor of safety instantly and antecedent rainfall plays a major role in the reduction of the factor of safety. The magnitude of the FoS started to increase as rainfall effectively stopped at the end of t = 20 days of Pattern 1 rainfall. However, the increase in the FoS value was considered small. It was also observed that the constant location of the slip surface and the value of the FoS were achieved towards the end of the Pattern 3 rainfall.

It may be inferred that the depth of the wetting fronts only influenced the depth of the slip surface and the magnitudes of FoS at certain periods of time. Changes of factor of safety and the position of the critical slip surface only occurred during the earlier stages of the rainfall duration. However, after a certain period of time, i.e. when the depth of the wetting front began deepening, it did not influence the magnitude of the factor of safety nor the position of the critical slip surface.

6.3 Presentation of the stability of the slopes in silty type soil

From Chapter 5, it can be seen that the depths of the wetting fronts in silty soil slopes were shallower at equivalent time periods compared with the depths observed in the sandy soil slopes. Thus, it is expected that it would take a longer time for the circular slip surface to move closer to the slope surface in silty soils.

In this section, the changes in the generated factors of safety for 1V:0.5H silty soil slopes and 1V:1H silty soil slopes at selected times for Pattern 1, Pattern 2 and Pattern 3 rainfall with total rainfalls of 310 mm and 496 mm are presented. At t = 0 (i.e. equilibrium phreatic surface – no rain), it was found that the factors of safety for the 1V:0.5H and 1V:1H silt slopes were 1.79 and 2.01 respectively.

6.3.1 1V:0.5H silty soil type slope

The magnitude of the factors of safety, the coordinates of the common points and the centres of circles for critical slip surfaces that were obtained at specific times during the application of Pattern 1 rainfall on a 1V:0.5H silty soil slope are tabulated in Table 6.7. The locations of the slip surfaces and other details are illustrated in Figure 6.8. It shows that the magnitudes of the factors of safety were slowly reduced with time. However for the lower cumulative rainfall of 310 mm over the 34 day period, the position of slip surface stayed at the location initially found at t = 1 day until the end of t = 3 days. A shallow slip surface was observed at the end of t = 6 days at the bottom of the slope and it widened and deepened with time just as the factor of safety continued to decrease with time. Throughout the 34-days rainfall duration, however, it may be seen that the magnitude of the FoS value was always greater than unity.

Table 6.7 The position of circular slip surface and the factor of safety due to the application of Pattern 1 rainfall on 1V:0.5H silt slope

Total rainfall (mm)	Time, t (day)	Cumulative rainfall (mm) at different 't'	Coordinates of the common point (m)			Critical circle				
						Centre			Radius (m)	FoS
			No.	x	y	location	x	y		
	0	0	20	49.5	20	t0	53	40	20.30	1.79
310	1	85	20	49.5	20	t1	53	40	20.30	1.76
	3	168	20	49.5	20	t3	53	40	20.30	1.63
	6	235	19	49	21	t6	61	32	16.28	1.63
	20	310	18	48.5	22	t20	71	44	31.47	1.23
	34	310	19	49	21	t34	73	46	34.66	1.14
496	1	137	20	49.5	20	t1	53	40	20.30	1.75
	3	268	8	43.5	32	t3	71	40	28.64	1.59
	6	376	19	49	21	t6	67	38	24.76	1.19
	20	496	19	49	21	t20	83	54	47.38	0.96
	34	496	19	49	21	t34	75	50	38.95	0.97

The application of the higher cumulative rainfall of 496 mm over the 34 day period resulted in a further reduction in the value of FoS. The position of the slip surface remained at the initial position until the end of t = 1 day. At the end of t = 3 days, a shallow slip surface was generated and again slowly deepened with time. From Table 6.7 and Figure 6.8, it can be seen that at the end of 20 days of Pattern 1 rainfall, the 1V:0.5H silty soil slope could already be considered as having failed as the value of FoS reduced to below unity.

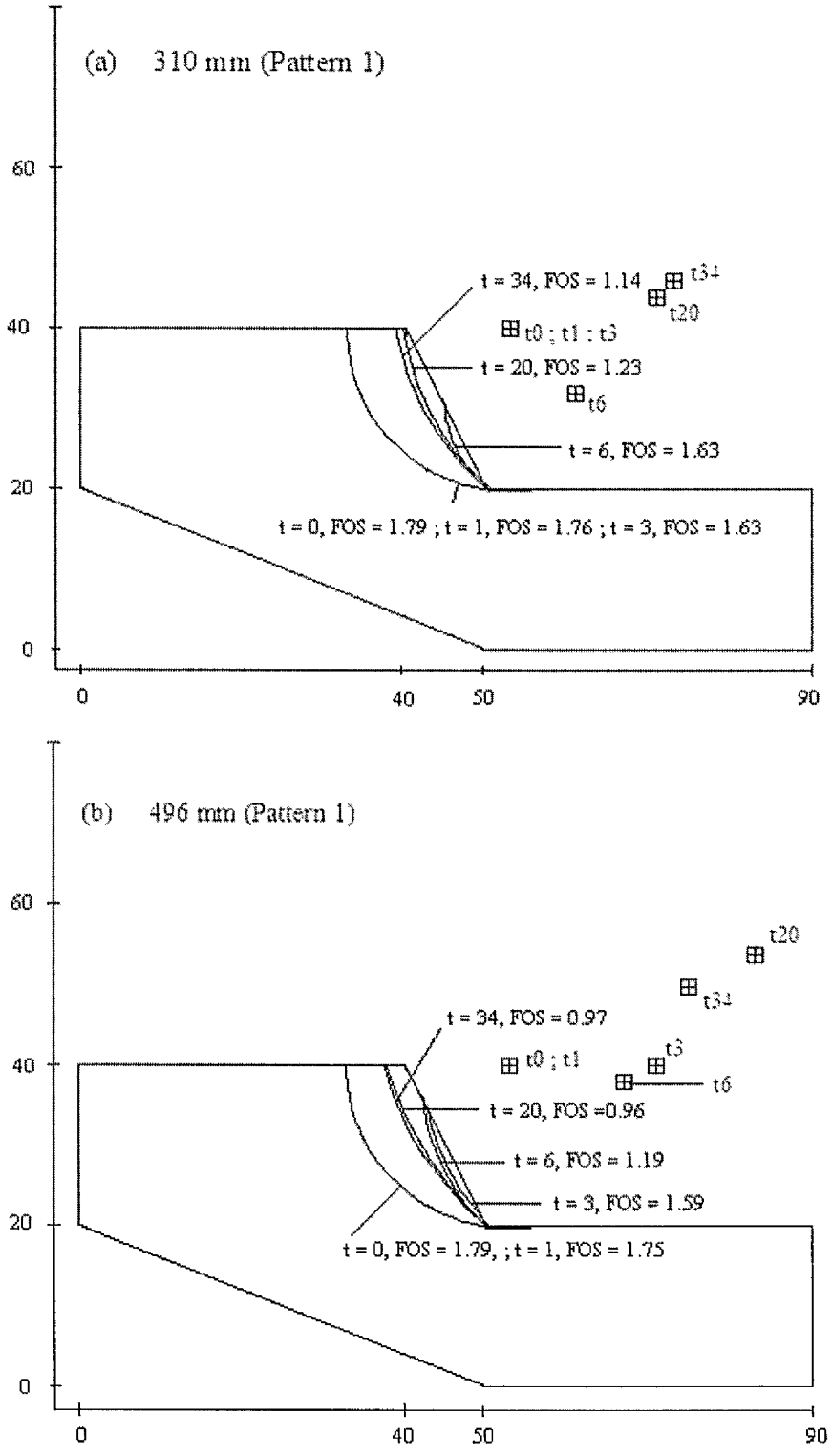

Figure 6.8 The location of the critical circular slip surface with time on a 1V:0.5H silty soil type slope subjected to Pattern 1 rainfall with total cumulative rainfall of (a) 310 mm and (b) 496 mm

The location of the critical slip surface due to the application of Pattern 2 rainfall on the 1V:0.5H silty soil slope was only affected at the end of t = 34 days. This is shown in Table 6.8 and Figure 6.9 below. It shows that even though the position of the slip surface stayed at the initial position found at the beginning of the rainfall period, the magnitude of the FoS continued to decrease slowly with time.

At the end of t = 26 days and t = 31 days of higher rainfall (i.e. 496mm), it can be seen that the application of a higher rainfall appears to cause an increase in the factor of safety by a marginal amounts, 0.04 and 0.03 respectively. These differences were considered small. It should be noted that the increase in FoS due to higher rainfall in this case was a bit suspicious. A large decrease in FoS to 1.02 was observed to have progressively occurred in the period just prior to t = 34 days.

Table 6.8 The position of circular slip surface and the factor of safety due to the application of Pattern 2 rainfall on 1V:0.5H silt slope

Total rainfall (mm)	Time, t (day)	Cumulative rainfall (mm) at different 't'	Coordinates of the common point (m)			Critical circle				
						Centre			Radius (m)	FoS
			No.	x	y	location	x	y		
	0	0	20	49.5	20	t0	53	40	20.30	1.79
310	22	20	20	49.5	20	t22	53	40	20.30	1.78
	26	50	20	49.5	20	t26	53	40	20.30	1.72
	31	143	20	49.5	20	t31	53	40	20.30	1.64
	34	310	19	49	21	t34	61	32	16.28	1.48
496	22	32	20	49.5	20	t22	53	40	20.30	1.78
	26	80	20	49.5	20	t26	53	40	20.30	1.76
	31	228	20	49.5	20	t31	53	40	20.30	1.67
	34	496	19	49	21	t34	65	36	21.93	1.02

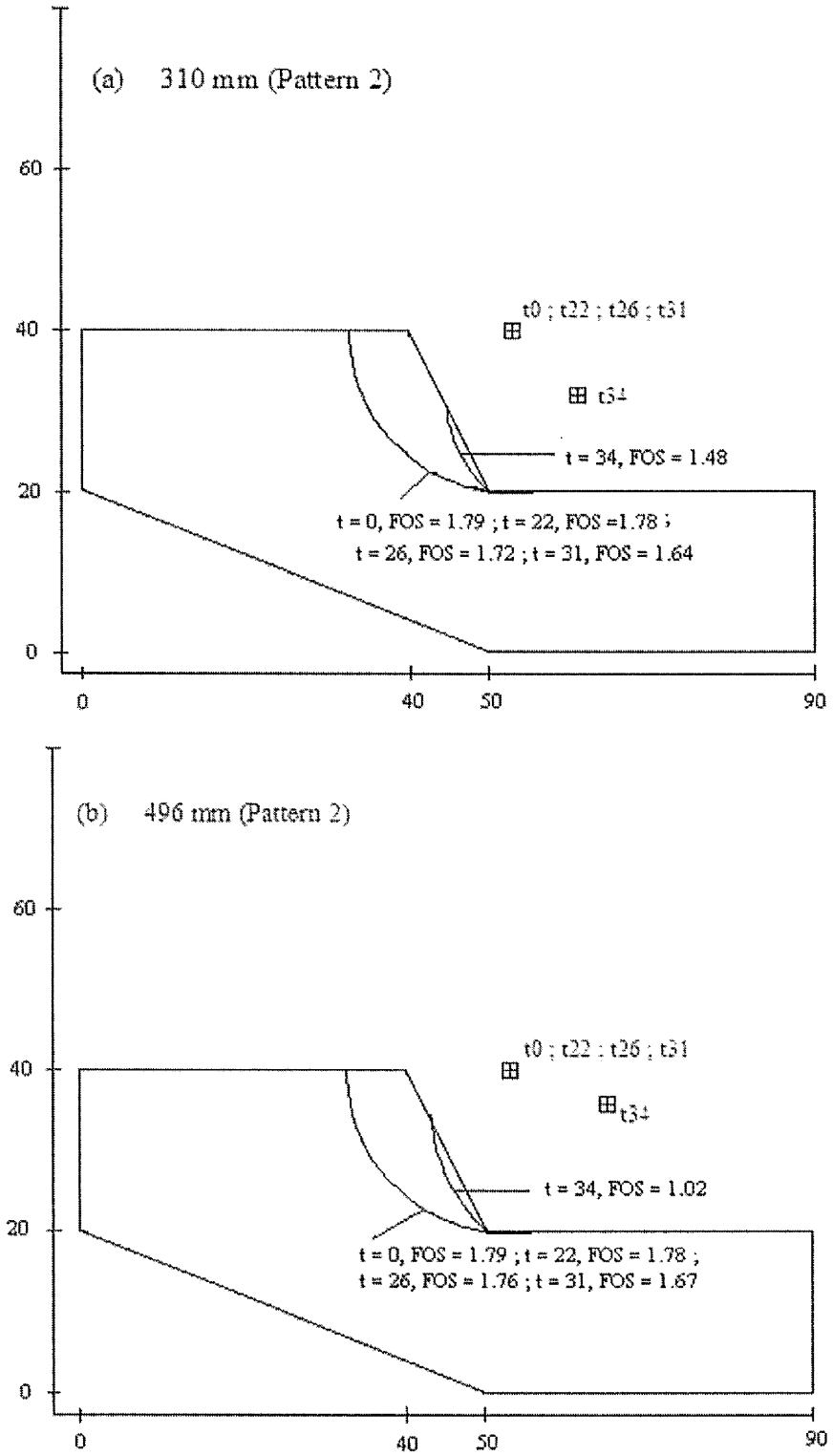

Figure 6.9 The location of the critical circular slip surface with time on a 1V:0.5H silty soil type slope subjected to Pattern 2 rainfall with total cumulative rainfall of (a) 310 mm and (b) 496 mm

As shown in Table 6.9 and Figure 6.10, the application of Pattern 3 rainfall with base case rainfall intensity of 310 mm did not affect the movement of the location of the

critical slip surface until about the end of t = 17 days. By the end of the period t = 26 days, a shallow critical slip surface was generated near to the surface of the slope progressively deepening to the end of t = 34 days. During the 34 day period of Pattern 3 rainfall, the FoS of the slope against failure continued to decrease with time, with the location of a potential slip surface remaining at the same position for approximately the first 17 days of the period.

The introduction of the higher intensity Pattern 3 rainfall on the 1V:0.5H silty soil slope resulted in a more rapid reduction in the degree of stability of the slope shown by a greater reduction in FoS than that observed during the base case rainfall period. Unlike in the case of the lower rainfall, the location of the critical slip surface only remained close to the position found at the start of the rainfall until the end of t = 8 days. At the end of t = 17 days, the location of the critical slip surface migrated towards a shallow position just below the slope surface and then moved down within the slope encapsulating an increasing mass of soil with further time. It can also be seen that at the end of t = 26 days and t = 34 days, the positions of the critical slip surfaces generated during both periods were almost very similar. As in the case of the Pattern 2 rainfall, the magnitudes of the FoS remained above unity throughout the 34 day rainfall period. The lowest value of FoS, i.e. FoS = 1.02, was obtained at the end of t = 34 days of the enhanced rainfall intensity of 496 mm.

Table 6.9 The position of circular slip surface and the factor of safety due to the application of Pattern 3 rainfall on 1V:0.5H silt slope

Total rainfall (mm)	Time, t (day)	Cumulative rainfall (mm) at different 't'	Coordinates of the common point (m)			Critical circle				
						Centre			Radius (m)	FoS
			No.	x	y	location	x	y		
	0	0	20	49.5	20	t0	53	40	20.30	1.79
310	8	73	20	49.5	20	t8	53	40	20.30	1.76
	17	155	20	49.5	20	t17	53	40	20.30	1.64
	26	237	19	49	21	t26	65	36	21.93	1.51
	34	310	18	48.5	22	t34	79	48	40.08	1.28
496	8	117	20	49.5	20	t8	53	40	20.30	1.70
	17	248	19	49	21	t17	65	36	21.93	1.49
	26	380	18	48.5	22	t26	87	54	50.06	1.12
	34	496	19	49	21	t34	75	46	36.07	1.02

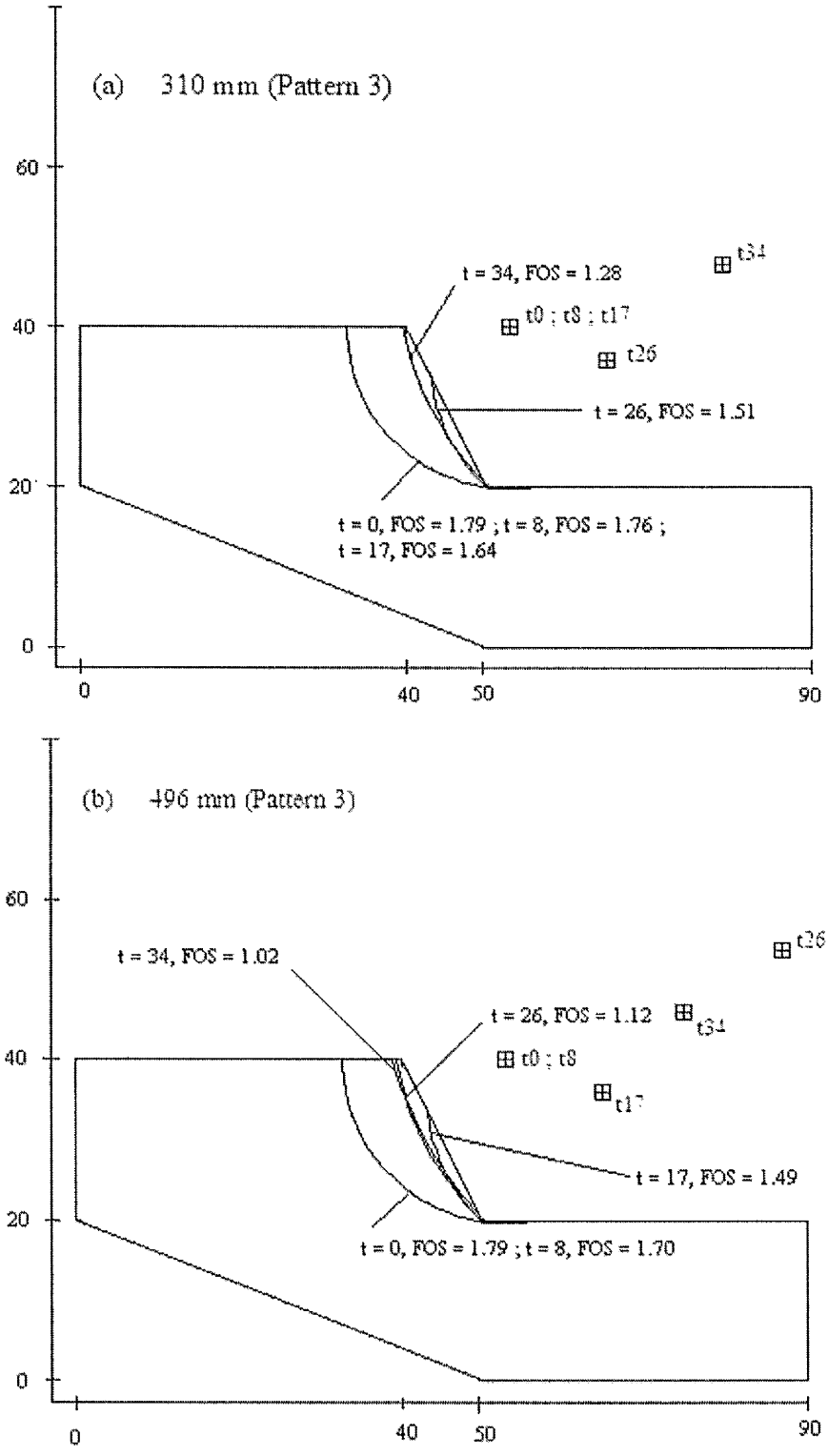

Figure 6.10 The location of the critical circular slip surface with time on a 1V:0.5H silty soil type slope subjected to Pattern 3 rainfall with total cumulative rainfall of (a) 310 mm and (b) 496 mm

6.3.2 1V:1H silty soil type slope

In this section the results of the effects on the stability of a 1V:1H silty soil slope are presented for three rainfall patterns and the two maximum cumulative rainfall values of 310 mm and 496 mm over the standard period of 34 days.

The coordinates of the common points and the centre of the circle for the location of the critical circular slip surface and the magnitude of the factor of safety at various times during the period of Pattern 1 rainfall are tabulated in Table 6.10 and the positions of these slip surfaces are also illustrated in Figure 6.11. It shows that for lower base case total rainfall of 310 mm, at the end of t = 1 day, the position of the critical slip surface was located just above the initial position (t = 0 days) remaining at this position until at least the end of t = 6 days. At the end of t = 1 day, the magnitude of the FoS reduced to 1.87. However, it shows that at the end of t = 3 days and at the end of t = 6 days, the FoS increased slightly to 1.88 and 1.90 respectively. From these small changes, the assumption is that the application of rainfall for the first 6 day period had only a minimal effect on both the location of the critical slip surface and the magnitude of FoS. However, at the end of t = 20 days, a shallow slip surface was observed forming within the slope and deepening slightly towards the end of t = 34 days. At the end of t = 34 days, the FoS reduced to the lowest value of 1.72.

In the case of the higher rainfall intensity, i.e. of 496 mm, the critical slip surface showed a small migration staying at this location until the end of t = 3 days. A shallow critical circular slip surface was observed at the end of t = 6 days. Thereafter the failure surface slowly deepened until the end of t = 34 days. At this time, the magnitude of the FoS was 1.44. It was observed that throughout the 34 days duration of pattern 1 rainfall, the value of the factor of safety for 1V:1H silt slope remained above unity.

Table 6.10 The position of circular slip surface and the factor of safety due to the application of Pattern 1 rainfall on 1V:1H silt slope

Total rainfall (mm)	Time, t (day)	Cumulative rainfall (mm) at different 't'	Coordinates of the common point (m)			Critical circle				
						Centre			Radius (m)	FoS
			No.	x	y	location	x	y		
	0	0	23	62	17	t0	58	40	23.35	2.01
310	1	85	22	61	18	t1	58	40	22.20	1.87
	3	168	22	61	18	t3	58	40	22.20	1.88
	6	235	22	61	18	t6	58	40	22.20	1.90
	20	310	18	57	22	t20	96	80	69.89	1.75
	34	310	18	57	22	t34	86	72	57.80	1.72
496	1	137	22	61	18	t1	58	40	22.20	1.86
	3	268	22	61	18	t3	58	40	22.20	1.87
	6	376	14	53	26	t6	90	78	63.82	1.74
	20	496	19	58	21	t20	80	64	48.3	1.47
	34	496	19	58	21	t34	82	68	52.77	1.44

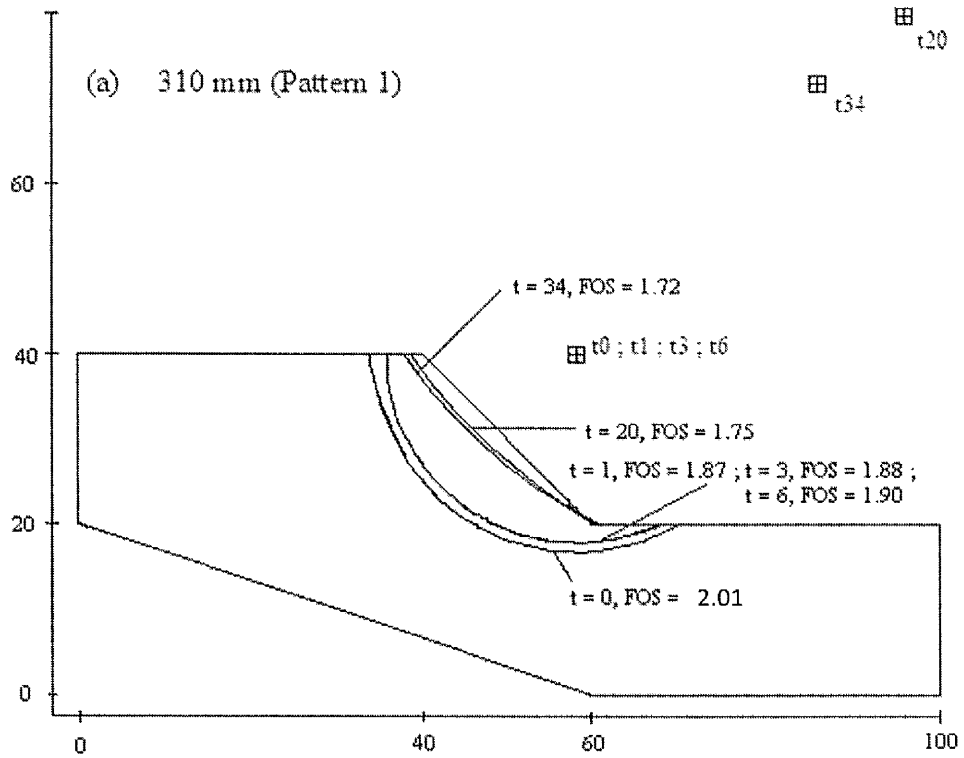

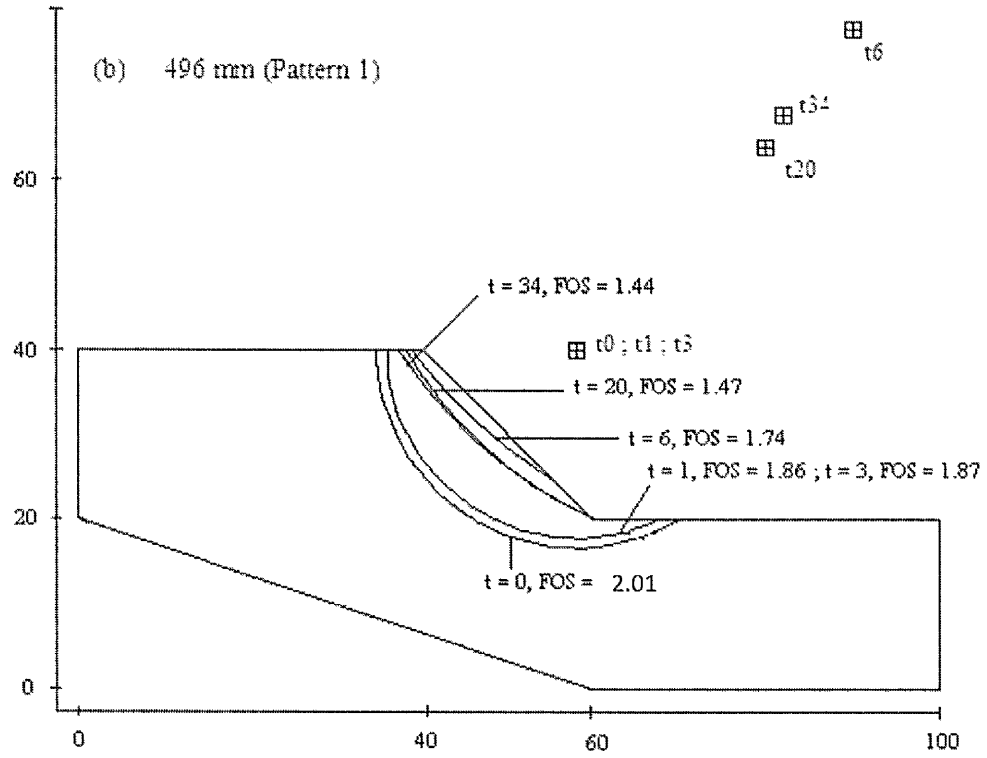

Figure 6.11 The location of the critical circular slip surface with time on a 1V:1H silty soil type slope subjected to Pattern 1 rainfall with total cumulative rainfall of (a) 310 mm and (b) 496 mm

The coordinates of the common points and the centres of critical surfaces for the changes of slip surface and the factor of safety due to the application of Pattern 2 rainfall at selected times are tabulated in Table 6.11 and also illustrated in Figure 6.12. For the case of the lower rainfall intensity, i.e. total of 310 mm, it can be seen that as rainfall was applied to the ground, a new slip surface was formed just above the initial location of the critical slip surface staying at this position until the end of the Pattern 2 rainfall. The value of FoS reduced very slowly with time and by the end of t = 34 days, the FoS only reduced to the lowest value of 1.86.

When the rainfall intensity was increased by 60%, the value of FoS and the location of the critical slip surface at the end of t = 22 days did not differ from those values of lower rainfall intensity. Further reduction in FoS values due to the higher rainfall intensity was observed by the end of t = 26 days and t = 31 days. However, the difference in the magnitude of FoS as a result of both the lower and higher rainfall intensities at equivalent times was only 0.01. It should be noted, however, that the location of the critical slip surface remained in the same position until the end of t =

31 days. At the end of t = 34 days, a shallow slip surface was observed to have formed from the crest to the mid section of the 1V:1H silt slope. The magnitude of the FoS at this time was 1.56. Similar to Pattern 1 rainfall, the FoS value throughout the 34-days of Pattern 2 rainfall was always above unity.

Table 6.11 The position of circular slip surface and the factor of safety due to the application of Pattern 2 rainfall on 1V:1H silt slope

Total rainfall (mm)	Time, t (day)	Cumulative rainfall (mm) at different 't'	Coordinates of the common point (m)			Critical circle				
						Centre			Radius (m)	FoS
			No.	x	y	location	x	y		
	0	0	23	62	17	t0	58	40	23.35	2.01
310	22	20	22	61	18	t22	58	40	22.20	1.92
	26	50	22	61	18	t26	58	40	22.20	1.91
	31	143	22	61	18	t31	58	40	22.20	1.88
	34	310	22	61	18	t34	58	40	22.20	1.86
496	22	32	22	61	18	t22	58	40	22.20	1.92
	26	80	22	61	18	t26	58	40	22.20	1.90
	31	228	22	61	18	t31	58	40	22.20	1.87
	34	496	14	53	26	t34	88	74	59.41	1.56

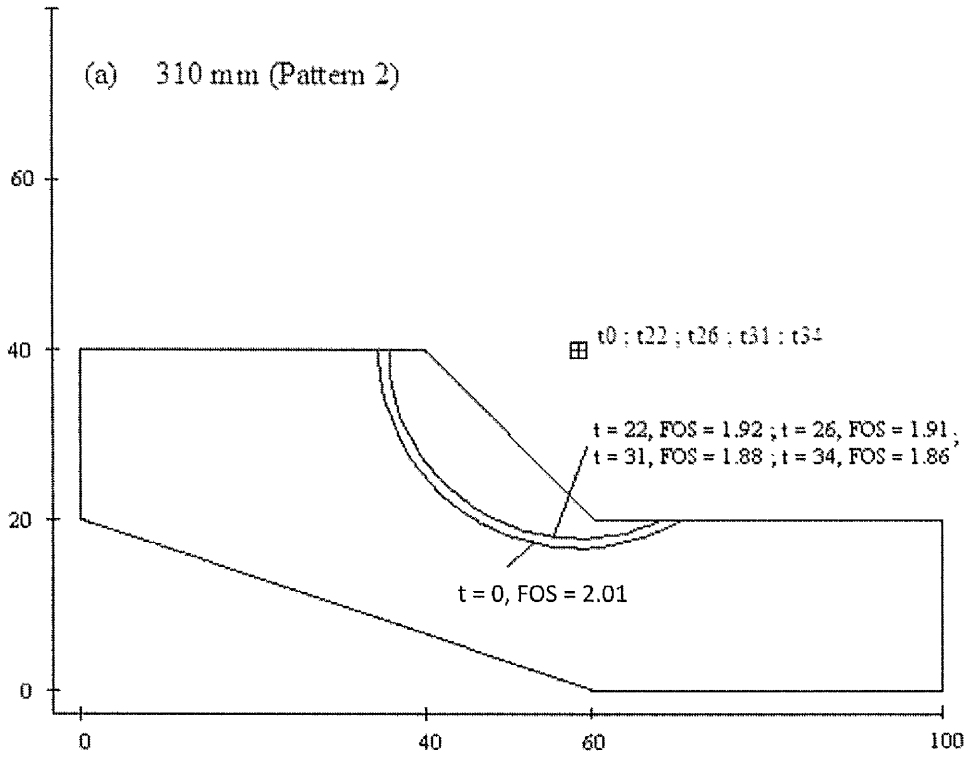

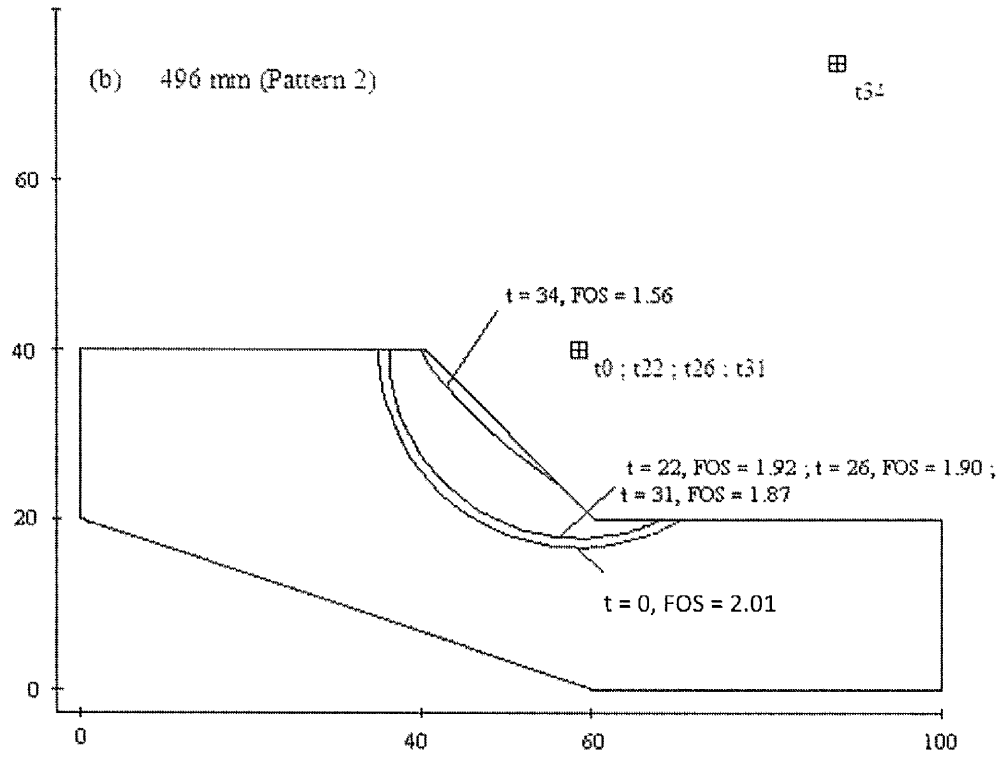

Figure 6.12 The location of the critical circular slip surface with time on a 1V:1H silty soil type slope subjected to Pattern 2 rainfall with total cumulative rainfall of (a) 310 mm and (b) 496 mm

As shown in Table 6.12 and Figure 6.13, the application of lower rainfall intensity of Pattern 3 rainfall on 1V:1H silt slope resulted in the migration of the critical circular slip surface to just above the initial slip surface. The position of critical slip surface stayed at this position until at least the end of t = 26 days. The variation in the factor of safety during this period was very small. At the end of t = 34 days, a shallow critical slip surface was generated near the surface of the slope. At this time the value of FoS = 1.83.

During the first 17 days of the higher intensity rainfall of type Pattern 3, a similar behaviour of the critical slip surface as that produced by the lower intensity rainfall during the same period was observed. However, at the end of t = 26 days, a shallow slip surface was generated just below the surface of the slope and the value of the FoS at this time reduced to 1.68. The critical circular slip surface migrated deeper into the slope by the end of t = 34 days and the FoS value continued to decrease to a terminal value of 1.49. As in the case of Pattern 1 and Pattern 2 rainfall, the factor of

safety against failure for the 1V:1H silty soil slope due to the application of Pattern 3 rainfall remained greater than unity.

Table 6.12 The position of circular slip surface and the factor of safety due to the application of Pattern 3 rainfall on 1V:1H silt slope

Total rainfall (mm)	Time, t (day)	Cumulative rainfall (mm) at different 't'	Coordinates of the common point (m)			Critical circle				
						Centre			Radius (m)	FoS
			No.	x	y	location	x	y		
	0	0	23	62	17	t0	58	40	23.35	2.01
310	8	73	22	61	18	t8	58	40	22.20	1.90
	17	155	22	61	18	t17	58	40	22.20	1.90
	26	237	22	61	18	t26	58	40	22.20	1.89
	34	310	18	57	22	t34	72	50	31.76	1.83
496	8	117	22	61	18	t8	58	40	22.20	1.89
	17	248	22	61	18	t17	58	40	22.20	1.90
	26	380	16	55	24	t26	76	60	41.68	1.68
	34	496	18	57	22	t34	88	72	58.83	1.49

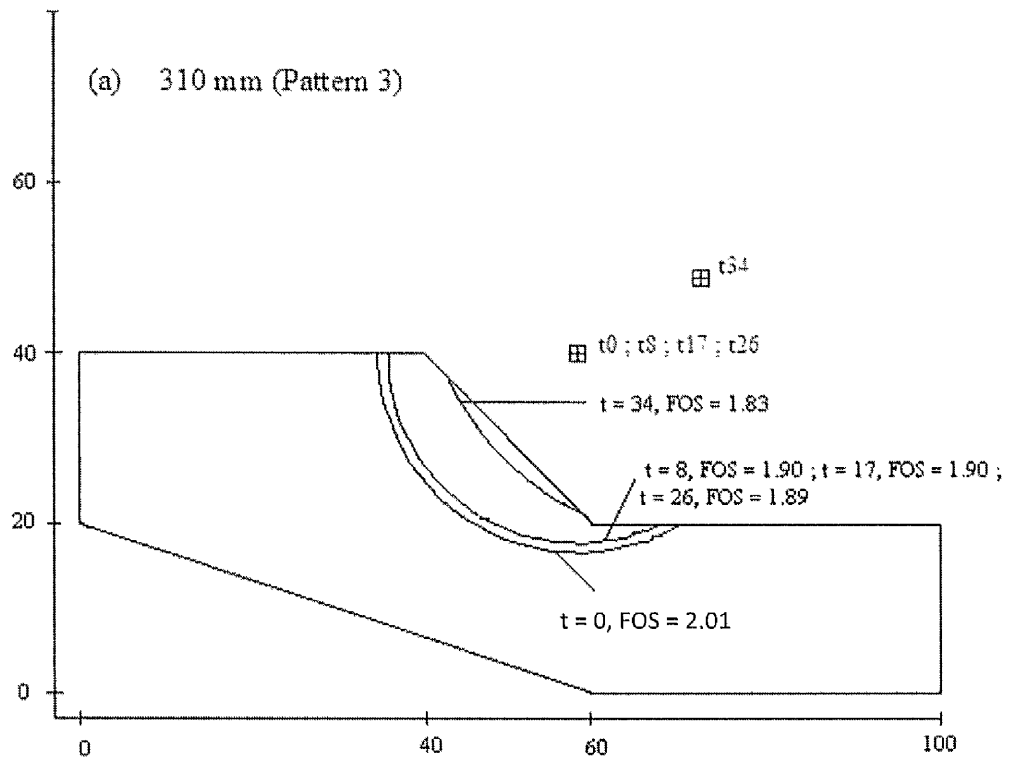

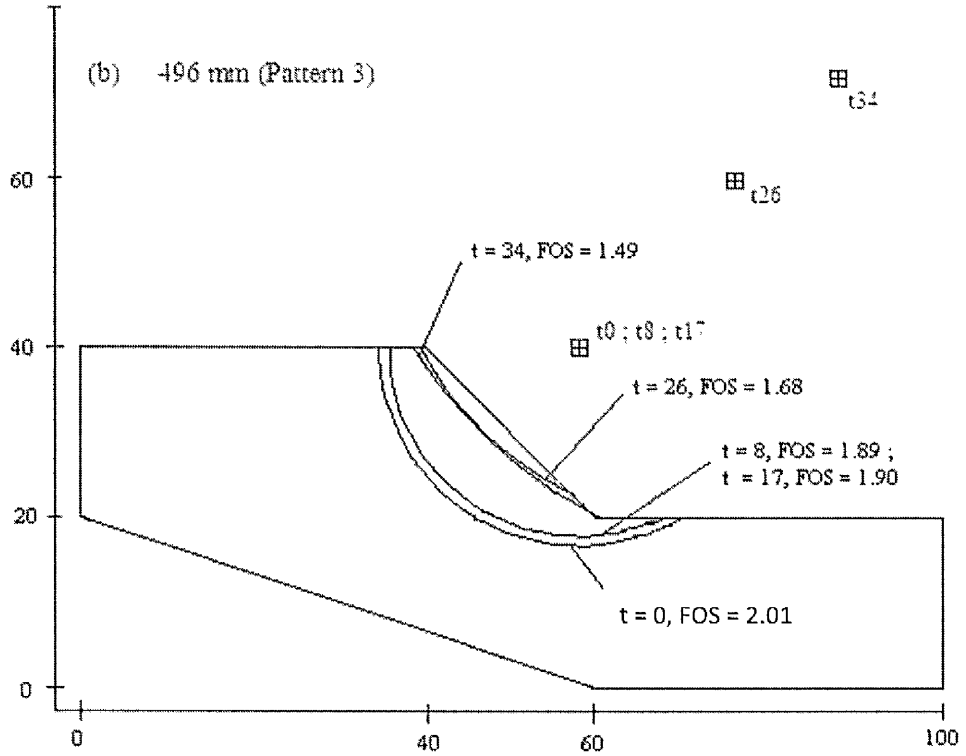

Figure 6.13 The location of the critical circular slip surface with time on a 1V:1H silty soil type slope subjected to Pattern 3 rainfall with total cumulative rainfall of (a) 310 mm and (b) 496 mm

6.3.3 Comparison of the effects on the 1V:0.5H and 1V:1H silty soil slopes

The changes in FoS with time as tabulated from Tables 6.7 to 6.12, for both 1V:0.5H and 1V:1H silt slopes is also illustrated in Figure 6.14.

Generally, based on the discussion above, the silty soil type slope appears to remain stable for the typical rainfall patterns applied to it, except at the end of t = 20 days and t = 34 days where the value of the FoS reduced to below unity (given the soil strength parameters) as shown in Table 6.7. These values of FoS were observed as a result of the application of the higher rainfall intensity of type Pattern 1 rainfall on the 1V:0.5H slope. However, it is also noted that even after the rainfall ceased at the end of t = 20 days of Pattern 1 rainfall, the magnitudes of the FoS continued to decrease to the end of t = 34 days. It is believed that the FoS value continued to reduce even after the 34-days rainfall duration as a result of further migration of the

pore water pressures through the slope, notwithstanding the termination of the rainfall.

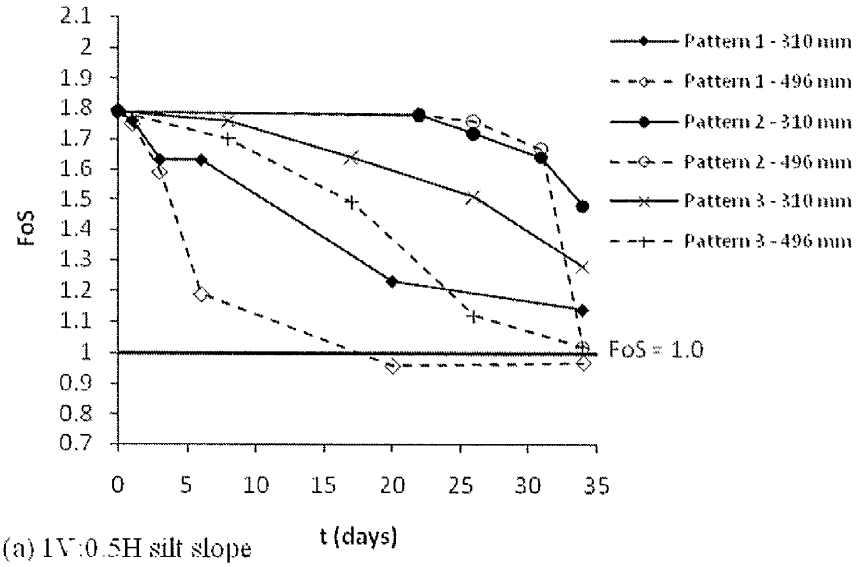

(a) 1V:0.5H silt slope

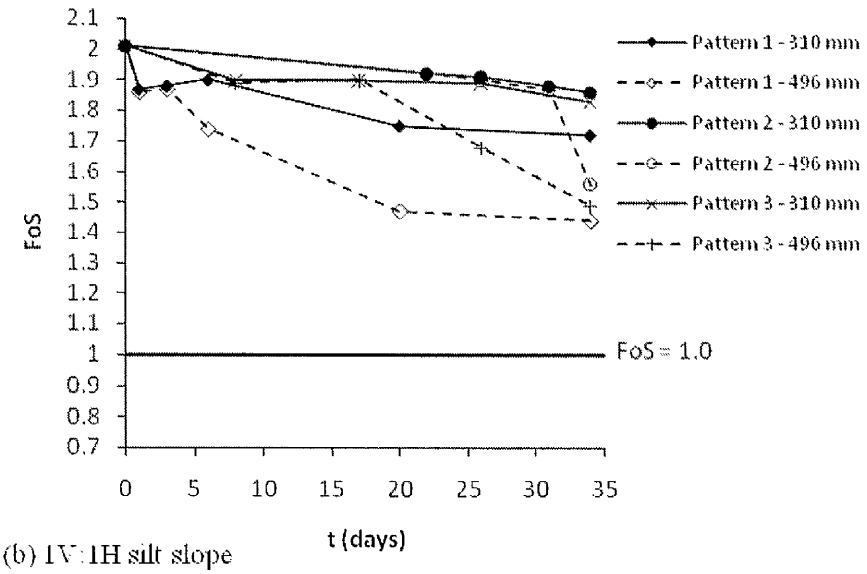

(b) 1V:1H silt slope

Figure 6.14 The changes in FoS with time for (a) 1V:0.5H silt slope and (b) 1V:1H silt slope for different rainfall patterns and total amount

It also demonstrates that the 1V:0.5H silty soil slope is more sensitive than 1V:1H silty slope to the effects of water infiltration and permeation and that the value of FoS against failure for the 1V:1H silt slope remained well above unity for the parameters adopted. For both geometries, Pattern 2 rainfall has less influence on the movement of the slip surface and the factor of safety during the earlier stages of the 34-days rainfall period. The changes in the location of the critical slip surface and

the factor of safety values were influenced the most by Pattern 1 rainfall. This behaviour corresponds to the behaviour of the wetting front as described in Section 5.3.

6.4 Presentation of the stability of the slopes in clayey type soil

In this section the locations of critical circular slip surfaces and the changes in the factors of safety values at selected times for clay material on 1V:0.5H and 1V:1H slope are discussed. As in the cases of the slope in silty and sandy type soils, the changes in FoS arising from the three rainfall patterns with the two rainfall intensities of cumulative rainfall of 310 mm and 496 mm respectively are presented.

At t = 0, the FoS value for 1V:0.5H clay slope was 1.79 and for 1V:1H clay slope was 2.01.

6.4.1 1V:0.5H clayey soil type slope

The coordinates of the common points and the centres of the circles for the locations of the critical slip surfaces and factors of safety due to the application of Pattern 1 rainfall on 1V:0.5H clay slope are tabulated in Table 6.13 and illustrated in Figure 6.15.

For the base case rainfall (total 310 mm in 34 days), the application of Pattern 1 rainfall on the 1V:0.5H clay slope did not affect the initial location of the critical slip surface until about t = 3 days. However, the magnitude of the FoS at the end of t = 1 day and t = 3 days reduced by 0.05 and 0.06 respectively from the initial magnitude. At the end of t = 6 days, the value of FoS was seen to have reduced further and the slip surface had migrated from its initial position. By the end of t = 20 days a shallow circular slip surface emerged from the mid section to the toe of the slope and thereafter migrated to a greater depth within the slope by the end of t = 34 days. At these times the magnitudes of the FoS were both 1.46.

The application of the increased rainfall (total of 496 mm in 34 days) reduced the value of FoS to a lower figure than in the same period under the lower rainfall intensity. As with the lower rainfall of 310 mm in 34 days, the application of the higher rainfall amount did not affect the location of the initial critical slip surface until about the end of t = 3 days. However, unlike the lower rainfall amount, by the end of t = 6 days, a shallow slip surface was forming immediately below the surface of the slope subsequently deepening with time. It should be noted, however, that from the end of t = 6 days to t = 34 days, the rainfall caused only small subsequent changes in the factor of safety against failure.

It was observed that the calculated FoS was greater than unity throughout the 34 days period of the application of Pattern 1 rainfall. It confirmed that the clay soil appears to be less sensitive to inundation due to high precipitation compared to a silty soil. Implementation of Pattern 1 rainfall on the 1V:0.5H slope comprising clayey soil resulted in the critical slip surface migrating to a shallow location at a later time in comparison with the same slope in silty soil.

Table 6.13 The position of circular slip surface and the factor of safety due to the application of Pattern 1 rainfall on 1V:0.5H clay slope

Total rainfall (mm)	Time, t (day)	Cumulative rainfall (mm) at different 't'	Coordinates of the common point (m)			Critical circle				
						Centre			Radius (m)	FoS
			No.	x	y	location	x	y		
	0	0	20	49.5	20	t0	53	40	20.30	1.79
310	1	85	20	49.5	20	t1	53	40	20.30	1.74
	3	168	20	49.5	20	t3	53	40	20.30	1.73
	6	235	20	49.5	20	t6	55	40	20.74	1.67
	20	310	19	49	21	t20	65	36	21.93	1.46
	34	310	19	49	21	t34	61	34	17.69	1.46
496	1	137	20	49.5	20	t1	53	40	20.30	1.72
	3	268	20	49.5	20	t3	53	40	20.30	1.65
	6	376	8	43.5	32	t6	71	40	28.64	1.12
	20	496	19	49	21	t20	67	38	24.76	1.11
	34	496	18	48.5	22	t34	83	52	45.72	1.12

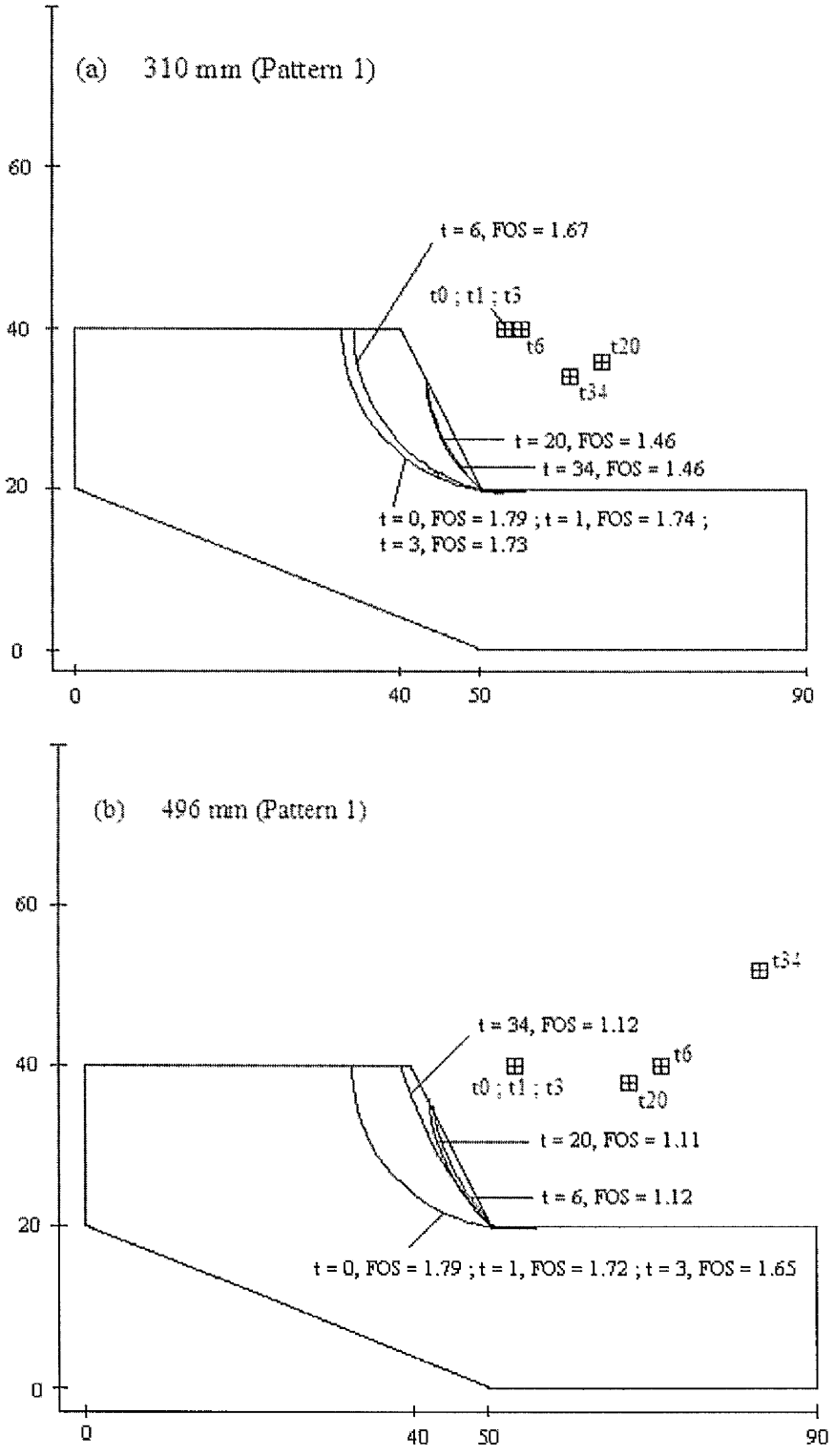

Figure 6.15 The location of the critical circular slip surface with time on a 1V:0.5H clayey soil type slope subjected to Pattern 1 rainfall with total cumulative rainfall of (a) 310 mm and (b) 496 mm

It can be seen from the data in Table 6.14, that, for lower rainfall intensity of 310 mm in 34 days, the location of the initial critical circular slip surface was not affected until about t = 31 days. At the end of t = 34 days, a small shallow critical slip surface in the lower part of the slope was generated. This is clearly shown in Figure 6.16. Throughout the 34 days duration of Pattern 2 rainfall, the FoS continued to decrease with time. The lowest value of FoS, i.e. of 1.41 was achieved at the end of t = 34 days.

The behaviour of the slope during the application of the higher rainfall intensity (496 mm in 34 days) was almost identical with respect to the position of slip surface and the factor of safety values as that during the lower rainfall intensity until about the end of t = 26 days. However, at the end of t = 31 days the position of the critical slip surface migrated upwards from the initial slip surface location. At the end t = 34 days, a shallow slip surface with the lowest FoS value of 1.15 was observed to occur in the lower part of the slope.

It should be noted that the volume of soil associated with the generation of the shallow critical slip surface observed at the end of t = 34 days for 1V:0.5H clay slope was smaller than that observed in the shallow slip surface that was generated in the 1V:0.5H silty soil slope.

Table 6.14 The position of circular slip surface and the factor of safety due to the application of Pattern 2 rainfall on 1V:0.5H clay slope

Total rainfall (mm)	Time, t (day)	Cumulative rainfall (mm) at different 't'	Coordinates of the common point (m)			Critical circle				
						Centre			Radius (m)	FoS
			No.	x	y	location	x	y		
	0	0	20	49.5	20	t0	53	40	20.30	1.79
310	22	20	20	49.5	20	t22	53	40	20.30	1.78
	26	50	20	49.5	20	t26	53	40	20.30	1.76
	31	143	20	49.5	20	t31	53	40	20.30	1.74
	34	310	19	49	21	t34	57	28	10.63	1.41
496	22	32	20	49.5	20	t22	53	40	20.30	1.77
	26	80	20	49.5	20	t26	53	40	20.30	1.76
	31	228	20	49.5	20	t31	55	40	20.74	1.68
	34	496	19	49	21	t34	57	28	10.63	1.15

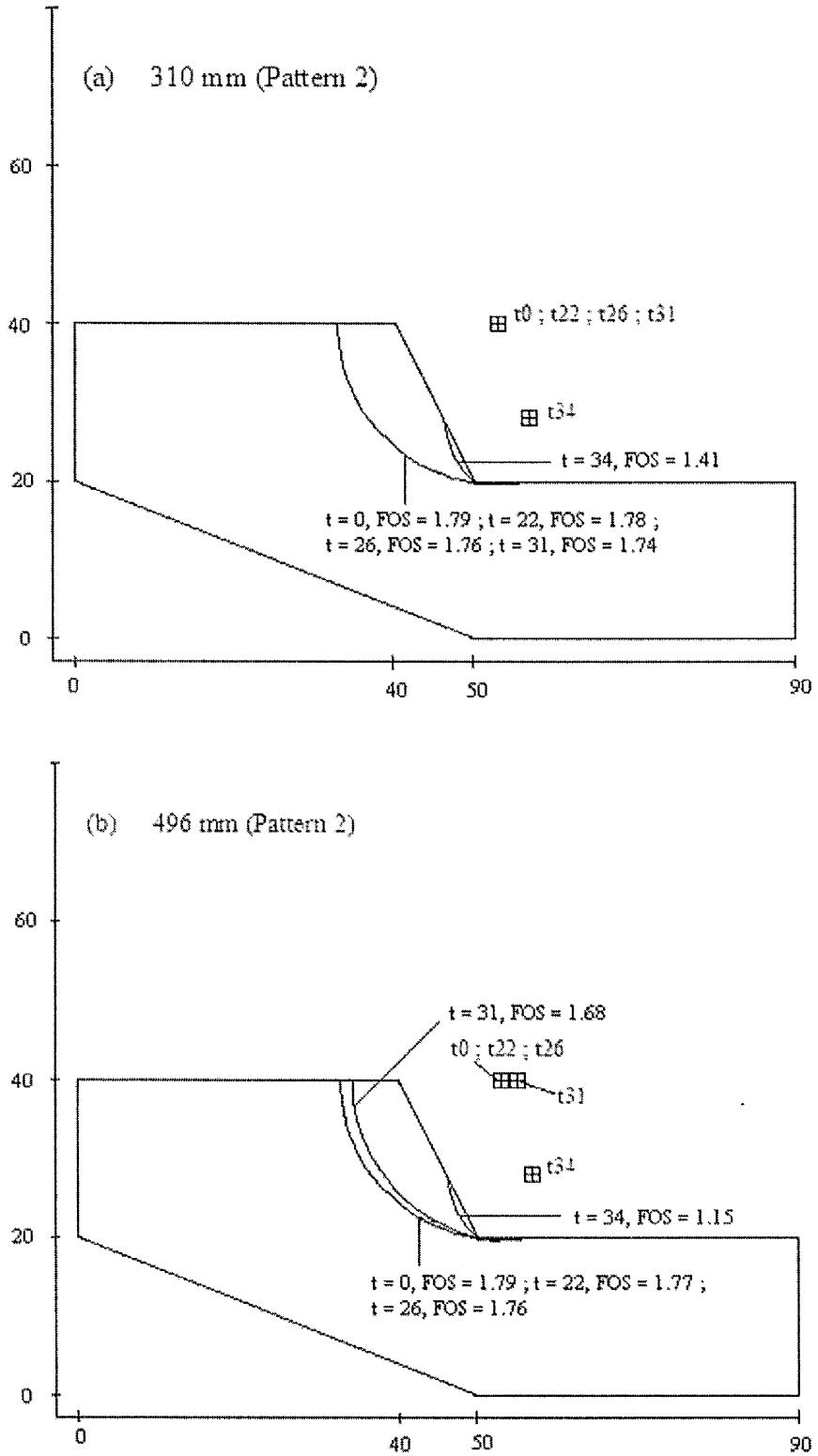

Figure 6.16 The location of the critical circular slip surface with time on a 1V:0.5H clayey soil type slope subjected to Pattern 2 rainfall with total cumulative rainfall of (a) 310 mm and (b) 496 mm

The coordinates of the common points and the centres of rotation of the circles for the locations of the critical slip surfaces and factors of safety as a result of the application of Pattern 3 rainfall on the 1V:0.5H clayey soil slope are tabulated in Table 6.15. It shows that even though the magnitude of the FoS continued to reduce as rainfall was applied into the ground, the location of the slip surfaces remained approximately in the initial position until the end of t = 26 days. At the end of t = 34 days, shallow critical slip surface with FoS = 1.47 was formed at the bottom of the slope.

Introducing the higher rainfall intensity of 496 mm in 34 days had a greater effect on the reduction in the value of the FoS. The critical slip surface appeared to remain in approximately the same position as it was at the commencement of the rainfall until the end of t = 8 days. By the end of t = 17 days, the critical slip surface migrated slightly above its original position at the start of the rainfall. At the end of t = 26 days, a shallow critical slip surface was formed just below the surface of the slope and continued to migrate to a deeper location by the end of t = 34 days. It was found that the FoS at the end of t = 26 days and at the end of t = 34 days was 1.24 and 1.02 respectively.

Table 6.15 The position of circular slip surface and the factor of safety due to the application of Pattern 3 rainfall on 1V:0.5H clay slope

Total rainfall (mm)	Time, t (day)	Cumulative rainfall (mm) at different 't'	Coordinates of the common point (m)			Critical circle				
						Centre			Radius (m)	FoS
			No.	x	y	location	x	y		
	0	0	20	49.5	20	t0	53	40	20.30	1.79
310	8	73	20	49.5	20	t8	53	40	20.30	1.76
	17	155	20	49.5	20	t17	53	40	20.30	1.70
	26	237	20	49.5	20	t26	53	40	20.30	1.68
	34	310	19	49	21	t34	61	32	16.28	1.47
496	8	117	20	49.5	20	t8	53	40	20.3	1.75
	17	248	20	49.5	20	t17	55	40	20.74	1.67
	26	380	19	49	21	t26	61	32	16.28	1.24
	34	496	19	49	21	t34	65	36	21.93	1.02

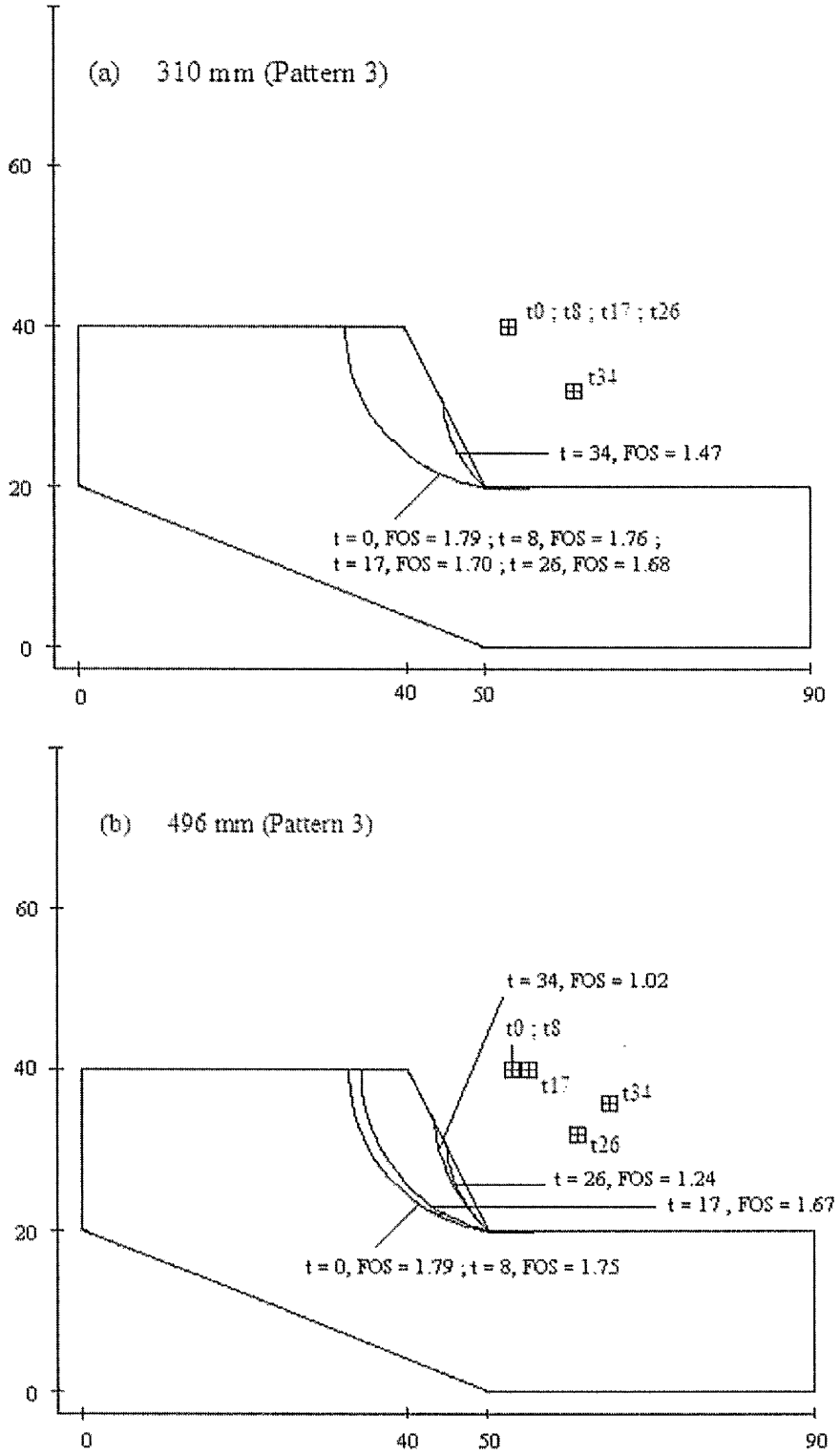

Figure 6.17 The location of the critical circular slip surface with time on a 1V:0.5H clayey soil type slope subjected to Pattern 3 rainfall with total cumulative rainfall of (a) 310 mm and (b) 496 mm

6.4.2 1V:1H clayey soil type slope

In this section, the development of the critical slip surfaces and associated factors of safety during the application of three rainfall patterns on 1V:1H clay slope are presented. As in the case of the 1V:0.5H clay slope, two rainfall intensities of 310 mm and 496 mm are considered.

The coordinates of common points and the centres of circles for the locations of the critical slip surfaces at various times being generated in the 1V:1H clay slope due to the application of Pattern 1 rainfall are presented in Table 6.16. An illustration of these critical slip surfaces is shown in Figure 6.18. When the base case rainfall intensity of 310 mm in 34 days was applied to the ground, the location of the critical circular slip surface migrated a modest distance from the initial position of slip surface at t = 0 days. It remained in this position until the end of t = 34 days. By the end of t = 1 day, the FoS against failure reduced from 2.01 to 1.83. However, from the end of t = 3 days onwards, the FoS slowly increased with time. It was found that by the end of t = 34 days, the FoS was 1.89.

Under the influence of the 496 mm in 34 day rainfall intensity the position of the critical slip surface in the 1V:1H clayey soil slope initially migrated slightly above its initial position, Remaining here until about the end of t = 3 days maintaining a value of 1.84. By the end of t = 6 days, a shallow critical slip surface with a FoS = 1.79 was formed just below the surface of the slope. The position of this slip surface continued to move deeper with time. By the end of t = 20 days, the value of the FoS was 1.62. When the rainfall stopped the FoS was 1.66.

It should be noted that unlike in the silty soil slope, after the rain stopped at the end of t = 20 days, there was a continued increase in the factor of safety until the end of t = 34 days. This behaviour was similar to that in the slope comprising sandy soil. However, it does show that for Pattern 1 rainfall, the FoS against failure in a slope comprising clayey soil was the least affected in comparison with the effects on the stability of the slopes in sandy and silty soils.

Table 6.16 The position of circular slip surface and the factor of safety due to the application of Pattern 1 rainfall on 1V:1H clay slope

Total rainfall (mm)	Time, t (day)	Cumulative rainfall (mm) at different 't'	Coordinates of the common point (m)			Critical circle				
						Centre			Radius (m)	FoS
			No	x	y	Location	x	y		
	0	0	23	62	17	t0	58	40	23.35	2.01
310	1	85	22	61	18	t1	58	40	22.20	1.83
	3	168	22	61	18	t3	58	40	22.20	1.84
	6	235	22	61	18	t6	58	40	22.20	1.85
	20	310	22	61	18	t20	58	40	22.20	1.88
	34	310	22	61	18	t34	58	40	22.20	1.89
496	1	137	23	62	17	t1	60	40	23.09	1.84
	3	268	23	62	17	t3	60	40	23.09	1.84
	6	376	17	56	23	t6	74	48	30.81	1.79
	20	496	19	58	21	t20	70	44	25.95	1.62
	34	496	19	58	21	t34	72	48	30.41	1.66

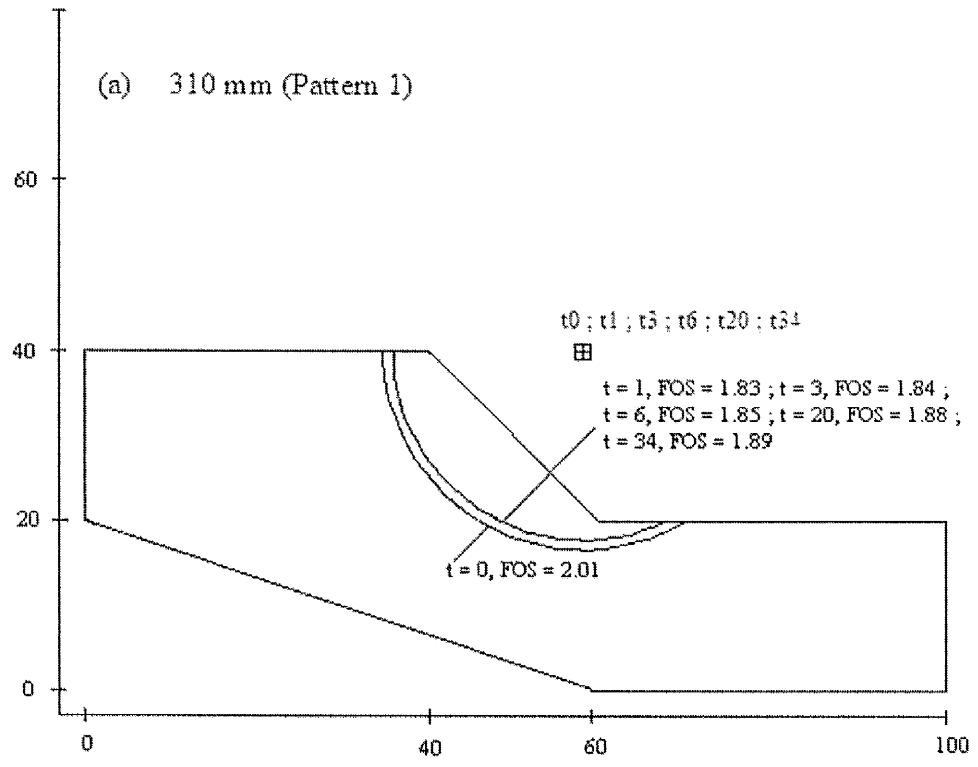

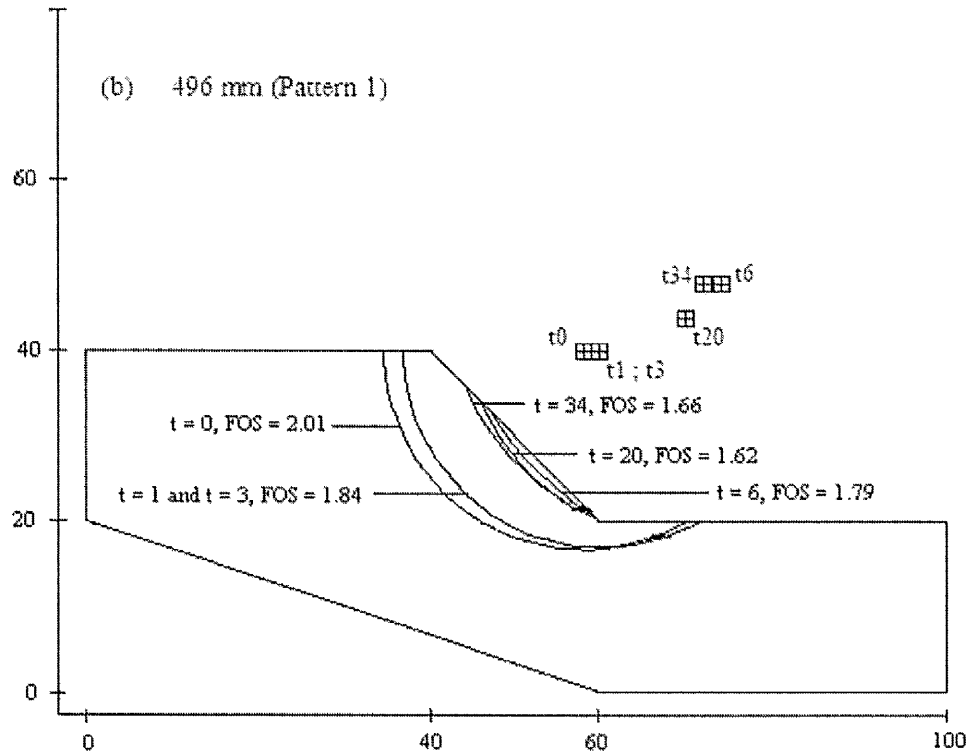

Figure 6.18 The location of the critical circular slip surface with time on a 1V:1H clayey soil type slope subjected to Pattern 1 rainfall with total cumulative rainfall of (a) 310 mm and (b) 496 mm

As tabulated in Table 6.17 and illustrated in Figure 6.19, for the lower rainfall intensity (310 mm in 34 days), the influence on the position of the critical slip surface in a 1V:1H clay slope due to the application of Pattern 2 rainfall was similar to that during an equivalent Pattern 1 rainfall period. At the end of t = 22 days, the position of the slip surface migrated further above its initial location and remained in this position until the end of t = 34 days. The magnitude of the FoS during the 34 day period continued to reduce with time. It was noted that, at the end of t = 34 days, where the slope received the highest short-term intensity of rainfall of 85.32 mm/day, the FoS was 1.83. This value was similar to that found in Pattern 1 rainfall at the end of t = 1 day.

It can be noted that, by comparing the application of Pattern 2 rainfall on a 1V:1H silty soil slope and 1V:1H clayey soil slope, it was found that the magnitudes of the FoS during the 34-day duration were lower in the slope of clayey soil than in the slope of silty soil. This appears to contradict the earlier conclusion where it was observed that the clayey soil was less sensitive to the influence of Pattern 1 rainfall

when applied to the 1V:1H slope in comparison with other soils. However, it should be recognised that during the application of Pattern 2 rainfall on both 1V:1H silt and 1V:1H clay slopes, the position of the critical circular slip surface at all times was considered to be very deep.

The magnitude of the FoS reduced further when the higher rainfall intensity (496 mm in 34 days) was applied. However, the difference in the magnitude of the factor of safety for the same circular slip surfaces when considering the lower rainfall and higher rainfall intensities at the end of t = 22 days, 26 days and 31 days was found to be negligible – about 0.01. A shallow slip surface was observed to have developed just below the surface of the slope by the end of t = 34 days. At this time, the magnitude of the FoS was 1.57

Table 6.17 The position of circular slip surface and the factor of safety due to the application of Pattern 2 rainfall on 1V:1H clay slope

Total rainfall (mm)	Time, t (day)	Cumulative rainfall (mm) at different 't'	Coordinates of the common point (m)			Critical circle				
						Centre			Radius (m)	FoS
			No.	x	y	location	x	y		
	0	0	23	62	17	t0	58	40	23.35	2.01
310	22	20	22	61	18	t22	58	40	22.20	1.91
	26	50	22	61	18	t26	58	40	22.20	1.88
	31	143	22	61	18	t31	58	40	22.20	1.85
	34	310	22	61	18	t34	58	40	22.20	1.83
496	22	32	22	61	18	t22	58	40	22.20	1.90
	26	80	22	61	18	t26	58	40	22.20	1.87
	31	228	22	61	18	t31	58	40	22.20	1.84
	34	496	17	56	23	t34	74	48	30.81	1.57

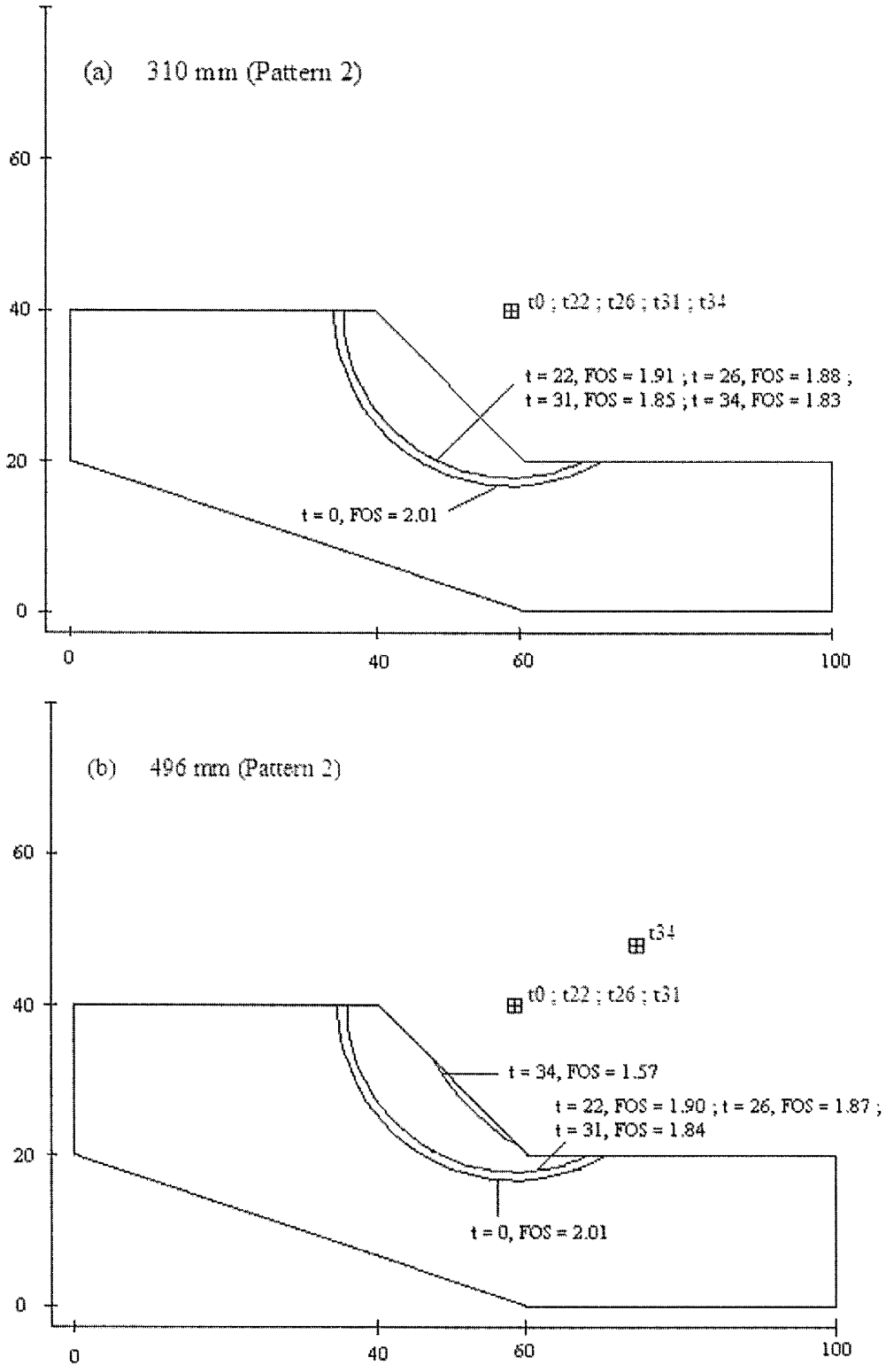

Figure 6.19 The location of the critical circular slip surface with time on a 1V:1H clayey soil type slope subjected to Pattern 2 rainfall with total cumulative rainfall of (a) 310 mm and (b) 496 mm

The application of the base case rainfall (310 mm in 34 days) in the form of Pattern 3 rainfall onto the 1V:1H clay slope caused the critical circular slip surface to migrate a little further above its initial condition. It remained at this location until the end of t = 34 days. This is shown clearly in Table 6.18 and illustrated further in Figure 6.20. At the end of t = 8 days, it was found that the FoS was reduced from 2.01 to 1.88, and slowly continued to decrease with time by a minimal amount of 0.01 for each time step. At the end of t = 34 days, it was noted that the magnitude of the FoS was 1.86.

As in the case of the lower rainfall intensity, it shows that at the end of t = 8 days, the application of higher rainfall (496 mm in 34 days) also caused the critical slip surface to migrate to just above its initial location, but it only stayed at this position until the end of t = 26 days. A shallow slip surface was later formed near the surface of the slope with an associated FoS equal to 1.59.

Throughout the period of 34 days, the factor of safety remained greater than unity. Furthermore, a shallow slip surface was only formed at the end of t = 34 days. By comparing the effect of Pattern 3 rainfall on 1V:1H sandy and silty slopes, it also shows that Patten 3 rainfall has the least affect on a 1V:1H clayey soil slope in comparison with other soil types.

Table 6.18 The position of circular slip surface and the factor of safety due to the application of Pattern 3 rainfall on 1V:1H clay slope

Total rainfall (mm)	Time, t (day)	Cumulative rainfall (mm) at different 't'	Coordinates of the common point (m)			Critical circle				
						Centre			Radius (m)	FoS
			No.	x	y	location	x	y		
	0	0	23	62	17	t0	58	40	23.35	2.01
310	8	73	22	61	18	t8	58	40	22.20	1.88
	17	155	22	61	18	t17	58	40	22.20	1.87
	26	237	22	61	18	t26	58	40	22.20	1.87
	34	310	22	61	18	t34	58	40	22.20	1.86
496	8	117	22	61	18	t8	58	40	22.20	1.86
	17	248	22	61	18	t17	58	40	22.20	1.86
	26	380	22	61	18	t26	58	40	22.20	1.85
	34	496	19	58	21	t34	68	40	21.47	1.59

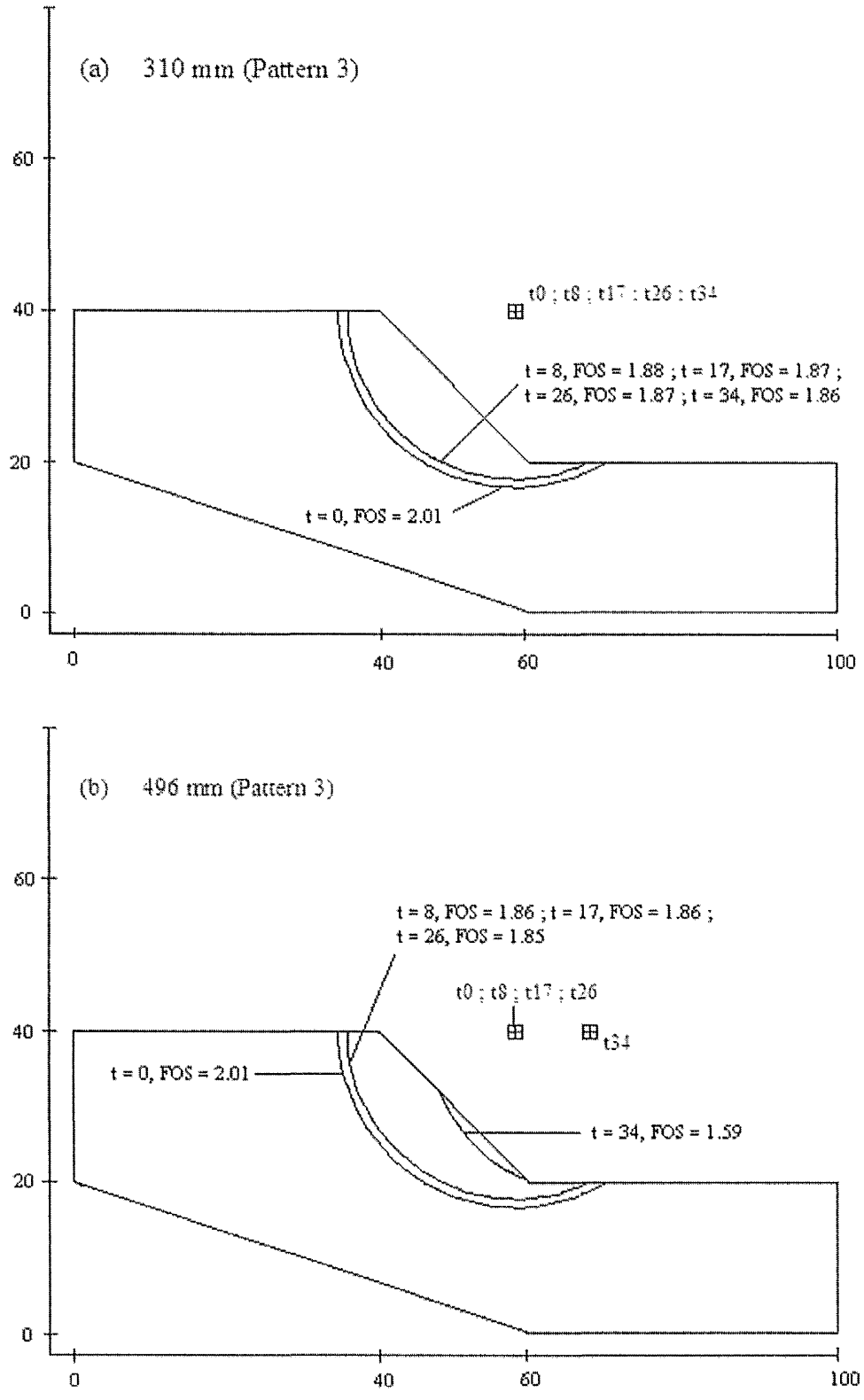

Figure 6.20 The location of the critical circular slip surface with time on a 1V:1H clayey soil type slope subjected to Pattern 3 rainfall with total cumulative rainfall of (a) 310 mm and (b) 496 mm

6.4.3 Comparison of the effects on the 1V:0.5H and 1V:1H clayey soil slopes

The changes in FoS with time as tabulated from Tables 6.13 to 6.18, for both 1V:0.5H and 1V:1H clay slopes is also illustrated in Figure 6.21.

In Chapter 5, it was shown that the pore water pressures in clayey soils in natural slopes were the least affected during equivalent rainfall in comparison with slopes comprising sandy and silty soils. This is replicated in the determination of the stability of slopes in clayey soils as described in this section.

It shows that the FoS remained above unity for all rainfall patterns that were applied on both clay slope geometries. The 1V:0.5H clay slopes were understandably more sensitive to changes in FoS compared with 1V:1H clay slopes. In the case of the 1V:0.5H clay slopes, it shows that the lowest value of FoS (1.02) was observed at the end of t = 34 days of Pattern 3 rainfall at the higher intensity. It also shows that the Pattern 2 rainfall had the least effect in comparison with other rainfall patterns. It should also be noted that the application of the higher rainfall (496 mm in 34 days) did affect the position of the critical slip surface and the magnitude of the FoS after a period of time.

In the case of the 1V:1H clay slope it was found that the lowest FoS observed was 1.57 and was generated at the end of t = 34 days of Pattern 2 rainfall at the higher intensity. However, it should also be noted that at the end of t = 34 days of Pattern 3 of higher rainfall, the magnitude of the FoS was 1.59. The application of the lower rainfall intensity i.e. 310 mm in 34 days, with the three different types of rainfall pattern on a 1V:1H clay slope resulted in the critical slip surface migrating just above its initial position. However, the locations of shallow critical slip surfaces were observed when the higher rainfall intensity was applied. It should be noted that for Pattern 2 and Pattern 3 rainfall, the shallow slip surface was only obtained approaching t = 34 days.

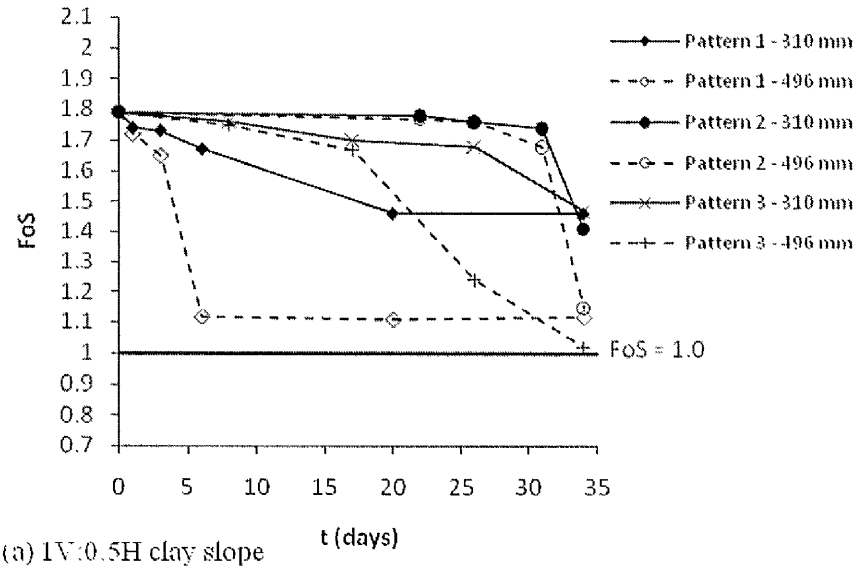

(a) 1V:0.5H clay slope

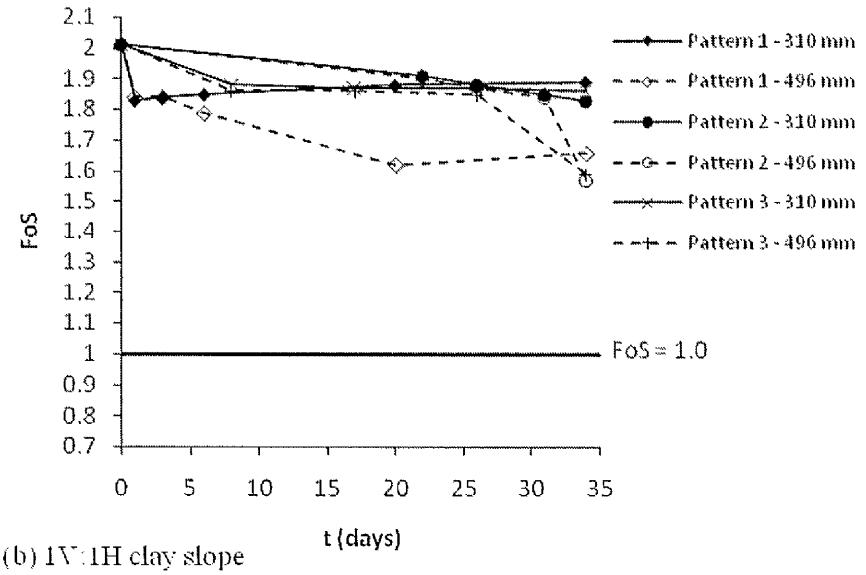

(b) 1V:1H clay slope

Figure 6.21 The changes in FoS with time for (a) 1V:0.5H clay slope and (b) 1V:1H clay slope for different rainfall patterns and total amount

6.5 Summary of the effects of different rainfall patterns and intensities on slope stability

Generally, changes in locations of the critical slip surfaces and the generated factors of safety are most apparent in slopes of sandy soils and the slopes in clay soils are least affected. This behaviour is mirrored by the changes in pore water pressure and the developing depth of the wetting fronts as described in Chapter 5.

Likewise, the increase in the rainfall intensity by 60% resulted in a reduction in the factor of safety with time during the rainfall period by a greater degree than the base case. A characteristic observed during the rainfall period was that an increase in the rainfall intensity by 60% over the rainfall period resulted in the location of the critical slip surface migrating very rapidly to the surface of the slope. This behaviour was particularly clear in slopes comprising silty or clayey soil (i.e. the lower permeability soils).

The application of higher intensity rainfall at t = 1 day on 1V:0.5H slopes of sandy soil by Pattern 1 rainfall type caused the initial position of the potential slip surface to migrate to a shallow slip location very rapidly. Conversely, the higher intensity of rainfall at the beginning of Pattern 1 did not affect the initial position of the critical slip surface for slopes comprising silty and clayey soils. The shallow slip surfaces in slopes of these two soils were formed at a later time in the rainfall period. However, the magnitude of the FoS against failure for the slope in sandy soil reduced to less than unity very quickly, i.e. at the end of t = 3 days, whereas for slopes in silty soils, this condition arose by t = 20 days, and only when the higher rainfall intensity (i.e. 60% increase) was applied to the slope. The 1V:0.5H clay slopes appeared to remain stable throughout the 34 day rainfall duration.

When Pattern 2 rainfall was applied to 1V:0.5H silty and clayey slopes, a deep failure mechanism was invoked until after approximately t = 31 days. A shallow slip surface was only formed at the end of t = 34 days. Both of these slopes remained stable throughout the 34 day duration. However, as shown earlier in Table 6.8, it is likely that the magnitude of FoS would be further reduced after the end this period. For slopes in sandy soil, however, the FoS was found to be less than unity at the end of t = 31 days of Pattern 2 rainfall, for both lower and higher total rainfall intensities.

When the base case intensity Pattern 3 rainfall (310 mm in 34 days) was applied to the 1V:0.5H sand slope, the FoS was found to be less than unity by the end of t = 17 days. However, when the rainfall was increased by 60%, it was observed that the slope was already unstable at the end of t = 8 days. For slopes in silty or clayey soils, the slopes were remained stable throughout the 34 day rainfall duration even when the rainfall intensity was increased by 60% (i.e. FoS>1.0). Again, it was

noticed that at the end of t = 34 days, when rainfall was increased by 60%, the FoS for slopes in silty and clayey soils was just above unity.

The behaviour of 1V:1H slopes under these conditions were basically similar to that of the 1V:0.5H slopes. However for all rainfall patterns and intensities, the computations showed that the 1V:1H slopes remained stable throughout the 34 day duration. The magnitudes of FoS in 1V:1H slopes were at all times higher than the FoS magnitudes in 1V:0.5H slopes at equivalent times under similar intensities and patterns of rainfall. In some cases, however, the migration of the critical circular slip surface from the deeper location to the shallow position was at a later time in 1V:1H slopes than in 1V:0.5H slopes.

It can be seen that the higher rainfall intensity during the 34 day period did not necessarily create a more unstable slope. The state of instability requires time to develop under the infiltration regimes, and the antecedent rainfall also plays an important role in the reduction of the value of factor of safety of the slopes.

It is very clear that in slopes of sandy soil after a certain period of time, the wetting fronts no longer influenced the location of the critical slip surface. In the case of slopes in silty or clayey soils, a change in stability state will certainly evolve as the wetting fronts, which move through the soil body at a slower rate than those in more permeable soils, continue to influence the magnitudes of pore water pressures in the soil body after the rain has stopped.

The stability of the slopes described above are contingent upon the soil strengths generated based on the effective stress soil parameters assigned to each particular soil. The discussions regarding the factors of safety are relative and they are not an indication in this case of incipient failure. A change in the input parameters will obviously result in a different set of factors of safety being generated.

Given the nature of the limit equilibrium analysis, a manipulation of the factors of safety provides an indication of the magnitude of a mobilisation of a ϕ angle to resist slope failure. This is used to develop a method to predict the onset of general slope failure given the soil parameters, the antecedent rainfall characteristics, the soil types and the slope geometry.

7 Discussion on the required mobilised phi values and the prediction of time to potential slope failure

7.1 Introduction

The effects of pore water pressure changes due to rainfall on the factor of safety against failure of the slope have been presented in Chapter 6. The analyses reported in Chapter 6 examined exclusively these effects by accommodating the pore water pressure variations with time during a rainfall period but keeping all other parameters which define the slope's resistance to failure constant.

In this chapter, a further discussion is presented where the factor of safety is represented as an angle of shear resistance, ϕ_m, which is required to be mobilised for limiting equilibrium of each slope. This was calculated for specific times during the application of each rainfall pattern for both the base case of 310 mm per 34 days and the increased rainfall intensity of 496 mm for the same period on both 1V:0.5H and 1V:1H slopes, comprising sandy, silty and clayey soils.

The mechanism for the calculation of the mobilised phi, ϕ_m, was to interpolate between values of ϕ' used to derive a factor of safety for a particular situation. This procedure was repeated at different selected times for each rainfall pattern with different overall intensity, geometry and soil type. At any specific time, different values of ϕ' were input into Slope12.01 in order to find different value of FoS, while other shear strength parameters, i.e. drained cohesion, c', of 5 kN/m^2 were kept constant throughout the analysis. In the process of finding the mobilised phi values, the position of slip surface changed with different values of ϕ', and in some cases, the position of the potential critical slip surface which was originally formed in a shallow position when $\phi' = 38^o$ migrated back to a deeper position when the mobilised phi, ϕ_m, was found.

An illustration of a plot of FoS against Phi values in order to obtain the value of mobilised phi, ϕ_m, is shown in Figure 7.1. It shows that for different values of phi

angle, different values of FoS were obtained for three different time steps, thus from Figure 7.1, a different value of ϕ_m, was obtained at three selected time steps, for instance at time 1, time 2 and time 3, the values of mobilised phi, ϕ_{m1}, ϕ_{m2} and ϕ_{m3} respectively were obtained.

As described earlier in Chapters 5 and 6 for observation time points, the value of mobilised angle of shear resistance, ϕ_m, was also found at different times during the 34 days rainfall period depending on the rainfall pattern applied. It was calculated at the end of t = 0 day, 1 day, 3 days, 6 days, 20 days and 34 days for Pattern 1 rainfall, at the end of t = 0 day, 22 days, 26 days, 31 days and 34 days for Pattern 2 rainfall, and at the end of t = 0 day, 8 days, 17 days, 26 days and 34 days for Pattern 3 rainfall.

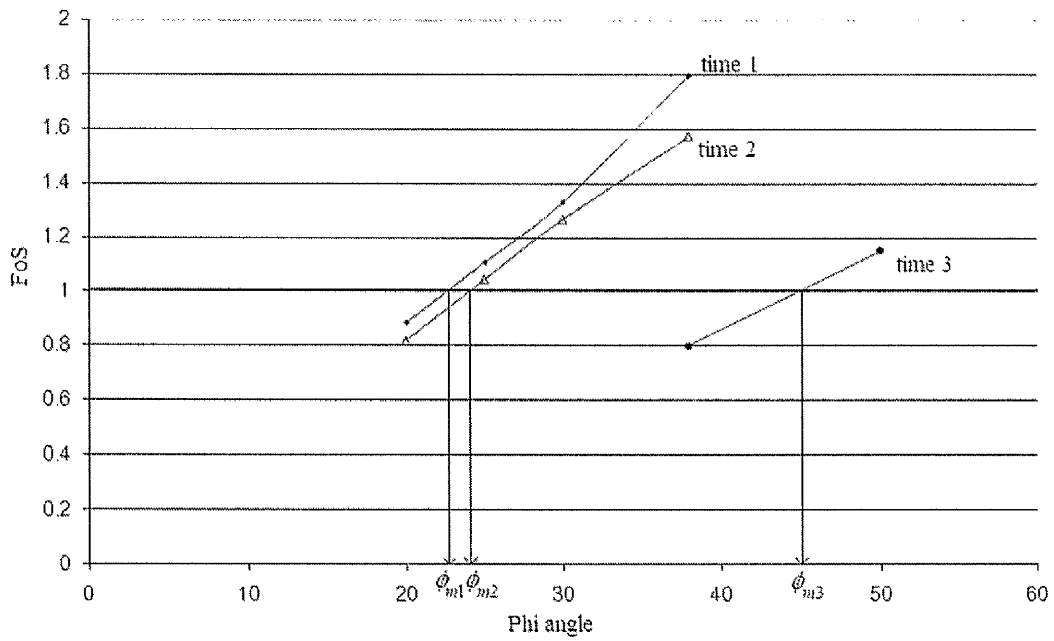

Figure 7.1 A plot of FoS against Phi value in order to find the value of mobilised phi, ϕ_m at different times.

7.2 Discussion of the mobilised phi values on sandy soil slopes

In this section, the value of mobilised phi, ϕ_m, at the selected times were determined for different rainfall patterns in both geometries of sandy soil slope i.e. 1V:0.5H and

1V:1H. The changes in the values of mobilised phi, ϕ_m, due to two different overall rainfall intensities of 310 mm and 496 mm are included in this presentation.

7.2.1 1V:0.5H sandy soil slopes for the base case rainfall and higher rainfall

The value of mobilised phi and the approximate location of the circular slip surface on 1V:0.5H sand slopes at each selected time for Pattern 1, Pattern 2 and Pattern 3 rainfall for both base case overall rainfall intensity of 310 mm per 34 days and the higher rainfall intensity of 496 mm in 34 days is tabulated in Table 7.1 and illustrated in Figure 7.2. The highlighted bold type 'Deep' that is shown in Table 7.1 under the column of 'position of slip surface' is an indication, as explained earlier, when the slip surface which was originally formed at a shallow position i.e. when $\phi' = 38^o$, migrated to a deeper position when the mobilised phi, ϕ_m , was calculated. This form of an indication is also used many times in other tabulated tables in this chapter.

From Table 7.1, it shows that at the initial condition of t = 0, the value of mobilised phi, $\phi_m = 22.6^o$. By the end of t = 1 day of Pattern 1 rainfall with the base case rainfall amount, the value of mobilised phi, ϕ_m, was increased to 24.0^o. The position of the slip surface during this time remained deep. However, a substantial increase in mobilised phi, ϕ_m, to 41.4^o was observed to be required by the end of t = 3 days, and the location of the slip surface migrated to a shallow location. A maximum value of mobilised phi, ϕ_m, of 46.9^o was found to be required by the end of t = 6 days. From Table 7.1 and Figure 7.2, it can be seen that by the end of t = 20 days, the magnitude of the required mobilised phi started to decrease steadily until the end of t = 34 days. When rainfall was increased by 60%, the magnitudes of the mobilised phi values necessary to maintain limiting equilibrium follow the same patterns as those of the mobilised phi values during the lower rainfall intensity. Understandably, however, the magnitude of mobilised phi necessary to give a FoS of unity was higher in the case of the higher rainfall intensity. The highest value of mobilised phi, ϕ_m, necessary for limiting stability, of 48.9^o was observed by the end of t = 6 days. It was also observed that the difference between the two required

mobilised phi values at the end of t = 20 days and t = 34 days for both base rainfall intensity cases were very small. This can be seen clearly in Figure 7.2 .

In the case of Pattern 2 rainfall, during the first 14 days of effectively no rainfall, it was assumed that the value of required mobilised phi, ϕ_m, remained similar to that of the initial condition of mobilised phi, ϕ_m, at t = 0 day. The low rainfall intensity at the beginning of the Pattern 2 rainfall, required only small changes in the value of mobilised phi even when the rainfall was increased by 60%. A high increase in mobilised phi was necessary by the end of t = 31 days. During the 34 days period of Pattern 2 rainfall, the maximum values of mobilised phi required for limiting stability were observed by the end of t = 34 days, where the magnitudes of maximum mobilised phi, ϕ_m, were 47.6° and 48.5° respectively for the base case and higher rainfall intensities respectively. From Figure 7.2, it can be seen that the changes in mobilised phi values needed between the base case and the higher rainfall intensities of Pattern 2 mostly occurred between t = 22 days and t = 34 days. At the end of t = 34 days, the increase in rainfall intensity by 60% only required small changes in mobilised phi.

Table 7.1 The values of the required mobilised phi, ϕ_m and the position of slip surface on 1V:0.5H sand slopes due to the application of three types of rainfall pattern with two 34-days total amount of rainfall of 310 mm and 496 mm

Total rainfall =		310 mm		496 mm	
Pattern	time (day)	mobilised phi (°)	position of slip surface	mobilised phi (°)	position of slip surface
Pattern 1	0	22.6	Deep	22.6	Deep
	1	24.0	**Deep**	26.5	Shallow
	3	41.4	Shallow	46.4	Shallow
	6	46.9	Shallow	48.9	Shallow
	20	45.7	Shallow	45.9	Shallow
	34	44.8	Shallow	44.9	Shallow
Pattern 2	0	22.6	Deep	22.6	Deep
	14	22.6	Deep	22.6	Deep
	22	23.6	Deep	24.3	Deep
	26	24.2	**Deep**	28.1	Shallow
	31	39.6	Shallow	45.5	Shallow
	34	47.6	Shallow	48.5	Shallow
Pattern 3	0	22.6	Deep	22.6	Deep
	8	28.2	Shallow	38.3	Shallow
	17	44.7	Shallow	46.7	Shallow
	26	46.3	Shallow	46.8	Shallow
	34	46.3	Shallow	46.8	Shallow

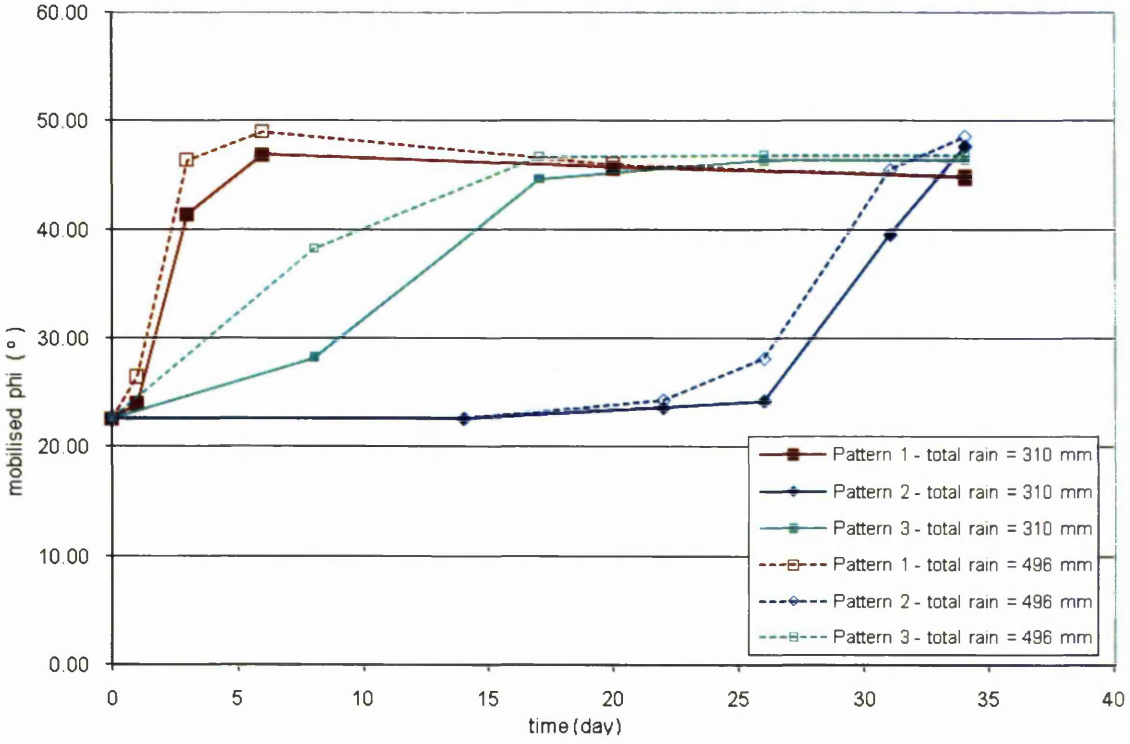

Figure 7.2 The values of mobilised phi (^{o}) against time (day) on 1V:0.5H sand slopes due to the application of three rainfall patterns with two 34-days total amount of rainfall of 310 mm and 496 mm

By looking at the base case of Pattern 3 rainfall, it can be seen that by the end of t = 8 days, only a small increase in the magnitude of mobilised phi was required for limiting stability. At this time, the location of the potential critical slip surface had migrated to the shallow position. The large increase in the magnitude of required mobilised phi of 44.7^{o} was observed by the end of t = 17 days. It was observed that from the end of t = 17 days, the increase in the required mobilised phi values by the end of t = 26 days and t = 34 days were 3.6% and 3.7% respectively. From Figure 7.2, it can be seen that the increase in rainfall intensity by 60% in the Pattern 3 rainfall required a large increase in mobilised phi values by the end of t = 8 days. However, from the end of t = 17 days onwards, the changes necessary in mobilised phi values between the base case rainfall intensity and the higher rainfall intensity were diminishing with time.

7.2.2 1V:1H sandy soil slopes for the base case rainfall and higher rainfall

Initially at t = 0, the required mobilised phi value, ϕ_m, for 1V:1H sand slope was found to be 20.2°. Table 7.2 and Figure 7.3 show that the behaviour of the magnitude of mobilised phi required for limiting stability with time for 1V:1H sand slope due to the application of different rainfall patterns and for both base case and higher case rainfall intensities is similar to those 1V:0.5H sand slope. However, it should be noted that the value of the magnitude of the required mobilised phi for 1V:1H sand slopes for all rainfall patterns was not higher than 33.7°.

Table 7.2 shows that by the end of t = 1 day of Pattern 1 rainfall, the magnitude of mobilised phi needed for equilibrium was only increased by a very small amount even when the rainfall intensity was increased by 60%. A high increase in required mobilised phi was only observed by the end of t = 3 days whereby during this time, the location of the slip surface migrated to a shallow position. The value of mobilised phi needed for limiting stability continued to increase with time. However from t = 6 days onwards, the difference of the required mobilised phi that was achieved between the base case rainfall and higher intensity rainfall was considered small. Similar to 1V:0.5H sandy type soil slope, by the end of t = 20 days onwards, the magnitude of the required mobilised phi started to decrease with time until the end of t = 34 days.

For the first 26 days of Pattern 2 rainfall, the magnitude of the required mobilised phi increased steadily with time. However, the increase in the mobilised phi value needed to maintain limiting equilibrium during this period was considered small even when the rainfall was increased by 60%. A high increase in the required mobilised phi value was observed at the end of t = 31 days during which the position of the circular slip surface migrated to a shallow location. The increase in the rainfall intensity by 60% during this time increased the magnitude of the required mobilised phi from 26.2° to 30.7°. These values continued to increase gradually towards the end of t = 34 days. However, it was observed that at the end of t = 34 days, the difference between the required mobilised phi value for the base case rainfall intensity and the higher case rainfall intensity was only 1.7°.

Table 7.2 The values of the required mobilised phi, ϕ_m and the position of slip surface on 1V:1H sand slopes due to the application of three types of rainfall pattern with two 34-days total amount of rainfall of 310 mm and 496 mm

Total rainfall =		310 mm		496 mm	
Pattern	time (day)	mobilised phi (°)	position of slip surface	mobilised phi (°)	position of slip surface
Pattern 1	0	20.2	Deep	20.2	Deep
	1	21.8	Deep	21.9	**Deep**
	3	27.2	Shallow	31.2	Shallow
	6	32.0	Shallow	33.3	Shallow
	20	32.2	Shallow	32.2	Shallow
	34	31.7	Shallow	31.8	Shallow
Pattern 2	0	20.2	Deep	20.2	Deep
	14	20.2	Deep	20.2	Deep
	22	21.6	Deep	21.7	Deep
	26	21.6	Deep	21.8	**Deep**
	31	26.2	Shallow	30.7	Shallow
	34	32.0	Shallow	33.7	Shallow
Pattern 3	0	20.2	Deep	20.2	Deep
	8	21.7	**Deep**	25.4	Shallow
	17	30.1	Shallow	32.5	Shallow
	26	32.5	Shallow	32.9	Shallow
	34	32.7	Shallow	32.9	Shallow

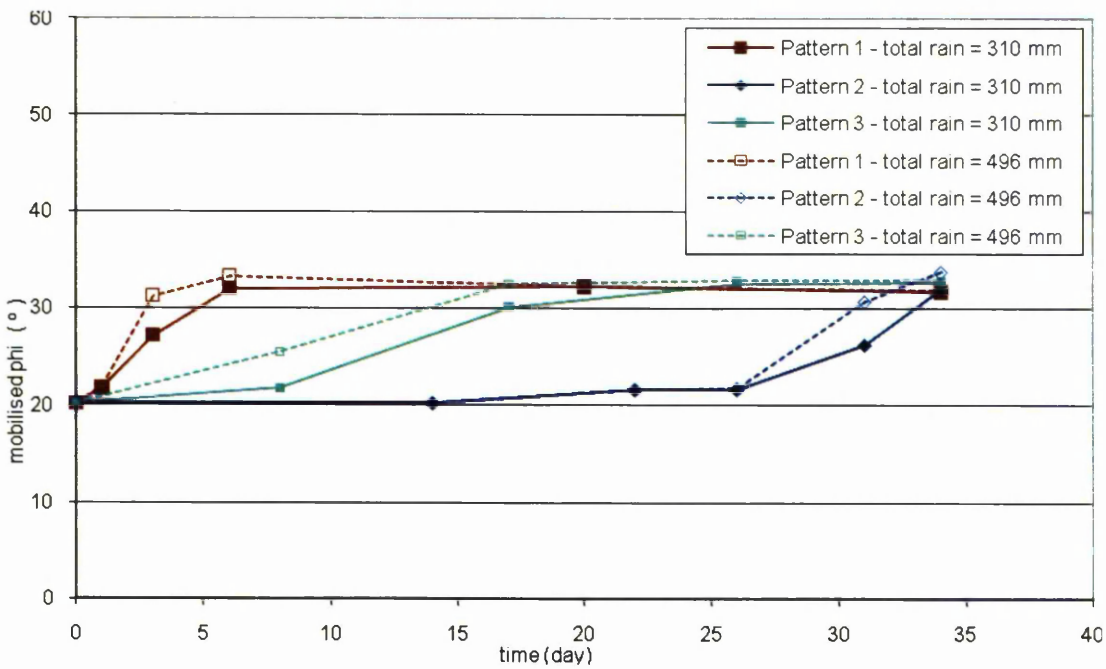

Figure 7.3 The values of mobilised phi (°) against time (day) on 1V:1H sand slopes due to the application of three rainfall patterns with two 34-days total amount of rainfall of 310 mm and 496 mm

For the base case of Pattern 3 rainfall, the shallow position of circular slip surface was only observed by the end of t = 17 days, during which the required mobilised phi value was increased to 30.1°. The magnitude of mobilised phi continued to increase steadily towards the end of t = 34 days, however it was noted that the change of the required mobilised phi between t = 26 days and t = 34 days was small. For the higher rainfall intensity that was increased by 60%, it shows that a shallow slip surface was already obtained at the end of t = 8 days and the magnitude of the required mobilised phi continued to increase progressively with time. At the end of t = 26 days and t = 34 days, it was found that the magnitude of the required mobilised phi for limiting stability at both times were similar.

It can be observed that for both sandy type soil slope geometries, the changes of the required mobilised phi values necessary for limiting stability with time show approximately the same behaviour. It was observed that at the end of the no rainfall period, i.e. at the end of t = 20 days of Pattern 1 rainfall, the magnitude of the required mobilised phi started to decrease with time. For both Pattern 2 and Pattern3 rainfalls, the maximum value of mobilised phi necessary for limiting stability was achieved at the end of t = 34 days and for Pattern 1 rainfall, the maximum value of the required mobilised phi was obtained at an earlier time. It was also observed that towards the end of Pattern 3 rainfall, the increase in the required mobilised phi was considered small even when the base case rainfall intensity was increased by 60%.

7.3 Discussion of the mobilised phi values on silty soil slopes

Similar to the previous section on sandy soil slopes, this section illustrates the changes of the mobilised phi value, ϕ_m, required for limiting stability at selected times due to the application of different rainfall patterns in both geometries of 1V:0.5H and 1V:1H silty soil slopes. These three rainfall patterns were also based upon the base case overall rainfall intensity of 310 mm in 34 days and the higher rainfall intensity of 496 mm in 34 days.

7.3.1 1V:0.5H silty soil slopes for the base case rainfall and higher rainfall

The changes of the required mobilised phi values at each selected time due to the application of different rainfall patterns on 1V:0.5H silty soil slope are tabulated in Table 7.3 and illustrated in Figure 7.4. By comparing Figure 7.2 for 1V:0.5H sandy soil slopes and Figure 7.4 for 1V:0.5H silty soil slopes, it shows that the effect of 60% increase in rainfall intensity on the required mobilised phi value was higher in silty soil slopes than in sandy soil slopes. However, the overall values of the required mobilised phi necessary for limiting stability in silty soil slopes were still lower in comparison with sandy soil slopes.

During the application of the base case rainfall intensity of Pattern 1, there was only a small increase in the magnitude of the required mobilised phi until the end of t = 6 days. At this time, the position of the slip surface was located at a deep position. The high increase in the required mobilised phi of 31.2° was only achieved at the end of t = 20 days, during which the position of the slip surface had already migrated to a shallow location. At the end of t = 34 days, even when the rainfall was stopped for 14 days, the magnitude of the required mobilised phi continued to increase to 33.8°. Unlike 1V:0.5H sandy soil slope, the increase in the rainfall intensity by 60% shows a larger increase in the magnitude of the required mobilised phi in 1V:0.5H silty soil slope. At the end of t = 6 days, the position of slip surface had already migrated to a shallow location during which the value of the required mobilised phi, ϕ_m = 31.6°. The magnitude of the required mobilised phi necessary for limiting equilibrium continued to increase until the end of t = 20 days. However, it was noticed that the magnitude of the required mobilised phi was lower by approximately 0.4° at the end of t = 34 days. This behaviour did not appear for the base case rainfall intensity of Pattern 1 rainfall.

The application of Pattern 2 rainfall on 1V:0.5H silty soil slope only shows a small increase in the magnitude of the required mobilised phi. For the base case rainfall intensity, the value of the required mobilised phi was only increased from 22.7° at the end of t = 0 day to 24.3° at the end of t = 34 days, during which time the slip surface was located in a deep position throughout the 34 days rainfall duration.

Table 7.3 The values of the required mobilised phi, ϕ_m and the position of slip surface on 1V:0.5H silt slopes due to the application of three types of rainfall pattern with two 34-days total amount of rainfall of 310 mm and 496 mm

Total rainfall =		310 mm		496 mm	
Pattern	time (day)	mobilised phi (°)	position of slip surface	mobilised phi (°)	position of slip surface
Pattern 1	0	22.7	Deep	22.7	Deep
	1	23.0	Deep	23.1	Deep
	3	24.1	Deep	24.5	**Deep**
	6	24.1	**Deep**	31.6	Shallow
	20	31.2	Shallow	39.3	Shallow
	34	33.8	Shallow	38.9	Shallow
Pattern 2	0	22.7	Deep	22.7	Deep
	14	22.6	Deep	22.6	Deep
	22	22.9	Deep	22.8	Deep
	26	22.9	Deep	23.1	Deep
	31	24.0	Deep	24.2	Deep
	34	24.3	**Deep**	37.1	Shallow
Pattern 3	0	22.7	Deep	22.7	Deep
	8	23.0	Deep	23.8	**Deep**
	17	24.0	Deep	24.3	Shallow
	26	24.2	Shallow	34.0	Shallow
	34	30.6	Shallow	37.5	Shallow

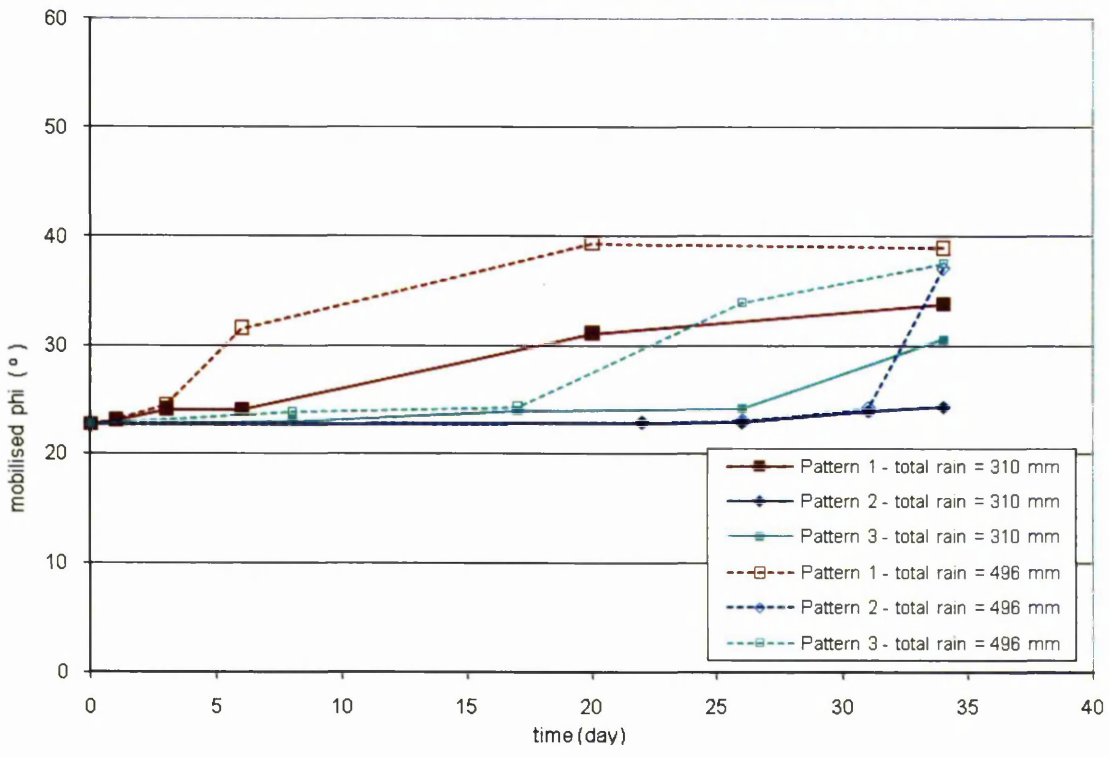

Figure 7.4 The values of mobilised phi (°) against time (day) on 1V:0.5H silt slopes due to the application of three rainfall patterns with two 34-days total amount of rainfall of 310 mm and 496 mm

When the overall rainfall intensity was increased by 60%, the same gradual increases in the required mobilised phi values were produced for the first 31 days of the Pattern 2 rainfall. However, it was observed that a high increase in the magnitude of the required mobilised phi of 37.1° was achieved at the end of t = 34 days. At this time, the location of circular slip surface migrated to a shallow position.

From Figure 7.4, during the application of the base case intensity of Pattern 3 rainfall, the magnitude of the required mobilised phi was increasing slowly with time. However, for the first 17 days of Pattern 3 rainfall, the location of the slip surface still remained in a deep position. The maximum value of the required mobilised phi of 30.6° was achieved at the end of t = 34 days, whereby during this time the location of the slip surface was already migrated to a shallow position. As the rainfall intensity was increased by 60% from the base case intensity, the magnitude of the required mobilised phi during the 34 day duration was also increased. However, a larger increase in the required mobilised phi value of 34.0° was only achieved at the end of t = 26 days and the magnitude of the required mobilised phi increased further by the end of t = 34 days.

At the end of t = 34 days of the base case overall rainfall intensity, the difference of the required mobilised phi values for limiting equilibrium between each rainfall pattern was larger in the 1V:0.5H silty soil slope compared to the 1V:0.5H sandy soil slope. However, a close approximation of the required mobilised phi value was achieved at the end t = 34 days when the rainfall intensity was increased by 60%. From Figure 7.4, it also shows that the increase of the rainfall intensity by 60%, shows a big increase in the magnitude of the required mobilised phi. The high daily intensity at the beginning of Pattern 1 rainfall, did not necessarily increase the magnitude of the required mobilised phi; time was also an additional factor that contributed to the increase in the required mobilised phi values. This behaviour is similar to the sandy soil slopes. By looking at Pattern 2 rainfall in Figure 7.4, it shows that the high daily intensity rainfall which was increased by 60% at the end of t = 34 days increased the magnitude of the required mobilised phi value instantly. Again, this behaviour shows the important effect of the antecedent rainfall of Pattern 2 on 1V:0.5H silty soil slope. Rainfall intensity alone is not the only factor that can

produce a high magnitude of the required mobilised phi; time and antecedent rainfall also play important role in achieving the high required mobilised phi value.

7.3.2 1V:1H silty soil slopes for the base case rainfall and higher rainfall

The changes of the magnitude of the required mobilised phi for limiting stability due to the application of different rainfall patterns, for these two overall total rainfall intensities of 310 mm and 496 mm in 34 days on 1V:1H silty soil slope are tabulated in Table 7.4 and illustrated further in Figure 7.5. These show that the application of the base case rainfall intensity of all three rainfall patterns on 1V:1H silty soil slopes shows a very little increase in the magnitude of the required mobilised phi throughout the 34 days rainfall duration. For all three rainfall patterns, the highest magnitude of the required mobilised phi was achieved at the end of t = 34 days, whereby by the end of Pattern 1, Pattern 2 and Pattern 3 rainfall, the required mobilised phi value was increased from the initial required mobilised phi value of 20.3° to 22.4°, 21.7° and 21.5° respectively. A shallow position of the slip surface was only produced at the end of t = 20 days of Pattern 1 rainfall, whereas for the case of Pattern 2 and Pattern 3 rainfall, the slip surface remained deep throughout the 34 days duration.

When the rainfall intensity was increased by 60%, it was also found that the position of the slip surface had already migrated to a shallow position by the end of t = 20 days of Pattern 1 rainfall. For Pattern 2 and Pattern 3 rainfall, the position of the shallow slip surface was obtained at the end of t = 34 days and t = 26 days respectively. Similar to the base case rainfall intensity, the maximum magnitude of the required mobilised phi was achieved at the end of t = 34 days of all three rainfall patterns. These values were 27.2°, 23.1° and 25.5° respectively for Pattern 1, Pattern 2 and Pattern 3 rainfall. By comparing the base case rainfall and the higher case rainfall intensities, it shows that the increase in rainfall amount by 60% was mostly affected by Pattern 1 rainfall and least affected by Pattern 2 rainfall.

Table 7.4 The values of the required mobilised phi, ϕ_m and the position of slip surface on 1V:1H silt slopes due to the application of three types of rainfall pattern with two 34-days total amount of rainfall of 310 mm and 496 mm

Total rainfall =		310 mm		496 mm	
Pattern	time (day)	mobilised phi (°)	position of slip surface	mobilised phi (°)	position of slip surface
Pattern 1	0	20.3	Deep	20.3	Deep
	1	21.7	Deep	21.7	Deep
	3	21.6	Deep	21.6	Deep
	6	21.5	Deep	21.6	**Deep**
	20	21.4	Shallow	26.4	Shallow
	34	22.4	Shallow	27.2	Shallow
Pattern 2	0	20.3	Deep	20.3	Deep
	14	20.3	Deep	20.3	Deep
	22	21.1	Deep	21.2	Deep
	26	21.3	Deep	21.4	Deep
	31	21.5	Deep	21.6	Deep
	34	21.7	Deep	23.1	Shallow
Pattern 3	0	20.3	Deep	20.3	Deep
	8	21.3	Deep	21.4	Deep
	17	21.4	Deep	21.5	Deep
	26	21.4	Deep	22.0	Shallow
	34	21.5	**Deep**	25.5	Shallow

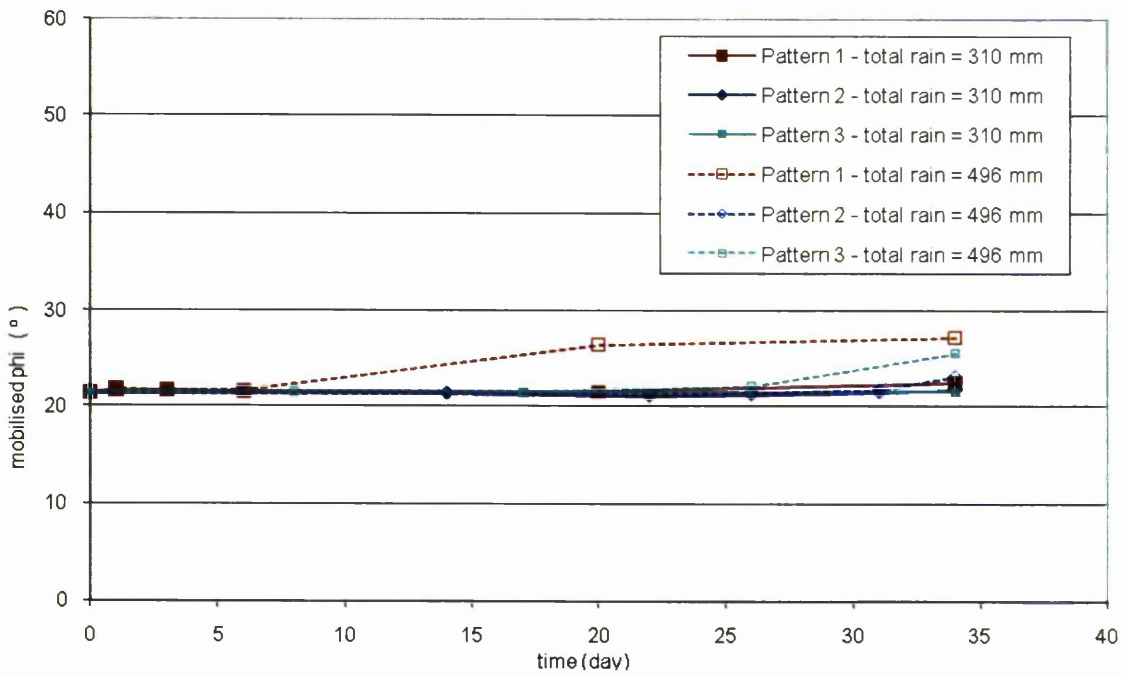

Figure 7.5 The values of mobilised phi (°) against time (day) on 1V:1H silt slopes due to the application of three rainfall patterns with two 34-days total amount of rainfall of 310 mm and 496 mm

The magnitude of the required mobilised phi was higher in the 1V:0.5H silty soil slope than in the 1V:1H silty soil slope. However, the presentation of the changes in the required mobilised phi values on 1V:1H silty soil slopes also shows the importance effect of antecedent rainfall and duration of rainfall on slope stability. It shows that by the end of t = 34 days of Pattern 1 rainfall, the magnitude of the required mobilised phi continued to increase even when there was no rainfall for the last 14 days period of Pattern 1 rainfall.

7.4 Discussion of the mobilised phi values on clayey soil slopes

This section illustrates the changes of the required mobilised phi value, ϕ_m, for limiting stability at the selected times due to the application of three rainfall patterns in both geometries of 1V:0.5H and 1V:1H clayey soil slopes. Similar to sandy and silty soil slopes, the three rainfall patterns that are presented in this section were also based upon the base case overall rainfall intensity of 310 mm and the higher rainfall intensity of 496 mm that was applied in a 34 day period.

7.4.1 1V:0.5H clayey soil slopes for the base case rainfall and higher rainfall

The changes in the required mobilised phi values for limiting stability on 1V:0.5H clayey soil slope for Pattern 1, Pattern 2 and Pattern 3 rainfall are tabulated in Table 7.5 and illustrated in Figure 7.6. Generally, the changes in the required mobilised phi values were lower in clayey soil slopes than in silty soil slopes. However, for the base case rainfall intensity of Pattern 2 rainfall, the magnitude of the required mobilised phi from t = 22 days to t = 34 days was higher in the 1V:0.5H clayey soil slope than in the 1V:0.5H silty soil slope. During this period, the position of the slip surface remained in a deep position. It should be noted that the differences in the required mobilised phi values for both cases were considered very small. This behaviour probably occurred due to an inconsistency during the calculation of pore water pressure from the finite element result and hence the piezometric value for the limit equilibrium analysis. It should be remembered that the mesh design for the

1V:0.5H clayey soil slope as explained in Chapter 4, was different in comparison with the 1V:0.5H sandy soil slope and the 1V:0.5H silty soil slope. Thus, there is a possibility that the numerical calculation to define the value of pore water pressure would be affected for clay material, especially at the deeper positions as the concentration of finer mesh was only designed for the upper part of the 1V:0.5H clayey slopes.

For the base case overall rainfall intensity of 310 mm on the 1V:0.5H clayey soil slope, a gradual increase in the magnitude of the required mobilised phi was observed for all three rainfall patterns. A shallow position of the slip surface was only obtained from the end of t = 20 days onwards of Pattern 1 rainfall, whereas for Pattern 2 and Pattern 3 rainfall, the circular slip surface remained in a deep position throughout the 34 days duration. The maximum magnitude of the required mobilised phi was obtained at the end of t = 34 days of each rainfall pattern, whereby the magnitude of the required mobilised phi at this time was 25.3°, 24.7° and 26.9° respectively for Pattern 1, Pattern 2 and Pattern 3 rainfall.

In general, the increase in the base case rainfall intensity by 60% would increase the magnitude of the required mobilised phi for all three rainfall patterns. However, it was noticed that for Pattern 2 rainfall, there were two occasions where the value of the required mobilised phi for the higher rainfall intensity was found to be lower than for the base case of Pattern 2 rainfall. During this period the position of the slip surface remained in a deep position. This behaviour was probably produced due to the inconsistency during the calculation of the magnitude of the required mobilised phi when there was only a very small change in the pore water pressure occurring in the deeper part of the domain during the first 31 days of Pattern 2 rainfall.

Table 7.5 The values of the required mobilised phi, ϕ_m and the position of slip surface on 1V:0.5H clay slopes due to the application of three types of rainfall pattern with two 34-days total amount of rainfall of 310 mm and 496 mm

Total rainfall =		310 mm		496 mm	
Pattern	time (day)	mobilised phi (°)	position of slip surface	mobilised phi (°)	position of slip surface
Pattern 1	0	22.7	Deep	22.7	Deep
	1	23.3	Deep	23.3	Deep
	3	23.4	Deep	24.5	Deep
	6	24.0	Deep	32.3	Shallow
	20	25.0	Shallow	34.4	Shallow
	34	25.3	Shallow	34.1	Shallow
Pattern 2	0	22.7	Deep	22.7	Deep
	14	22.7	Deep	22.7	Deep
	22	23.1	Deep	22.9	Deep
	26	22.9	Deep	23.1	Deep
	31	24.0	Deep	23.9	Deep
	34	24.7	**Deep**	30.4	Shallow
Pattern 3	0	22.7	Deep	22.7	Deep
	8	23.0	Deep	23.1	Deep
	17	23.6	Deep	24.0	Deep
	26	24.4	Deep	29.2	Shallow
	34	26.9	**Deep**	37.2	Shallow

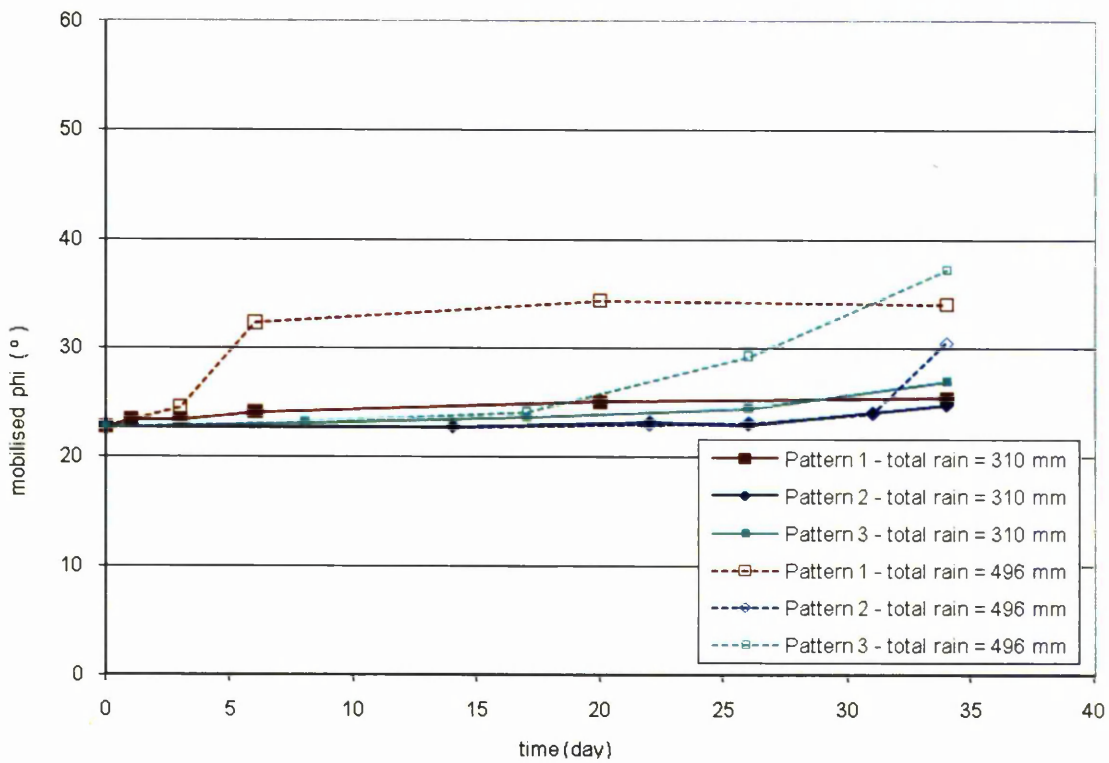

Figure 7.6 The values of mobilised phi (°) against time (day) on 1V:0.5H clay slopes due to the application of three rainfall patterns with two 34-days total amount of rainfall of 310 mm and 496 mm

When the rainfall intensity was increased by 60%, unlike the base case rainfall intensity of Pattern 1 rainfall, the maximum magnitude of the required mobilised phi of 34.4° was obtained at an earlier time i.e. by the end of t = 20 days. It was observed that the shallow position of the circular slip surface on the 1V:0.5H clayey soil slope due to the application of Pattern 1 rainfall was obtained at an earlier time, i.e. at the end of t = 6 days. In the case of Pattern 2 rainfall, when the rainfall intensity was increased by 60%, a shallow slip surface was only formed by the end of t = 34 days, with the value of the required mobilised phi, ϕ_m = 30.4°; and for Pattern 3 rainfall, the shallow slip surface was already formed by the end of t = 26 days and the maximum magnitude of the required mobilised phi of 37.2° was calculated at the end of t = 34 days.

7.4.2 1V:1H clayey soil slopes for the base case rainfall and higher rainfall

The changes in the required mobilised phi values due to the application of the base case overall rainfall intensity of 310 mm in 34 days and the higher overall rainfall intensity of 496 mm on 1V:1H clayey soil slope are tabulated in Table 7.6 and illustrated in Figure 7.7. These show that the position of the slip surface due to the application of the three base case rainfall patterns with overall amount of 310 mm remained deep thoroughout the 34 days duration. Initially, at t = 0, the value of mobilised phi, ϕ_m = 20.3°. For Pattern 1 rainfall, the maximum magnitude of the required mobilised phi of 22.0° was obtained at the end of t = 1 day before it decreased slowly towards the end of t = 34 days, with the magnitude of the required mobilised phi, ϕ_m = 21.5°. For Pattern 2 and Pattern 3 rainfall, even though the position of the slip surface remained in a deep position, the magnitude of the required mobilised phi increased gradually with time. The maximum value of the required mobilised phi of 22.1° and 21.8° was found at the end of t = 34 days of Pattern 2 and Pattern 3 rainfall respectively.

Table 7.6 The values of the required mobilised phi, ϕ_m and the position of slip surface on 1V:1H clay slopes due to the application of three types of rainfall pattern with two 34-days total amount of rainfall of 310 mm and 496 mm

Total rainfall =		310 mm		496 mm	
Pattern	time (day)	mobilised phi (°)	position of slip surface	mobilised phi (°)	position of slip surface
Pattern 1	0	20.3	Deep	20.3	Deep
	1	22.0	Deep	22.1	Deep
	3	21.9	Deep	22.0	Deep
	6	21.8	Deep	22.0	**Deep**
	20	21.6	Deep	22.5	Shallow
	34	21.5	Deep	22.7	Shallow
Pattern 2	0	20.3	Deep	20.3	Deep
	14	20.3	Deep	20.3	Deep
	22	21.2	Deep	21.3	Deep
	26	21.5	Deep	21.6	Deep
	31	21.9	Deep	22.0	Deep
	34	22.1	Deep	22.1	**Deep**
Pattern 3	0	20.3	Deep	20.3	Deep
	8	21.6	Deep	21.7	Deep
	17	21.7	Deep	21.8	Deep
	26	21.6	Deep	21.9	Deep
	34	21.8	Deep	22.7	Shallow

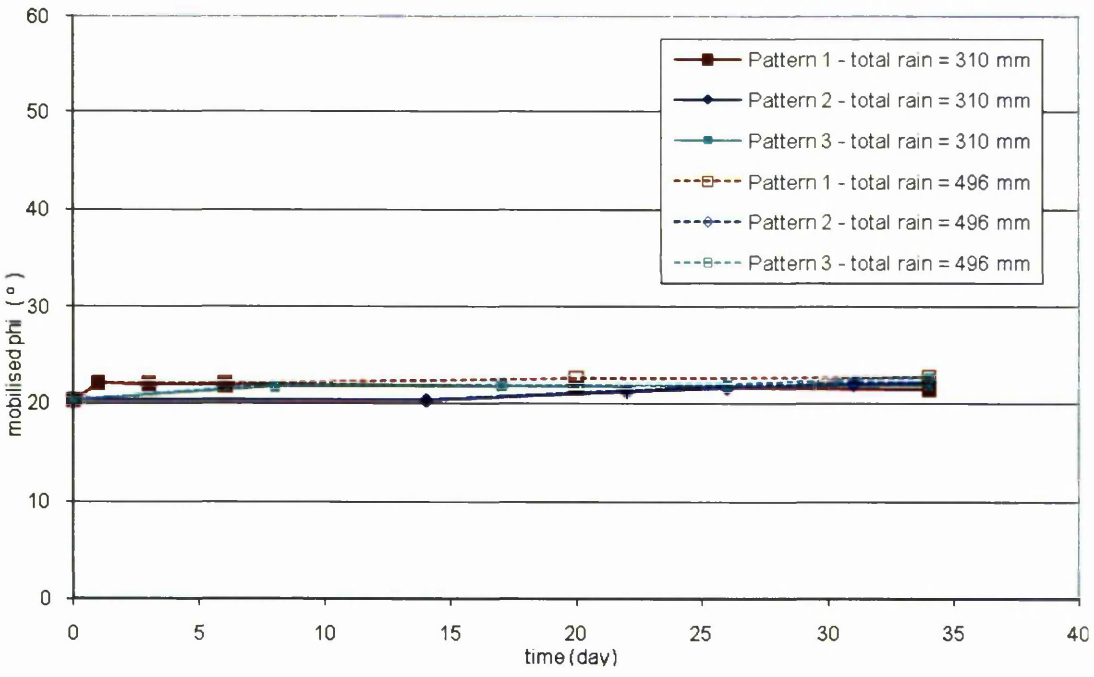

Figure 7.7 The values of mobilised phi (°) against time (day) on 1V:1H clay slopes due to the application of three rainfall patterns with two 34-days total amount of rainfall of 310 mm and 496 mm

There was only a small increase in the changes of the magnitude of the required mobilised phi when the base case rainfall intensity was increased by 60%. For Pattern 1 rainfall, the location of the slip surface migrated to a shallow position at the end of t = 20 days, and the maximum magnitude of the required mobilised phi of 22.7^{o} was achieved at the end of t = 34 days. Pattern 2 rainfall shows the least effect when the rainfall intensity was increased by 60%. It was calculated that the value of the required mobilised phi at the end of t = 34 days of Pattern 2 rainfall was almost similar to that obtained at the end of t = 34 days of the base case Pattern 2 rainfall, and the position of the slip surface remained in a deep position throughout the 34 days duration even when the rainfall intensity was increased by 60%. For Pattern 3 rainfall, the shallow slip surface was obtained at the end of t = 34 days when rainfall was increased by 60%. At this point, the value of the required mobilised phi, ϕ_m = 22.7^{o}.

7.5 Summary of the influence of rainfall patterns on the required mobilised phi for slopes in sandy, silty and clayey soils.

The location of the critical slip surface at certain selected times during the application of each rainfall pattern on each slope with the different soils and geometries were illustrated earlier in Chapter 6. However, this determination was based upon the changes in pore water pressure alone with time with the soil strength parameters kept constant. The value of angle of internal shear resistance, ϕ' that was used in Chapter 6 to calculate the limiting equilibrium was an arbitrary 38^{o}. It can be seen that in the stability calculations and hence the subsequent determination of mobilised phi values as tabulated in Table 7.1 to Table 7.6, there were few occasions where the position of slip surface migrated from a shallow location to a deep slip surface. These were highlighted in bold type in Table 7.1 to Table 7.6.

Generally, the magnitude of the required mobilised phi was highest in slopes in sandy soils and the lowest in clayey soils, and 1V:0.5H slopes demonstrated the necessity of higher mobilised phi values than 1V:1H slopes. This is to be expected. The increase, however, in the base case rainfall intensity by 60% influenced the need for an increase in the value of mobilised phi. However, in the case of slopes in sandy

soils, by the end of t = 34 days this increase in the rainfall intensity by 60% made very little difference to the magnitude of the required mobilised phi values. In all probability the relatively high permeability of the sandy soil enabled rapid infiltration and subsequent drainage of the water through the soil. As seen in the behaviour of the 1V:0.5H slopes in silt and clay soils, the increase in the base case rainfall intensity by 60% produced a higher increase in the required value of mobilised phi by the end of t = 34 days.

It is apparent that there is a difficulty in predicting which rainfall pattern would give rise to the requirement of the highest value of mobilised phi as this all depends on rainfall intensity, type of soil within the slope and the slope geometry. For slopes in sandy soils, for instance, the application of the base case rainfall intensity on a 1V:0.5H sandy slope (i.e. high permeability soil), gave rise to the requirement of a maximum value of mobilised phi at the end of t = 34 days of Pattern 2 rainfall. However when the rainfall was increased by 60%, the maximum value of mobilised phi was obtained at the end of t = 6 days of Pattern 1 rainfall. In the case of the 1V:1H geometry sandy slopes, the maximum value of mobilised phi was seen to be required at the end of t = 34 days of the base case of Pattern 3 rainfall. However, as the base case rainfall was increased by 60%, the maximum value of mobilised phi was seen to be required at the end of t = 34 days of Pattern 2 rainfall.

For 1V:0.5H silt slope, when the base case rainfall amount was increased by 60%, the time at which the mobilised phi reached its maximum changed from t = 34 days to t = 20 days of Pattern 1 rainfall, whereas for the base case and higher rainfall intensity that was applied to the 1V:1H silty soil slope, the maximum required value of mobilised phi was obtained at the same time, i.e. at the end of t = 34 days of Pattern 1 rainfall.

For 1V:0.5H clay slope, the maximum value of mobilised phi was required at the end of t = 34 days of Pattern 3 rainfall for both base case and higher rainfall case. However, for the application of the base case rainfall intensity on 1V:1H clay slope, the maximum value of required mobilised phi was obtained at the end of t = 34 days of Pattern 2 rainfall, and for the higher rainfall intensity, the maximum value of required mobilised phi was found to be at the end of t = 34 days of Pattern 1 rainfall.

7.6 Use of the mobilised ϕ-time graphs to predict time to potential slope failure

The examination of each individual slope's stability assumed the existence of an idealised slope – of either 1V:1H or 1V:0.5H configuration and of a standard 20 m height. These slopes comprised soils characterised as c', ϕ' materials with arbitrarily assigned values to both c' and ϕ'. The slopes were also characterised by their permeability, this being associated with the soil type. It was the influence of this permeability on the behaviour of pore water pressure within the slope as a result of infiltration under standard rainfall patterns which resulted in the observations above.

Whilst the general geology of the Brunei area is documented, the composition of individual slopes, many of which have been steepened through tropical erosion and rainfall, anthropogenic interference and, in some cases, defoliation, is not currently known. Given the hypothesis of the three rainfall patterns presented over a period of 34 days, based on data derived from the meteorological office in Brunei, it is possible to make a rapid assessment of the level of risk of failure of any slope and when in the rainfall cycle this would most likely occur by examination of the Figures 7.2 to 7.7.

A rudimentary site investigation would reveal the type of soil comprising a particular slope deemed to be at risk. Likewise the site investigation would also produce average soil strength parameters through either insitu or simple laboratory tests. An assessment of the soil's permeability and the effective stress parameters would be sufficient to allow the figures above to be used to predict the time to potential failure given daily rainfall records. Figure 7.8 below demonstrates the method in the case of a slope which has been assessed to comprise a sandy type soil, having an associated permeability and an angle of internal friction of 42°. The slope is measured as approximately 1V:0.5H. The rainfall records suggest a Pattern 1 type rainfall.

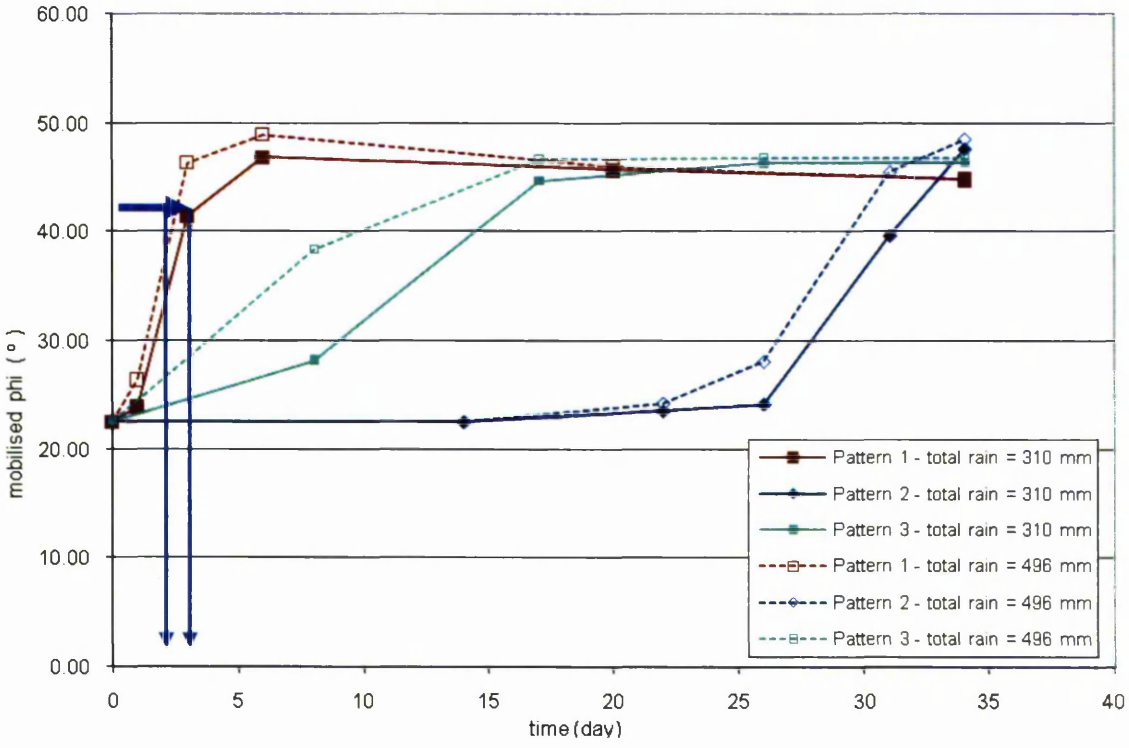

Figure 7.8 The demonstration of the time at which the slope may suffer failure due to Pattern 1 rainfall on 1V:0.5H sandy soil slope

From the above Figure 7.8 it can be seen that the slope may well suffer failure after 2 to 3 days. In the event that the rainfall data are ambiguous, suggesting a rainfall pattern which is between Pattern 1 and 3, an assessment may be made associated with the predicted time to failure; i.e. when the mobilised angle of internal friction required to maintain the slope's stability is only necessary sometime between twelve and sixteen days after the start of the rainfall period.

Likewise other slopes may be examined in a similar manner, bringing to bear the influence of the migrating pore water regime on the stability of the particular slope. Many of the observations made during the execution of this research have been either self-evident or intuitive. The benefit of the presentation of the data from the analyses has been to quantify the periods required for the mobilisation of shear resistance within the slopes under given specific slope geometries and rainfall conditions.

8 Concluding remarks and Recommendations for Future Work

8.1 Aims and Objectives of the research

The aim of this research, as set out in chapter one of the thesis, was;-

"to improve the understanding of the behaviour of water infiltration into slopes with the commensurate generation of transient pore water pressure regimes due to different rainfall patterns and the consequential effect this has on the overall stability of steep slopes in different types of soil in Brunei in order to develop a method to predict when a failure might occur in these slopes."

This was achieved by firstly examining what rainfall patterns might be expected over a prolonged period of time in Brunei. This was achieved by analysing typical rainfall records available for a period of 20 years, i.e. from 1985 to 2004. Whilst pattern recognition analysis demonstrated that a statistically significant and regular seasonal system could not be identified, alternative analysis showed that over short periods of approximately one month three clear types of rainfall pattern could be identified. Using these as base rainfall patterns, and by means of a reliable and commercially available finite element program, the infiltration of water into the idealised slopes was modelled over the one month rainfall periods.

The effects of these different infiltration patterns on the stability of the slopes was then examined by a simple effective stress based limit equilibrium method. In order to isolate the effects of the transient water pressure systems generated in the slopes, both in the unsaturated and saturated zones, on the slope stability, all stability analyses were undertaken with the same soil effective stress parameters (c' and ϕ'), soil unit weight and slope heights. In subsequent analyses the parameter essentially characterising the soil strength (ϕ') was then considered. This was done to permit an examination of the limiting equilibrium of any slope at any time in terms of the magnitude of the mobilised ϕ' which would be required to maintain slope stability.

The outcome of this analysis was the development of a simple means by which known parameters of a slope in Brunei similar in geometry and height which is

subjected to severe rainfall could be used to predict if and when the slope is in danger of instability during such a period of rainfall.

8.2 Research approach

The approach to this research has been essentially parametric without recourse to field examples. With the exception of comprehensive rainfall data for the region, the authorities in Brunei were unable to provide any coherent data on the behaviour of steep slopes, in particular during periods of intense rainfall. The research would certainly have been enhanced by access to field pore water pressure data from instrumented slopes. Regrettably this was not an option in this case.

The use of industry and research validated finite element and limit equilibrium analytical instruments to examine the behaviour of infiltrated water and its effect on the stability of slopes, provides, it is believed, some assurance that the results obtained and the trends observed are rational and that may be expected. Many of the results found have been considered intuitive, but there have been some which have appeared unusual.

8.3 Outcomes and observations

The research findings are analysed comprehensively in Chapter 7. The effects of the infiltrated water on the pore water pressure regime within the slopes so far as it influenced the potential for the slope to resist failure are dealt with for all soil types, characterised by their permeability. The location of the wetting fronts, the distribution of the magnitude of pore water pressure with time in the different soil types caused a variation of potential slip surfaces to be generated.

For all soil slopes, the depth of the wetting front increased as the amount of rainfall continue to increase. However, this behaviour depended on the permeability of the soil and the patterns of rainfall. Understandably, the depths of the wetting fronts were the greatest for sandy soil slopes for the same patterns applied to the clayey soil slopes, which showed the least penetration into the slope. It was found that the duration of rainfall infiltration become an important factor for the migration of the

location of the critical slip surface from a deep position to a shallow slip surface. For lower permeability soil slopes, it was found that it took a longer time for the deep slip surface to migrate to a shallower position. It was also noted that in determining the magnitude of the required mobilised phi angle, it was found that there were few occasions where the critical slip surface migrated from a shallow location to a deep location. In all cases, however, a pattern of critical slip surface migration to a deep location and then returning to a shallow position emerged.

Whilst the limit equilibrium analyses showed that with the application of the base case ϕ' to the analysis, there were a number of cases where the slope was inherently stable. This was shown to be particularly in the cases of the slopes comprising clayey soils. This was as a result of the low dissipation of the pore water pressure due to the lower overall permeability of these soils. The sensitivity analyses then demonstrated that essentially a much lower magnitude of mobilised ϕ' was necessary in these cases to ensure continued stability of the slopes. Conversely slopes in sandy soils clearly showed that with the anticipated range of effective stress parameters for relict clays in tropical zones such as Brunei the slopes would in all probability be in a state of incipient failure within a very short period after the start of the rainfall.

In relation to previous research in the literature, the behaviour of the distribution of pressure head as shown in Appendix B was comparable to the behaviour of pore water pressure presented by Vargas et al. (1990). The pattern of pressure heads was similar for all three soil type, and the depth of the wetting fronts were influence by the water retention parameters and saturated hydraulic conductivity of the soil. As mentioned earlier, the depth of penetration of the wetting front was more significant for highly permeable soil than less permeable soil, this behaviour also agreed with the result found by Tsaparas (2002) and Tsaparas et al. (2002). Unlike that found by Tsaparas et al. (2002), however, the pore water pressure that was formed near the surface of the slope due to the infiltration of rainfall only reached 0 kN/m^2, whereas as reported in Tsaparas et al. (2002), the introduction of major rainfall after a period of antecedent rainfall on high permeability soil produced a positive value of pore water pressure below the surface of the slope.

Similar to Alonso et al. (1995), it can also be suggested that these hydraulic parameters of the soil control the stability of slope during rainfall. For instance, by comparing the behaviour of the 1V:0.5H sandy soil slope (Section 6.2.1) with the 1V:0.5H silty soil slope (Section 6.3.1) under Pattern 1 rainfall of higher intensity, it shows that it takes a longer time for a slope of silty type soil to produce a value of FoS below unity in comparison with a slope of sandy type soil. This behaviour was also found by Rahardjo H. et al.(2008).

In addition to this, it was also found that the highest daily rainfall intensity on Day 1 of Pattern 1 rainfall reduced the FoS instantly. However the reduction of FoS increased further when antecedent rainfall was applied at the beginning of Pattern 2 rainfall, before the highest daily rainfall intensity was introduced on Day 34. This behaviour was similar with that observed by Ng and Shi (1998a), Ng and Shi (1998b) and Rahardjo et al. (2001). In this study it was found that the ground water level beneath the toe of all three type slopes rose to a level during the 34 day duration of any three rainfall pattern which agreed with the study concluded by Rahardjo et al. (2001). It should be added in this study, however, that the increase in ground water level beneath the toe of the slope also depends on the soil type, i.e. the water retention parameters and saturated hydraulic conductivity of the soil slope.

8.4 Prediction of time to failure

Using the observations of the variation of mobilised ϕ' against time generated from the various analyses for different slopes and conditions, information on the effective stress parameters from individual slopes in Brunei may be matched against the observations from this research in a attempt to predict when the onset of failure may be expected.

Whilst this is a simple approach, it could be very effective given reliable and relevant data from slopes under examination in the field. This research has concentrated on a few typical configurations and soil types. A more comprehensive study incorporating a greater degree of complexity in terms of the slope characteristics, strengths, heterogeneity etc would certainly provide a better basis for examination.

8.5 Recommendations for further research

It is clear that the outcomes from this research have lacked calibration with field data. Furthermore the analytical tools available to predict the onset of failure were rudimentary, not allowing any prefailure deformation to be examined and to assess this with respect to the further variation of the pore water pressure regime within the slopes immediately prior to failure.

It is believed that the following avenues of future research would benefit this work;-

- A more comprehensive study of a greater variation of slope, height and soil types, including heterogeneity, should be addressed to provide a better basis for the prediction of the onset of failure.
- A finite element based stability analysis should be used to assess slope mechanical behaviour using the transient pore water systems prevailing at any time during the rainfall period.
- The periods immediately after the cessation of rainfall should be examined in more detail to see if the ongoing pore water pressure migration has any significant effect on the stability of the slopes.
- The results of a more comprehensive analysis should be in dimensionless format so that the prediction method may be applied to more general cases.
- The analyses should take into account the effects of vegetation, denudation and erosion.
- This research assumed a steady state condition for the water table prior to the start of the rainfall period. This may well not be the case if the antecedent rainfall immediately prior to a base case rainfall period was sufficiently close in time so as to prevent the water table from equilibrating under zero rainfall conditions. This should be considered. The same approach adopted here may be applied to a number of rainfall cycles thus providing a more realistic preconditioning of the water table.
- For unsaturated soil, it is more appropriate to consider an additional parameter from the extended Mohr Coulomb failure envelope, ϕ^b as mentioned earlier in Chapter 2. This should be the subject of further consideration in adopting a more relevant soil model.

- The soil water retention curve is an important factor in the behaviour of the pore water pressure in the vadose zone. A comprehensive investigation of the soil water retention model through ground water monitoring should be studied for soil types in Brunei using real field data.

References

Abdul Halim, Q. (1992). "Geological resources." *Singapore Journal of Tropical Geography*, 13(1), 38 - 51.

Alonso, E. E., Gens, A., Delahaye, C., and Lloret, A. (1995). "Effect of rain infiltration on the stability of slopes." Proceedings of the 1st International Conference on Unsaturated Soils. Part 1 (of 2), Sep 6-8 1995, Paris, France, 241 - 249.

Au, S. W. C. (1993). "Rainfall and slope failure in Hong Kong." *Engineering Geology*, 36(1-2), 141-147.

Bishop, A. W. (1955). "The use of the slip circle in the stability analysis of slopes." *Geotechnique*, 5(1), 7-17.

Blight, G. E. (1997). "Interactions between the atmosphere and the earth." *Geotechnique*, 47(4), 715-766.

Blyth, F. G. H., and De Freitas, M. H. (1984). *A geology for engineers*, 7th Edition, Edward Arnold, London.

Borin, D. L. (2003). *SLOPE - Slope stability and reinforced soil analysis and design program - Users manual*, Geosolve, London.

Brand, E. W. (1992). "Slope instability in tropical areas." Proceedings of the 6th International Symposium on Landslides, Christchurch, New Zealand, 2031 - 2051.

Brand, E. W., Premchitt, J., and Phillipson, H. B. (1984). "Relationship between rainfall and landslides in Hong Kong." Proceedings of the 4th International Symposium on Landslides, Toronto, Canada, 377 - 384.

Brooks, R. H., and Corey, A. T. (1964). "Hydraulic properties of porous media." *American Society of Agricultural Engineers -- Transactions*, 7(1), 26-28.

Brunig, E. F. (1970). "On the ecological significance of drought in the equatorial wet evergreen forest of Sarawak." The water relations of Malaysian forests, J. R. Flenley, ed., University of Hull, Department of Geography, Miscellaneous Series 11, 66.

BS 5930. (1999). *The code of practice for site investigations*, British Standards Institution, London.

Burroughs, W. J. (2007). *Climate change : a multidisciplinary approach*, Cambridge University Press, Cambridge.

Carsel, R. F., and Parrish, R. S. (1988). "Developing Joint Probability-Distributions of Soil-Water Retention Characteristics." *Water Resources Research*, 24(5), 755-769.

Charbeneau, R. J. (2000). *Groundwater hydraulics and pollutant transport*, Prentice Hall, Upper Saddle River, NJ.

Craig, R. F. (1997). *Soil mechanics, 6th Edition*, E & FN Spon, London.

Dale, W. L. (1963). "Surface temperatures in Malaya." *Journal of Tropical Geography*, 17, 57.

Delleur, J. W. (1999). *The handbook of groundwater engineering*, CRC Press, Boca Raton, Florida.

Duncan, J. M., and Wright, S. G. (2005). *Soil strength and slope stability*, John Wiley & Sons, Hoboken, New Jersey.

Dykes, A. P. (1994). "Hydrological controls on shallow mass movements and characteristics slope forms in the tropical rainforest of Temburong District, Brunei," PhD Thesis, King's College London, University of London.

Feddes, R. A., Kowalik, P. J., and Zaradny, H. (1978). *Simulation of field water use and crop yield*, Centre for Agricultural Pub. and Documentation, Wageningen.

Fetter, C. W. (2001). *Applied hydrogeology*, Prentice Hall, Englewood Cliffs, N.J.

Fredlund, D. G., and Rahardjo, H. (1993). *Soil mechanics for unsaturated soils*, Wiley, New York, N.Y.

Fredlund, D. G., and Xing, A. (1994). "Equations for the soil-water characteristic curve." *Canadian Geotechnical Journal*, 31(4), 521-532.

Gasmo, J. M., Rahardjo, H., and Leong, E. C. (2000). "Infiltration effects on stability of a residual soil slope." *Computers and Geotechnics*, 26(2), 145-165.

Griffiths, D. V., and Lu, N. (2005). "Unsaturated slope stability analysis with steady infiltration or evaporation using elasto-plastic finite elements." *International Journal for Numerical and Analytical Methods in Geomechanics*, 29(3), 249-267.

Haji Sirabaha, H. S. (2005). Private Communication.

Henson, R. (2008). *The rough guide to climate change*, Rough Guides Ltd.

Jali, D., and Choudhury, J. E. E. (1992). "Soil: Agriculture and engineering properties." *Singapore Journal of Tropical Geography*, 13(1), 1 - 14.

Lockwood, J. G. (1974). *World climatology : an environmental approach*, Edward Arnold, London.

Lu, N., and Likos, W. J. (2004). *Unsaturated soil mechanics*, J. Wiley, Hoboken, N.J.

Lumb, P. (1965). "Residual soils of Hong Kong." *Geotechnique*, 15(2), 180-194.

Lumb, P. (1975). "Slope failures in Hong Kong." *Quarterly Journal of Engineering Geology*, 8, 31 - 65.

Meteorological Office, Brunei (2005) Private Communication

Mualem, Y. (1976). "A new model for predicting the hydraulic conductivity of unsaturated porous media." *Water Resources Research*, 12(3), 513-522.

Negara Brunei Darussalam Master Plan. (1986). "Geology and Mineral Resources." Ministry of Development (unpublished), Brunei Darussalam.

Ng, C. W. W., and Shi, Q. (1998a). "Influence of rainfall intensity and duration on slope stability in unsaturated soils." *Quarterly Journal of Engineering Geology*, 31(pt 2), 105-113.

Ng, C. W. W., and Shi, Q. (1998b). "Numerical investigation of the stability of unsaturated soil slopes subjected to transient seepage." *Computers and Geotechnics*, 22(1), 1-28.

Powrie, W. (1997). *Soil mechanics : concepts and applications*, E & FN Spon, London.

Quazi, A. H. (1999). "Landslides and Urban Development in Brunei Darussalam." Construction Industry Directory 1999, Hj Hamdani Hj Mohd Jamil, Hj Md Yunus Hj Yusof, Mohammad Ozair Mian, and Mazlan Ahmad, eds., Ministry of Development, Brunei, 128 - 129.

Rahardjo, H., Aung, K. K., Leong, E. C., and Rezaur, R. B. (2004). "Characteristics of residual soils in Singapore as formed by weathering." *Engineering Geology*, 73(1-2), 157-169.

Rahardjo, H., Li, X. W., Toll, D. G., and Leong, E. C. (2001). "The effect of antecedent rainfall on slope stability." *Geotechnical and Geological Engineering*, 19(3-4), 371-399.

Rahardjo H., Leong E. C., and Rezaur R. B. (2008). "Effect of antecedent rainfall on pore-water pressure distribution characteristics in residual soil slopes under tropical rainfall." *Hydrological Processes*, 22(4), 506-523.

Rassam, D., Simunek, J., and Van Genuchten, M. T. (2004). *Modelling variably saturated flow with HYDRUS-2D*, ND Consult, Brisbane, Australia.

Sandal, S. T. (1996). *The Geology and Hydrocarbon Resources of Negara Brunei Darussalam*, Syabas, Bandar Seri Begawan.

Schaap, M. G., and Leij, F. J. (2000). "Improved prediction of unsaturated hydraulic conductivity with the Mualem-van Genuchten model." *Soil Science Society of America Journal*, 64(3), 843-851.

Schaap, M. G., Leij, F. J., and Van Genuchten, M. T. (2001). "Rosetta: A computer program for estimating soil hydraulic parameters with hierarchical pedotransfer functions." *Journal of Hydrology*, 251(3-4), 163-176.

Simunek, J., Sejna, M., and Van Genuchten, M. T. (1999). "The Hydrus2D software package for simulating the two-dimensional movement of water, heat, and multiple solutes in variably-saturated media, Version 2.0 (manual)." U.S. Salinity Laboratory, Agricultural Research Service, U.S. Department of Agriculture, Riverside, California.

Singh, H., and Huat, B. B. K. (2004). "Origin, formation and occurrence of tropical residual soils." Tropical residual soils engineering, B. B. K. Huat, G. S. Sew, and F. H. Ali, eds., A. A. Balkema, Leiden, 1 - 19.

Smith, G. N., and Smith, I. G. N. (1998). *Elements of soil mechanics*, Blackwell Science, Oxford.

Spencer, E. (1967). "Method of analysis of stability of embankments assuming parallel inter-slice forces." *Geotechnique*, 17(1), 11-26.

Summerfield, M. A. (1991). *Global geomorphology : an introduction to the study of landforms*, Longman Scientific & Technical, Harlow.

Terzaghi, K. (1943). *Theoretical soil mechanics*, Wiley, New York ; London.

Tsaparas, I. (2002). "Field measurement and numerical modelling of infiltration and matric suctions within slopes," PhD Thesis, University of Durham.

Tsaparas, I., Rahardjo, H., Toll, D. G., and Leong, E. C. (2002). "Controlling parameters for rainfall-induced landslides." *Computers and Geotechnics*, 29(1), 1-27.

Tsaparas, I., and Toll, D. G. (2002). "Numerical analysis of infiltration into unsaturated residual soil slope." Unsaturated Soils : Proceedings of the 3rd International Conference on Unsaturated Soils, J. F. T. Juca, T. M. P. de Campos, and F. A. M. Marinho, eds., Swets & Zeitlinger, Recife, Brazil, 755 - 762.

van Genuchten, M. T. (1980). "A closed-form equation for predicting the hydraulic conductivity of unsaturated soils." *Soil Science Society of America Journal*, 44(5), 892-898.

Vargas, E. A., Velloso, R. C., and de Campos, T. M. P. (1990). "Saturated-unsaturated analysis of water flow in slopes of Rio de Janeiro, Brazil." *Computers and Geotechnics*, 10(3), 247-261.

Verruijt, A. (1970). *Theory of groundwater flow*, Macmillan, London.

Wicander, R., and Monroe, J. S. (1995). *Essentials of geology*, West Publishing, St Paul (Minn.).

APPENDIX A

The 30 days cumulative rainfall pattern with 10 days interval from the initial time, t_i = 0 day to the initial time, t_i = 330 days during each year from 1986 to 2004

Appendix A

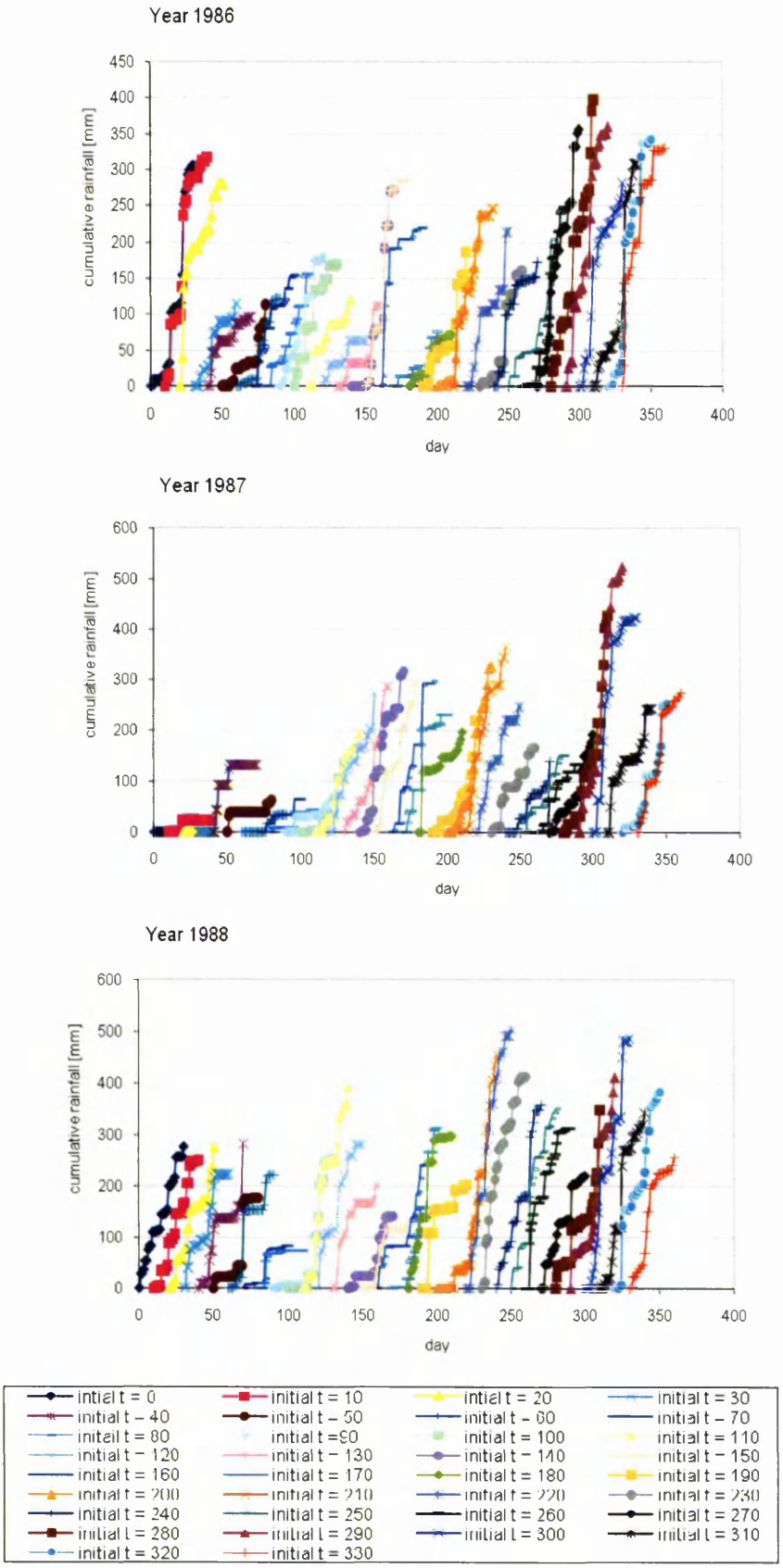
Year 1986
cumulative rainfall [mm]
day
Year 1987
cumulative rainfall [mm]
day
Year 1988
cumulative rainfall [mm]
day
intial t = 0
initial t = 10
intial t = 20
initial t = 30
initial t – 40
initial t – 50
initial t – 60
initial t – 70
initeil t = 80
initial t =90
initial t = 100
initial t = 110
initial t – 120
initial t – 130
initial t – 140
initial t – 150
initial t = 160
initial t = 170
initial t = 180
initial t = 190
initial t = 200
initial t = 210
initial t = 220
initial t = 230
initial t = 240
initial t = 250
initial t = 260
initial t = 270
initial t = 280
initial t = 290
initial t = 300
initial t = 310
initial t = 320
initial t = 330

Appendix A

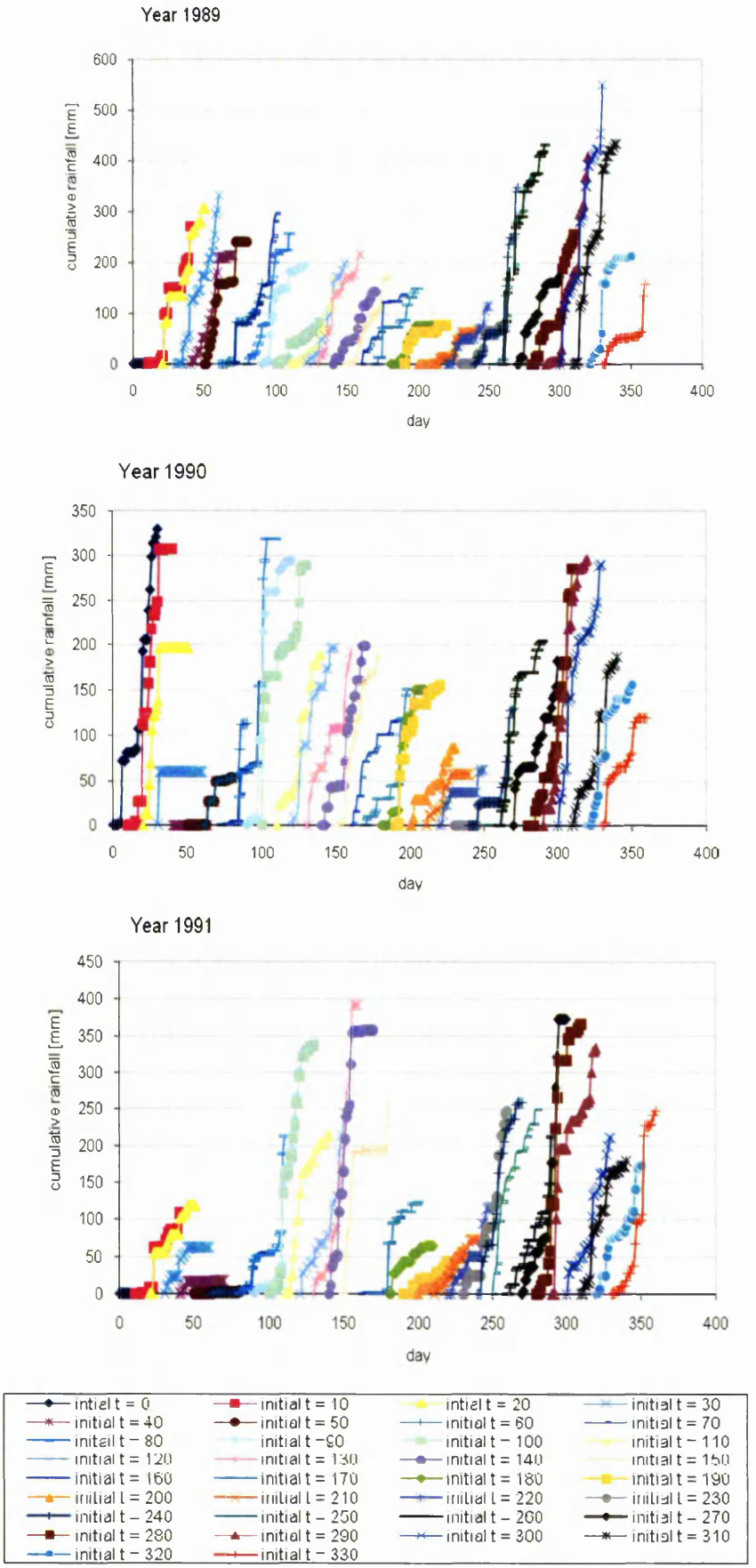
Year 1989
cumulative rainfall [mm]
day
Year 1990
cumulative rainfall [mm]
day
Year 1991
cumulative rainfall [mm]
day
intial t = 0
initial t = 10
intial t = 20
initial t = 30
initial t = 40
initial t = 50
initial t = 60
initial t = 70
initail t = 80
initial t = 90
initial t = 100
initial t = 110
initial t = 120
initial t = 130
initial t = 140
initial t = 150
initial t = 160
initial t = 170
initial t = 180
initial t = 190
initial t = 200
initial t = 210
initial t = 220
initial t = 230
initial t = 240
initial t = 250
initial t = 260
initial t = 270
initial t = 280
initial t = 290
initial t = 300
initial t = 310
initial t = 320
initial t = 330

Appendix A

Year 1992

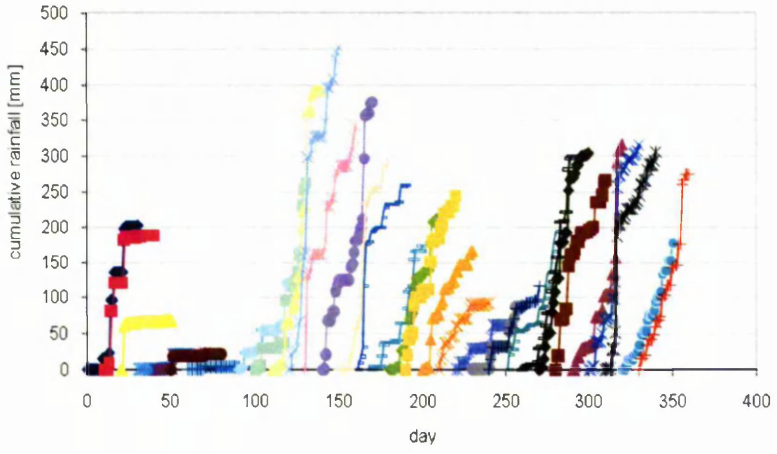

Year 1993

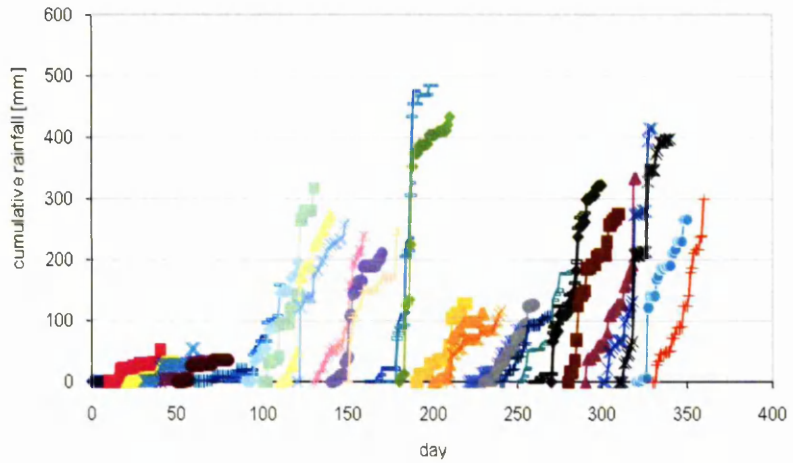

Year 1994

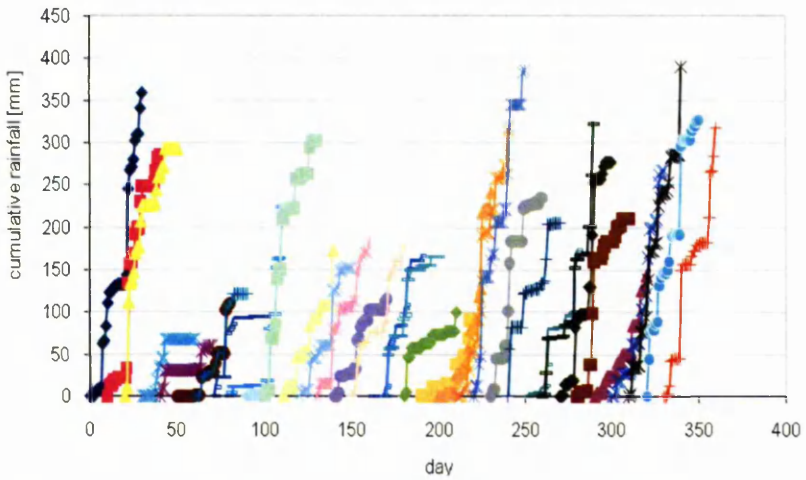

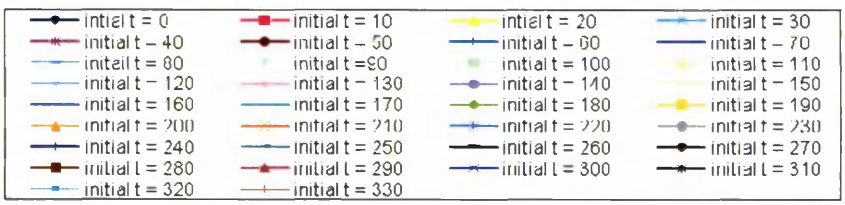

Appendix A

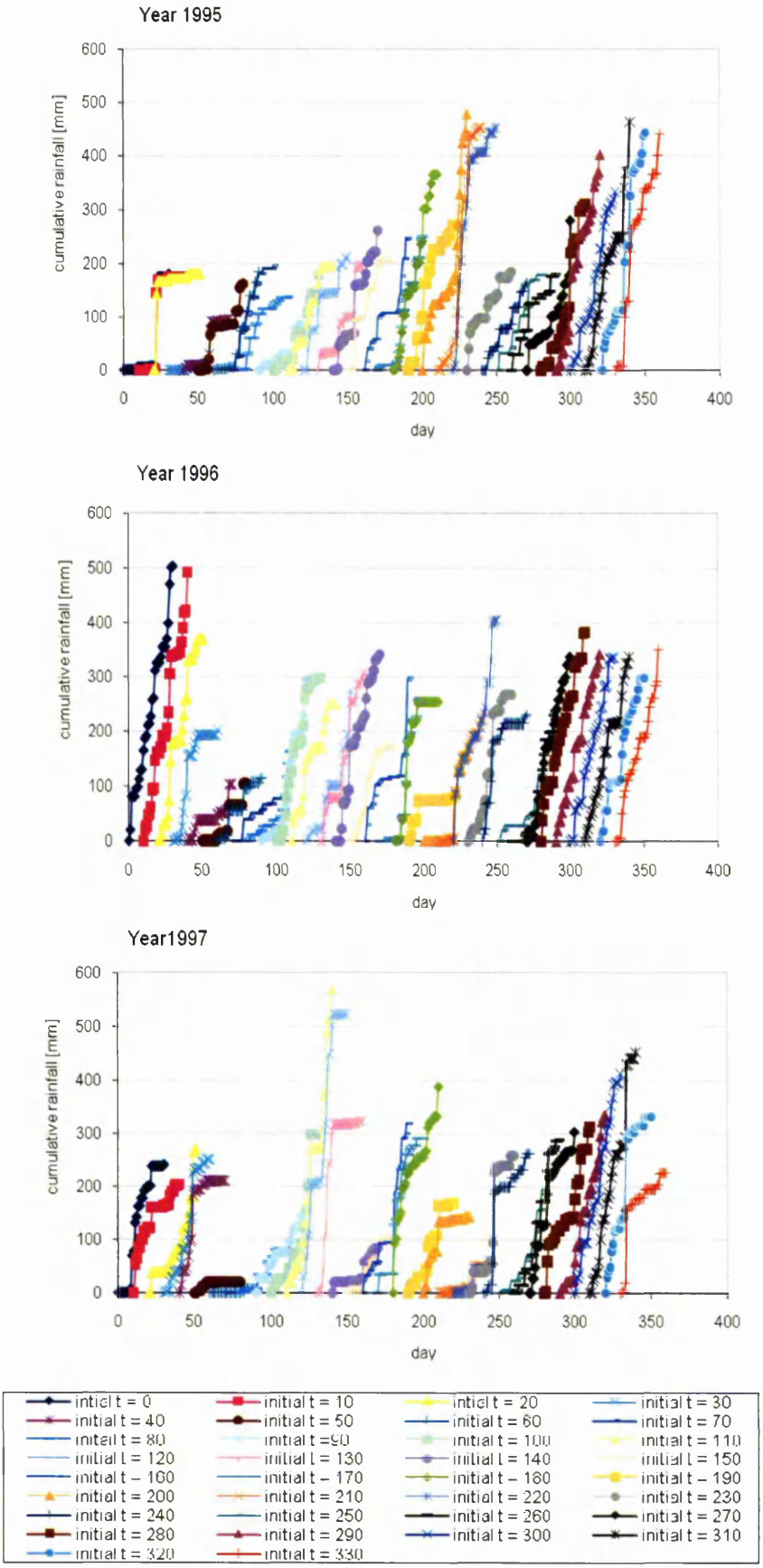
Year 1995
cumulative rainfall [mm]
day
Year 1996
cumulative rainfall [mm]
day
Year1997
cumulative rainfall [mm]
day
initial t = 0
initial t = 10
initial t = 20
initial t = 30
initial t = 40
initial t = 50
initial t = 60
initial t = 70
initial t = 80
initial t = 90
initial t = 100
initial t = 110
initial t = 120
initial t = 130
initial t = 140
initial t = 150
initial t = 160
initial t = 170
initial t = 180
initial t = 190
initial t = 200
initial t = 210
initial t = 220
initial t = 230
initial t = 240
initial t = 250
initial t = 260
initial t = 270
initial t = 280
initial t = 290
initial t = 300
initial t = 310
initial t = 320
initial t = 330

Appendix A

Year 1998

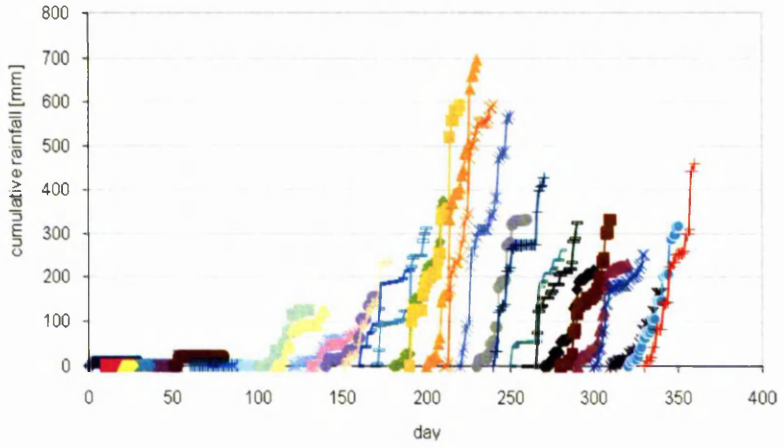

Year 1999

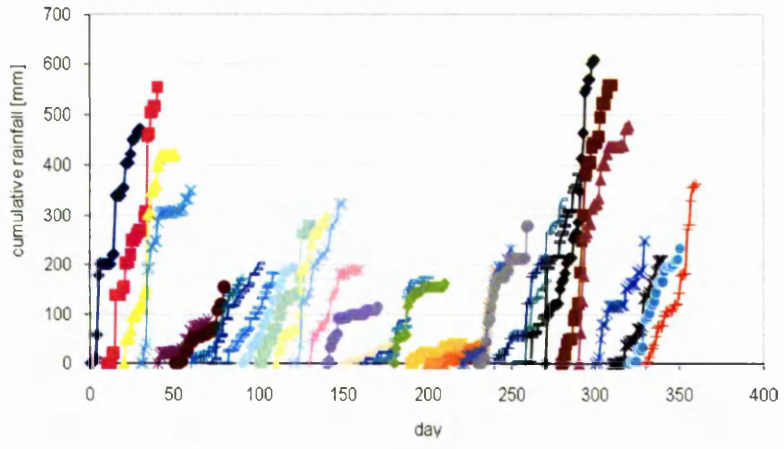

Year 2000

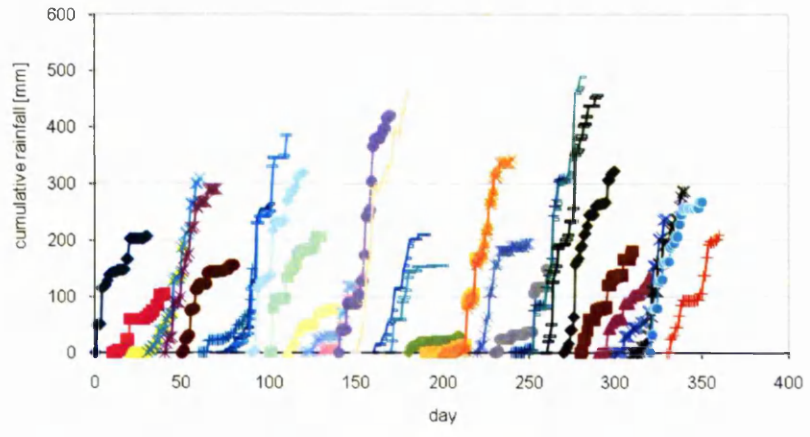

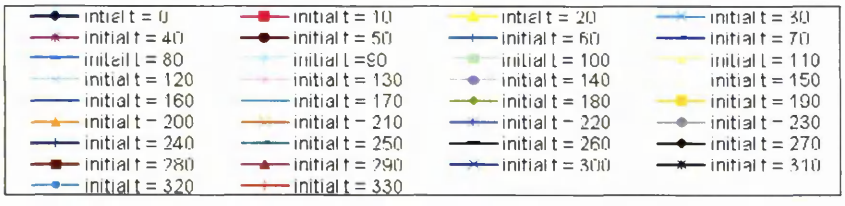

Appendix A

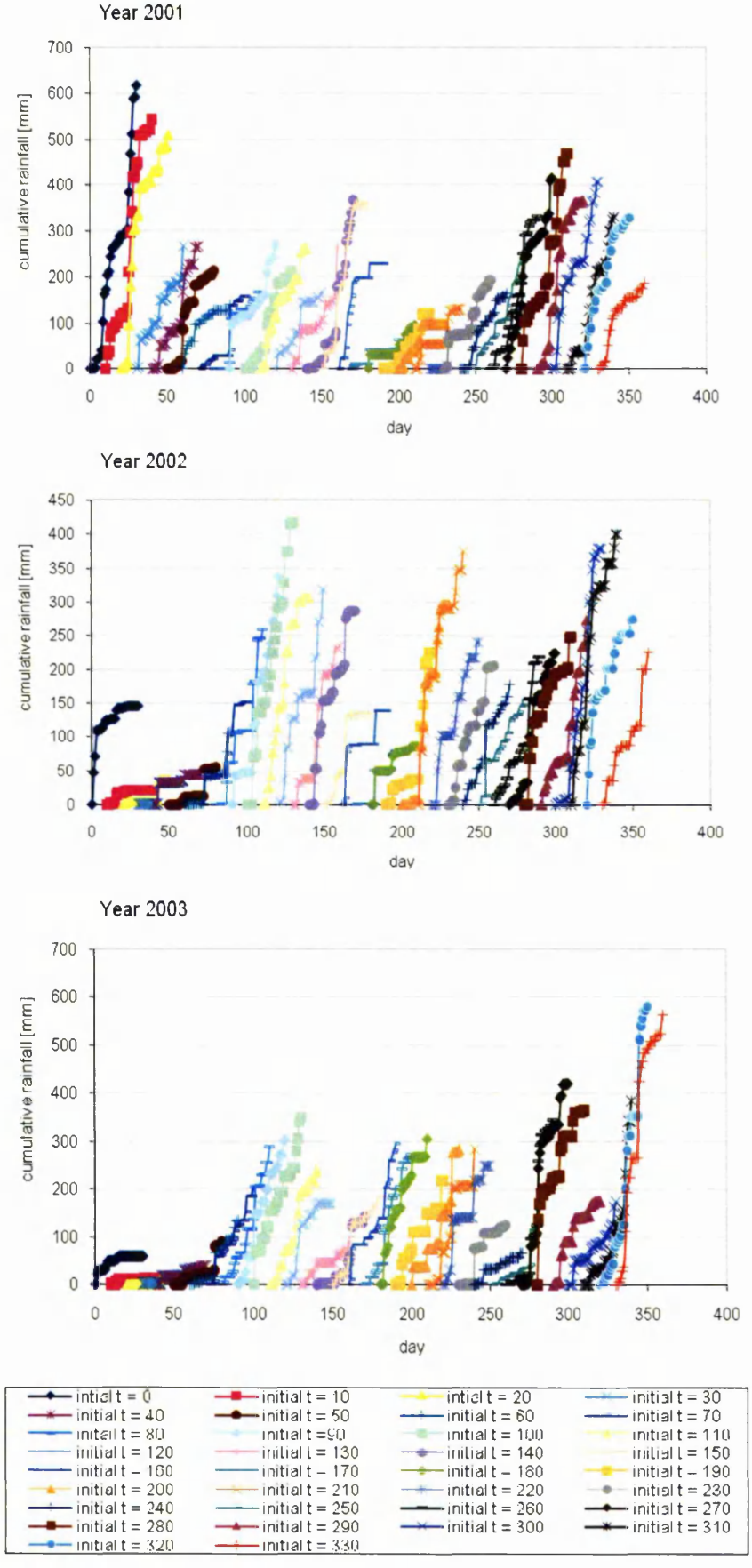
Year 2001
cumulative rainfall [mm]
day
Year 2002
cumulative rainfall [mm]
day
Year 2003
cumulative rainfall [mm]
day
initial t = 0
initial t = 10
initial t = 20
initial t = 30
initial t = 40
initial t = 50
initial t = 60
initial t = 70
initial t = 80
initial t = 90
initial t = 100
initial t = 110
initial t = 120
initial t = 130
initial t = 140
initial t = 150
initial t = 160
initial t = 170
initial t = 180
initial t = 190
initial t = 200
initial t = 210
initial t = 220
initial t = 230
initial t = 240
initial t = 250
initial t = 260
initial t = 270
initial t = 280
initial t = 290
initial t = 300
initial t = 310
initial t = 320
initial t = 330

Appendix A

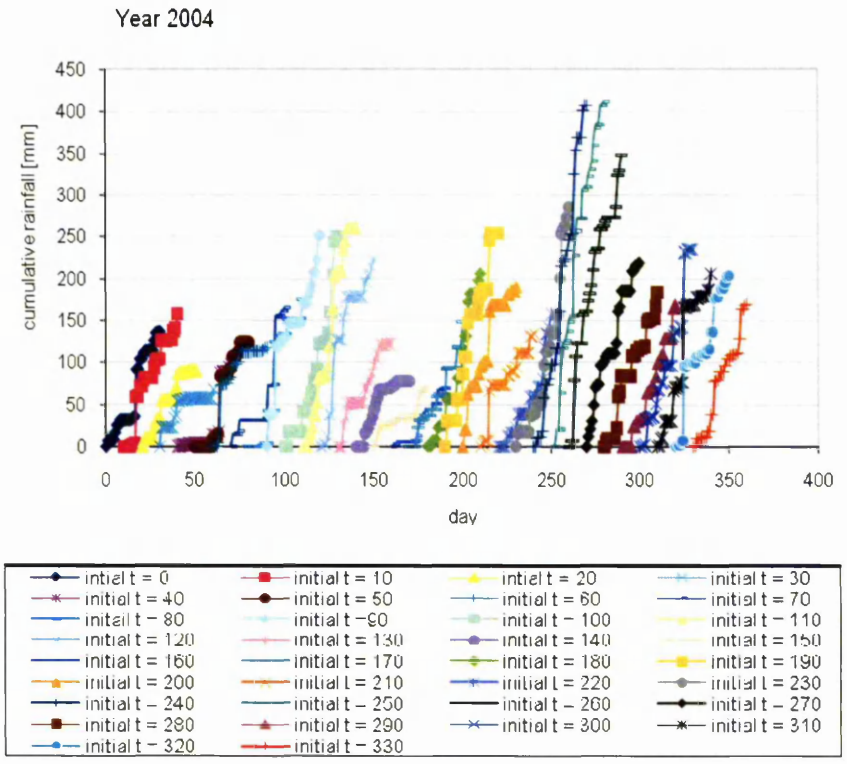
Year 2004
cumulative rainfall [mm]
450
400
350
300
250
200
150
100
50
0
0
50
100
150
200
250
300
350
400
day
intial t = 0
initial t = 10
intial t = 20
initial t = 30
initial t = 40
initial t = 50
initial t = 60
initial t = 70
initail t = 80
initial t = 90
initial t = 100
initial t = 110
initial t = 120
initial t = 130
initial t = 140
initial t = 150
initial t = 160
initial t = 170
initial t = 180
initial t = 190
initial t = 200
initial t = 210
initial t = 220
initial t = 230
initial t = 240
initial t = 250
initial t = 260
initial t = 270
initial t = 280
initial t = 290
initial t = 300
initial t = 310
initial t = 320
initial t = 330

APPENDIX B

The two dimensional contours of the pressure head values (m) observed at the end of t = 34 days of all three rainfall patterns, with 34-days total rainfall amount of 310 mm and 496 mm; for the area around the slopes with two slope geometries of 1V:0.5H and 1V:1H, comprising sandy, silty and clayey soils.

List of Appendix B:

Appendix	Description	Total rainfall [mm]
Appendix B-1	Contours of pressure head values at t = 34 days for three rainfall patterns on 1V:0.5H **SAND** slopes	310.26
Appendix B-2	Contours of pressure head values at t = 34 days for three rainfall patterns on 1V:0.5H **SAND** slopes	496.42
Appendix B-3	Contours of pressure head values at t = 34 days for three rainfall patterns on 1V:1H **SAND** slopes	310.26
Appendix B-4	Contours of pressure head values at t = 34 days for three rainfall patterns on 1V:1H **SAND** slopes	496.42
Appendix B-5	Contours of pressure head values at t = 34 days for three rainfall patterns on 1V:0.5H **SILT**	310.26
Appendix B-6	Contours of pressure head values at t = 34 days for three rainfall patterns on 1V:0.5H **SILT**	496.42
Appendix B-7	Contours of pressure head values at t = 34 days for three rainfall patterns on 1V:1H **SILT**	310.26
Appendix B-8	Contours of pressure head values at t = 34 days for three rainfall patterns on 1V:1H **SILT**	496.42
Appendix B-9	Contours of pressure head values at t = 34 days for three rainfall patterns on 1V:0.5H **CLAY** slopes	310.26
Appendix B-10	Contours of pressure head values at t = 34 days for three rainfall patterns on 1V:0.5H **CLAY** slopes	496.42
Appendix B-11	Contours of pressure head values at t = 34 days for three rainfall patterns on 1V:1H **CLAY**	310.26
Appendix B-12	Contours of pressure head values at t = 34 days for three rainfall patterns on 1V:1H **CLAY** slopes	496.42

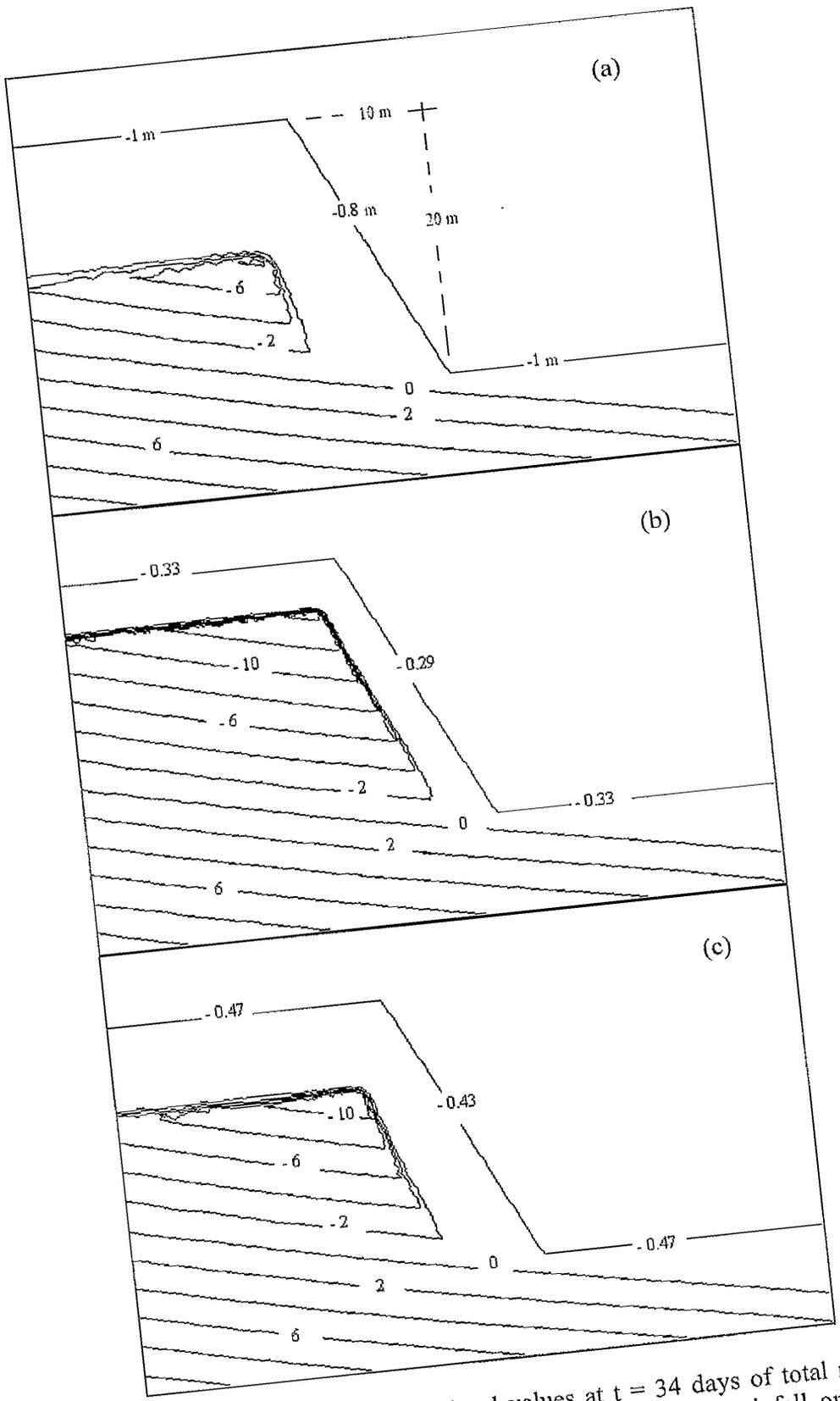

Appendix B-1 Contours of pressure head values at t = 34 days of total rainfall of 310.26 mm for (a) Pattern 1 (b) Pattern 2 and (c) Pattern 3 rainfall on 1V:0.5H SAND slopes

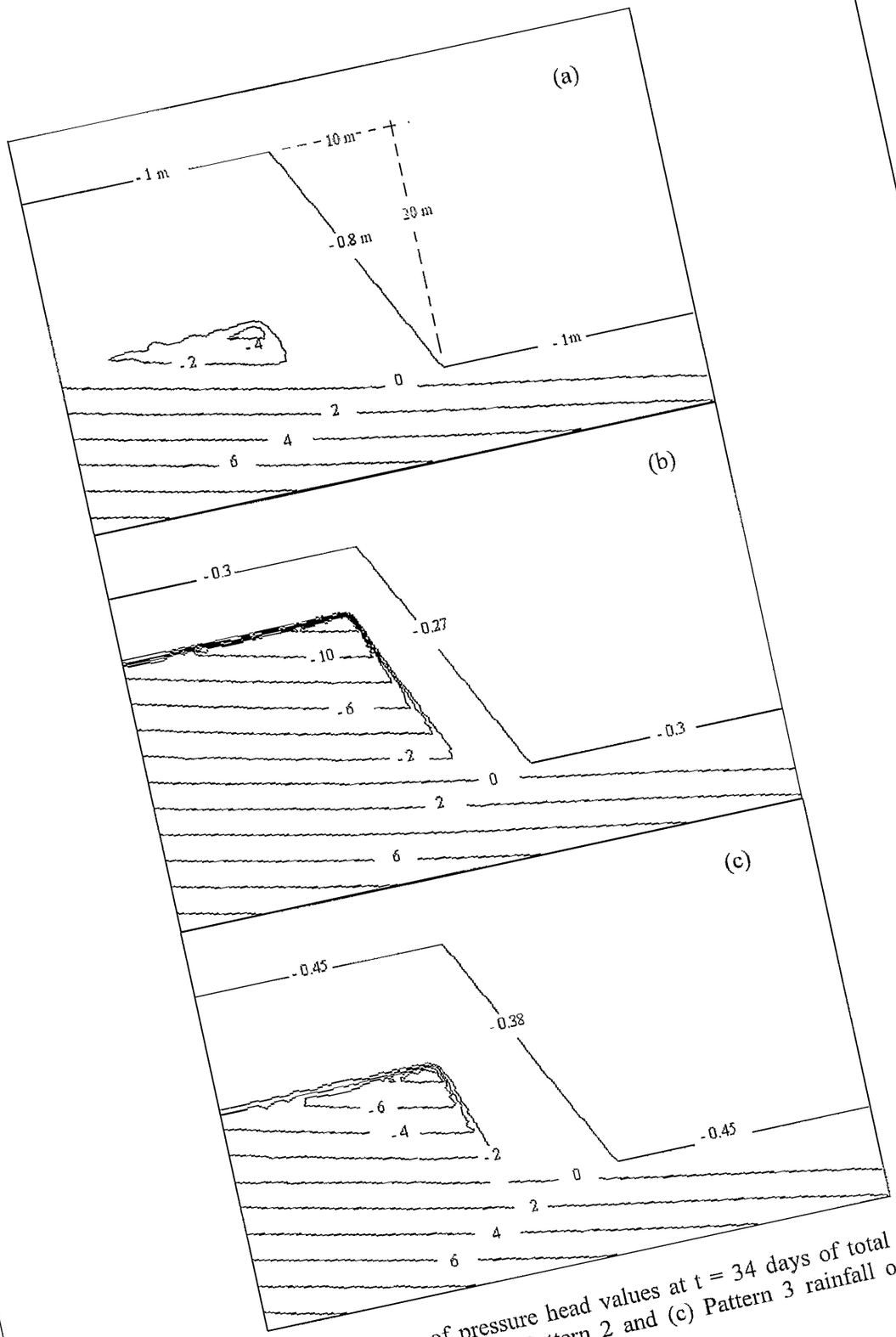

Appendix B-2 Contours of pressure head values at t = 34 days of total rainfall of 496.42 mm for (a) Pattern 1 (b) Pattern 2 and (c) Pattern 3 rainfall on 1V:0.5H SAND slopes

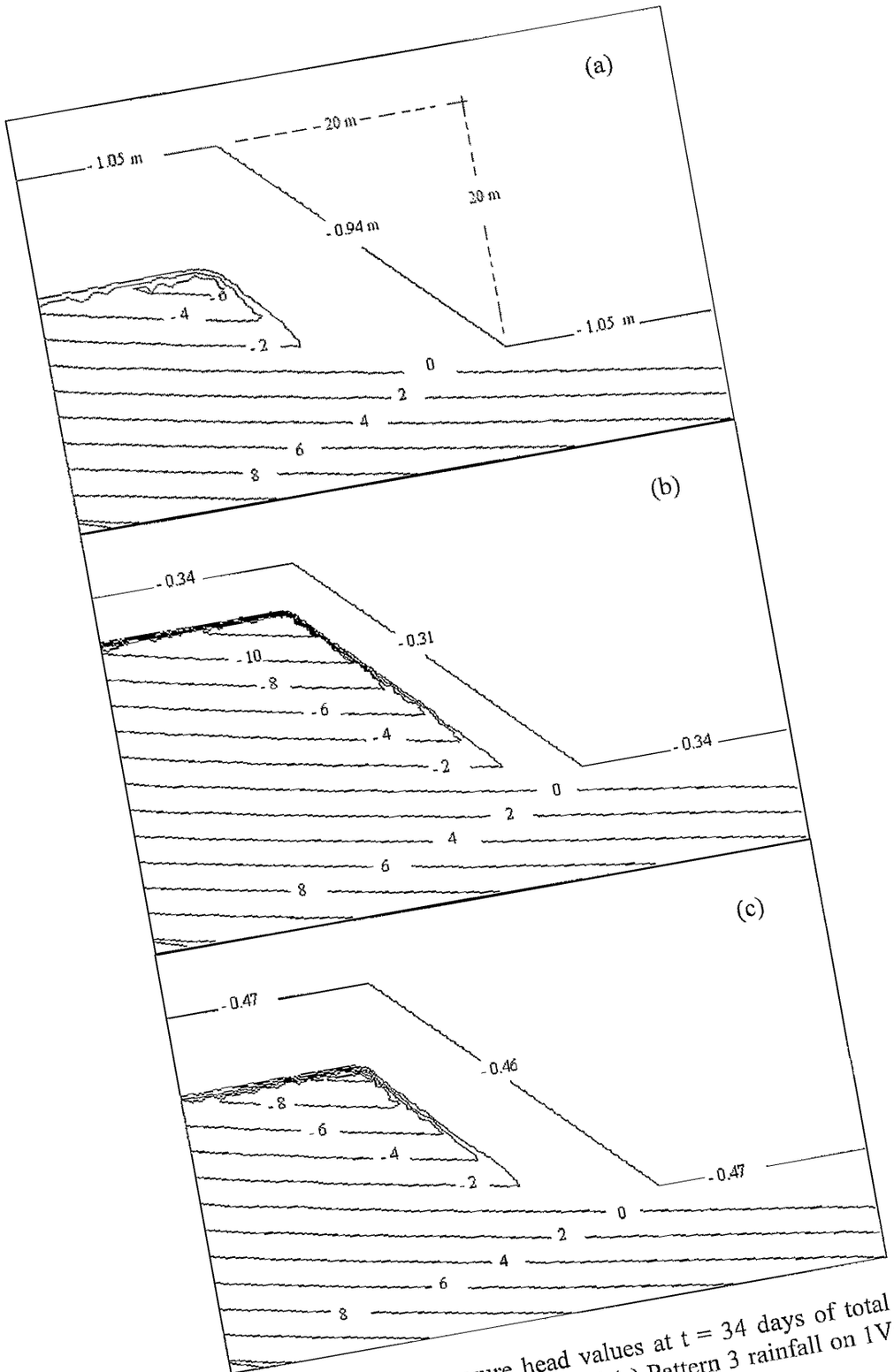

Appendix B-3 Contours of pressure head values at t = 34 days of total rainfall of 310.26 mm for (a) Pattern 1 (b) Pattern 2 and (c) Pattern 3 rainfall on 1V:1H SAND slopes

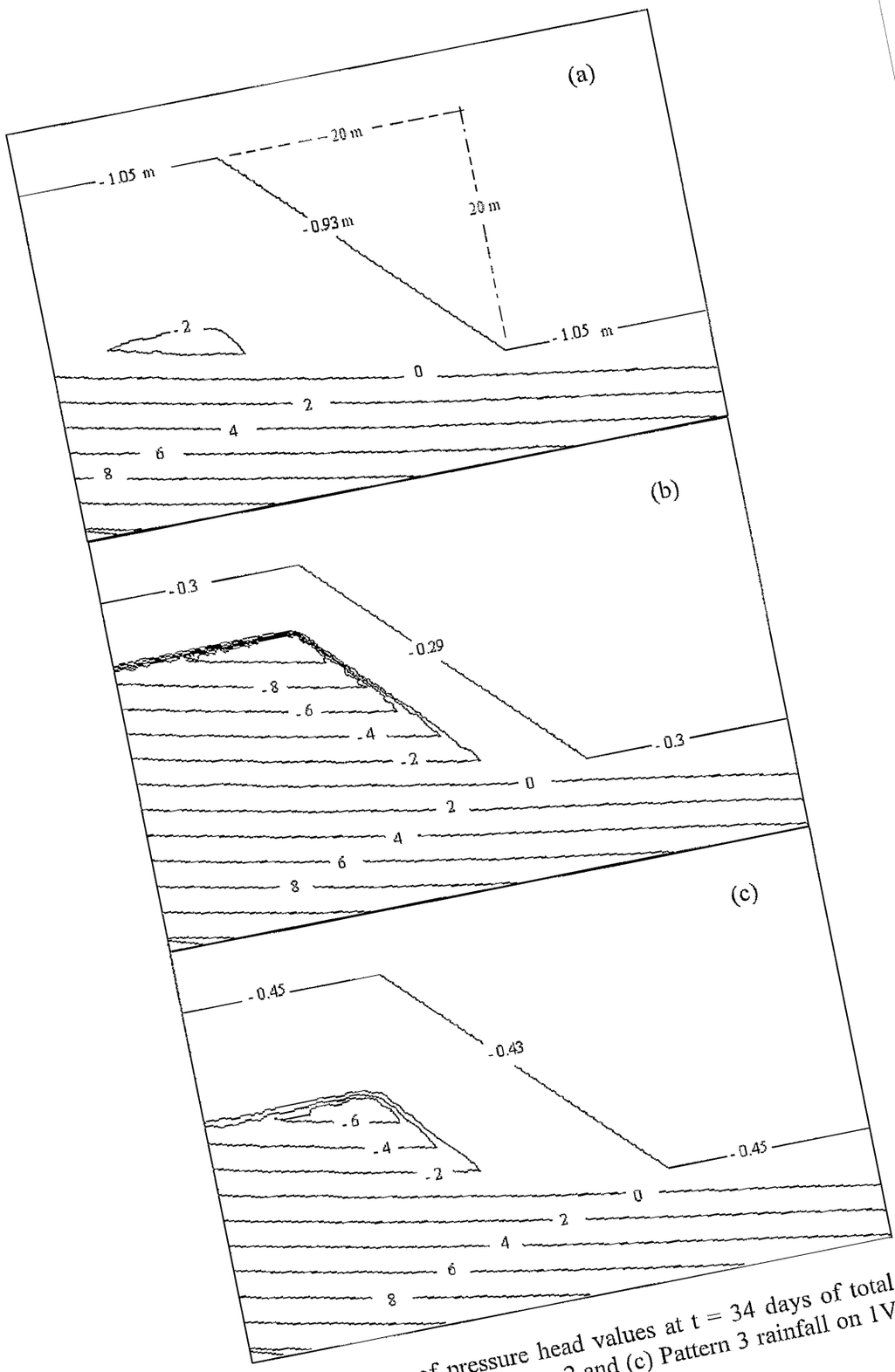

Appendix B-4 Contours of pressure head values at t = 34 days of total rainfall of 496.42 mm for (a) Pattern 1 (b) Pattern 2 and (c) Pattern 3 rainfall on 1V:1H SAND slopes

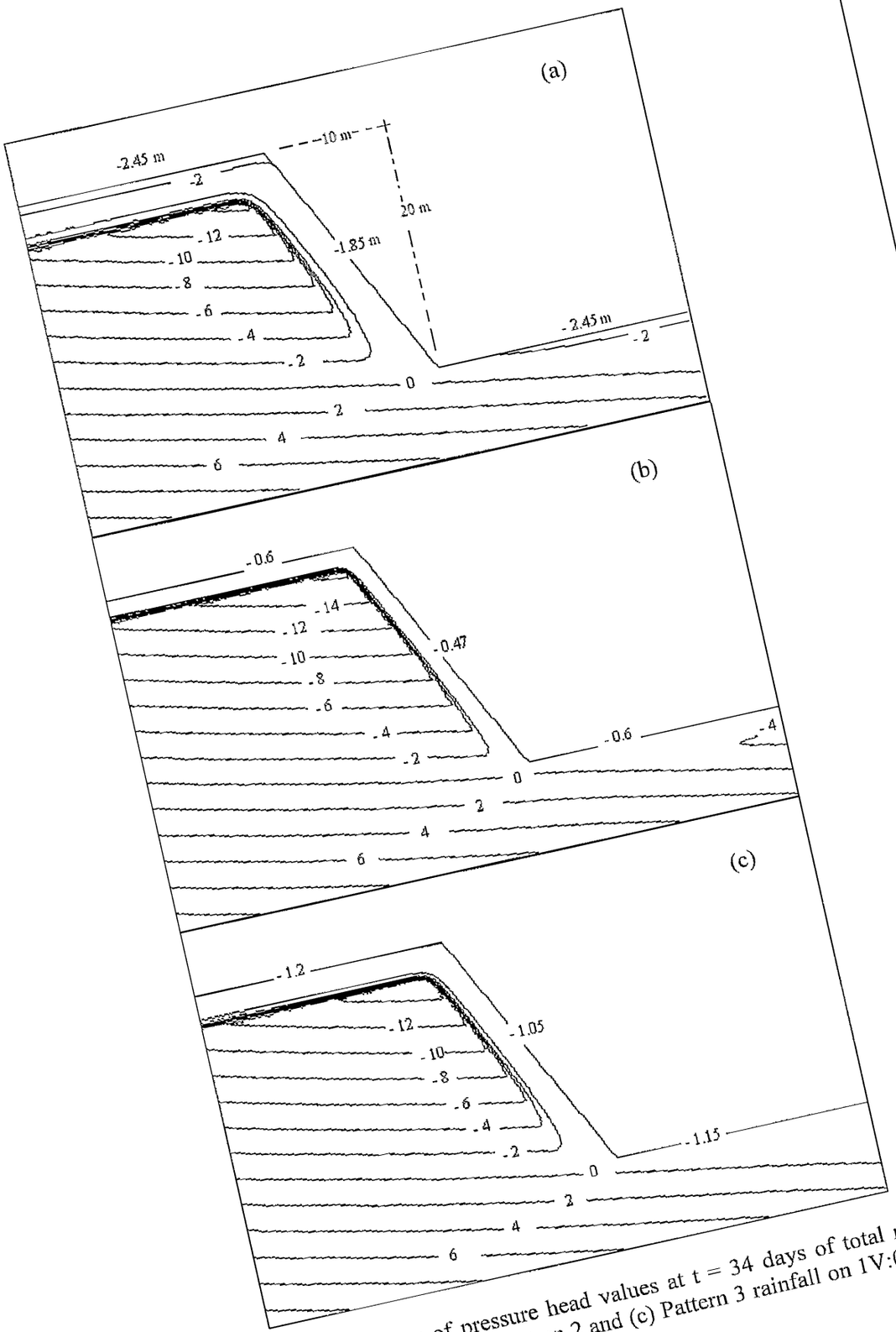

Appendix B-5 Contours of pressure head values at t = 34 days of total rainfall of 310.26 mm for (a) Pattern 1 (b) Pattern 2 and (c) Pattern 3 rainfall on 1V:0.5H SILT slopes

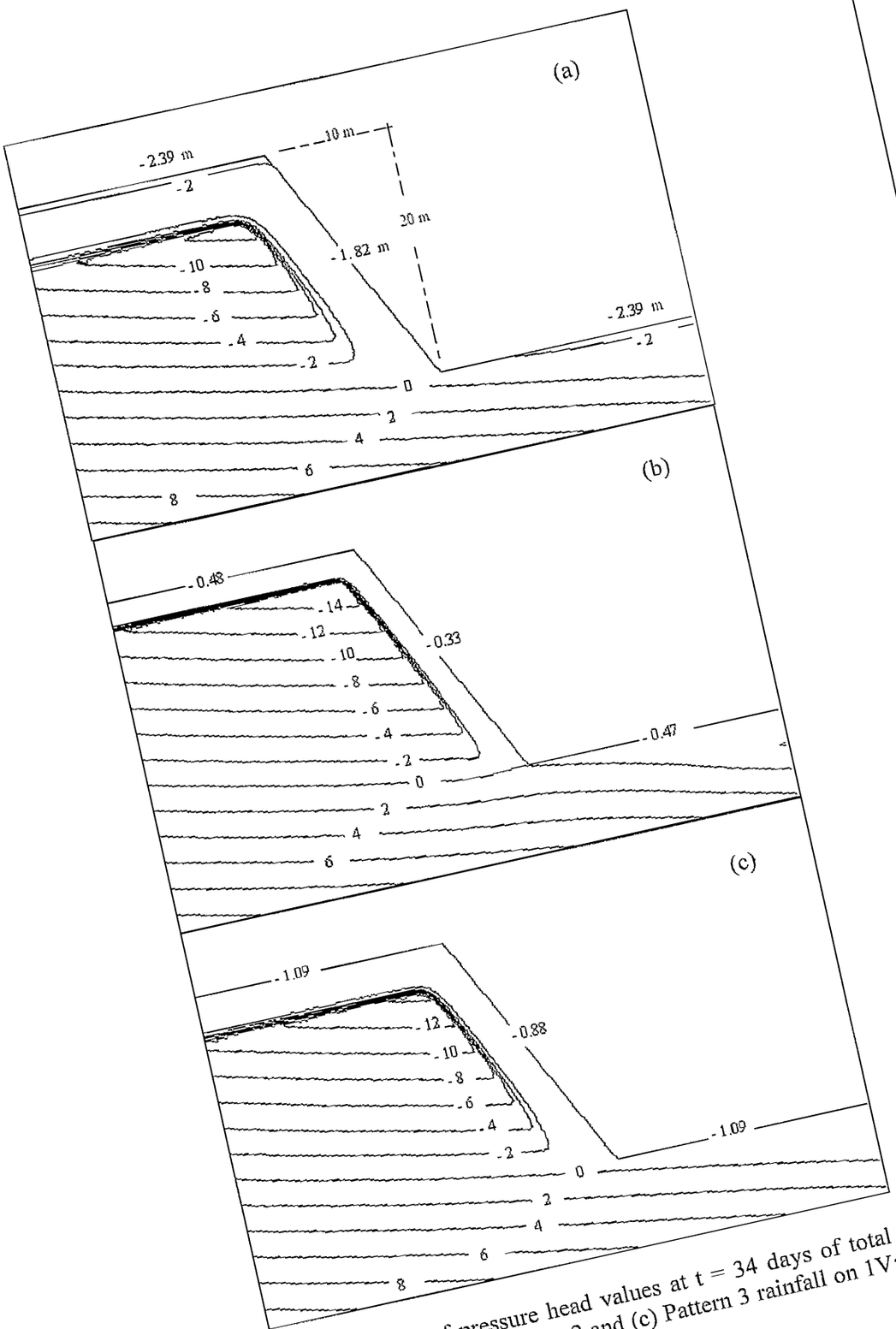

Appendix B-6 Contours of pressure head values at t = 34 days of total rainfall of 496.42 mm for (a) Pattern 1 (b) Pattern 2 and (c) Pattern 3 rainfall on 1V:0.5H SILT slopes

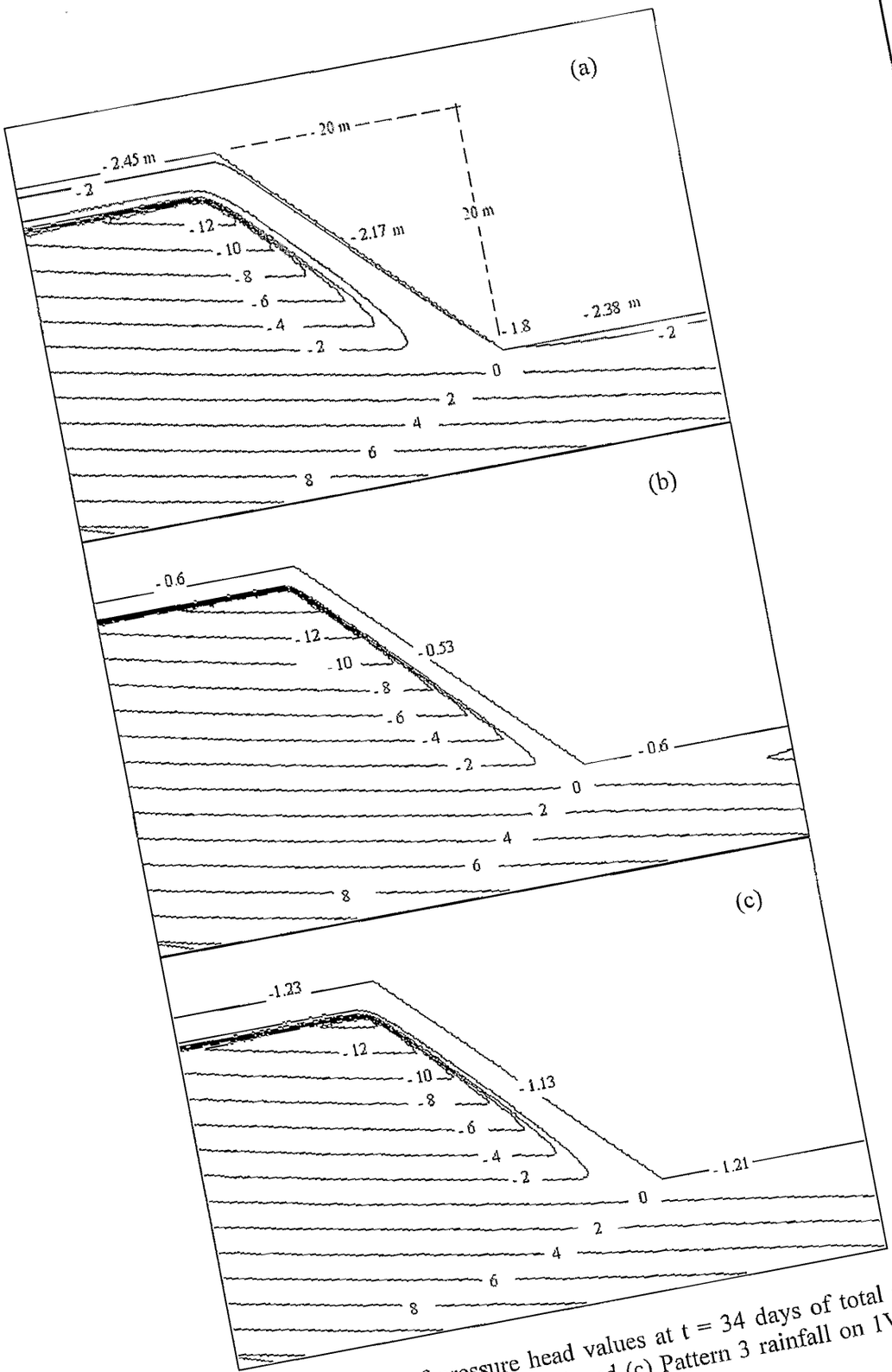

Appendix B-7 Contours of pressure head values at t = 34 days of total rainfall of 310.26 mm for (a) Pattern 1 (b) Pattern 2 and (c) Pattern 3 rainfall on 1V:1H SILT slopes

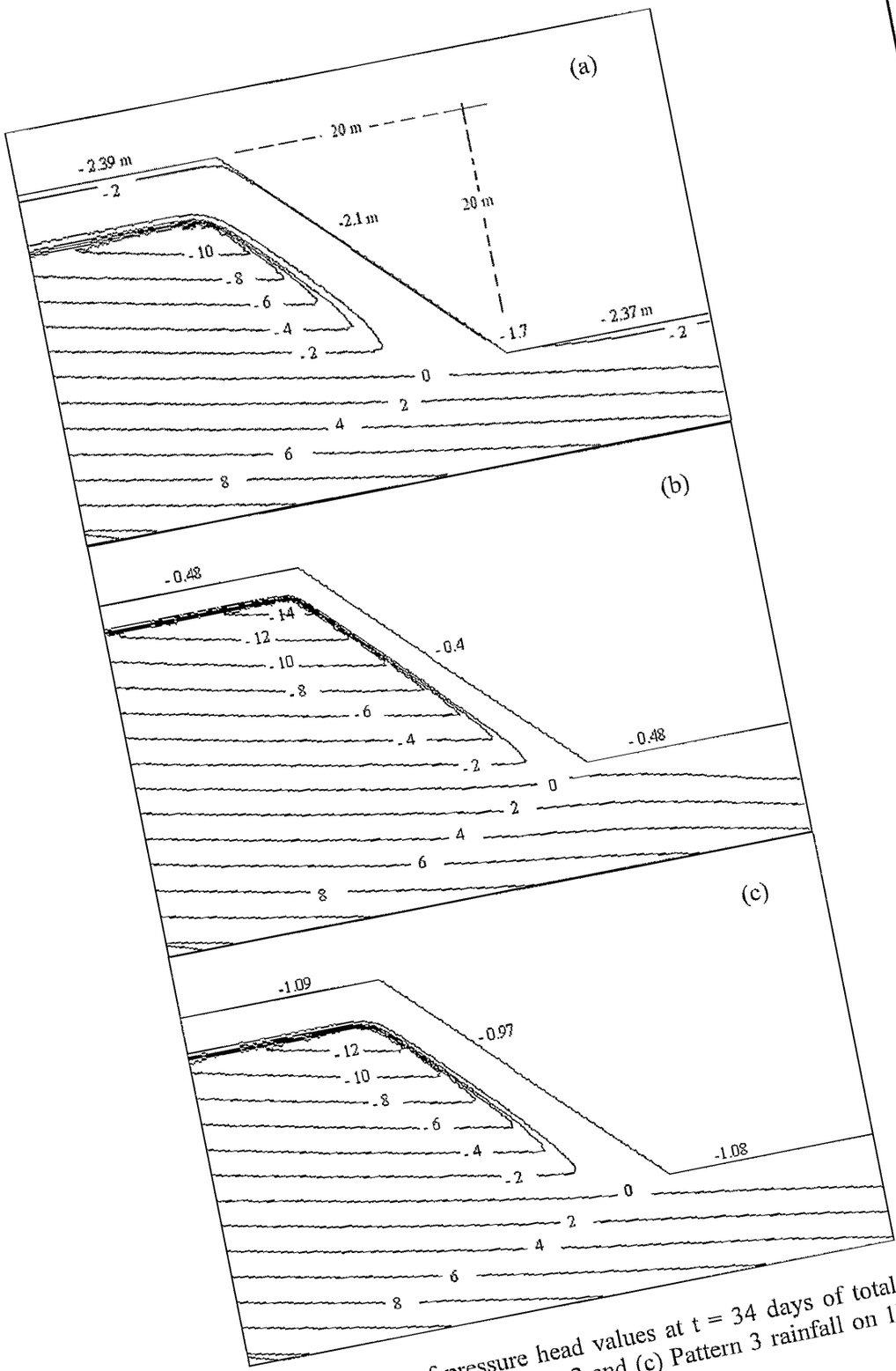

Appendix B-8 Contours of pressure head values at t = 34 days of total rainfall of 496.42 mm for (a) Pattern 1 (b) Pattern 2 and (c) Pattern 3 rainfall on 1V:1H SILT slopes

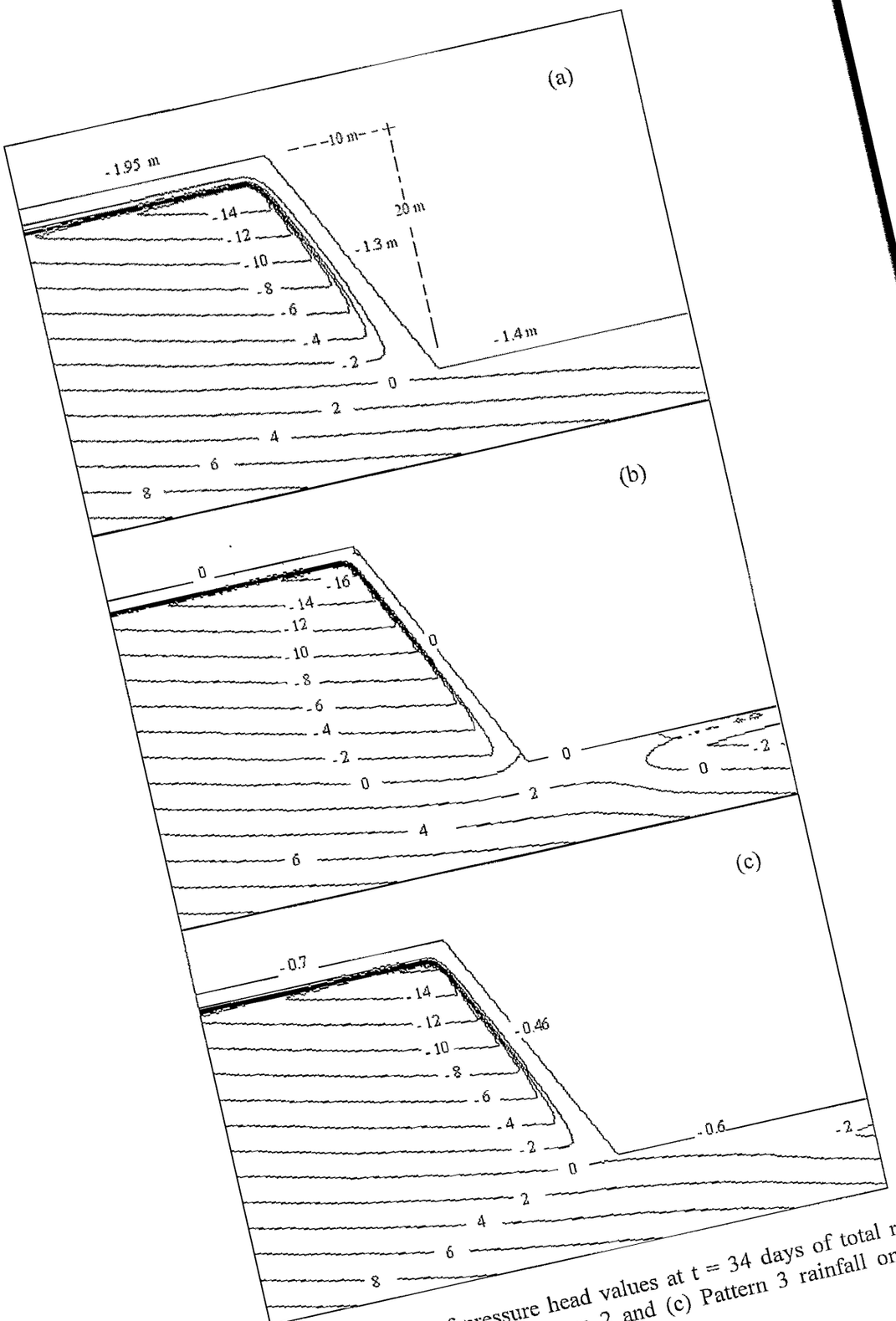

Appendix B-9 Contours of pressure head values at t = 34 days of total rainfall of 310.26 mm for (a) Pattern 1 (b) Pattern 2 and (c) Pattern 3 rainfall on 1V:0.5H CLAY slopes

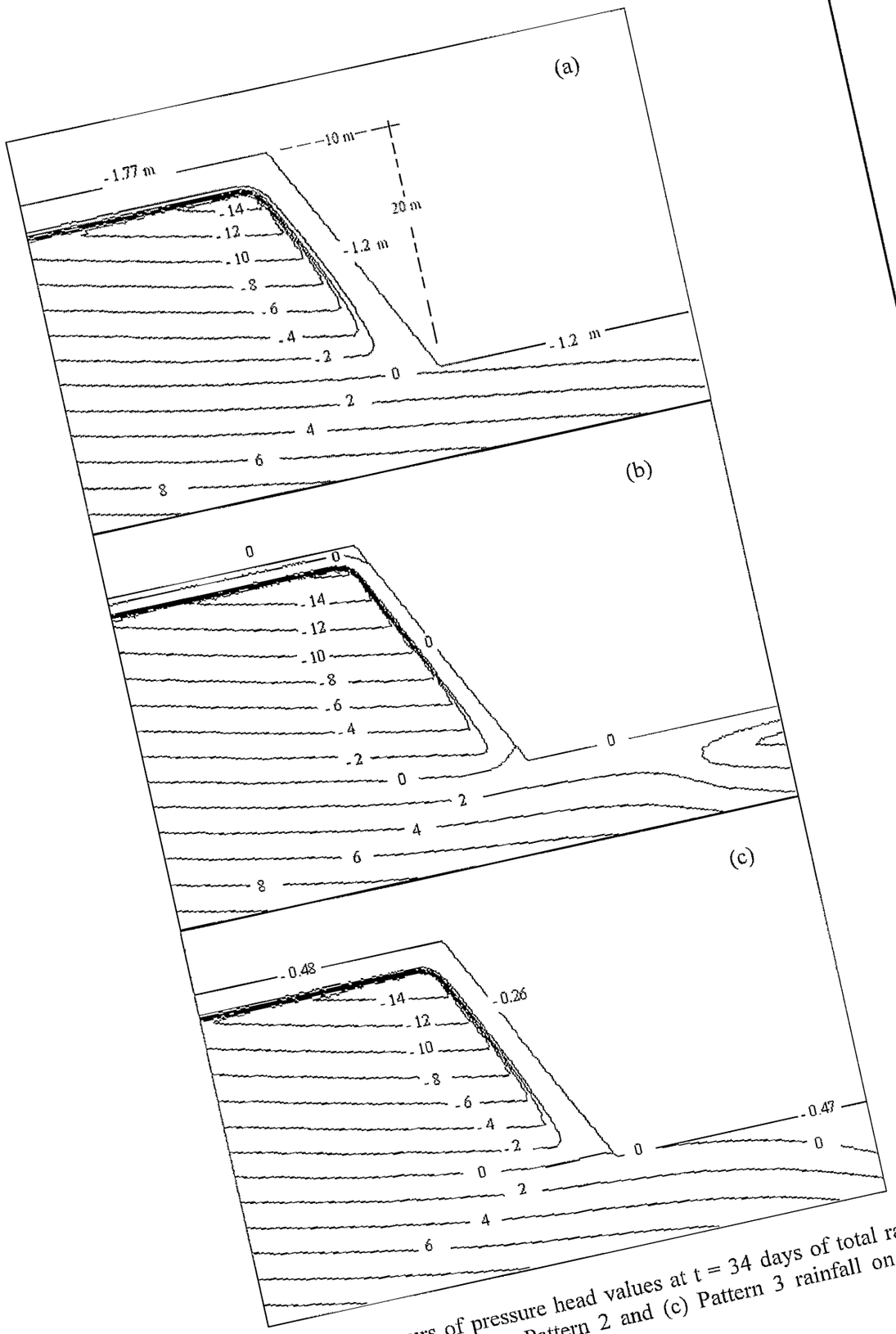

Appendix B-10 Contours of pressure head values at t = 34 days of total rainfall of 496.42 mm for (a) Pattern 1 (b) Pattern 2 and (c) Pattern 3 rainfall on 1V:0.5H CLAY slopes

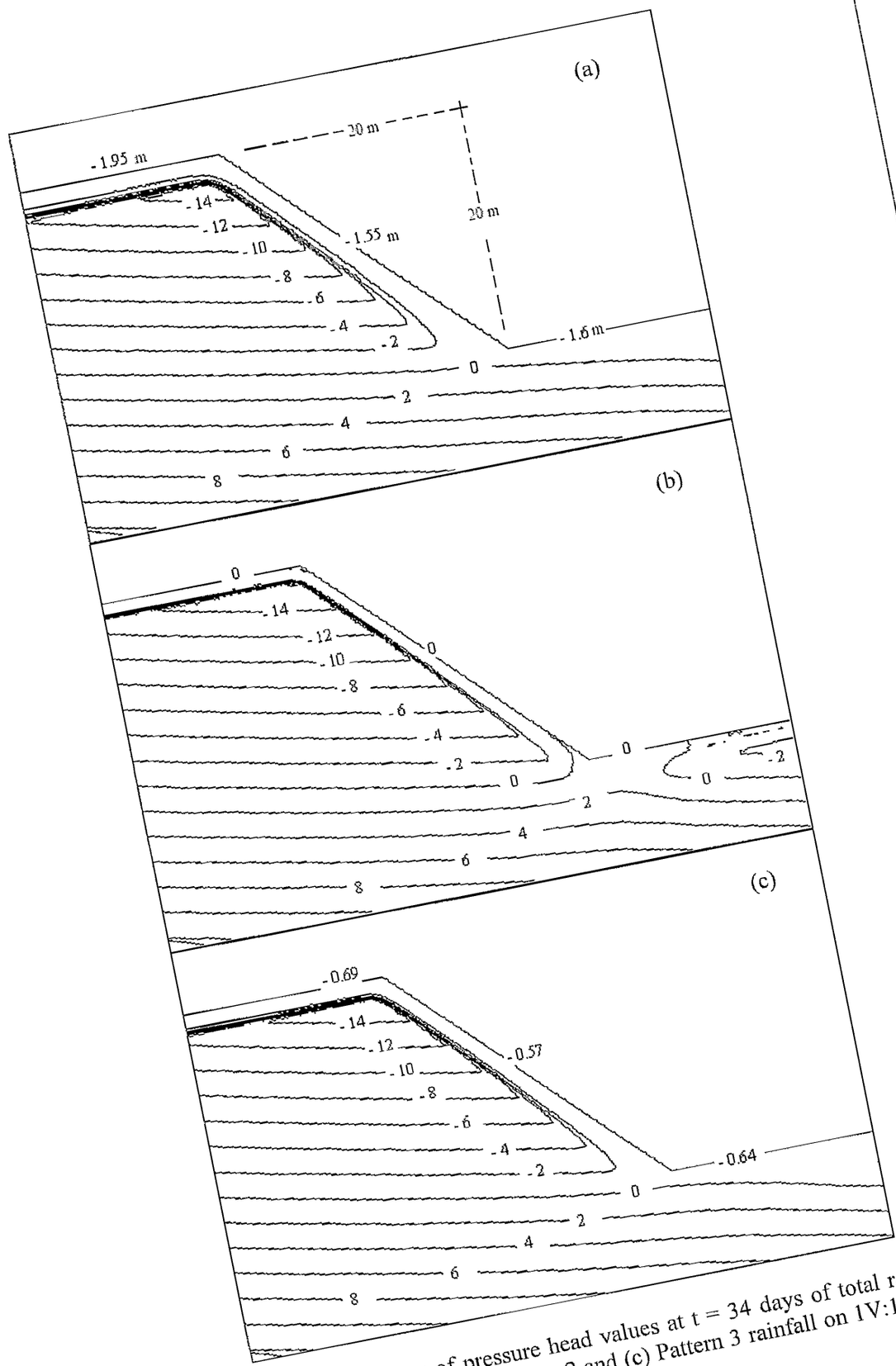

Appendix B-11 Contours of pressure head values at t = 34 days of total rainfall of 310.26 mm for (a) Pattern 1 (b) Pattern 2 and (c) Pattern 3 rainfall on 1V:1H CLAY slopes

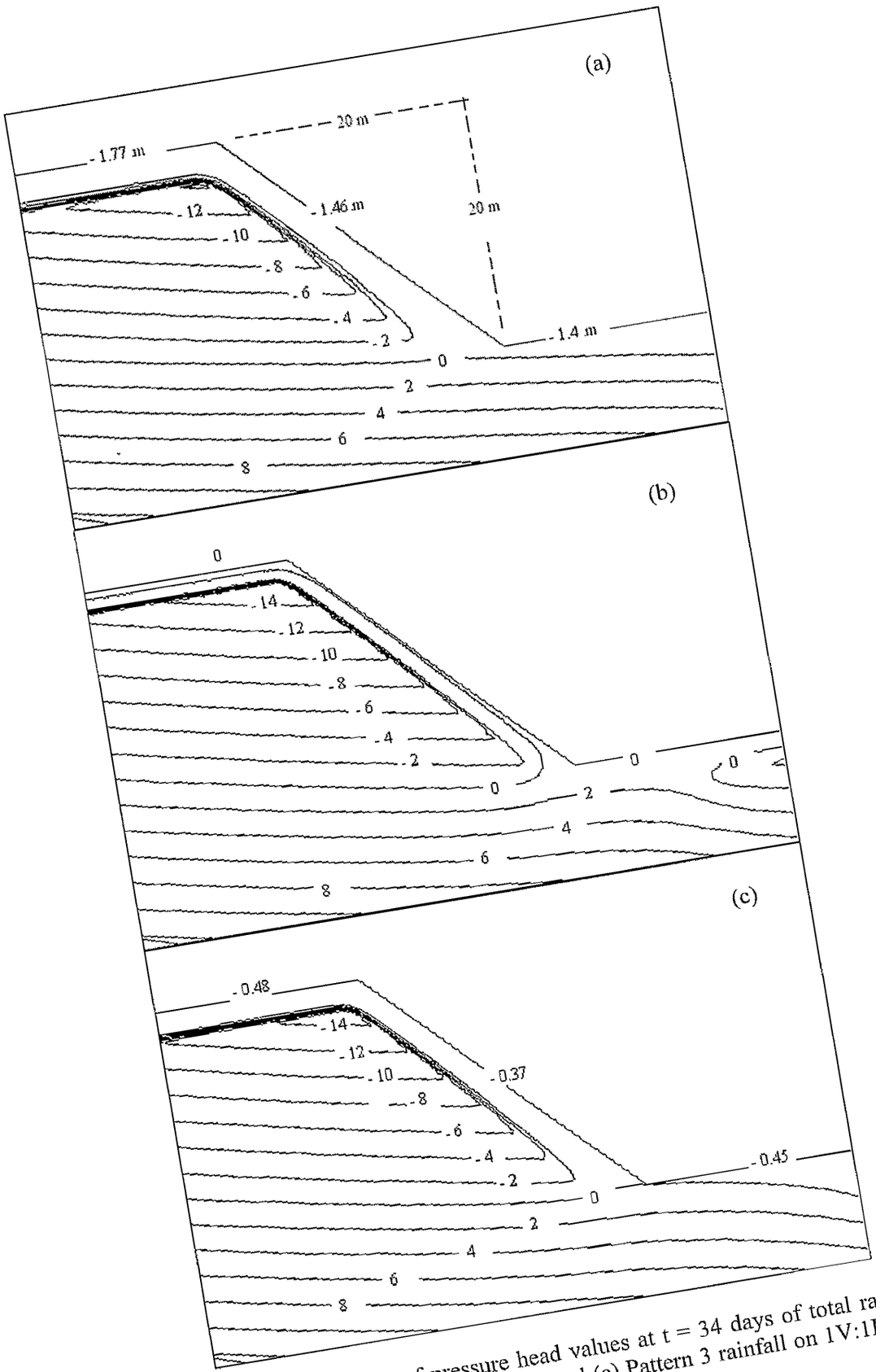

Appendix B-12 Contours of pressure head values at t = 34 days of total rainfall of 496.42 mm for (a) Pattern 1 (b) Pattern 2 and (c) Pattern 3 rainfall on 1V:1H CLAY slopes